Alkaline Magmatism of the Earth and related strategic metal deposits

Proceedings of XXXII International Conference

7-14 August 2015

VERNADSKY INSTITUTE OF GEOCHEMISTRY AND ANALYTICAL CHEMISTRY OF RUSSIAN ACADEMY OF SCIENCES (GEOKHI RAS)

GEOLOGICAL INSTITUTE OF KOLA SCIENCE CENTRE OF RUSSIAN ACADEMY OF SCIENCE (GI KSC RAS)

CRITICAL METALS WORKSHOP. INTERNATIONAL NON-COMMERCIAL ORGANIZATION

Alkaline Magmatism of the Earth and Related Strategic Metal Deposits

Proceedings of XXXII International Conference

7-14 August 2015

Apatity

The present volume was prepared for the XXXII international conference Alkaline Magmatism of the Earth and Related Strategic Metal Deposits. It contains short papers representing the frontier of geological, geochemical, petrologic, mineralogical and isotopic research on alkaline rocks, carbonatites and their associated deposits of critical (strategic) metals. The contributions assembled here address key problems of igneous petrology and metallogeny, including lithospheric and sublitospheric mantle processes, evolution of magmas from their mantle sources to highly differentiated systems, and behavior of critical metals in igneous and supergene environments. Some of the contributions discuss current issues facing critical metal exploration and extraction technology.

The cover picture of "Pink mountains" (Khibiny, oil on canvas, 1989) was painted by artist Belkov I.V.

Belkov Igor Vladimirovich was doctor of geology-mineralogy sciences, director of the Geological Institute KFAN the USSR from 1961 to 1985. He was greatest scientist in the field of geology, geochronology, petrology, mineralogy and metallogeny of granites and genesis of metamorphic rocks. Together with Batyeva I. D., he discovered the Sakharyok and Kulyok alkaline massifs in the Kola Peninsula.

Content

6

9

Chromites from Late Vendian K-alkali Volcanics in the Olenek Uplift
(Northeastern Siberian Craton)

Afanasiev V.P., Nikolenko E.I., Egorova E.O.

Institute of Geology and Mineralogy, Siberian Branch of the Russian Academy of Sciences, Novosibirsk,
Russia

avp-diamond@mail.ru

Placer chromites of a particular variety discovered in the Siberian craton were interpreted as false kimberlite indicators and called Kungur-type chromite after the place of their first find. Although overlapping with kimberlite compositions (Afanasiev et al., 2000), they crystallized in different conditions and, hence, differ in crystal morphology. The sources of the Kurung-type chromites remained unknown until recently, but we found the primary deposits in the northeastern part of the craton: on the northern slope of the Olenek uplift, in the Beenchime and Kuoika catchments south of Olenek, and among Triassic sediments along the Lena River (fields 1, 2, and 3, respectively, in Fig. 1). The chromites are identical over the whole territory and may have a still wider spread. Search for their sources revealed their similarity with chromites from Vendian K-alkali volcanic pipes (Shpunt and Shamshina, 1989) in the crest of the Olenek uplift (Figs. 1, 2). The pipes were observed within an area of 2000 km^2 s but may exist over a much larger territory buried beneath Phanerozoic sediments, judging by the great extent of the derived placer chromites. Therefore, Vendian potassic-alkalic magmatism in the northeastern Siberian craton was an important geological and metallogenic event which provided large-scale chromite mineralization of Vendian-Early Cambrian rocks.
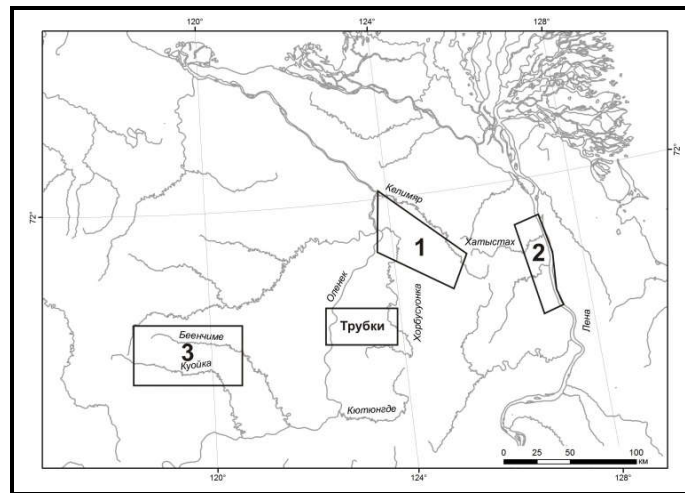
Fig. 1. Occurrences of placer chromites.
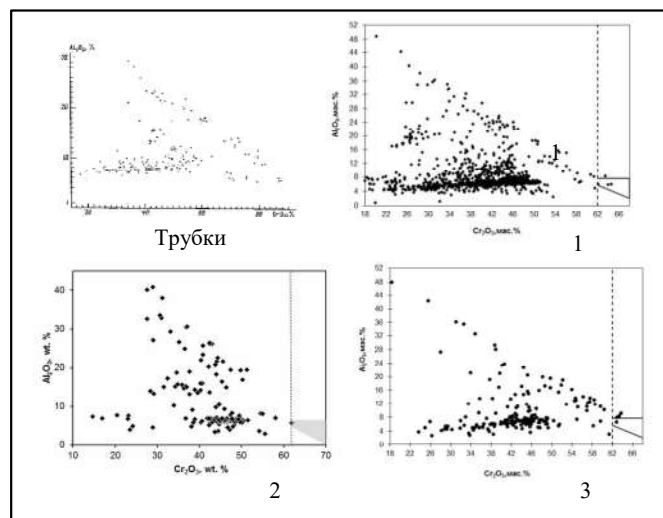
Fig. 2. Major-element compositions of chromites. Data on pipe compositions are from (Shpunt and Shamshina, 1989). 1, 2, 3 refer to samples from the respective chromite fields in Fig. 1.

The placer chromites coexist with placer diamonds of exotic varieties (V-VII and II according to the classification of Orlov): rounded dodechedroids, some with fine fibrous structure and with dissolution signatures) which are either absent from kimberlite or occur in minor amounts. The diamonds may be derived from Precambrian non-kimberlite sources (Afanasiev et al., 2009, 2011) and involved in Phanerozoic sedimentation in the latest Triassic, together with the discovered placer chromites. The Vendian chromites, abundant in younger placers, became "hydraulic companions" of non-kimberlite diamonds in the latest Triassic when the crest of the rapidly growing Olenek uplift was exposed to erosion. The erosion affected Vendian sediments, including conglomerates and gravelstones of the Turkut and Khatyspyt formations, which may have been intermediate reservoirs of exotic placer diamonds. This provides another proof for the origin of exotic diamonds from Precambrian primary deposits (Afanasiev et al., 2009).

References

Afanas'ev V. P., Pokhilenko N. P., Logvinova A. M., Zinchuk N. N. *, Efimova E. S.,

Saf'yannikov V. I. *, Krasavchikov V. O., Podgornykh N. M., and Prugov V. P. , 2000. Problem of false kimberlite indicators: a new morphogenetic type of Cr-spinellide in diamondiferous areas. Russian Geology and Geophysics 41(12), 1676-1689,

Afanasiev, V.P., Zinchuk, N.N., Logvinova, A.M., 2009. Distribution of placer diamonds derived from Precambrian sources. Reports of the Russian Mineralogical Society, Issue 2, 1-13. (in Russian)

Afanasiev, V.P., Lobanov, S.S., Pokhilenko, N.P., Koptil, V.I., Mityukhin, S.I., Gerasimchuk, A.V., Pomazansky, B.S., Gorev, N.I., 2011. Polygenesis of diamonds of the Siberian Platform. Russian Geology and Geophysics 52 (3), 335-353.

Shpunt, B.R., Shamshina, E.A., 1989. Late Vendian K-alkali volcanics of the Olenek Uplift (northeastern Siberian craton). Doklady AN SSSR 307 (3), 678-682.

Paleozoic magmatism of the Fennoscandian Shield: from tholeiites to carbonatites and agpaitic syenites

Arzamastsev A.A.
Institute of Precambrian Geology and Geochronology, St.Petersburg, Russia,
e-mail: arzamas@ipgg.ru

The Kola Paleozoic alkaline province, formed in the northeastern part of the Fennoscandian Shield is characterized by features, which give logical reasons to consider them as the typical manifestations of plume magmatism. Province includes large plutons, made up of agpaitic syenites, carbonatite intrusions, and numerous dikes of alkaline rocks, as well as remnants of subalkaline and alkaline extrusives.

The earliest manifestations of Paleozoic magmatism in the region are represented by the normal dolerite dikes forming three swarms: Pechenga, the Barents Sea, and East Kola. These swarms include a series of large vertical dikes of submeridional trend (NE 10°), some of which have been traced to a distance of more than 80 km. The largest dykes are 10–40 m thick; they cross all the Precambrian structures. Based on $^{40}Ar/^{39}Ar$ dating, the biotite and plagioclase fractions from several dykes of the three Barents Coast swarms yielded age of 385 ± 15 Ma. These data are the same as those obtained with the $^{40}Ar/^{39}Ar$ method for dolerite dikes in the Varanger Peninsula.

The next stage of Paleozoic magmatism is represented by subalkaline volcanics which are exposed in the Kontozero caldera and in the roof of the Lovozero alkaline massif and subalkaline intrusion Kurga. The latter exhibit the U-Pb zircon age of 387±7 Ma [Arzamastsev et al., 1999]. The main stage of Paleozoic magmatic activity is represented by ultrabasic alkaline massifs with carbonatites and agpaitic syenite plutons. Among the 19 ultrabasic alkaline massifs of the Kola province, the Vuoriyarvi and Kovdor massifs, ultrabasic alkaline complex of the Khibiny Massif, and intrusions of the Khabozero group were chosen for U–Pb geochronological investigations. The Khabozero intrusions were chosen because each of them is represented by a single phase and composed of more than 90% of a single rock type: olivinite (Lesnaya Varaka Massif), pyroxenite (Afrikanda Massif), and foidolite (Ozernaya Varaka Massif). The geological and petrological data suggest that all the above intrusions are complementary and were formed during a single differentiation process of the parental melts of the ultrabasic alkaline series. In contrast to typical carbonatite massifs with alkaline ultramafic rocks, in which ultrabasic and, then, ultrabasic alkaline melts were injected through a common conduit, derivatives of the Khabozero group were sequentially emplaced through different conduits, which resulted in the formation of a group of intrusions spaced apart by 5– 8 km. We believe that the absence in each of these intrusions of later derivatives of the ultrabasic alkaline series minimizes the probability of the disturbance of isotopic systems of early differentiates and allows us to obtain the most correct age estimates. Fifteen mineral separates of perovskite

representing all rocks varieties of the ultrabasic alkaline series were chosen for U–Pb dating. In accordance with the geological data, the oldest ages were obtained for perovskite from the olivinites and pyroxenites. Taking into account the errors, their age is 385–377 Ma. Age estimates for perovskite from the more evolved rocks of the series range from 376 to 367 Ma. The age of perovskite from sample 13-OV appeared to be significantly older compared with perovskites from the other foidolites. Petrographic examination showed that this sample is a dike rock similar in composition to olivine melanephelinite and contains numerous xenocrysts of olivine, Cr-bearing clinopyroxene, garnet, and perovskite. It is reasonable to suppose that the perovskite analyzed could be formed at an earlier stage of differentiation of the ultrabasic alkaline series. The analysis of rare perovskite grains from the rocks of the Khibiny Massif revealed significant differences between the ages of the pyroxenite and xenoliths of ultrabasic alkaline rocks (383 ± 7 Ma) and apatite–nepheline ores (370 ± 3 Ma), which is consistent with geological observations of rock relationships.

The age estimates reported here for perovskite from the olivinite, pyroxenite, and perovskite bearing pyroxenite (perovskite ore) of the Lesnaya Varaka, Afrikanda, and Kovdor massifs fall within the range 385–377 Ma. A slightly younger age of 376–367 Ma was obtained for perovskite from the foidolite members of the ultrabasic alkaline series, which is in general consistent with geological observations indicating that the ijolite–melteigite intrusions cross cut the pyroxenites and olivinites. The analysis of data for different intrusive phases from a single massif suggests that each multiphase intrusion developed autonomously within a specific age interval. For instance, the similarity of ages of the early ultrabasic rocks and late carbonatites of the Kovdor Massif indicates that it was formed within the range 380–378 Ma. On the other hand, the formation of the Vuoriyarvi Massif occurred approximately 368–361 Ma ago. The analysis of the published data and geochronological estimates obtained here suggests that most of the ultrabasic alkaline massifs of the Kola province were formed at 379 ± 5 Ma. A comparison of these data with Rb–Sr isochron ages indicates significantly younger ages of the agpaitic syenites of Khibiny (367 ± 5 Ma) and Lovozero (370 ± 7 Ma) [Kramm and Kogarko, 1994]. Additional $^{40}Ar/^{39}Ar$ age determinations for phlogopite from a diatreme cutting the nepheline syenite of Khibiny (363 ± 5 Ma) [Arzamastsev et al., 2009] and zircons from the contact aureole (359 ± 5 Ma) and zircon bearing alkaline syenites of the Lovozero Massif (347 ± 8 Ma) [Arzamastsev et al., 2007] suggest that magmatic activity within these giant alkaline plutons continued for at least several million years after the formation of the main rock complexes. In the light of the available isotopic evidence, the age of perovskite from pyroxenite xenoliths at Khibiny (383 ± 7 Ma) coincides with the age of formation of the ultrabasic alkaline series of carbonatite intrusions of the Kola province. In contrast, the obtained age of perovskite from the apatite–nepheline ore of Khibiny (370 ± 3 Ma) corresponds to the emplacement of agpaitic syenites. This provides indirect evidence that the apatite mineralization of Khibiny is linked to the agpaitic series, which is represented by a complex of potassic nepheline syenites (rischorrites) and massive urtites, rather than to the ultrabasic alkaline series [Arzamastsev et al., 1987].

The existing geochronological database includes more than 120 age estimates obtained by different methods. Almost all the massifs of the Kola alkaline province, as well as dike complexes and volcanics were dated with varying accuracy. Together with geological observations, these data allow us to distinguish the following stages of Paleozoic magmatism in the northeastern Fennoscandian Shield.

393–381 Ma. Emplacement of subalkaline dolerite dikes in the distal zone adjacent to the Barents Sea region of the Kola–Kanin monocline [Arzamastsev et al., 2009; Baluev et al., 2012].

387 ± 7 Ma. Origination of a series of faults in Late Archean tonalites, trondhjemites, and granodiorites; formation of the Kurga Massif [Arzamastsev et al., 1999] and ultrabasic and subalkaline volcanics in the northeastern part of the future Lovozero ring structure.

388 ± 6 Ma. Formation of a series of ring faults and the origin of the Khibiny sagging caldera at the contact of the Late Archean complex of tonalites, trondhjemites, and granodiorites and the Paleoproterozoic Pechenga–Imandra–Varzuga paleorift complex; injection of the first portions of melanephelinite magma and formation of framing ring dikes [Arzamastsev et al., 2009].

383 ± 7 Ma. Emplacement of ultrabasic alkaline melts in the northern part of the Khibiny caldera and the northeastern part of the Lovozero caldera; formation of olivine pyroxenite, melilitolite, and olivine melteigite bodies.

379 ± 5 Ma. Formation of ultrabasic alkaline complexes with carbonatites in the Kovdor Massif, as well as the Turiy Mys, Afrikanda, Lesnaya Varaka, Ozernaya Varaka, Ivanovka, Pesochnyi, and other massifs.

372–367 Ma. Development of the main plutonic complexes of agpaitic syenites in the Khibiny and Lovozero calderas. Khibiny: (a) emplacement of agpaitic syenites along outer cone shaped faults (khibinite intrusion); (b) continuing sagging of the caldera and formation of a layered ijolite–melteigite complex along a system of ring faults; (c) formation of coneshaped faults in the rocks of the ijolite–melteigite complex and emplacement of an apatite bearing urtite–juvite–kalsilite syenite intrusion along them (370 ± 7 Ma); and (d) breakup of the central part of the caldera and emplacement of nepheline syenite melts, which formed the core of the massif (foyaite intrusion). Lovozero: (a) filling of the entire depression with agpaitic magmas and formation of a layered loparite bearing lujavrite–foyaite–urtite complex; (b) breakup of the central part of the massif and

formation of a shallow intrusion of eudialyte lujavrites; and (c) emplacement of an alkali syenite (pulaskite) intrusion in the central part of the Lovozero caldera.

367–366 Ma. Intrusion of carbonatite and pulaskite stocks in the eastern part of the Khibiny caldera.

377–362 Ma. Formation of postintrusion dike swarms in the framing of the agpaitic and ultrabasic alkaline massifs. Emplacement of autonomous dikes and formation of diatremes of alkali picrite, kimberlite, olivine melanephelinite, nephelinite, and phonolite mainly in the framing of the Kandalaksha paleorift structure.

359 ± 5 Ma. Formation of late microcline–albite veins with ilmenite and zircon in the framing of the Lovozero Massif.

347 ± 8 Ma. Late magmatic processes in the alkali syenites of the central part of the Lovozero Massif marking the termination of magmatic activity in the Khibiny and Lovozero calderas.

Types of carbonatite and relative associated silicate rocks groups – by re-analysisis of the Database Woolley and Kjarsgaard

Asavin A.M.
Vernadsky Institute of Geochemistry and Analytical Chemistry RAS, Moscow, Russia, Moscow
aalex06@inbox.ru

The development of metallogenic deposits database is a new, underdeveloped approach in the field of ore geochemistry. The carbonatites is one of the lucky exception of the present state in the Earth of Science.

Now published and open databases "World Carbonatite" [Woolley & Kjarsgaard 2009, Woolley & Kjarsgaard 2008] and "Carbonatite and Kimberlite" [Frolov et al. 2006, Burmistrov et al. 2008] and "Metallogenic of the intraplate magmatism complexes" editor by Mejelovski et al. 2001 [Bagdasarov et al 2001].

This gives us unique chance to analyze the metallogenic relationships in this type of deposit on the quantitative level.

Only the single attempt to analyze information from "World Carbonatite" was made by Woolley and Kjarsgaard in 2008 year.

The authors created the classification of associations of silicate rocks linking with carbonatites. It highlighted several associations (10-12) [Woolley & Kjarsgaard 2008]. These associations were ranked from different paragenetic types of carbonatite location (8) in different geodynamic structures. It allowed to build a reasonable model of carbonatite genesis.

The disadvantages of this work are in two factors: the fact that classification was performed separately for two (hydrothermal and intrusive) independent groups of carbonatites. While a further analysis showed that, this kind of separation does not work. And the second fact that they did not attempt to divide carbonatites by chemical composition. This approach prevents to emphasize certain ore associations of carbonatites and to find links to paragenesis of silicate, intrusive rocks in depend of this factor.

In addition, selected group are mixed in hypabyssal and intrusive rock types. Several types of rocks (syenite for example) add in 5 of the 12 groups. It indicates a large variation within the selected groups.

The accumulated information allows us after 7 years repeat a re-analysis of data from public databases and appreciate the sustainability of receiving conclusions. The development of information processing techniques gives us the efficient possibilities for gaining new information from databases.

Table 1. Classification plutonic associations from carbonatite localities (M- mono phase association; Poly_ - poly phases association more then 3-4 types of the rocks).

This work		Woolley & Kjarsgaard 2008	
M-dunite-olivinite			
M-pyroxenite	0		
Poly_UO	6	Ol-Pyx uo rock + syenite	
Poly_UO_melilitolite	3		
Poly_melilitolite			
M-melilitolite		Melilitolite	6

14

melilitolite-Ne-syenite		Melilitite, melillite-nephelinite extrusive (±Melilitolite)	4
Dunite-ijolite-Ne-syenite			
Dunite-pyroxenite-ijolite			
ijolite-urtite-Ne-syenite	6		
ijolite-urtite-Ne-syenite(Px)	5		
ijolite-urtite-Ne-syenite(Px-gabbro)	6		
ijolite-urtite-Ne-syenite(granite)			
M-ijolite-urtite	3		
M-ijolite-urtite(Px)		Melteigute-ijolite-Urtite (±uo rock syenite)	7
M-ijolite-urtite(Px-gabbro)		Nephelinite extrusive (± M-I-U)	8
M-gabbro			
gabbro-syenite	0	Basanite, tephrite alkaline gabbro essexite	
gabbro-syenite(Px)			
gabbro-syenite-granite(Px)			
syenite-Ne-syenite	6	Phonolite, FSp syenite	8
Ne-syenite(Px)	3	Pyroxenite+syenite	3
syenite-Ne-syenite-granite(Px)	6	Trachyte, Q-trachyte, syenite, Q-syenite	3
granite			
Total massive	15		03

Results of re-analysis of database "World Carbonatite" [Woolley & Kjarsgaard 2009] and other database are shown in tabl.1 (also compared with classification schema Woolley & Kjarsgaard 2008) The main peculiarities of our classification are that we have identified mono phase (M-) massive (with 1-2 types of the rocks) and poly phases massive. This is the effect of strong detalization of our classification. In the old classification mono association is absent (tabl. 1 right off columns). Also on the histogram (Fig.1) we can observe gradual frontiers between different groups of the rocks. We believed that this picture is close to the real nature of carbonatite massives. The histogram also reflects the view of previous studies about the allocation of the three major formations: ultramafic-alkaline, gabbro, and miaskitic syenite-granite [Bagdasarov 2007; Ternovoy 1977]. Relatively recently selected group of linear carbonatite bodies can be attributed to the miaskitic syenite-granite group apparently [Rass 2011, Nedosekova 2007].
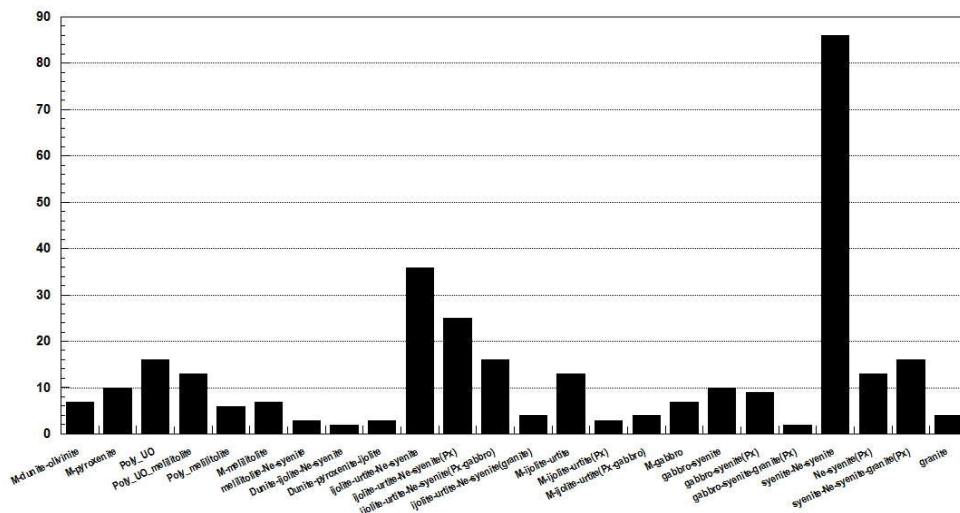
Fig. 1. Histogram of plutonic association from carbonatite localities as result of databases re-analysis.

In the next stage of work, we evaluate the distribution of carbonatites types from occurrences (Fig.2). The calculating methods of the frequency of different types of carbonatites in occurrences also were developed based on database re-analysis. Main minerals included in association are : CC – calcite, Dol – dolomite, Ank – ankerite. The types of rocks: sill – silico-carbonatite, Phosc – phoscorite (also include nelsonite, magnetitolite), hydro – calcite vein with TR-minerals, Ba-TR_CC – benstonite bearing with bastnesite and calcite. The vast majority sevite, mono calcite carbonatite type (236 occurrences) is shown in the histogram off scale - an arrow (gray column).
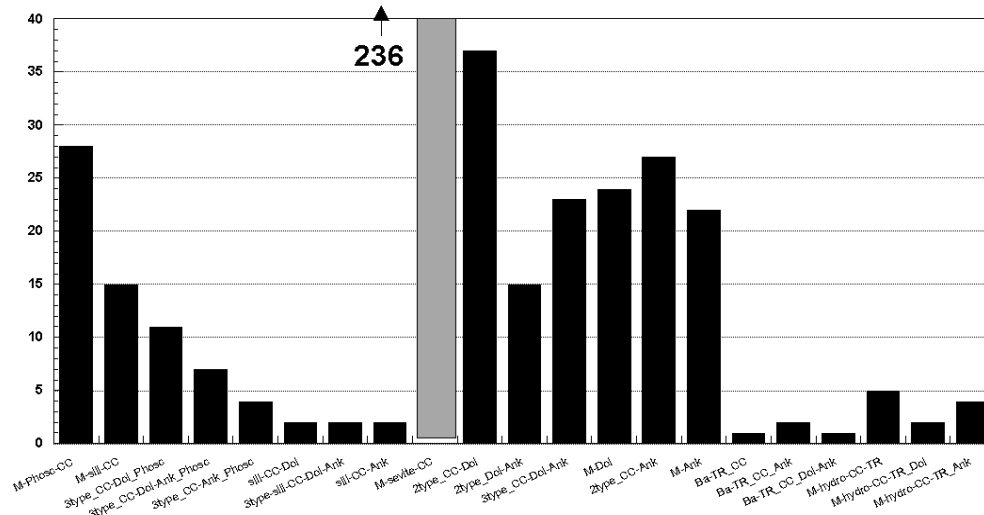
Fig. 2. Histogram of distribution of carbonatite association in occurrences as result of databases re-analysis (detail legend see in text).

Calcite carbonatites are permanent members of the association with other types of carbonatite. This is emphasized by the presence of large number (236) of localities in which contains only sevite carbonatites. Therefore, we can consider the binary association phoscorite-sevite, silico-carbonatite-sevite as mono association. Which is reflected in the histogram mark M. 2type and 3type marks on histogram axis marked the arrays were present the association consisting from 3, 4 additional types of carbonatites.

We have developed the classification mainly based on the division of the main mineral types of carbonatites, but this is a first approximation. In fact, sevite carbonatites allocate several types of calcite generations with different ore contents. It should be considered in the future.

Table 2. Classification of carbonatite associations from carbonatite localities (M- mono phase association; 2type, 3type - poly phases association with more then 3-4 types of the carbonatite).

Petrography association	Count	Legend on histogram
Phoscorite (nelsonite, magnetitolite)+sevite	28	M-Phosc-CC
Silicocarbonatite+sevite	15	M-sill-CC
Sevite+Dolomite+phoscorite	11	3type_CC-Dol_Phosc
Sevite+Dolomite+ankerite+phoscorite	7	3type_CC-Dol-Ank_Phosc
Sevite+ankerite+phoscorite	4	3type_CC-Ank_Phosc
Silicocarbonatite+sevite+Dolomite	2	sill-CC-Dol
Silicocarbonatite+sevite+Dolomite+ankerite	2	3type-sill-CC-Dol-Ank
Silicocarbonatite+sevite+ankerite	2	sill-CC-Ank
Sevite	236	M-sevite-CC
Sevite+Dolomite	37	2type_CC-Dol
Sevite+Dolomite+ankerite	15	2type_Dol-Ank
Sevite+Dolomite+ankerite	23	3type_CC-Dol-Ank
Dolomite (rauhaugite, beforcite)	24	M-Dol
Sevite+ankerite	27	2type_CC-Ank

16

Ankerite	22	M-Ank
Benstonite-bearing carbonatites+ Sevite+ Bastnesite-	1	Ba-TR_CC
Benstonite-bearing carbonatites+ Sevite+ Ankerite	2	Ba-TR_CC_Ank
Benstonite-bearing carbonatites+ Sevite+ Dolomite +Ankerite	1	Ba-TR_CC_Dol-Ank
Hydrothermal calcite vein with REE (Fluorite-rich sevite)	5	M-hydro-CC-TR
Hydrothermal calcite vein with REE, +Dolomite	2	M-hydro-CC-TR_Dol
Hydrothermal calcite vein with REE,+ankerite	4	M-hydro-CC-TR_Ank
Total	470	

The histogram gives sufficient evidence of a clear genetic separation of phoscorite phase from the main sevite phase. On the histogram phoscorites and close to them rocks are separated from the sevite type by significant gap. The same conclusion can be made for hydrothermal calcite veins and barium carbonatites with TR mineralization. On the other hand the link between calcite (sevite) and dolomite (beforsite) carbonatite types very close. This is indicated by a large numbers of occurrences with intermediate types associations between these extreme members.

Unfortunately, the volume of abstract does not allow further analysis of the spatial distribution of selected association types for different geodynamic conditions of localities. But this question is quite interesting. Possible, if we use our classification the result will be better than the fuzzy picture obtained by Burmistrov [Burmistrov et al., 2008].

The next question is whether there is a link between the types of carbonatite and association types of igneous rock? Our preliminary analysis shows that the M-sevite type meets with all associations, but other more rare types of carbonatites are still mostly associated with certain types of associations silicate rocks.

Further development of the information content in database allows us to receive new, not obvious conclusions. But we need to perform a re-analysis of the database, perform data mining, as well as to create new algorithms.

References
Bagdasarov U.A. Carbonatites formation of the alkaline rocks and their peculiarities of mineralogy// in. Doneck 24 International conference: Alkaline magmatism of the Earth and their ore potential" 2007, P.10-11 (in Cyrillic)

Burmistrov A. A. , V. I. Starostin, and D. R. Sakya Tectonic Aspects of the Evolution and Ore Potential of Carbonatite and Kimberlite Magmatism // Doklady Earth Sciences. 2008, V.418, No. 1, pp. 19–23.

Krasnobaev, A. A., Rusin, A. I., Valizer, P. M., & Busharina, S. V Zirconology of calcite carbonatite of the Vishnevogorsk massif, southern Urals // Doklady Earth Sciences 2010, Vol. 431, No. 1, pp. 390-393

Nedosekova I.L. New data on carbonatites of the Il'mensky-Vishnevogorsky alkaline complex, the southern Urals, Russia. // Geology of Ore Deposits. 2007, 49 (2), pp. 129-146.

Rass I.T. Carbonatites – derivate of the mantle magmas // www.ises.su/2011/pdf/rass_carbonatites.pdf VII International school from the Earth Science I.S.E.S. 2011, 3pp. (in Cyrillic)

Ternovoy V.I. Carbonatite massives and their deposit // L. Leningradsky University 1977, 188 pp. (in Cyrillic)

Woolley A. R., Kjarsgaard B. A. Book Review. // Journal of petrology. 2009, V. 50, N. 1, pp. 195-196.

Woolley Alan R. Igneous silicate rocks associated with carbonatites: their diversity, relative abundances and implications for carbonatite genesis // Per. Mineral. 2003, V .72. Spec. Issue: Eurocarb, p. 9-17.

Woolley Alan R. , Bruce A. Kjarsgaard Paragenetic types of carbonatite as indicated by the diversity and relative abundances of associated silicate rocks: evidence from a global database // The Canadian Mineralogist. 2008, V.46, pp. 741-752.

Neoarhaean alkaline magmatism of Fennoscandian Shield of Arctic region is an oldest plume in the history of the Earth?

Bayanova T.B., Chshashin V.V., Kudryashov N.M., Elizarov D.V., Serov P.A.
Geological Institute of Kola Science Centre RAS, Apatity, Russia, tamara@geoksc.apatity.ru

In the N-E part of the Baltic of Fennoscandian Shield there are about 30 massifs of high Ba, Sr, LREE sanukitoids. Isotope U-Pb data on zircon from sanukitoids granites of Karelia region (massifs Nukozersky, Xaytavaarsky, Elliysky et set.) and eastern Finland (massifs Kiiittila, Silvevaara, Tasanvaara et set.) and connected with sanukitoids lamprophyres dykes (2.68 Ga) have yielded Neoarhean age interval origin from 2.74- to 2.70 Ga (Chekulaev et all., 2004, Lobach-Zhuchenko et all., 2005; Kudryashov et al., 2013). Sanukitoids in genesis are result of enriched mantle reservoir (Lobach-Zhuchenko et all., 2005; Egorova, 2014).

For the first time in Murmansk domene zircon from albite syenite of Paneavrsky massif yielded U-Pb age with 2653±9 Ma (Petrovsky et.all, 2009). New U-Pb ages 2668±7Ma on zircon gave for eugerin-auvgite granosyenite Mt.Sylngyraz (Table 1).

In Keivy terrane Neoarhean alkaline granite and sienite are widespread with massifs Belaya Tundra (U-Pb age on zircon 2654±5Ma), Zapadno-Keivsky (2674±6 Ma), Saharjok, Ponoisky et.set. For zircon from Saharjok massif with zircon deposit has been yielded 2613±35 Ma for late phase of nepheline syenite. The U-Pb age on zircon from yearly phase of the massif is 2682±10 Ma. For the first time baddeleyite have been separated from carbonatites of Siilinjarvy (Finland) and U-Pb age gave 2613±18 Ma which are coeval on U-Pb age on big zircon crystal with 2611±10 Ma (Bayanova, 2006).

Table 1. Summarizing of U-Pb and Sm-Nd data for Neoarhean basite and alkaline rocks of Fennoscandian Shield (from Bayanova, 2004).

Rocks	U-Pb, Ma (zircon, baddeleyite)	Sm-Nd
Murmansk domene		
Paneavrsky (albite syenite)	2653±9	T_{Dm} = 3.1 Ga; ε_{Nd}(T) = -1.5 – -4.0
Sylnguraz (subalkaline eugerine- avgite granosyenite)	2668±7	T_{Dm} = 3.1 Ga; ε_{Nd}(T) = -2.0
Keivy structure		
Tsaga (monzogabbro) (gabbro-norite) (monzonite)	2668±10 2660±80 2659±3	T_{Dm} = 3.0 Ga; ε_{Nd}(T) = +2
Medvezhje-Schuchieozersky (anorthosite)	2663±7	- " -
Achinsky (anorthosite)	2678±16	- " -
Western-Keivsky (granosienite)	2674±6	- " -
White Tundra (alkaline granites)	2654±3	T_{Dm} = 3.1 Ga; ε_{Nd}(T) = -1.4
Sakharijok (nepheline syenite)	2682±10	- " -
Sakharijok (alkaline syenite)	2613±35	- " -
Central-Kola domene		
Kanozero (alkaline granites)		T_{Dm} = 3.0 Ga; ε_{Nd}(T) = -1.2
Finland		
Siilinjärvi (carbonatite)	2611±10	T_{Dm} = 3.1 Ga; ε_{Nd}(T) = +0.4
Siilinjärvi (carbonatite)	2613±18	2615±57; ε_{Nd}(T) = +0.4 – +0.2

Kanozersky massif of alkaline granite lies in Central –Kola Arhean domene and zircon yielded U-Pb age 2667±16 Ma. Therefore take into account all U-Pb isotope data on zircon and baddeleyite duration of Neoarhean alkaline magmatism are more than 60 Ma from interval 2.61 to 2.67 Ga (Table 1).

All isotope data for alkaline granites-syenites and sanukitoids of Fennoscandian Shield of Arctic region of Neoarhean structures and carbonatites of Siilinjarvy which based on εNd, ISr, REE and He[3]/He[4] data belong to enriched mantle EM-2 reservoir according to (Zozulya et all., 2007; Egorova, 2014). This epoch (130 Ma) formation from 2.74 to 2.61 Ga of alkaline, subalkaline, basite and carbonatite magmatism is corresponded time of origin Kenorland supercontinent according to investigation (Lubnina, 2009).

All investigations are in frame in the IGCP-SIDA 599.

References:

Bayanova T.B. Age of key geological complexes of Kola region and duration of magmatic processes.// Nauka. Saint-Petersburg. 2004. 176 P.

Bayanova T.B. Baddeleyite a prospect geochronometer of alkaline and mafic magmatism // Petrology. 2006. T.14. N.2. P.203-216.

Chekulaev V.P., Bayanova T.B., Arestova N.A., Kovalenko A.V., Levkovich N.V. About age of high-Mg granitoids of Nukozersky massif, Karelia region // Doclady RAS. 2004. T.394. N.1. P.101-104.

Egorova Y. Sanukitoids of Fenno-Karelian provinces of the Baltic Shield: geology, composition, sources // Abstract of candidate dissertation. Saint-Petersburg. 2014. 20 P.

Kudryashov N.M., Petrovskiy M.N., Mokrushin A.V., Elizarov D.V. Neoarhean sanukitoids magmatism of Kola region: geological, petrochemical, geochronological and isotope-geochemistry data // Petrology. 2013. V.21. № 4. P.389-413.

Lobach-Zhuchenko S.B., Kovalenko A.V.,Chekulaev V.P.,Arestova N.A., Guseva N.S. Sanukitoids of Karelia as possible source of information about geodynamics substance in late Arhean on Baltic Shield // Geology and geodynamic of Arhean // Materials of Russian conference on problem geology and geodynamic of Precambrian. Saint-Pet.: centre of information culture. 2005. P. 236-242.

Lubnina N.V. Earst-European craton from Neoarhean to Paleozoic time on paleomagnetic data. // Abstract of doctoral dissertation. Moscow. 2009. 41 P.

Petrovskiy N.M., Mitrofanov F.P., Petrovskaya L.S., Bayanova T.B. New massif of Arhaean alkaline syenites in Murmansk domene in Kola Peninsula // Doclady RAS. 2009. T.424. N.1. P. 89-94.

Zozulya D.R., Bayanova T.B., Serov P.V. Age and isotope-geochemical characteristics of Arhaean carbonatites and alkaline rocks of the Baltic Shield // Doclady RAS. 2007. T.415. P. 383-388.

Effects of sodium on ferric/ferrous ratio in silicate melts: an experimental study

Borisov A.A.

Institute of Geology of Ore Deposits, Petrography, Mineralogy, and Geochemistry (IGEM),
Russian Academy of Sciences, Moscow, Russia.
aborisov@igem.ru.

Our understanding of the ferric/ferrous ratio in natural magmas is primary based on experimental work of Carmichael' s group (Sack et al., 1980; Kilinc et al., 1983, etc.) who suggested an empirical equation in the form:

$$\ln(Fe_2O_3/FeO) = a \cdot \ln(fO_2) + b/T + \Sigma d_i X_i + c \qquad (1),$$

where T in K, a, b and c = const, X_i are mole fractions of petrogenic oxides and d_i are empirical coefficients. However, as it was shown recently (Borisov et al., 2015), the effects of melt composition on ferric/ferrous ratio cannot be predicted accurately as a function of $\Sigma d_i X_i$ while silicate melts seem to be more complex than symmetric regular solutions. In the same time the strict application of the model of asymmetric regular solutions to predict the ferric/ferrous ratios in multicomponent systems is not realistic (36 interaction terms would be necessary to apply this approach for an 8-component melt). Instead, we propose to use the simple $\sum d_i X_i$ expression but with a few additional terms for some "critical" components. Such "critical" components need to be identified on the base of the experimental studies.

During last a few years we have experimentally studied the effects of main network-forming oxides (SiO_2, TiO_2, Al_2O_3, P_2O_5) on ferric/ferrous ratio. One network-modifier (MgO) was also studied (Borisov et al., 2013; 2015). Two components (Al_2O_3 and MgO) were found to be "critical". For example, the increase of MgO concentration in a basaltic melt results in a moderate increase of Fe^{3+}/Fe^{2+} ratio but has a negligible effects in more silicic melts. We demonstrated that two additional terms in eq. (1) are necessary, $d_{AlSi}X_{Al2O3}X_{SiO2}$ and $d_{MgSi}X_{MgO}X_{SiO2}$ (Borisov et al., 2015).

The aim of present investigation is to further experimentally study the effects of melt composition on ferric/ferrous ratio with more emphasize on strong network-modifiers, first of all, sodium.

The earlier investigations with sodium have been conducted in rather simple systems, e.g., Na_2O-FeO_t-SiO_2 (Lange and Carmichael, 1989). To the best our knowledge the only similar study in multicomponent melt is the paper of Thornber et al. (1980). These investigators modified an initial diabase composition by increasing Na_2O up to 8.5 wt %. They found an increase of Fe^{3+}/Fe^{2+} value with Na increasing. However, the scatter of experimental points is very big and the experiments with only one basic melt composition do not allow clarifying if Na_2O is "critical" components or not.

We have studied Fe^{3+}/Fe^{2+} ratio in DA+Fe_2O_3±SiO_2±Al_2O_3 melts (DA = Di-An eutectic compositions) modified with different amount of Na_2O. The experiments were done at 1500°C in a one atmosphere vertical tube furnace with the loop technique. We have analyzed the ferric/ferrous ratios in experimental glasses by wet-chemical method (Wilson, 1960) in modification of Schuessler et al. (2008).

We worked at air condition where the loss of alkalis from silicate melts at 1 atm total pressure is not as dramatic as at more reducing conditions (e.g., Borisov et al., 2006). Nevertheless, working with a loop

technique, one must expect some alkali exchange between high- and low-alkali melt samples occurring side by side in a single run (Borisov, 2008). However, we hoped that ferric/ferrous reequilibration in the samples is faster than Na lost or Na gain. Fig. 1 supports this idea.

It was found that the increase of sodium content in all compositions results in an essential increase of ferric/ferrous ratio (Fig. 2). The slopes of $\log(Fe^{3+}/Fe^{2+})$ vs. X_{Na2O} in silicic and more basic melts (including alumina-rich ones) are slightly different (2.6±0.2, 2σ and 3.4±0.3, 2σ, correspondently). However, this difference is not very large and we expect that $d_{Na2O} \cdot X_{Na2O}$ term in type (1) equation may be sufficient to describe the effects of sodium on ferric/ferrous ratio.
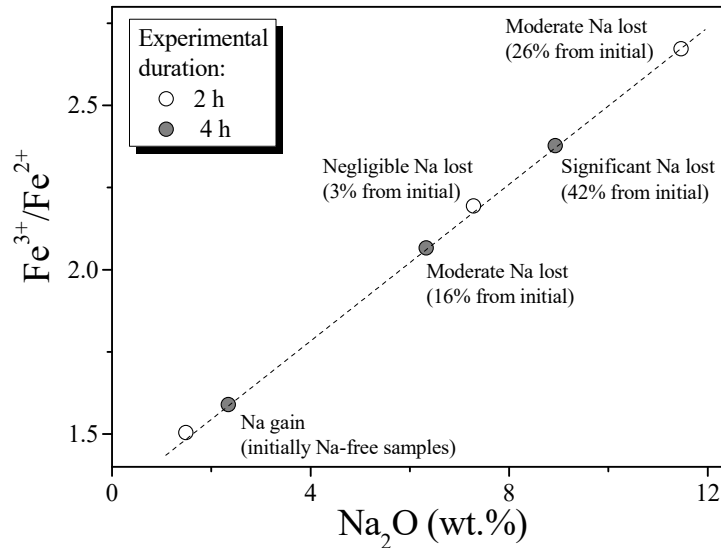
Fig. 1. Ferric/ferrous equilibrium in air at 1500°C in silicic melts (DAFS+Na series) suffering Na lost/Na gain.
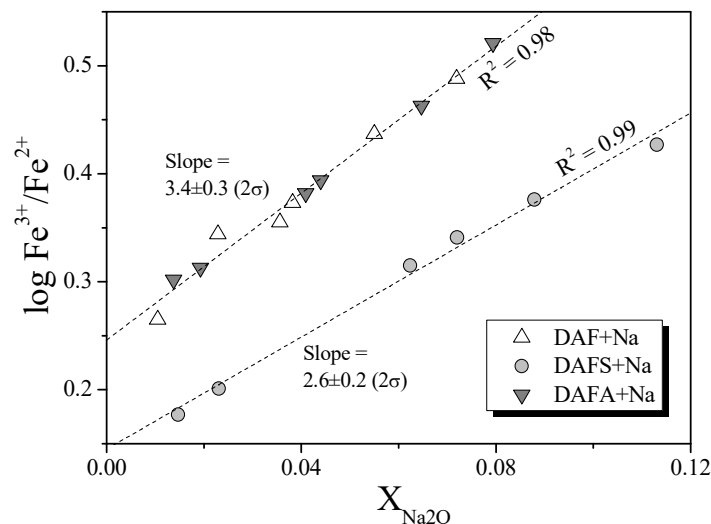
Fig. 2. Effects of sodium on ferric/ferrous ratio in silicate melts at air conditions and 1500°C.
DAF+Na - haplobasalts, DAFS+Na - silica enriched melts, DAFA+Na - alumina enriched melts.

References:

Borisov A., Behrens H. and Holtz F. (2013) The effect of titanium and phosphorus on ferric/ferrous ratio in silicate melts: an experimental study. Contribution to Mineralogy and Petrology, V. 166, 1577-1591.

Borisov A., Behrens H. and Holtz F. (2015) Effects of melt composition on $Fe^{3+}/Fe^{2}+$ in silicate melts: a step to model ferric/ferrous ratio in multicomponent systems. Contributions to Mineralogy and Petrology, V. 169, Article 24.

Borisov A., Lahaye Y. and Palme H. (2006) The effect of sodium on the solubilities of metals in silicate melts. American Mineralogist V. 91, 762-771.

Borisov A.A. (2008) Experimental Investigation of K and Na Partitioning between Miscible Liquids. Petrology, V. 16, 552-564.

Kilinc A., Carmichael I.S.E., Rivers M. and Sack R.O. (1983) The ferric-ferrous ratio of natural silicate liquids in air. Contribution to Mineralogy and Petrology, V. 83, 136-140.

Lange R.A. and Carmichael I.S.E. (1989) Ferric/ferrous equilibria in Na_2O-FeO-Fe_2O_3-SiO_2 melts: Effects of analytical techniques on derived partial molar volumes. Geochimica et Cosmochimica Acta, V. 53, 2195-2204.

Sack R.O., Carmichael I,S.E., Rivers M.L. and Ghiorso M.S. (1980) Ferric-ferrous equilibria in natural silicate liquids at 1 bar. Contributions to Mineralogy and Petrology, V. 75, 369-376.

Schuessler J.A., Botcharnikov R.E., Behrens H., Misiti V., and Freda C. (2008) Oxidation state of iron in hydrous phono-tephritic melts. American Mineralogist, V. 93, 1493-1504.

Thornber C.R., Roeder P.L. and Foster J.R. (1980) The effect of composition on the ferric-ferrous ratio in basaltic liquids at atmospheric pressure. Geochimica et Cosmochimica Acta, V. 44, 525-532.

Wilson A.D. (1960) The micro-determination of ferrous iron in silicate minerals by a volumetric and a colorimetric method. Analyst, V. 85, 823-827.

About metasomatic nature Khibiny apatite-nepheline deposits

Borutzky B.Ye.
Mineralogical Museum of A.Ye. Fersman, Russian Academy of Sciences, Moscow, Russia.
borborutzky2012@yandex.ru

Famous apatite deposits in the Khibiny massif on the Kola Peninsula is unique for its unusual mineral composition (apatite + nepheline), the quality of ore containing phosphorus, strontium, rare earth elements, fluorine, aluminum, rare alkaline elements, niobium, etc., and huge reserves. Apatite-nepheline rocks as industrial deposits not yet found anywhere in the world, especially on such a scale. What is so unique in its composition and ore reserves are set in the alkaline massifs composed agpaitic nepheline syenites, which had never been associated elevated concentrations of phosphorus, indicates the non-triviality and the uniqueness and the conditions of their formation.

The theses of this report it is impossible to carry out a detailed analysis of all khibiny problems using the vast amount of literature the Khibiny, and the specific details and references, we refer to some our publications (Borutzky, 1988, 2004, 2010, 2012), based on a comparison data of geological and petrological with data of mineralogical and geochemical researches.

Detailed geological and petrological analysis of the Khibiny massif became possible since the initial "hand-written" (1930) map by B.M. Kupletskiy, V.I. Vlodavets and O.A. Vorob'eva was refined after geological mapping that took place in 1931-1936s by a team of scientists from Academy of Sciences, "Apatite" trust, Leningrad geological trust, Scientific-research institute of fertilizers, Sevzapsoyuzredmetrazvedka, TSNIGRI institute, "Arctica" institute etc (A.S. Amelandov, E.V. Volodin, N.A. Volotovskaya, O.A.Vorob'eva, E.I. Denisov, E.N. Egorova, N.P. Lupanova, P.M. Murzaev, V.I. Namoyushchko, V.N. Numerov, I.S. Ozhinskiy, K.K. Sudislavlev et al) at scale of 1:25000 and later was reduced N.A. Eliseev, I.S. Ozhinskiy and E.N. Volodin (1939) to the sketch 1:75000 map. As conceptual model of formation of the Khibiny massif N.A. Eliseev applied the concept of the "intrusions of central type" by English geologist E.M. Anderson and method of structure analysis of plutonic bodies by G. Kloos – A.A. Polkanov. According to this dynamic model, the Khibiny pluton was formed as a result of magmatic intrusion of alkaline magma along the system of alternate circular and conic faults sequentially from the periphery towards its central core (from west to east) as a series of the nepheline syenite intrusions. According to this model melteigite-urtites were trapped in the time between plug nepheline syenites, what is not usual. Conception N.A. Eliseev is the "official" for more than 70 years.

The ideas by N.A. Eliseev were fully shared by S.I. Zak, N.M. Abramov, V.N. Bolysheva, M.M. Kalinkin, Ye.A. Kamenev, F.V. Minakov and other employees of Sevzapgeolupravleniye, that conducted new geological mapping of the massif in 1957-1960s at a scale 1:50000 and in 1959-1963s – mapping of the productive ijolite-urtite intrusion at scale 1:10000 with detailed prospecting for apatite by F.V. Minakov, A.I. Alexandrov, Ye.A. Kamenev, A.I. Konovalova, I.I. Perekrest et al. (Zak et al., 1972). In this intrusion ijolite-urtites was divided into 3 subphase: early and late - presented finely/medium trachytoid (gneissic) melteigite-

ijolites, and the average - folded coarse-grained massive urtites, feldspar urtites and juvitts, which observed the spatial (and possibly genetic) relationship with apatite-nepheline deposits.

Return to the question on genesis the Khibiny apatite-nepheline deposits. Using advances in the enrichment technology apatite from nepheline, A.Ye. Fersman wrote in 1931: "Flotation repeats the geochemical process, which took place in the nature. It raises the concentrate upward, i.e, apatite and partly sphene, immerses nepheline to the bottom, and further flotation of the nepheline tails results in purified nepheline concentrate, which sinks to bottom as a sediment, which corresponds to the best and most pure sort of urtite rock." (Fersman, 1959, p. 758). This is the reason, the massive coarse-grained urtites, underlying apatite deposits, are that significant for genesis and prospecting.

After "conditioned" geological mapping the massif a number of different hypotheses of magmatic, metamorphic and metasomatic origin of apatite were proposed. The most detailed apatite problem dealt T.N. Ivanova. She suggested the idea of a Second Khibiny sub-vulkane (Ivanova, 1963) and divided melteigite-urtites into 5 sub-phase (three pre-ore - trachytoidal and massive fine-grained and massive medium-grained together with apatite-nepheline rocks, ristshorrites and lujavrites in the Western sub-vulkane and two post-ore – rest of trachytoidal ijolites, massive medium-grained feldspar urtites and juvites in the Eastern sub-vulkane). In her opinion, formation of apatite-nepheline rocks referred to independent intrusion of agile "apatite" magma which penetrated into thin cracks, rich in volatiles, highly mobile, able to recrystallize surrounding rocks and genetically unrelated to ijolite-urtite. That is, she subscribe to opinion F.U. Levinson-Lessing, A.N. Labuntsov, B.M. Kupletskiy, M.P. Fiehweg, V.I. Vlodavets, L.B. Antonov and B.M. Melent'ev on the existence of *apatite magma*, in contrast to opinions N.N. Gutkova linking apatite formation with the residual pegmatite melt, A.S. Amelandov on pneumatolytic-hydrothermal genesis of apatite (Ivanova, 1969). She did not agree with the metasomatic hypothesis origin of apatite ores by S.M. Kurbatov and L.L. Solodovnikova from hydrothermal solutions, although observed substitution of original aegirine-diopside by apatite in lenses of fine-grained ijolite and partly by nepheline during they collective recrystallization, but at the same time, recognize the metasomatic genesis of apatite deposits Poachvumchorr, assuming in this case replacement of nepheline and feldspar by apatite in ristchorrites.

Modern views on the geology of the Khibiny massif were changed. The interpretation of trachytoidal and banding structures, by N.A. Eliseev as a result of a melt intrusion alongside circular faults, became doubtful. Thus, G.M. Virovlyanskiy demonstrated that it is directed not from below upwards but from above downward, and that the rocks of the Khibiny pluton sunk into subsidence caldera for 1.5–2 km alongside a number of cylindrical faults, and between blocks were clamped of various ancient roof rocks as xenoliths. Such xenoliths between massive and trachytoidal khibinites were diagnosed as paleovulcanic (rhomben-porphyres and other) in the "Western Arc" of the Khibiny massif and were also found within lyavochorrites (Borutsky, 1988). Numerous xenoliths of alkaline-ultrabasic rocks, were earlier described by A.V. Galakhov. Paleovulcanites were described by A.I. Serebritsky in foyaites of central part of the massif and were found by V.P. Pavlov, I.I. Perekrest, V.V. Smirnov and others within nepheline syenites during structural deep drilling. In the Khibiny were also discovered the tubes explosion and carbonatites.

The new principal data were obtained on the nature, composition and structure of the Khibiny melteigite-urtites of the "Central arch" massif. Their stratification was determined even earlier by N.A. Eliseev (1939), but this fact was not taken into account. According to the detailed mineralogical-petrological investigations by E.A. Kamenev, F.V. Minakov, V.N. Titov, I.I. Perekrest, A.D. Kozlowskiy, S.M. Kravchenko, V.I. Nozdrya, T.N. Ivanova, A.A. Arzamastsev, A.N. Korobeynikov, and others the rocks from melteigite-urtite series can be divided into two complexes by the chemical composition of the rock-forming minerals and structural-textural features. They are: early, differentiated fine/medium-grained trachytoidal melteigite-urtites and late coarse-grained massive urtites, and the latter may be united into one complex with feldspar-urtites, juvites and ristschorrites, similar by chemical composition, structure and typomorphic features of the minerals contained. The rocks of the first complex is close to the common alkaline-ultrabasic rocks, enriched by sodium and iron (with high agpaitic coefficients), and according by S.M. Kravchenko, D.A. Mineev, A.Ye.Belyakov, L.N. Kogarko and others took plase after intrusion of alkaline-ultrabasic rocks into surrounding nepheline syenites "in situ", by crystallized or gravitatively-crystallized differentiation. The scientist were not confused by the fact, that stratification of the rocks strikes not horizontally, as usual does in stratified rocks, but drops towards the center of the massif under the angle of 15-30 to 40-50º and by the fact, that according to the drilling data, conducted by geologist from the Khibinogorsk party (V.P. Pavlov, I.I. Perekrest, V.V. Smirnov and others), stratified rocks this complex disappear with the depth, are underlied by khibinites, and cut abruptly by lyavochorrites. I.e. this stratum is not an intrusion, but was entrapped by nepheline syenites as a giant bow-shaped xenolith (or relict), similar by its geological position to xenoliths of paleovulcanites. The rocks of the second complex – are specific feldsparbearing coarse-grained with unusual poikilitic structure, enriched with potassium and silicon. The authors consider them as a consequently intruded rocks, which were formed within an independent magmatic chamber during the directed crystallized differentiation trend: coarse-grained urtites → feldspar urtites → juvites → ristschorrites.

22

Nevertheless according the investigations by S.M. Kurbatov (1948), L.L. Solodovnikova, S.A. Rudenko, V.N. Titov, G.M. Kuznetsov and athor of this report, it is more likely that giant-grained rocks of the ristchorrite complex are metasomatic rocks arising by effect of alkaline fluid solutions, split from nepheline-syenite magma (i.e. fenitization) as a result of recrystallization and subsequent K-feldspathization ijolite-urtites with the scheme: coarse-grained urtite → juvite → ristchorrite (Borutzky, 1988).

In accordance with the considered views of the nature of the rocks the"Central arc" we believe that the Khibiny apatite formed as a result of substitution aegirine-diopside inlenses of fine-grained ijolites as earlier intended S.M. Kurbatov (1948), during fenitization the relic melteigte-urtites when exposed to fluids, split off from the nepheline syenite magma (Zotov, 1989; Borutzky, Zotov, 2010), followed by recrystallization under the influence of alkaline solutions with enrichment for Sr and La relatively Ce. It is assumed that phosphorus brings a potassium (and optionally sodium) fluoride-phosphate complexes.

References:

Borutzky B. Ye. Rock-forming minerals of high-alkaline complexes. M: Nauka. 1988. 212 p. (in Rus.)

Borutzky B. Ye. Mineralogical mapping of melteigite-urtites in the Khibiny plutonic-volcanic complex // Mineralogy its wide meaning. I Fersman scientific session of the Kola branch of RMO, dedicated to the 120th anniversary of the birth of A.Ye. Fersman and A.N. Labuntsov. Apatity. 22-23 April 2004. Apatity: Geol. Inst. Kola SciCentre RAS. 2004, pp 17-23. (in Rus.)

Borutzky B.Ye. Modern ideas on the nature and geological history of the Khibiny alkaline massif formation. (Critical correlation of the hypotheses suggested, with comments to them) // Unique geological objects of the Kola Peninsula: Khibiny. 80th anniversary of the Kola SciCenter RAS Academy scientific-practical conference materials. Apatity. 2010. P. 7-30. (in Rus.)

Borutzky B.Ye. The sketches on the fundamental and genetic mineralogy: 6. Experience on employment of the detailed mineralogical researches for solution the petrogenetic and ore deposition problems on example of the Khibiny massif // New Data on Minerals. 2012. Vol. 47. C. 128-157. (in English)

Borutzky B.Ye., Zotov I.A. Fundamentally new geological and petrological model of the Khibiny apatite deposits and its value to search apatite concentrations // Unique geological objects of the Kola Peninsula: Khibiny. 80th anniversary of the Kola SciCenter RAS Academy scientific-practical conference materials. Apatity. 2010. P.31-34. (in Rus.)

Eliseev N., Ozhinsky I.S, Volodin E.N. Geological-petrographic essay on the Khibiny tundras. Geological map of the Khibiny // Proceedings of the Leningrad Geol. Dept. 1939. Vol. 19. C. 1-68. (in Rus.)

Zak S.I., Kamenev Ye.A., Minakov F.V. et al. The Khibiny alkaline massif. L .: Nedra. 1972. 170 p. (n Rus.)

Zotov I.A. Transmagmatic fluids in magmatism and ore formation. M.: Nauka. 1989. 215 p. (in Rus.)

Ivanova T.N. Apatite deposits of the Khibiny tundras. M.: Gosgeoltekhizdat. 1963. 282 p. (in Rus.)

Ivanova T.N. Apatite-bearing of the Kola Peninsula // Apatity. M.: Nauka. 1968. P. 59-85. (in Rus.)

Kurbatov S.M. On a genesis of apatite deposits on the mountain Kukisvumchorr in the Khibiny tundras // Report at the scientific session at the Kola base of the AN USSR in Kirovsk. August 1948. (in Rus.)

Fersman A. Ye. Geochemical arches of the Khibiny tundras // Dokl. AN USSR. A. 1931. № 14. P. 367-376. After: Selected works. T. 5. M.: AN USSR. 1959. P. 755-763. (in Rus.).

HREE-enrichment in late-stage apatite from carbonatites; comparison of apatite from the Songwe, Tundulu and Kangankunde carbonatites, Malawi

Broom-Fendley S.L., Wall F.*, Gunn A.G.**, Brady A.E.****

Camborne School of Mines, University of Exeter, United Kingdom, s.broom-fendley@ex.ac.uk
**British Geological Survey, Keyworth, Nottingham*
***Mkango Resources Ltd., Suite 1400, 700 - 2nd Street SW, Calgary, Alberta, Canada*

Rare-earth element (REE)-minerals currently extracted from carbonatites (such as the REE-fluorcarbonates and monazite-(Ce)) are typically rich in light (L)REE and poor in heavy (H)REE, where LREE denotes La—Sm and HREE denotes Eu—Lu + Y (Wall, 2014). The price of the LREE has been decreasing since the peak of 2011, and so carbonatites have become less attractive to exploration companies. Heavy REE prices have also dropped since 2011 but they are still worth two orders of magnitude more than the LREE. Thus, any mechanism to increase the percentage of extractable HREE from carbonatite deposits would greatly increase the value of the REE resource.

Fluorapatite ($Ca_5(PO_4)_3F$), which is ubiquitous in carbonatites, usually comprises 2–5 modal % of the rock and can be the main REE host. It is typically a liquidus phase, but can occur throughout carbonatite

emplacement, from early magmatic, through to late hydrothermal stages (Hogarth, 1989). It is a remarkably tolerant mineral to structural distortion and chemical substitution, being able to accept many different elements into its structure, including the REE. Concentrations of up to 5 wt. % REE in apatite have led to the suggestion that it may be a viable by-product or co-product of phosphate extraction, although the REE-distribution is often LREE-enriched (e.g. Mariano & Mariano, 2012).

Ngwenya (1994), Ting et al. (1994), Walter et al. (1995), Wall & Mariano (1996) and Broom-Fendley et al. (2013; 2015 *in prep*) have described late-stage apatite from the Tundulu, Sukulu, Juquiá, Kangankunde and Songwe carbonatites, respectively. In these examples apatite grains often have distinct turbid cores and clear rims, although a fine-grained, anhedral texture is more prominent in the apatite at Sukulu and Songwe. Distinct enrichment in SrO, REE and Na$_2$O is present in the late stage apatite relative to earlier-crystallised apatite, which often forms cores or euhedral/ovoid grains. Analyses of apatite from Tundulu and Juquiá also display evidence of HREE-enrichment in the late-stage apatite rims, while Wall & Mariano (1996) described crystallisation of xenotime-(Y) in association with the apatite rims at Kangankunde. However, evidence of HREE-enrichment in late-stage apatite has been limited to inferences from bulk-rock REE analyses and EPMA analyses of a few of the REE. The REE-distribution of late-stage apatite is not fully understood. In this study it is suggested that late-stage apatite in carbonatites can host the HREE, potentially up to economically significant concentrations. It is also proposed that the changing REE and trace-element contents of apatite, through the different paragenetic stages, can be used to infer REE behaviour during the last vestiges of carbonatite emplacement.

To test the proposed hypotheses, late-stage apatite from Tundulu and Kangankunde is re-examined, and new apatite data from the Songwe Hill carbonatite are presented. Optical microscopy, cold-cathodoluminescence (CL), BSE-imaging and EDS mapping are used to elucidate upon the complex paragenesis of the apatite at these localities. Spatially-resolved REE, major and trace element analyses from EPMA and LA-ICP-MS have been acquired from each site in order to better understand the evolution of REE, Sr, Na, U and Th from early to late-stage apatite.

Fluorapatite from Kangankunde and Tundulu are texturally similar, with turbid cores and clear overgrowths, confirming previous work (Styles, 1988; Ngwenya, 1994; Wall & Mariano, 1996). CL imagery of the Kangankunde cores and rims emphasises the textural difference, with cores displaying green—violet luminescence and rims showing muted brown/purple colours. CL imagery of the Tundulu apatite, however, reveals a much more complex crystallisation history, with luminescence colours varying from (cores to rims) bright-blue, green, maroon and mauve. These changing luminescence colours are attributed to changing proportions of the CL-activators: Ce^{3+} (violet); Dy^{3+}, Tb^{3+} and Mn^{2+} (yellow); and Sm^{3+} (red/orange). Additionally, at Tundulu, new petrographic observations indicate that the LREE-fluorcarbonates crystallised *after* the development of apatite rims. Apatite from Songwe does not display core/rim textures and can be broadly subdivided into two textures: early, ovoid grains and late fine-grained, anhedral stringers. Early apatite luminesces violet, while late-apatite is typically creamy/brilliant white. At Songwe the late-stage apatite crystallised prior to the crystallisation of the REE-fluorcarbonate synchysite-(Ce). Very late-stage apatite at Songwe is associated with xenotime overgrowths.

Major and trace element analyses and spatially resolved X-ray maps of Kangankunde and Tundulu confirm the results of the previous analyses, with the later-stage apatite crystallisation broadly displaying enrichment in SrO, REE and Na$_2$O. At Kangankunde, REE concentrations are greater in the rims than the cores, but both core and rim REE distributions are LREE-enriched, peaking at Sm. At Tundulu, however, REE distribution is considerably more complex. Several different distribution patterns are observable in the cores, with a LREE-rich distribution, a curved, convex-up, MREE-enriched distribution and a LREE-poor, HREE-rich distribution. In some cases the HREE concentration can reach 1 wt. %. The complexity of the REE-distribution in the cores contrasts with analyses from the rim, where most analyses are MREE-enriched with a steep decrease towards the HREE. However, maroon-luminescent rims from Tundulu are chemically different to all the previously described occurrences of late-stage apatite. These rims are enriched in Na, but do not show the Sr and REE enrichment observed at other localities. Indeed, none of the elements analysed were positively correlated with Na. Such high Na concentrations are unlikely without a charge-balancing coupled-substitution. Based on infrared spectrometry of a similar sample from Tundulu (Styles, 1988), the increased Na concentration in this apatite type is, therefore, interpreted to be due to a coupled-substitution with CO$_3$. While they have low REE concentrations, these rims display flat to HREE-enriched REE distribution patterns. A negative Y-anomaly is observable in the distribution of both cores and rims of the apatite from both localities. At Songwe, major and trace element analyses reveal a complex crystallisation history. Early, ovoid, apatite is LREE-enriched, as observed in liquidus apatite from many carbonatites. The late, anhedral, apatite at Songwe, however, is HREE-enriched, reaching up to 2.5 wt. % HREE. REE distributions are varied, ranging from flat; convex-up, MREE-enriched; through to prominently LREE-depleted and HREE-enriched. As observed in late-stage apatite from other carbonatites, the increase in REE concentration is associated with a concomitant increase in Na and Sr concentration. At Songwe, Tundulu and Kangankunde, increasing HREE concentration is associated with an

24

increase in U and Th. Interestingly, in comparison to late apatite from Kangankunde and Tundulu, none of the apatite from Songwe displays a Y-anomaly.

Comparison of these apatite analyses with published carbonatite-derived and granitoid-derived apatite shows that carbonatite-hosted apatite can reach higher degrees of HREE-concentration in the late-stages of carbonatite emplacement. Late-stage apatite from Kangankunde appears to have anomalously low HREE concentrations compared to late-stage apatite from Songwe and Tundulu. However, co-crystallisation of xenotime-(Y), as observed by Wall & Mariano (1996), is likely to preferentially partition the HREE into the xenotime structure and would explain the relatively low HREE concentration in apatite from this locality. The composition of the analysed apatite extends the known range of HREE content in carbonatitic apatite to levels hitherto occupied only by granitoids. This suggests that carbonatites are potential sources of the M/HREE, which are currently in great demand for new and green technologies. Indeed, mineral processing test work is currently underway to beneficiate apatite and synchysite-(Ce) from the Songwe Hill carbonatite (Brady et al. 2014).

The similarities of increasing HREE, Sr and Na concentration in late-stage apatite, and the tendency of this late-stage apatite to form prior to LREE-fluorcarbonates, in many different carbonatite complexes suggests that all of these intrusions are subject to similar processes. It is suggested that the apatite crystallised from a hydrothermal fluid and it can be inferred, based on associated mineralogy, that this fluid was rich in F, CO_2, P and SO_4, although a Cl-rich fluid cannot be ruled out. One possibility is that of a fenitising fluid; these are commonly inferred to be Na- and F-rich and cause large-scale hydrothermal alteration of country-rocks surrounding carbonatites. Comparison with apatite from fenite at Songwe, however, indicates that the late-stage fluids which led to apatite crystallisation are probably not related to fenitising fluids. Apatite derived from fenite is LREE-enriched, with a chondrite-normalised distribution sloping towards low HREE concentrations, and displays a prominent negative Eu-anomaly. Such a distribution has been described for fenite-derived apatite from other carbonatites and is interpreted to be a distinct fenite signature (Dowman, 2014). This contrasts to the HREE-enriched apatite observed in the Malawian carbonatites. Rather, the crystallisation of the late-stage apatite in these examples is interpreted to be caused by carbonatite-derived fluids expelled late in the crystallisation sequence. It is suggested that complexation by F, CO_2, P and/or SO_4 could be potential transport mechanisms for the REE.

References:

Brady, A.E., et al., The mineralogy of the Songwe Hill REE deposit, Malawi, and the implications for mineral processing. // Proceedings of the Canadian Institute of Mining, 2014.

Broom-Fendley, S., et al., Carbonatite-hosted late-stage apatite as a potential source of the heavy rare earth elements. // SGA Conference abstracts, 2013, 4, 1694

Dowman, E. Mineralisation and fluid processes in the alteration zone around the Chilwa Island and Kangankunde carbonatite complexes, Malawi. // Ph.D. thesis, Kingston University. 2014.

Hogarth, D. Pyrochlore, apatite and amphibole: distinctive minerals in carbonatite. // in: Bell, K. (Ed) Carbonatites: genesis and evolution. Unwin Hyman, London, 1989, 105.

Mariano, A. N. & Mariano, A. Rare earth mining and exploration in North America. // Elements, 2012, 8, 369

Ngwenya, B. Hydrothermal rare earth mineralization in carbonatites of the Tundulu complex, Malawi: Processes at the fluid/rock interface. // GCA, 1994, 58, 2061–2072.

Styles, M. A preliminary report on the mineralogy of the Tundulu and Songwe carbonatite complexes, Malawi. // Technical report, British Geological Survey Mineralogy and Petrology report: WG/88/6R, 1988

Ting, W., et al. Characterisation and petrogenetic significance of CO_2, H_2O and CH_4 fluid inclusions in apatite from the Sukulu Carbonatite, Uganda. // EJM, 1994, 6, 787.

Wall, F. & Mariano, A. Rare earth minerals in carbonatites: a discussion centred on the Kangankunde Carbonatite, Malawi. // in: Jones et al. (Eds) Rare Earth minerals, The Mineralogical Series, 7, 193.

Wall, F., Rare Earth Elements // in: Gunn, A.G. (Ed) Critical Metals Handbook, John Wiley & Sons, Oxford. 2014.

Walter, A.-V., et al. Behaviour of major and trace elements and fractionation of REE under tropical weathering of a typical apatite-rich carbonatite from Brazil. // EPSL, 1995, 136, 591.

Primordial and radiogenic noble gases in fluid inclusions in Seblyavr massive carbonatites and pyroxenites

Buikin A.I.*,**, Hopp J.**, Sorokhtina N.V.*, Trieloff M.**,***, Kogarko L.N.*
*Vernadsky Institute of Geochemistry and Analytical Chemistry RAS, Moscow, Russia
**Institut für Geowissenschaften, Universität Heidelberg, Heidelberg, Germany
***Klaus-Tschira-Labor für Kosmochemie, Universität Heidelberg, Heidelberg, Germany

The alkaline–ultramafic Seblyavr ring intrusion occurs in the NW part of the Kola Peninsula (68°42′ N, 32°05′ E). Covering an area of approximately 20 km^2, this Paleozoic massif is one of the largest of its type within the Kola Alkaline Provinces. The Seblyavr massif has a concentric-zone structure and consists of the following rocks (listed in order from older to younger): olivinites, clinopyroxenites, ijolite–melteigites, phoscorite and carbonatite series of rocks, numerous postmagmatic rocks and fenites formed after country Archean gneiss [Afanas'ev, 2011].

The majority of magmatic rock types show traces of intense hydrothermal alteration and thin veinlets with dolomite–strontianite–ancylite-(Ce)-sulfide mineralization ubiquitously developed in contact zones between the carbonatites and earlier magmatic host rocks. We conclude that fluid phases played an active role throughout the whole course of rock formation and subsequent alteration. To better understand the sources and evolution of fluid phases we performed noble gas isotope analyses extracting gases by stepwise crushing of three mineral separates: diopside from clinopyroxenite (Sbl97-47Px), calcite from a carbonatite vein cutting the clinopyroxenite (Sbl97-47Cal) and calcite from calcite-amphibole carbonatite (Sbl97-11Cal). The samples were collected from different drill sites, with depths of the samples ranging from 40 to 65 meters.

The ^{4}He concentrations vary less than an order of magnitude and are slightly higher in Sbl97-47Px (3.8×10^{-5} cc/g) compared to the calcites (9.8×10^{-6} cc/g and 5.6×10^{-6} cc/g) in Sbl97-47Cal and Sbl97-11Cal respectively. The variations of concentrations of primordial ^{3}He are much higher – up to 3 orders of magnitude (9.0×10^{-10} cc/g, 7.2×10^{-11} cc/g and 8.1×10^{-13} cc/g) for Sbl97-47Px, Sbl97-47Cal and Sbl97-11Cal respectively. This is reflected in ^{4}He/^{3}He ratios which vary from typical values of deep mantle plumes (around 20000-30000 [Trieloff et al. 2000, Marty et al. 1998]) to essentially radiogenic values typical for crustal materials. The higher the ^{3}He concentration (Fig. 1), the lower the ^{4}He/^{3}He ratios, which approach the Kola plume values [Tolstikhin et al. 2002, Marty et al. 1998].
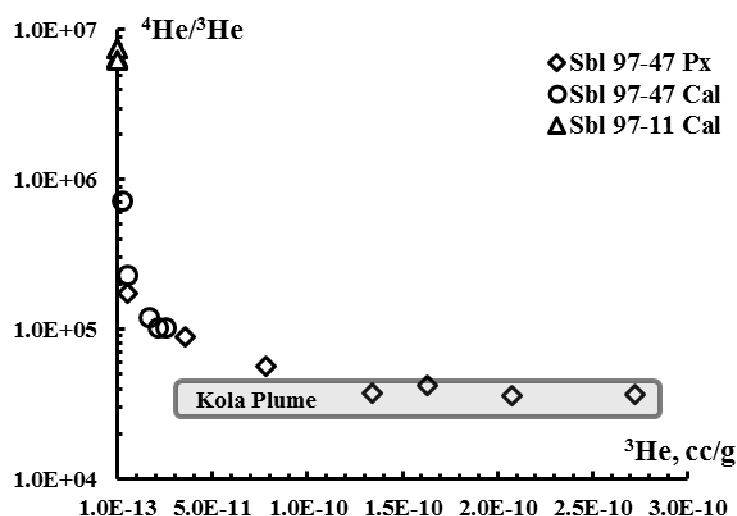
Fig. 1. Dependence of ^{4}He/^{3}He ratios on ^{3}He concentrations.

It is worth noting that ^{4}He/^{3}He ratios increase with progressive crushing which is most probably the result of addition of *in situ* radiogenic helium from *in situ* U+Th decay that is extracted with increasing number of strokes while

primordial helium is decreasing. The highest ^{4}He/^{3}He ratios are observed in Sbl97-11Cal, where the ^{3}He content is three orders of magnitude lower than in Sbl97-47Px. Interestingly, the ^{3}He concentration in calcite (Sbl97-47Cal) from the later calcite vein is ten times lower than in pyroxene from the same pyroxenite, which could point to He escape from the magmatic system.

Neon results are shown in Fig. 2. The data points of the very first crushing steps of 97-47 Px and Cal samples plot close to the Reunion mixing line [e.g. Hopp et al. 2005]. Further, with progressive crushing (as also for He) one can observe an increase of the nucleogenic component in the neon budget. Only for Sbl97-11Cal

(which is the least contaminated by atmospheric and nucleogenic components) we obtained a well correlated mixing line and evaluated the $^{21}Ne/^{22}Ne$ mantle end member (at $^{20}Ne/^{22}Ne$ = 12.5) as 0.0426±0.0019.

The argon isotopic composition is in good agreement with our previous data on these samples [Buikin et al. 2014]. Very high $^{40}Ar/^{36}Ar$ ratios in Sbl97-47Px (up to 30000) well correlate with high $^{4}He/^{3}He$ ratios (Fig. 3), and thus cannot be explained by a MORB-type mantle component. Most probably, they are the result of redistribution of *in situ* radiogenic argon from phlogopite grains which are abundant in the host pyroxene. Due to the dominating neon and argon mantle component in Sbl97-11Cal we could evaluate the mantle end-member $^{40}Ar/^{36}Ar$ ratio of the Kola plume. Extrapolation of the regression line (Fig. 4) to mantle Ne ($^{20}Ne/^{22}Ne$ = 12.5) yields $^{40}Ar/^{36}Ar$ = 4579±342 (1 σ), which is consistent with the value of 5000±1000 reported by Marty et al. (1998) but more precise.

Thus, on the base of new high precision and well correlated neon and argon isotope data we obtained a better evaluation of the $^{40}Ar/^{36}Ar$ ratio of the Kola mantle plume source (4579±342). The correlation of radiogenic argon and helium (and nucleogenic neon) in crushing steps of Sbl97-47Px allowed us to exclude the presence of a MORB-type mantle component in Seblyavr pyroxenites. The most plausible source of radiogenic helium and argon and nucleogenic neon in progressive crushing steps of Sbl97-47Px are redistributed *in situ* radiogenic/nucleogenic gases, but we still can't exclude the presence of abundant very small fluid inclusions carrying crustal noble gas components (i.e. extracted by circulating waters from wall Archean gneisses).
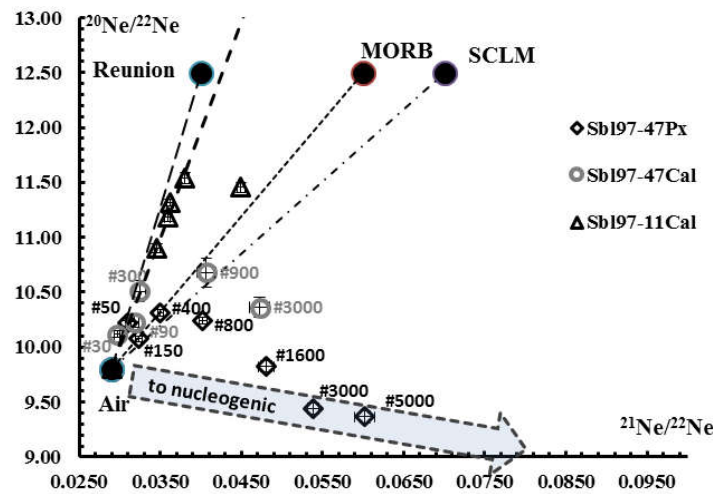
Fig. 2. Neon three isotope diagram. Mixing lines for Reunion plume, MORB and SCLM as well as cumulative number of strokes and trend of crustal (nucleogenic) neon component are indicated.
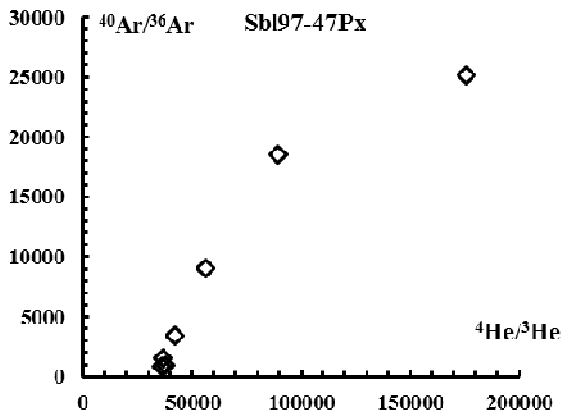
Fig. 3. Correlation of radiogenic to non-radiogenic isotope ratios of helium and argon indicates crustal or in situ radiogenic nature of high $^{40}Ar/^{36}Ar$ ratios in late crushing steps of Sbl97-47Px.
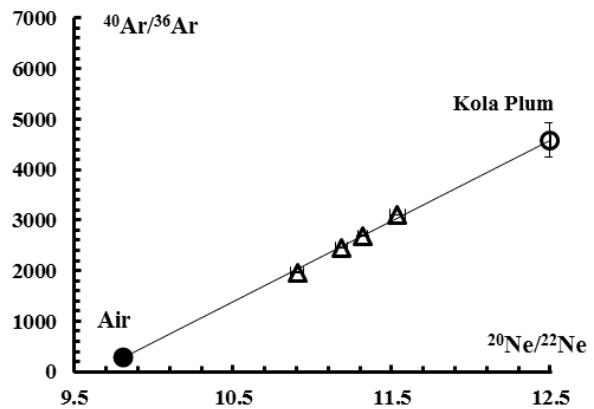
Fig. 4. Argon-neon isotope systematic of Sbl97-11Cal. The data reflects mixing between atmospheric and mantle components of neon and argon.

References:

Afanasyev B.V., Mineral Resources of Alkali–ultramafic Complexes of the Kola Peninsula // Roza Vetrov Press, St. Petersburg 2011. (224 pp., in Russian).

Trieloff M., Kunz J., Clague D.A., Harrison D., Allègre C.J. The nature of pristine noble gases in mantle plumes, 2000. Science 288, 1036-1038.

Marty B., Tolstikhin I.N., Kamensky I.L, Nivin V., Balaganskaya E., Zimmermann J.L.,1998. Plume-derived rare gases in 380 Ma carbonatites from the Kola region (Russia) and the argon isotopic composition in the deep mantle. Earth Plan. Sci. Lett. 164, 179-192.

Tolstikhin I. N., Kamensky I. L., Marty B., Nivin V. A., Vetrin V. R., Balaganskaya E. G., Ikorsky S., Gannibal M., Weiss D., Verhulst A., and Demaiffe D. Rare gas isotopes and parent trace elements in ultrabasic-alkaline-carbonatite complexes, Kola Peninsula: Identification of lower mantle plume component. Geochim. Cosmochim. Acta. 2002. **66**(5), 881-901.

Hopp J., Trieloff M., Refining the noble gas record of the Réunion mantle plume: Implications on mantle geochemistry, 2005. Earth Plan. Sci. Lett. 240, 573-588.

Buikin A.I., A.B. Verchovsky, N.V. Sorokhtina, L.N. Kogarko. Composition and Sources of Volatiles and Noble Gases in Fluid Inclusions in Pyroxenites and Carbonatites of the Seblyavr Massif, Kola Peninsula // Petrology, 2014, Vol. 22, No. 5, pp. 507–520. DOI: 10.1134/S0869591114050038.

Towards the issue about the source of carbonic matter in paleozoic ultrabasic dykes within Spitsbergen Archipelago

Burnaeva M.Yu.
FGUP VNIIOkeangeologia named after I.S. Gramberg, St. Petersburg, Russia

Today we know over 30 ultrabasic dykes within West Spitsbergen Archipelago (east and south of Andre Earth – western coast of Vejde-Fiord nearby Krosspynten and Petermann capes, Purpurdallen Valley, northern coast of Ekmanfiord, and nearby Rubinbreen Glacier – Haakon Earth VII) which occur as both singular bodies and accumulations. These dykes lie across low-Devonian terrigenic rocks of Wood Bay and Grey Hook suites. All the dykes are of submeridional and meridional strikes, subvertical and vertical gradients. Thickness and visible length are 0.3 to 1.5 m and up to 1.5 km, respectively. Macroscopically, the dykes are composed by picrite-like fine-grained dense massive and almond-shaped carbonized rocks dark-grey to black in color. Bodies with coarse impregnations of clinopyroxene and mica and bodies with inclusions of deep xenolithes take place. Recorded among the dykes are both differentiated and poorly differentiated bodies. Prominent among the differentiated dykes are decolorized fine-grained selvages (up to 5-7 cm in size) and coarse-grained central part deeper in color. No visible differentiation is observed in the other dykes, but phlogopite megacristae up to 5 cm large are present (1). The bodies intruded in post-orogenic epi-Caledonian development stage of the archipelago are structurally related to a subzone of major strike-slip oblique faults of submeridional strike within the Vejde- and Aust-fiords fault zone. The low-Devonian terrigenic rocks of Wood Bay and Grey Hook suits serve an enclosing strata.

The rocks show ultrabasic composition and are described in more detail in (1). Prominent among the dykes are both bodies with preserved primary structure and composition and those all-carbonized. Isotope studies have been carried out in order to define a source of dyke carbonization.

The isotope analysis was carried out at VSEGEI Isotope Research Center by IRM-MS methods with the use of DELTA plus XL mass-spectrometer (ThermoFinnigan, Germany, Bremen) supplied by Gasbench preparative add-on device. All the values of $^{13}C/^{12}C$ and $^{18}O/^{16}O$ isotope ratios are presented as their bias ($\delta^{13}C$ and $\delta^{18}O$) relative to the standard (PDB or VSMOW). Inaccuracy of measurements (1σ) was within 0.1-0.2‰ for carbon and 0.1-0.3‰ for oxygen.

The isotope analysis for $\delta^{13}C$ and $\delta^{18}O$ was carried out for core samples from 7 dykes. One of the dykes is composed by ankaramite, one by basalt and five by picrite-like rock. Two of the latter five dykes are saturated by almond-shaped bodies and contain coarse enough (occasionally up to 5 cm large) biotite, and the other three contain inclusions of deep xenolyths. Carbonate of hydrothermal veins and fine-grained rock-saturating carbonate were analyzed for two of the dykes. The values obtained mainly vary between: -2.7 and -3.9 for $\delta^{13}C$, 15.1 and 20.0 for $\delta^{18}O$ (table 1, fig.1). Fallen out of the total isotope values are ankaramite dyke (2464-1) characterized by carbon (-6.8) and oxygen (13.8) light-weight relative to the other dykes and also carbonate from a carbonate vein of basalt dyke 1455 wherein the content of $\delta^{13}C$ was recorded as maximum among the other values obtained.

28

Table 1. Isotope composition of oxygen and carbon in dykes.

N	N sample	$\delta^{13}C$, $^o/_{oo, PDB}$	$\delta^{18}O$, $^o/_{oo, VSMOW}$
1	222-7	-3.6	16.2
2	222-7*	-2.7	15.1
3	41-04	-2.9	18.0
4	7-1	-3.3	17.3
5	2464-1	-6.8	13.8
6	2743-1	-3.3	18.7
7	1455*	-1.8	19.0
8	1455	-3.9	20.0
9	2686	-3.8	17.0

*- carbonate from veins.
1455 - basalt, 2464 – ankaramite, the rest dykes are
composed by picrite-like rock.

Analyzed for two core samples (222-7 and 1455) were both fine-grained carbonate saturating the groundmass and coarser carbonate from veins. The hydrothermal carbonate contains relatively heavier carbon and somewhat light-weight oxygen.

Deep-seated rocks and ordinary chondrites mainly show values of $\delta^{18}O$ to vary within 5 to 6. Isotope composition of oxygen in carbonatites mainly varies between 6 and 9 for $\delta^{18}O$ (2). These values are the benchmark for interpreting isotope variations while geological processes. The main values of $\delta^{13}C$ for carbonatite carbon vary within -8 to -6 and coincide with isotope composition of diamond carbon (3). For carbonic product these values represent the criterion of a pattern of the mantle (fig.1). Among the core samples studied, none of the values falls within the mantle interval for oxygen. For carbon, isotope composition of this element is shown only by the ankaramite dyke. Based on the above, we may suggest crustal nature of the carbonate product and significant assimilation by carbonate dykes from enclosing and superposing rocks of sedimentary genesis. The values obtained also tend to vary that suggests different degree of assimilation. In the diagram, the values for the carbonate from veins are above isotope parameters obtained for the carbonate from groundmass of the same dyke that may also be the evidence for its primary sedimentary genesis (insert, fig.1). Enrichment of the dykes in crustal products is also evidenced by $^{87}Sr/^{86}Sr = 0.710$ obtained before for samples 222-7 and 41 (1).
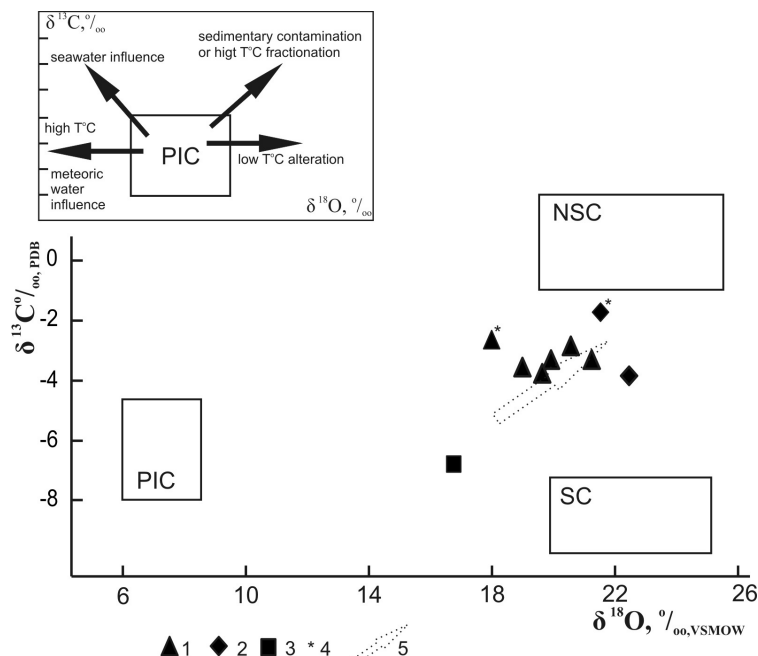
Fig.1. Points of isotope composition of carbon and oxygen from Paleozoic ultramafic dykes of Spitsbergen Archipelago in $\delta^{18}O$ - $\delta^{13}C$ diagram.
1 – picrite-like rocks, 2 – basalt, 3 – ankaramite, 4 – carbonate from vein, 5 – variations in $\delta^{18}O$ - $\delta^{13}C$ values for picrite-like dykes.

The diagram shows the fields of compositions: PIC ("primary igneous carbonatites") – primary magmatogenic carbonatites (6); NSC ("normal sedimentary carbonates") – marine normal sedimentary carbonates, SC ("soil carbonates") soil carbonates (5); variations in composition relative to increasing role of crustal products, and the insert showing the influence of different processes to variations in isotope composition of primary carbonatite product (4, 7).

References:
1. Burnaeva M.Yu. Mineralogical and Petrochemical Features of Paleozoic Picrite within Spitsbergen Archipelago // Regionalnaya Geologia i Metallogenia. 2011. № 48. Pp. 37-49.
2. Kuleshov V.N.. Isotope Composition and Genesis of Deep-Seated Carbonate. M.: Nauka. 1986. 128 p.
3. O'Neil J.R. Stable Isotope Geochemistry of Rocks and Minerals // Lectures in Isotope Geology. Ed. E Jager and J.C. Hunziker, M. Nedra. 1984. Pp. 250-279.
4. Demény A., Ahijado A., Casillas R., Vennemann T.W. Crustal contamination and fluid/rock interaction in the carbonatites of Fuerteventura (Canary Islands, Spain): a C, O, H isotope study.// Lithos. 1998. V. 44. Pp. 101-115
5. Salomons W. Chemical and isotopic composition of carbonates in recent sediments and soils from Western Europe. //J. Sediment Petrol. 1975. 45. Pp 440-449.
6. Taylor, H. P., Frechen, J. and Degens, E. T. () Oxygen and carbon isotope studies of carbonatites from the Laacher See District, West Germany and the Alnö District, Sweden //Geochim. Cosmochim. Acta. 1967. V. 31. Pp 407-430
7. Vrublevskii V.V., Gertner I.F. Origin of carbonatite-bearing complexes from fold systems: isotopic evidence for the mantle-crust interaction// Problems of sources of deep magmatism and plumes. Proceedings of V International Geochemistry Workshop, 15-23 August, 2005. Petropavlovsk-Kamchatsky.

Geochemistry of the basanite dyke Swarms, South Anatolia (Kahramanmaraş/Turkey)

Cansu Z., Öztürk H.
İstanbul University Department of Geology, İstanbul, Turkey.
zeynep.oru@istanbul.edu.tr

The Şekeroba (Türkoğlu-Kahramanmaraş) barite deposit which is one of the biggest and purest (high quality) barite deposit in Turkey is accompanied by alkaline dyke /sill swarms. These alkaline dyke/sill swarms, which only seen on underground mining gallery do not outcrop on the surface, have 0,5-1,20 m thickness and 5-10 m length. They are also so fresh, dense, black coloured rocks and mainly consist of feldspar, feldspatoid (some sections include more losite) , titanaugite, olivine, alkali amphiboles, titanian magnetite, apatite and secondary calcite and barite in amygdaloidal cavities. The age of these rocks determined as Miocene (13.2 ± 0.5 and 15.8 ± 1.0 Ma $\pm 2\sigma$.) by K-Ar Method (Öztürk et al. 2014).

Geochemical analysis of 10 samples from 5 location were analysed by ICP-MS. Mean major oxide values of the ten basanite samples are determined as follows(%); SiO_2:42,12 Al_2O_3: 13,39, Fe_2O_3:12,86, MgO: 8,31 CaO: 8,29, Na_2O:2,78, K_2O: 1,6, TiO_2: 2,55, MnO: 0,15, P_2O_5: 0,76. These values locate tephrite/basanite, trachy basalt and basalt field on silica versus total alkali diagram (TAS) (Fig.1).
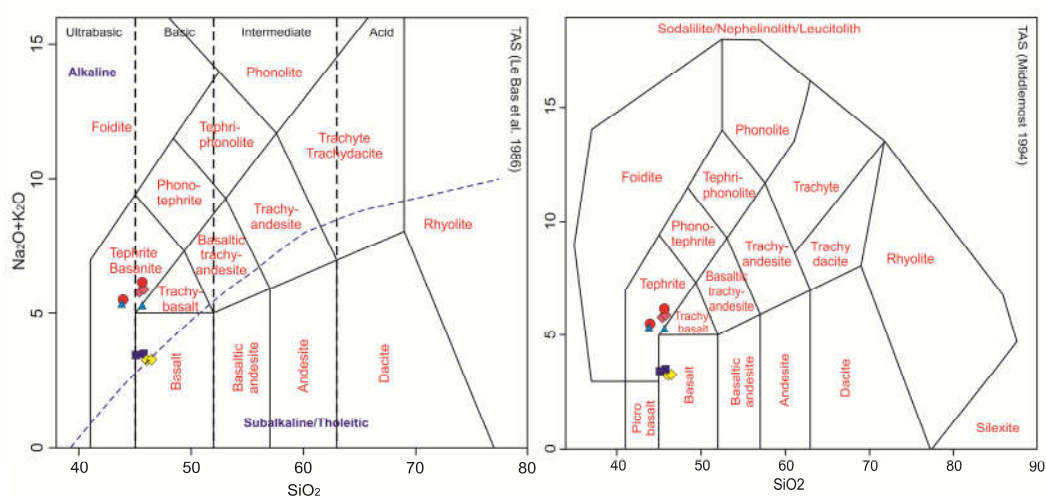
Fig 1. Şekeroba alkaline porphiritic rocks ploted on total alkali versus silica classification diagrams.

Basanite dyke/sill swarms unexpectedly haven't so rich for REE composition. They show so lineer patern with a depletion from L-REE to H-REE on the chondrite normalised REE diagrams(Fig.2). There is no any of rare earth element anomaly. Mean value of the total REEs of the basanite is 176,45 ppm.
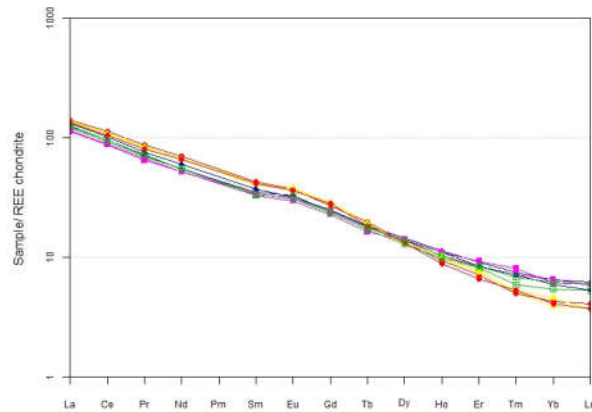
Fig 2. Chondrite-normalised REE patern of basanites (normalization values of Boynton, 1984).

The trace element composition of the basanite samples are also interpreted and ploted on THE tectonic discrimination diagrams. They are mainly fall in within plate alkaline rocks' area in Th-Hf/3-Nb/16 , Th-Zr/117-Nb/16, Th-Hf/3-Ta ternary diagrams(Fig.3) (Wood 1980).
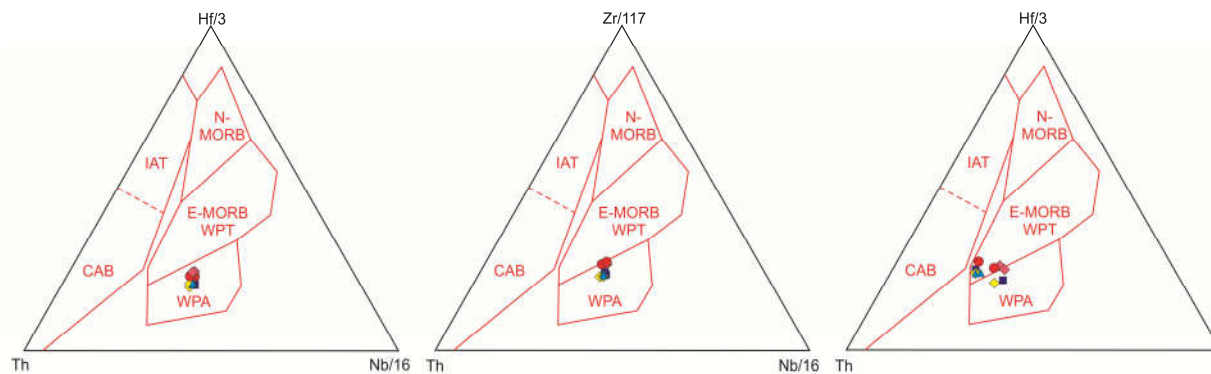
Fig 3. Th–Hf–Ta tectonomagmatic classification diagrams (Wood,1980) and plots of Şekeroba basanites.

This Miocene aged   basanites should have been intruded into the Ordovician aged clastic rocks, possibly by mantle plumes under the local tensional conditions.

References:

Boynton, W. V.. Geochemistry of rare earth elements: meteorite studies. In: Henderson P. ed. Rare Earth Element Geochemistry, Elsevier, Amsterdam.1984. pp.63-114.

Le Bas, M. J., Le Maitre, R. W., Streckeisen, A. & Zanettin, B. A chemical classification of volcanic rocks based on the total alkali–silica diagram. Journal of Petrology. Le Bas, M. J., Le Maitre, R. W., Streckeisen, A. & Zanettin, B. 1986. A chemical classification of volcanic rocks based on the total alkali–silica diagram. Journal of Petrology.vol. 27, 745–750.

 Middlemost, E. A. K.. Naming materials in the magma/ igneous system. 1994. Earth-Science Reviews. vol.37. pp.215–224.

Öztürk, H., Cansu Z., Nikiforov A.E., Zhukovsky V.M.. K-Ar And Sem Results Of The Alkaline Porphyritic Stocks In The Şekeroba Barite Deposit, Kahramanmaraş, Turkey, 30th International Conference on 'Ore Potencial of Alkaline, Kimberlite and Carbonatite Magmatism', ANTALYA, TÜRKIYE. 29 Eylül - 2 Ekim 2014. vol.1, pp.126-126

Wood, D. A. The application of a Th–Hf–Ta diagram to problems of tectonomagmatic classification and to establishing the nature of crustal contamination of basaltic lavas of the British Tertiary volcanic province. Earth and Planetary Science Letters. 1980. Vol. 50.pp. 11–30.

Precambrian carbonatitic magmatism in Manitoba (central Canada): an overview

Chakhmouradian A.R.*, Couëslan C.G., Mumin A.H.***, Böhm C.O.**, Martins T.**, Reguir E.P.*, McFarlane C.****, Demény A.*****, Sal'nikova E.B.******, Simonetti A.*******, Lepekhina E.N.********, Kressall R.D.*, Reimer E.*, Kamenov G.D.*********

*University of Manitoba, Winnipeg, Manitoba, Canada
**Manitoba Geological Survey, Winnipeg, Manitoba, Canada
***Brandon University, Brandon, Manitoba, Canada
****University of New Brunswick, Fredericton, New Brunswick, Canada
*****Institute for Geochemical Research, Budapest, Hungary
******Institute of Precambrian Geology and Geochronology, St. Petersburg, Russia
*******University of Notre Dame, Notre Dame, Indiana, USA
********Center for Isotopic Research, VSEGEI, St. Petersburg, Russia
*********University of Florida, Gainesville, Florida, USA*

Prior to the discovery of carbonatites at Eden Lake (Mumin, 2002), this type of rocks had not been recognized in the Province of Manitoba, central Canada, in striking contrast to the adjacent parts of the Superior craton in Ontario, where carbonatitic magmatism has been known for at least 60 years, and used as an important source of information for the development of isotopic models for carbonatites (Bell et al., 1982; Rukhlov and Bell, 2010). In Precambrian settings affected by deformation and metamorphism, igneous carbonate rocks can easily pass unrecognized during routine regional-scale mapping due to their small size, metamorphic fabrics and obscured exposure, particularly in a wet temperate climate. Most of the discoveries in Ontario were made by mineral exploration companies pursuing large aeromagnetic anomalies, such as the 7.5 × 5 km cluster of anomalies at Nemegosenda Lake that turned out to represent a ring complex composed of magnetite-bearing feldspathoid rocks cut by carbonatite dikes (Sage, 1987). Whereas geophysical methods, such as magnetic and vertical-gradient gravity surveys, are effective exploration tools in the search for magnetite-, ilmenite- and pyrochlore-bearing carbonatites emplaced in intracontinental extensional settings (e.g., Drenth, 2014), they do not work very well for carbonatites emplaced in orogenic settings, and typically lacking the aforementioned minerals. In addition, this latter type of carbonatites commonly undergo deformation and low-grade metamorphism in the waning stages of, or following, the orogeny to produce a metacarbonate rock that can be easily mistaken for part of a supracrustal sequence unrelated to any mantle magmatism. In the absence of a robust U-Pb geochronometer (such as zircon), the age of such rocks and their correct placement in a geodynamic context are both subject to uncertainty due to thermal resetting. These challenges require the development of a completely new exploration approach applying geochemical and mineralogical criteria to the search for (post)orogenic carbonatites and associated deposits of rare earth elements (REE).

The fortuitous discovery of carbonatite outcrops during a scoping study funded by Rare Earth Metals Corp. (Vancouver, Canada) in the eastern part of Eden Lake in northern Manitoba (Mumin, 2002) was a turning point, in that the Trans-Hudson Orogen (THO) began to emerge as the area of Precambrian carbonatitic magmatism, and that our understanding of carbon cycling had to be revised to account for this and other occurrences unrelated to continental rifting. At Eden Lake, dikes of sövite intruded postorogenic silica-saturated syenitic rocks of shoshonitic affinity, which were transformed into coarse-grained tinatite(±andradite)-bearing fenites at the contact (Chakhmouradian et al., 2008). Both silicate and carbonate rocks were emplaced after the closure of the Paleoproterozoic Manikewan Ocean and assembly of the northern part of the THO 1815 ± 8/15 Ma (U-Pb zircon and titanite ages, respectively). The postorogenic suite is crosscut by aplites and granitic pegmatites of anorogenic affinity, which manifest far-field effects of collisional processes elsewhere in the Orogen ca. 1750 Ma (reset titanite age). The most remarkable mineralogical characteristics of the Eden Lake sövite are the presence of microcline and aegirine-augite megacrysts and evidence of post-emplacement ductile flow accompanied by remobilization of REE from the primary igneous paragenesis (fluorapatite and calcite) to form allanite. Although REE are locally present here in high concentrations (up to 16.7 wt.% total REE oxide), the minerals hosting these elements are not amenable to economic REE recovery, which led to a halt in exploration activities in 2011.

Subsequently (Couëslan, 2008), postorogenic carbonatites were recognized Paint Lake in central Manitoba in a completely different structural setting confined to the northwestern margin of the Superior craton (in present-day coordinates) deformed during its collision with the Reindeer Zone and the consolidation of the THO. At this occurrence, calcite-dolomite and calcite carbonatites postdate the final stage of the Hudsonian orogeny by ~30 Ma (a Rb-Sr isochron based on phlogopite samples gave 1703 ± 15 Ma) and are not associated with any alkaline silicate rocks. Trace-element data suggest that both rock types originated from the same mantle-derived dolomitic magma by fractionation. Their closest "contemporary" analogue is Cenozoic carbonatites of the Himalayan Mianning-Dechang Belt in China (Hou et al., 2009).

Our recent work in eastern Manitoba indicated that carbonatitic magmatism linked to collisional tectonics occurred already during the assembly of the Superior Craton in the Late Archean. At Cinder Lake in the Oxford Lake – Knee Lake greenstone belt, veinlets of calcite carbonatite crosscut cumulate syenites associated with

diverse feldspathoid syenites. The veinlets were identified as igneous on the basis of their trace-element and isotopic characteristics, and the presence of REE minerals (monazite and britholite) in association with Sr-REE-rich calcite. The areas of carbonatite distribution are surrounded by extensive metasomatic halos comprising albite, muscovite (sericitized feldspar) and, in feldspathoid rocks, andradite. U-Pb geochronology of zircon from the silicate rocks and of andradite associated with the carbonatites shows that the two rock suites are coeval within the error (2705 ± 2 and 2710 ± 5 Ma, respectively). The emplacement of these rocks in a Neoarchean collision zone between the North Caribou and North Superior microcontinents heralded the consolidation of the Superior craton; carbonatites of broadly similar age (2.61-2.69 Ga) have been previously identified in the Slave craton, northern Quebec, Greenland and Finland. However, the Cinder lake carbonatite is at present the oldest known occurrence of such rocks in the world. Some 60 km WSW of Cinder Lake within the same Neoarchean Oxford Lake – Knee Lake greenstone belt, orthometamorphic rocks of the Bayly Lake complex (> 2.73 Ga) host an unusual dike (Anderson et al., 2013) that was interpreted as primary dolomite carbonatite fragmented and incorporated into a somewhat younger calcite carbonatite. The two rock types are cogenetic, but developed independently, as suggested by trace-element distributions in the principal rocks-forming minerals (calcite, dolomite, amphibole and phlogopite). This dike is, undoubtedly, a manifestation of voluminous postcollisional mantle-derived igneous activity in the Oxford-Stull domain, and further discoveries of similar rocks are to be expected elsewhere in Neoarchean greenstone belts in the Superior and other cratons.

The above discoveries are important because they show that carbonatitic magmas are a relatively common product of melting processes in the mantle associated with, and probably triggered by, subduction. The ascent of carbonate melts is related to relaxation, either in a transtensional regime, or in response to postoogenic relaxation. Our findings also suggest that plate tectonics as we know it was already operating 2.7 billion years ago.

The only occurrence of anorogenic carbonatite in Manitoba known at present is at Wekusko Lake, where dikes of macrocrystic beforsite intruded Paleoproterozoic supracrustal rocks long after the consolidation of the THO (U-Pb measurements on zircon macrocrysts gave 556 ± 4 Ma). The dikes contain spinel and ilmenite macrocrysts compositionally similar to those found in kimberlites, but the rest of its mineralogy and geochemistry is more consistent with carbonatites (Chakhmouradian et al., 2009). The Wekusko Lake beforsite is interpreted to have crystallized from primary mantle-derived melts produced by localized extension in the THO probably in response to far-field stresses related to the breakup of Rodinia in the Neoproterozoic. This locality is the youngest known expression of igneous activity in Manitoba.

References:

Anderson, S.D., Kremer, P.D., Martins, T. Preliminary results of bedrock mapping at Oxford Lake, northwestern Superior province, Manitoba (parts of NTS 53L13, 14) // Report of Activities, Manitoba Mineral Resources, Manitoba Geological Survey. 2013. Pages 7-22.

Bell, K., Blenkinsop, J., Cole, T.J.S., Menagh, D.P. Evidence from Sr isotopes for long-lived heterogeneities in the upper mantle // Nature. 1982. Volume 298. Pages 251-253.

Chakhmouradian, A.R., Böhm, C.O., Demény, A., Reguir, E.P., Hegner, E., Creaser, R.A., Halden, N.M., Yang, P. "Kimberlite" from Wekusko Lake, Manitoba: Actually a diamond-indicator-bearing dolomite carbonatite // Lithos. Volume 112S. Pages 347-357.

Chakhmouradian, A.R., Mumin, A.H., Demény, A., Elliott B. Postorogenic carbonatites at Eden Lake, Trans-Hudson Orogen (northern Manitoba, Canada): Geological setting, mineralogy and geochemistry // Lithos. 2008. Volume 103. Pages 503-526.

Couëslan, C.G. Preliminary results from geological mapping of the west-central Paint Lake area, Manitoba (parts of NTS 63O8, 9, 63P5, 12) // Report of Activities, Manitoba Science, Technology, Energy and Mines, Manitoba Geological Survey. 2008. Pages 99-108.

Drenth, B.J. Geophysical expression of a buried niobium and rare earth element deposit: The Elk Creek carbonatite, Nebraska, USA // Interpretation. 2014. Volume 2. Number 4. Pages SJ23-SJ33.

Hou, Z., Tian, S., Xie, Y., Yang, Z., Yuan, Z., Yin, S., Yi, L., Fei, H., Zou, T., Bai, G., Li, X. The Himalayan Mianning–Dechang REE belt associated with carbonatite-alkaline complexes, eastern Indo-Asian collision zone, SW China // Ore Geology Reviews. 2009. Volume 36. Pages 65-89.

Mumin, A.H. Discovery of a carbonatite complex at Eden Lake (NTS 64C9), Manitoba // Report of Activities, Manitoba Industry, Trade and Mines, Manitoba Geological Survey. 2002. Pages 187-197.

Rukhlov, A.S., Bell, K. Geochronology of carbonatites from the Canadian and Baltic Shields, and the Canadian Cordillera: clues to mantle evolution // Mineralogy and Petrology. 2010. Volume 98. Pages 11-54.

Sage, R.P. Geology of carbonatite-alkalic rock complexes in Ontario: Nemegosenda Lake Alkali Rock Complex, District of Sudbury // Ontario Geological Survey Study. Vol. 34. 132 pages.

The new demand paradigm: environmentally progressive rare earths –
Mountain Pass mine, California, USA

Cordier D., Landreth J., Sims J.
"Molycorp Inc," Greenwood Village, Colorado,USA
Dan.Cordier@Molycorp.com

Today's rare earth industry is undergoing significant and rapid evolutionary change toward greater reliability and diversity of supply, increased security of supply chains, and better price predictability. In particular, technology innovation is helping producers such as Molycorp meet the growing demand by downstream consumers for rare earth materials made with environmentally progressive processes. Advances in rare earth material science are lessening the need for relatively scarce heavy rare earths in high-performance neodymium-iron-boron (NdFeB) permanent rare earth magnets, which is making more NdFeB magnetic materials available for a broader range of downstream applications and markets. This is especially important to applications in the clean energy and energy efficiency spaces, where the use of NdFeB magnets drive better performance, greater energy savings, and associated reductions in air emissions. All of these trends are helping to restore the confidence of customers and other stakeholders in the rare earth space. That increased confidence is likely to drive both additional global demand for rare earth materials and increased utilization of these remarkable materials.

Critical factors in the rare earth market

Cox C.
The Anchor House, Inc., Chicago, USA

The rare earth element (REE) market has been extremely volatile over the last decade, and it has become very difficult to predict future market growth rates and prices for each of the elements. The future outlook of the market directly affects the financing of potential future supplies. There are a number of factors to consider when seeking to understand the direction of the market, including: the world economy, Chinese policy, reduction & replacement of REE usage, new applications, new processing methods, and new REE resources outside of China. Each of these factors will be examined and placed in historical context, as they each have the capability to shift the market.

World Economy

REE demand is closely linked to world economic growth. When the world economy declined sharply in 2008-2009, the rare earth market declined along with it. The purchase of products that utilize rare earths fluctuates as the world market expands and contracts.

Chinese Policy

Chinese policy has a profound affect on the REE market. Export and production quotas have been used to control the REE market—so much so that Japan, the EU, and the USA field and won a World Trade Organization (WTO) complaint. Chinese response to the WTO's ruling will shift the market and its regulation. Also, as new leadership has come to power in China, it will be very important to see how they treat rare earths in their new 5-year plan.

Rare Earth Crisis of 2010 and Aftermath

Much of the attention focused on the rare earth market is due to the crisis of 2010 and following. During 2010, the Chinese drastically cut export quotas and Japanese companies had some difficulty in acquiring material from China. The market response included a price spike (and subsequent drop), end-users re-evaluating rare earth usage in their products, and an explosion in the number of prospective rare earth projects outside of China.

Reduction & Replacement of REE Usage

As a result of the rare earth crisis, many sectors that use rare earths have lessened or replaced their dependence on REEs. The polishing industry has learned to recycle much more efficiently, magnet manufacturers have reduced or eliminated the use of dysprosium where possible, and the phosphor industry has significantly reduced usage (perhaps as much from the acceptance of LED lighting—which uses less REEs—as intentional reduction).

New Processing Methods

Many new methods for processing rare earths have been touted over the last decade. However, many of these methods re-visit older technologies and do not provide any new or substantial economic advantage. There has been some increased efficiency introduced across many rare earth processing steps, but these have, thus far, provided only incremental improvements.

The industry has been closely following the progress of Molycorp's Mountain Pass project and Lynas' Mount Weld project, to see if there will be viable, competitive REE production outside of China on a large scale. In addition to these companies, there are a number of other junior miners, and potential possibilities for by-product production.

Rare earth elements in charoite rocks, Murun complex

Dokuchits E.Yu., Vladykin N.V.
Institute of Geochemistry SB RAS, Irkutsk, Russia, esfor@rambler.ru, vlad@igc.irk.ru

The Murun alkaline complex is the largest complex of potassic agpaitic rocks, that is located in north-west part of Aldan shield (the border of Irkutsk state and Yakutia). This complex is one of Mesozoic alkaline complexes of Aldan alkaline province and doesn't have any analogues in the world.

Main minerals of charoite rocks are charoite, quartz, microcline, K-arfvedsonite, tinaksite, fedorite, apophyllite, frankamenite, pectolite phenocrysts. They are rimmed by charoite, charoite-pyroxene-tinaksite aggregate in cases with calcite. There are some rare and even unique minerals in charoite rocks. [Vladykin et al. 1983].

Charoite rocks are composed of these main petrogenic elements: Si, K, Na, Ca, Ba, Sr and water. Variations of these elements in particular determine chemical composition of charoite rocks.

[Rozhdestvenskaya et al. 2010] deciphered the structure of charoite:

$$(K,Sr,Ba,Mn)_{15-16}(Ca,Na)_{32} [(Si_{70} (O,OH)_{180})] (OH,F)_{4.0} \times nH_2O$$

The completed crystal chemical formula of charoite can be written as:

$$(K_{13.88}Sr_{1.0}Ba_{0.32}Mn_{0.36})_{15.56}(Ca_{25.64}Na_{6.36})_{32}$$
$$[(Si_6O_{11}(O,OH)_6)_2(Si_{12}O_{18}(O,OH)_{12})_2(Si_{17}O_{25}(O,OH)_{18})_2](OH,F)_{4.0} \times 3.18H_2O$$
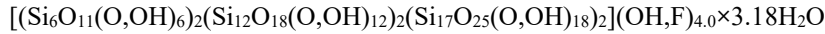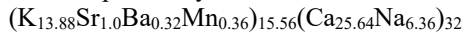
Double correlation plots of petrogenic elements (fig. 1) show common trends of composition changes. Divergence of some dots from a trend line is caused by small volume of samples (1 kg), and by processes of melt-fluid differentiation, which continued, while charoite rocks crystallized [Dokuchits. 2014].
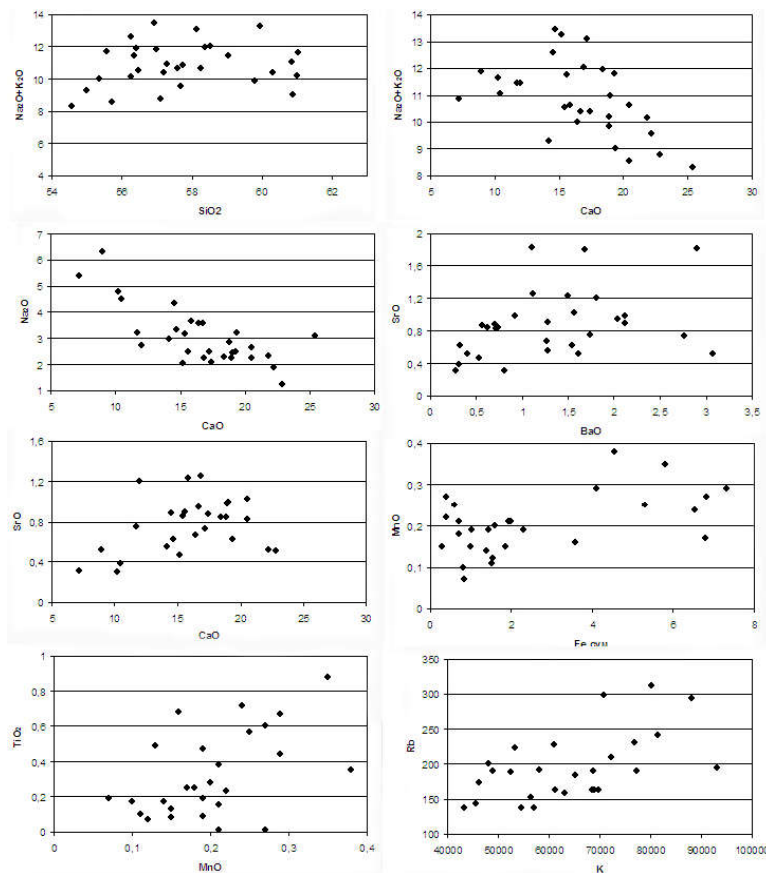
Fig. 1 Double correlation plots of petrogenic elements of charoite rocks.

We investigated a behavior of rare earth elements in charoite rocks. On fig. 2 shown ternary correlation plots of rare-erath elements inside whole group of these elements (with and without Y) in charoite rocks. Clear correlation dependences between elements are to be observed, that explain genesis of charoite rocks from melt-fluid.
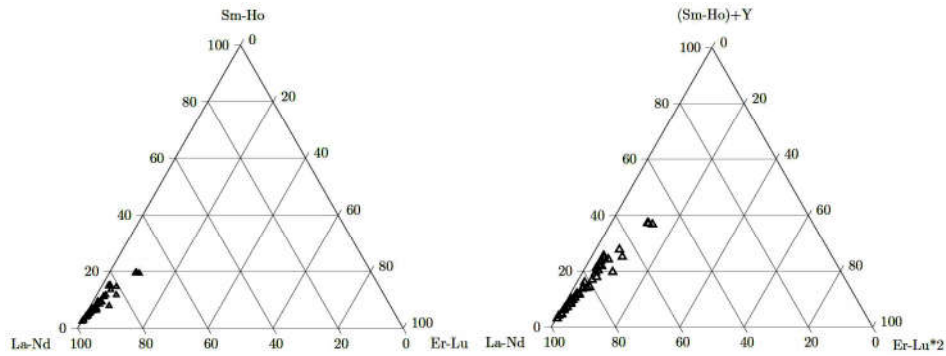
Fig. 2. Ternary correlation plots of charoite rocks.

The fig. 3 presents double correlation plots of rare-earth elements. Clear straight correlation dependences with quiet wide diapason of concentration of these elements are to be observed. The same dependences for another rare elements (Ba, Sr, Zr, Hf, Nb, Ta, Pb, Zn, Sn, Be) may be observed in fig. 4.
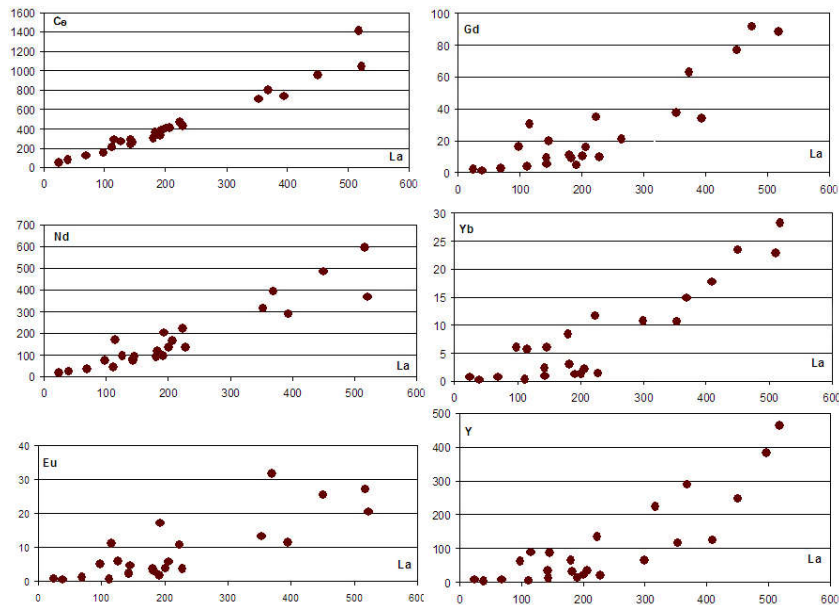
Fig. 3. Double correlation plots of REE in charoite rocks.
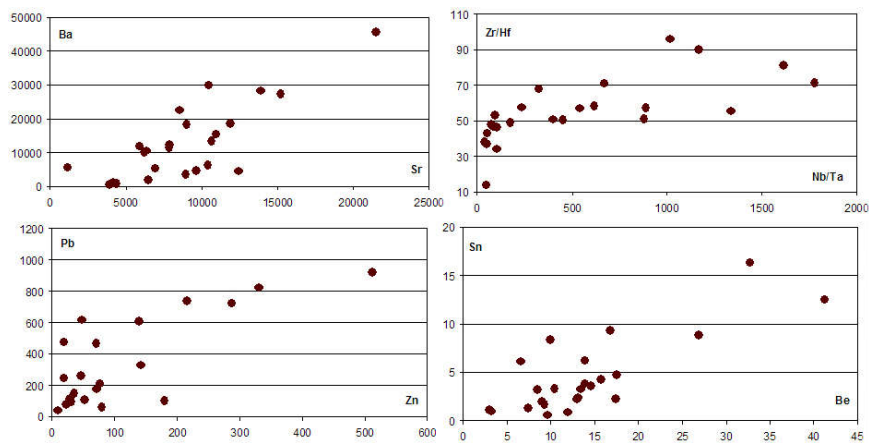
Fig. 4. Double correlation plots of rare elements in charoite rocks.

36

The regular behavior of petrogenic and rare elements in charoite rocks is evidence of quite stable conditions of crystallization of these rocks from silicate-carbonate melt-fluid. These patterns of conduct of rare elements in charoite rocks are close to those of the same elements in silicate rocks of Murun complex, which witness of their common genetic relation.

References:

Dokuchits E.Yu. Features of chemical and mineral composition of charoite rocks, Murun complex // Vestnik of Irkutsk state technical university. Irkutsk, 2014. Vol. 84(1). P. 34-40. [in russian]

Rozhdestvenskaya I., Mugnaioli E., Czank M., Depmeier W., Kolb U., Reinholdt A. and Weirich T. The structure of charoite, $(K,Sr,Ba,Mn)15-16(Ca,Na)32[(Si70(O,OH)180)](OH,F)4.0''nH2O$, solved by conventional and automated electron diffraction. Mineralogical Magazine, February 2010, Vol. 74(1), pp. 159-177.

Vladykin N.V., Matveeva L.N., Bogacheva N.G., Alekseev Yu.A. The new data about charoite and charoite rocks // Mineralogy and genesis of gems of East Siberia. Novosibirsk, 1983. P. 41-56. [in russian]

Role of tectonics during formation of alkaline rock associations of South-Western part of Russian Platform

Donskoy A.N., Donskoy N.A., Legkaya L.I.
N.P. Semenenko Institute of Geochemistry, Mineralogy and Ore Formation, Kiev, Ukraine
donick_gg@mail.ru

About twenty nepheline rock massifs of Proterozoic and Paleozoic series are indicated on the territory of South-Western part of Russian Platform. Most of them are on the territory of Ukraine, Belarus and Lithuania. There are some preconditions of findings in Rostov oblast' of Russia and Poland [1-5].

Similarity of petrological, geochemical and mineragenical features by means of comparison of main peculiarities of alkaline rocks of Proterozoic syenite series and Devonian basic-ultrabasic ones is indicated. It can note the following points.

Both series related to tectonic active zones of Precambrian geologic structures were formed at final stages of Proterozoic and Devonian tectonic activity. Alkaline magmatic melts' generating, alkaline fluids formation and their migration in lithosphere, their compositional ratio with host rocks are due generally to geodynamics of tectonic activity of certain consolidated structures.

Alkaline rocks of Proterozoic syenite series have no defined difference between magmatism products and metasomatism ones. There are no effusive and extrusive rocks. Pegmatate process is widespread. The rocks of sodium and sodium-potassium branches are prevailed. Increasing of rare elements' content associates sodium, aluminum content with total alkali. Among the rocks alkaline syenites are more widespread. Carbonatites are indicated.

In Devonian series in addition to plutonic rocks the effusive and extrusive ones are widespread. So, including kimberlites which are likely to be associated with diamond formation. Potassium branch rocks are prevailed. Comparing Proterozoic and Devonian rocks, first ones have higher K, Ti, F, Ba contents; Devonian metasomatites have increased Nb and Be contents, Zr and Ta are practically absent.

Alkaline rock association of Proterozoic and Devonian age contain deposits of nepheline ores, rare metal (Zr, Nb, Ta, Be and etc.) metasomatites and TR ones. As well as increased K, Na, P, Ti, Sr, Ba, Pb, Zn, Cu, F concentrations.

Comparison of alkaline rock associations of the region with other regions of the world indicates the following.

Nepheline syenite massifs associate ancient Proterozoic platforms, such structures as the Ukrainian and Baltic Shields, and Canadian platform. Besides nepheline series emergence meets eras of tectonic and magmatic activity which correspond periods of global Earth crust alteration. All massifs of syenite series were formed after an end of Archean and Early Proterozoic folding. They associate lifted early consolidated blocks of edge zones of Proterozoic faults, usually intersection of the faults which approach lower part of earth's crust and mantle. On the platforms they associate lineaments which transport fluids from the depth. Simultaneous with alkaline massifs of the region are Saharjok, Eletozero and Gremyakha-Vyrmes massifs of the Baltic Shield, Yellowknife, Kaminak, Haliburton Bancroft, Blue Mountain of the Canadian Shield, Palabora, Spitzkoppe of the Southern Africa region [6].

The middle Paleozoic era is characterized by widening of regions of the alkaline rock series and their diversity. Among Hercynian orogenic structures of the Urals the miascite massifs were formed, the Lovozero and Khibiny plutons on the Baltic Shield in paleorift zone. Middle Paleozoic magmatism associates similar rocks

in Kazakhstan, Central Asia, Altai-Sayan region, Nothern Mongolia, Transbaikalia and Nothern Baikal region [7-9].

References:
1. Ainberg L.F. Pryazovia alkaline massif // Trudy Vsesouzn. geol.-razved. obyedinenia. Leningrad: Moscow., 1933. – Issue. 196. – 100 pg. (in Russian)
2. Donskoy A.N. Nepheline complex of Oktyabrsky alkaline massif. – Kiev: Nauk. dumka, 1982. – 150 pg. (in Russian)
3. Donskoy A..N., Legkaya L.I., Stremovskiy A.M. Ore and geochemical specialization of Devonian magmatic complex rocks and associated metasomatic rocks in junction zone of Dnieper-Donetsk Depression and Azov part of the Ukrainian Shield // Geochemistry and Ore Formation. – 1984. - No 12. – Pg. 39-52. (in Russian)
4. Luchitskiy V.I., Lebedev P.I. Petrography of Ukraine // Trudy Petrograf. instituta. – Leningrad: Izd-vo AS Ukr SSR, 1934. – Ser. 1. – Issue. 3. – 324 pg. (in Russian)
5. Donskoy A.N., Zhvikas A.B., Marfin S.S., Skripkina T.S. On finding of nepheline rocks in western part of Eastern European platform (the Varena area, Lithuania) // DAN Ukr SSR. – Ser. B. – 1990. - No 9. – Pg. 5-8.
6. Donskoy A.N. Comparison of alkaline complexes of South of Eastern European Platform with other regions of the world // Geochemistry and Ore Formation. – 1991. - No 18. – Pg. 64-77. (in Russian)
7. Donskoy A.N., Kulish E.A., Donskoy N.A. Nepheline ores of Ukraine – complex aluminium-alumina and rare-metals ores. – Kiev: Logos, 2004. – 222 pg. (in Russian)
8. Donskoy A.N. Role of structural factors during formation of Oktyabrsky alkaline massif (Eastern Priazovia) // Collection of papers dedicated to G.I. Kalyaev, IGNS NAS «Tectonics, minerageny, mineral resources». – Kiev: Logos, 2005. – Vol. I. – Issue. 11. – Pg. 126-134. (in Russian)
9. Donskoy N.A. Tectonic structure of junction zone between Donbass and Azov block of the Ukrainian Shield and manifestations of Devonian magmatism within its territory // Collection of papers dedicated to G.I. Kalyaev, IGNS NAS «Tectonics, minerageny, mineral resources». – Kiev: Logos, 2005. – Vol. I. – Issue. 11. – Pg. 132-139. (in Russian)

Crystal chemistry and genesis of organic minerals: the interaction between organic molecules and heavy metals in hydrothermal environments

Echigo T., * *Kimata M.* **
Faculty of International Resource Sciences, Akita University, Akita, JAPAN, tak.echigo@gmail.com
**Graduate School of Life and Environmental Sciences, University of Tsukuba, Tsukuba, JAPAN*

Organic minerals are natural organic compounds with both a well-defined chemical composition and crystallographic properties; their occurrences reveal traces of the high concentration of certain organic compounds in natural environments. 45 species of organic minerals are approved by the Commission on New Minerals, Nomenclature and Classification of International Mineralogical Association (IMA/CNMNC); these minerals consist of the structural units containing carbon-carbon covalent bonds, for example, hydrocarbon molecules and organic acid anions (Gaines et al. 1996, Bojar et al. 2010). Echigo & Kimata (2010) divided the organic minerals (45 species) into the following two groups: (1) ionic organic minerals, in which organic anions and various cations are mainly held together by ionic bonds, and (2) molecular organic minerals, in which electro-neutral organic molecules are bonded by weak intermolecular interactions. The former group contains 27 species of organic minerals and the latter comprises 18 species (Echigo & Kimata 2010). The most typical ionic organic minerals are oxalate minerals that contain oxalic anion (Fig. 1a), various cations and water molecules. Coronene ($C_{24}H_{12}$: Fig. 1b) and picene ($C_{22}H_{14}$: Fig. 1c) molecules, which are polycyclic aromatic hydrocarbons (PAHs), are bonded by van Deer Waals forces and make up the crystal structures of the most typical molecular organic minerals, karpatite and idrialite, respectively (Echigo et al. 2007, 2009).
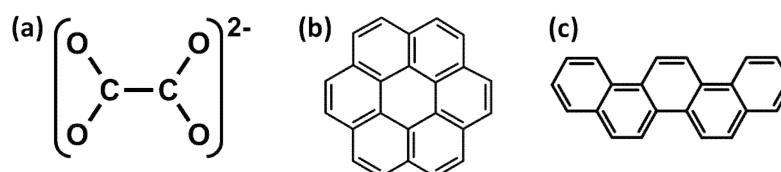
Fig. 1. Chemical structures of (a) oxalate anion, (b) coronene and (c) picene.

38

In general, organic minerals occur in low-temperature environments, e.g., marine sediments, carbonate concretion and coal. However, both whewellite [$Ca(C_2O_4)\cdot H_2O$] and natroxalate [$Na_2(C_2O_4)$], the most typical oxalate minerals, also occur in the late hydrothermal stages of peralkaline pegmatites of the Khibiny and Lovozero agpaitic massifs at Kola peninsula, Russia (e.g., Khomyakov et al. 1996). Not only these oxalate minerals, but also complex non-crystalline organic matters called solid bituminous matters (SBMs) occur in such peralkaline pegmatites (Chukanov et al. 2007). These SBMs are characterized by the association with Th- and rare earth elements (REEs) minerals that show relatively high concentration of Ce, La, Nd, Y, Sr, Th, U, Ti, Nb and Ba, and hence the role of such organic matters in the transportation of REEs in hydrothermal fluids was studied in detail (e.g., Chukanov et al. 2005). In addition, the most typical molecular organic minerals, karpatite (molecular crystal of coronene, Fig. 1b) and idrialite (molecular crystal of picene, Fig. 1c) occur in some epithermal Au-Hg deposits in California, USA (Sherlock 2000). Thus, the effects of organic molecules in hydrothermal fluids on the capturing of heavy metal elements/cations have been discussed for long time.

We studied the crystal chemistry and genesis of both oxalate and PAH minerals in detail because they are the most typical ionic and molecular organic minerals, respectively (e.g., Echigo et al. 2005, 2007, 2009). These studies have revealed that the cations and oxalate anions ($C_2O_4^{2-}$) in oxalate minerals are strongly bonded to form fundamental building blocks (FBBs) in their crystal structures and that FBBs in PAH minerals are individual PAH molecules and these are loosely bonded by weak intermolecular interactions. In addition, carbon isotope ratios of karpatite ($C_{24}H_{12}$) and idrialite ($C_{22}H_{14}$) occurring in mercury deposits in California, USA, were analyzed and suggested that these PAH minerals derive their origins from hydrothermal alternation of biogenic organic substances in oceanic sediments (hydrothermal petroleum) (Echigo et al. 2007, 2009). Itomuka mercury deposit in Hokkaido, Japan formed by Neogene/Quaternary volcanic activities in subduction zone is similar to mercury deposits in California that produce PAH minerals. We investigated the mercury ore from Itomuka mine and found out some solid organic matters associated with quartz and native mercury (Fig. 2c). Our study indicates that organic molecules in hydrothermal fluids play a significant role in the concentration of Hg (and Au) in subduction zone, as well as peralkaline pegmatites in Kola Peninsula.
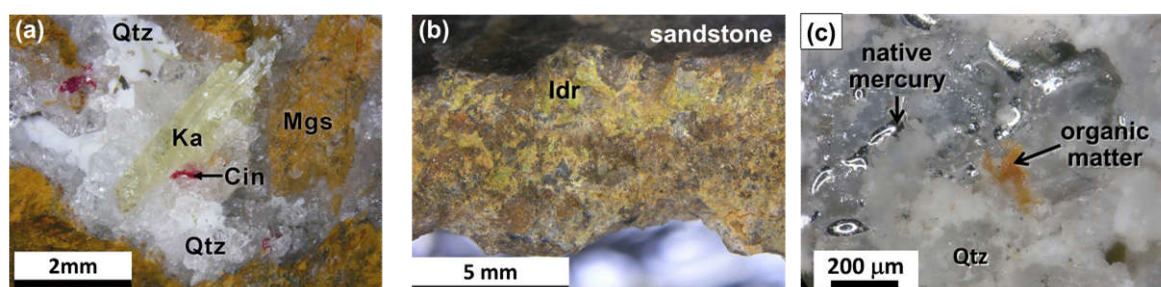
Fig. 2. Organic minerals/matters occurring in hydrothermal mercury deposits: (a) karpatite from San Benito mercury deposit (Ka: karpatite, Cin: cinnabar, Mgs: magnesite, Qtz: quartz), (b) idrialite from Skaggs Springs mercury deposit (Idr: idrialite) and (c) organic matter from Itomuka mercury deposit (Qtz: quartz).

References:

Bojar, H.-P., Walter, F., Baumgartner, J., & Färber, G. (2010): Ammineite, $CuCl_2(NH_3)_2$, a new mineral species with an ammine complex: mineral data and crystal structure. Can. Miner., 48, 1359-1371.

Chukanov, N. V., Pekov, I. V. & Ermolaeva, V. N. (2008) The role of organic matter in peralkaline pegmatites: Comparison of minerogenetic and technological processes. *In* Minerals as Advanced Materials I (S. V. Krivovichev, ed.). Springer-Verlag, Berlin (pp. 221-230).

Chukanov, N. V., Ermolaeva, V. N., Pekov, I. V., Sokolov, S. V., Nekrasov, A. N. & Sokolova, M. N. (2008) Rare-metal mineralization connected with bituminous matters in late assemblages of pegmatites of the Khibiny and Lovozero massifs, New data on minerals, 40, 80-95.

Gaines, R. V., Skinner, H. C. W., Foord, E. E., Mason, B. & Rosenzweig, A. (1997): Dana's New Mineralogy: the System of Mineralogy of James Dwight Dana and Edward Salisbury Dana (8th ed.). John Wiley & Sons, New York.

Echigo, T., Kimata, M., Shimizu, M. & Hatta, T. (2005) Re-investigation of the crystal structure of whewellite [$Ca(C_2O_4)\cdot H_2O$] and the dehydration mechanism of caoxite [$Ca(C_2O_4)\cdot 3H_2O$], Miner. Mag., 69, 63-74.

Echigo, T., Kimata, M. & Maruoka, T. (2007) Crystal-chemical and carbon-isotopic characteristics of karpatite ($C_{24}H_{12}$) from the Picacho Peak Area, San Benito County, California: Evidences for the hydrothermal

formation. Amer. Miner., 92, 1262-1269.

Echigo, T., Kimata, M., Maruoka, T., Shimizu, M. & Nishida, N. (2009) The crystal structure, origin and formation of idrialite ($C_{22}H_{14}$): Inferences from the microbeam and bulk analyses, Amer. Miner., 94, 1325-1332.

Echigo, T. & Kimata, M. (2010) Crystal chemistry and genesis of organic minerals — A review on oxalate and polycyclic aromatic hydrocarbon minerals, Can. Miner., 48, 1329-1358.

Khomyakov, A. P. (1996) Natroxalate $Na_2C_2O_4$, a new mineral. Zap. Vser. Mineral. Obshchest. 125, 126-132.

Sherlock, R. (2000) The association of gold–mercury mineralization and hydrocarbons in the coast ranges of northern California. *In* Organic Matter and Mineralization: Thermal Alternation, Hydrocarbon Generation and Role of Metallogenesis (M. Glikson & M. Mastalerz, eds.). Kluwer Academic Publications, Dordrecht (pp. 378-399).

Leaching of rare-earth and radioactive elements from lovozerite lujavrite (Lovozero alkaline massif, Kola Peninsula)

Ermolaeva V.N.*, Mikhailova A.V.**, Kogarko L.N.**
* IEM RAS, Chernogolovka, Russia
** GEOKHI RAS, Moscow, Russia
cvera@mail.ru

We studied leaching of rare-earth and radioactive elements from lovozerite lujavrite, which is rare-metal ore, with different reagents in order to determine the most effective ones. As a reagents for leaching, we used 4% solution of HCl, 2% solutions of ammonium oxalate, trilon B and ammonium difluoride, as well as mixtures (1:1) of HCl solution with 2% solutions of ammonium oxalate, trilon B and ammonium difluoride. The determination of the elements was carried out by using of ICP MS method. The results of leaching show, that *REE* and Th from lovozerite lujavrite are leached most effective by mixtures of HCl solution with ammonium oxalate, trilon B and ammonium difluoride solutions, as well as by HCl solution. Somewhat smaller quantities of *REE* and Th are leached by solutions of ammonium oxalate, trilon B and ammonium difluoride. U are leached most effective by mixtures of HCl solution with ammonium oxalate, trilon B and ammonium difluoride solutions, as well as by HCl and ammonium difluoride solutions. Thus a mixtures of HCl solution with trilon B and ammonium difluoride more effective extracts *LREE*, and mixture of HCl solution with ammonium oxalate – *HREE* (table 1, figure 1).

This work is important from the practical point of view: the high contents of rare (including rare-earth) elements in alkaline rocks of Lovozero massif make it possible to consider it as potential object for their industrial extraction.

Table 1. Element contents (ppm) and leaching results from lovozerite lujavrite (Lovozero alkaline massif, Kola Peninsula), ICP MS method. Experiments were made without volume control of the analyzed solutions.

Element	Contents in sample, ppm	Leaching results (in % from total content)						
		4% HCl solution	2% ammonium oxalate solution	2% trilon B solution	2% ammonium difluoride solution	4% HCl solution + 2% ammonium oxalate solution	4% HCl solution + 2% trilon B solution	4% HCl solution + 2% ammonium difluoride solution
La	413.60	62.62	5.46	17.60	2.63	85.55	87.98	~100
Ce	738.96	73.84	6.27	21.87	3.34	90.25	~100	~100
Pr	89.47	77.93	7.56	24.72	3.29	87.41	~100	~100
Nd	331.09	85.74	8.86	28.74	3.58	91.12	~100	~100
Sm	69.11	96.05	11.06	34.36	3.67	95.93	~100	~100
Eu	20.89	92.09	12.30	33.42	3.24	~100	~100	~100
Gd	66.96	92.42	11.79	32.62	3.29	95.99	~100	~100

Tb	12.32	82.89	11.20	28.47	2.65	91.44	97.76	94.02
Dy	71.75	88.36	13.23	28.41	3.70	~100	~100	~100
Ho	15.47	80.94	12.35	23.79	3.37	~100	96.20	93.44
Er	50.96	79.22	12.42	21.90	3.50	~100	93.25	91.15
Tm	7.21	76.79	10.48	19.33	2.75	~100	90.23	89.18
Yb	41.20	80.25	11.51	20.47	4.10	~100	92.55	91.74
Lu	5.09	75.65	9.64	18.54	2.40	~100	88.11	88.39
Th	338.91	81.13	8.50	25.54	4.75	93.66	93.88	~100
U	103.92	82.12	9.82	19.47	77.97	~100	94.75	94.45
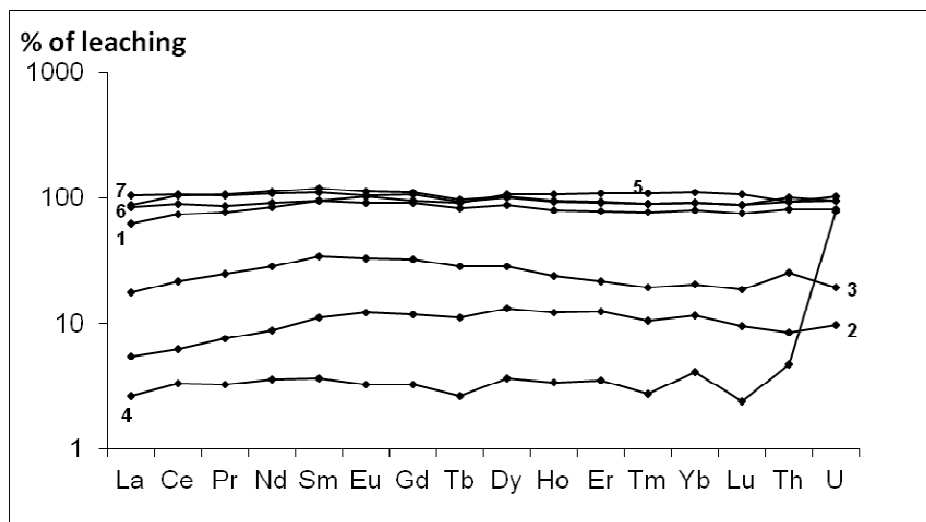
Figure 1. Results of *REE*, Th and U leaching (in % from total content) from lovozerite lujavrite (Lovozero massif, Kola Peninsula) with solutions: 1 – HCl, 2 – ammonium oxalate; 3 – trilon B, 4 - ammonium difluoride, 5 – HCl+ammonium oxalate, 6 - HCl+ trilon B, 7 - HCl+ammonium difluoride. ICP MS data.
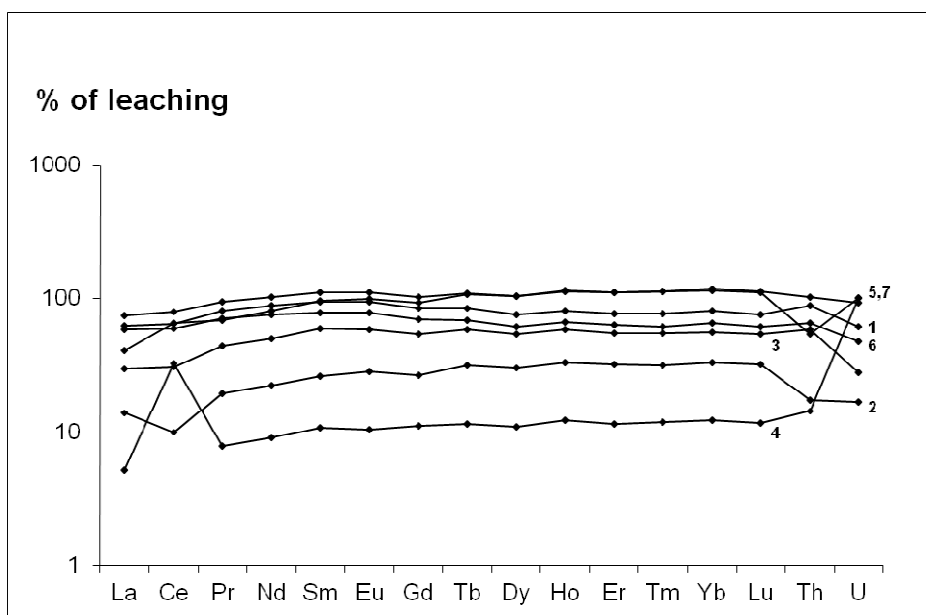
Figure 2. Results of *REE,* Th and U leaching (in % from total content) from porphyric lujavrite (Lovozero massif, Kola Peninsula) with solutions: 1 – HCl, 2 – ammonium oxalate; 3 – trilon B, 4 - ammonium difluoride, 5 – HCl+ammonium oxalate, 6 - HCl+ trilon B, 7 - HCl+ammonium difluoride. ICP MS data.

In comparison with porphyric lujavrite (Ermolaeva et al., 1014) single solutions of ammonium oxalate, trilon B and ammonium difluoride leaching some smaller quantities of *REE,* Th and U. In case of leaching with

other solutions we observe similar result for lovozerite and porphyric lujavrite. Unlike lovozerite lujavrite for porphyric lujavrite we can see Ce maximum for ammonium difluoride leaching and Th minimum for HCl+ammonium difluoride solution.

Reference

Ermolaeva V.N., Mikhailova A.V., Kogarko L.N. Leaching of rare-earth elements from porphyric lujavrite (Lovozero alkaline massif, Kola Peninsula // 30th International Conference on "Ore Potential of Alkaline, Kimberlite and Carbonatite Magmatism". Antalya - TURKEY. 29 September - 02 October 2014. P. 52-53.

Mantle carbonatites or crustal metacarbonates? Challenge from carbonate-dykes in the Ivrea-Verbano Zone (NW Italy / S Switzerland)

Galli A., Grassi D.N., Gianola O.A., Rickli J.
Department of Earth Sciences, ETH Zurich, Sonnegstrasse 5, 8092 Zurich, Switzerland
andgalli@hotmail.com

In the Ivrea-Verbano Zone (NW Italy / S Switzerland) one of the best mantle-crust sections worldwide is exposed. The geological evolution of the IVZ has been characterized by the Permian underplating of voluminous, mantle-derived basic magmas ("Mafic Complex") in to the amphibolites to granulite facies basement of the Southern Alps ("Kinzingite Formation").

In the Ivrea-Verbano Zone, numerous marble and calcsilicate-bodies are present as concordant bodies intercalated with metasediments of the Kinzingite Formation, or as up to 40 m thick, partly discordant carbonate-dykes associated with different rock types, such as upper amphibolites to granulite facies paragneisses and micaschists, mafic granulites, gabbros and ultramafic rocks. Usually, these carbonate-dykes display sharp contacts to the host rocks without any evidences of extensive alteration zones. Typical mineral assemblage consists of calcite, scapolite, diopside, sphene. Up to 50 cm large, angular or rounded xenoliths of the host rocks, in part disrupted and/or metasomatised, are enclosed within the dykes.

Nevertheless, in Val Mastallone (western IVZ) and in Val Fiorina (northern IVZ) the carbonate-dykes show distinct characteristics, different from the other dykes of the IVZ. In Val Mastallone (VM), an up to 40 m thick carbonate-dyke occurs within mafic granulites. This dyke is composed of coarse-grained calcite and contains numerous clinopyroxene clasts. The contacts to the host granulite are outlined by a 1.5 m thick zone of alteration constituted of actinolite, chlorite, clinozoisite, plagioclase, calcite, apatite, sphene, biotite, quartz and opaques. Up to 10-15 cm thick carbonate-apophyses intrude the host granulite. The VM dyke displays up to 2 m large xenoliths of black, coarse-grained, spinel-bearing clinopyroxenite, with strong petrological and geochemical affinities to late Permian pyroxenite bodies described in the area and interpreted as alkaline UM pipe. This suggests that the clinopyroxenite was transported from a remarkable distance.

The carbonate-dyke of Val Fiorina (VF) is spatially related to phlogopite-bearing peridotites, hornblendites and garnet-bearing clinopyroxenites occurring as pipes within stronalites and mafic granulites. The dyke is mostly composed of calcite and encloses numerous, polymict inclusions of stronalite, mafic granulite, hornblendite, clinopyroxenite and Triassic oligoclasite.

Geochemical investigations revealed compositional differences between the VM and VF dykes and the other carbonates dykes of the IVZ. Both VM and VF carbonate-dykes are richer in REE (Σ REE$_{VM}$: 338 ppm; REE$_{VF}$: 202 ppm; REE$_{IVZ}$: 55-192 ppm), are rich in Sr (Sr$_{VM}$: 1458 ppm; Sr$_{VF}$: 3950 ppm; Sr$_{IVZ}$: 207-5100 ppm) and display a primitive mantle-like Y/Ho ratio (Y/Ho$_{VM}$: 27; Y/Ho$_{VF}$: 29; Y/Ho$_{IVZ}$: 25-40). On the chondrite normalized REE abundances diagram, both VM and VF dykes show no Eu anomaly, in contrast to the other IVZ carbonates, which display a prominent Eu anomaly. The primitive mantle-normalized pattern of both VM and VF dykes show negative anomalies at Cs, Rb, K,Pb,Zr, Hf, and Ti and a positive Ba anomaly. Instead, the other IVZ carbonate-dykes are characterized by positive Cs, Pb and Sr anomalies, as well as by a strong Ba positive anomaly.

General concentrations and pattern of the IVZ carbonates are consistent with a sedimentary origin. Instead, the VM and VF dykes have strong geochemical similarities with the "world average carbonatites" but, in comparison with them, the dykes show lower absolute trace element concentrations. Nevertheless, the measured values are significantly higher than typical limestone compositions and similar to cumulate carbonatites found elsewhere in the world (e.g. India, China and Brazil).

Therefore, we propose that the IVZ carbonate-dykes are partly molten crustal sediments formed by local thermal anomalies and fluid flux during the emplacement and crystallization of alkaline UM pipes. Conversely, the VM and VF carbonate-dykes are carbonatites crystallized in the lower crust as carbonate "cumulates",

probably related to the alkaline UM pipes. This carbonatitic magmatism is related to the Permo-Triassic CO_2-bearing alkaline magmatism and metasomatism occurring in the Ivrea-Verbano Zone during the early stage of the opening of the Thetyan Ocean.

Further Nd-Sr isotopic investigations should elucidate the nature of the different types of carbonate-dykes, indicating if the VM and VF carbonate-dykes are in fact primary carbonatites arising from the mantle.

Natural diamonds in space and time

Garanin V.K.,**, Garanin K.V.***
A.E. Fersman Mineralogical Museum of RAS, Moscow, Russia;
***Geological Faculty, M.V. Lomonosov Moscow State University, Moscow, Russia*
vgaranin@mail.ru

Various types of natural diamond-bearing rocks from cosmic objects to the Earth's crustal rocks are well known now. There are gigantic cosmic bodies composed of diamond substance, meteorites, impactites, mantle peridotites and eclogites (from depths 150-200 km), ultra-high pressure rocks (from depths up to 700 km), kimberlites and lamproites, ophiolites, metamorphic rocks, calc-alkaline lamprophyres, komatiites, foliated plutonic rocks, and carbonatite complexes. All of these rocks were formed at different time intervals, environment, physical and chemical conditions of rocks and minerals crystallization, including diamond. Diamonds are varying consequently in size, shape, composition, structure, physical properties, admixtures, etc.

Cosmic diamond objects or giant diamonds (white dwarfs) with large-diameter (at least one has diameter ~ 4000 km), distanced 50-900 light-years away from the Earth according to National Radio Astronomy Observatory's (NRAO) astrophysics. Such objects are the most ancient cold bodies, and one of them (cosmic diamond PSR J2222-0137) is about 11 billion years old, it has the same age as the Milky Way (Deller et al., 2013). Among these cosmic diamonds, are interstellar black hydrogen-rich diamonds (mostly carbonado) crystallized in space and delivered to the Earth by asteroids fall (Garai et al., 2006). Initially such asteroids generated in a process of supernova stars explosions.

Diamonds from meteorites are dated at 4.5 Ga. These diamonds discovered in all types of meteorites crystallized in the Fe-Ni system (camacite, taenite) in association with troilite. Such diamonds presented by small cubic, octahedral and cubic-octahedral crystals up to 1 mm (usually <100 μm), with a huge excess of noble gases, and ^{14}N concentration is three times higher in these diamonds than the concentration of this isotope within the Earth.

Diamonds from impactites are small (up to several mm), irregularly shaped cloudy grains and aggregates with fragmental outlook. Mostly these diamonds presented by lonsdaleite (hexagonal modification of carbon). Polyphase aggregates composed by diamond, lonsdaleite and graphite. They do not contain nitrogen, have a high hardness, isotopically light and characterized by a sufficiently sustained $\delta^{13}C$ range from -13.2 to -18,7 ‰, enriched by radioactive (uranium, thorium), and rare earth (RE) elements. One of the most famous impact structure is the Popigay crater (ring-structure) with huge diamond resources formed 37 Ma ago.

Mantle diamonds discovered in mantle rocks (peridotites and eclogites) and phenocrysts in *kimberlites and lamproites*. Their size ranges from μm to cm. They have predominantly octahedral, dodecahedral, and cubic habit. The content of diamonds is varying in fragments of these rocks from single to hundreds. Mantle diamondiferous eclogite-peridotite rocks are situated at 150-200 km depths and transported by kimberlite and lamproite rocks intrusions to the Earth's surface. Furthermore, kimberlites and lamproites are also sources of its own diamonds (mostly small octahedrons). The content of diamonds in kimberlites and lamproites range from <0.1 to 8 ct/t, with average grade 0.5-2 ct/t for industrial kimberlitic pipes (deposits). Research shows that most diamonds range in age between 1 and 3.3 Ga.

Diamonds from ultra-high pressure rocks of Transition and Lower Mantle (from depths 200-700 km). These diamonds content of unique mineral inclusions with superdense crystal structures: wadsleyite, ringwoodite, majorite Mg-wostite, Mg-perovskite, Ca-perovskite and others The mantle is diamond-bearing substrate at depths of 150-700 km. These ancient diamonds are not cosmic origin, but formed in the depths of the Earth during its formation and evolution.

Diamonds from ophiolites have been extracted from peridotites and chromitites of ophiolites in China, Myanmar, and Russia (Yang, 2014). These diamonds are accompanied by a wide range of highly reduced minerals, such as Ni-Mn-Co alloys, Fe-Si and Fe-C phases, and moissanite (SiC); these have been found as either mineral separates or inclusions in diamonds and indicate growth under superreducing conditions. The diamond-bearing chromite grains likely formed near the mantle transition zone and were then brought to shallow levels in the upper mantle to form podiform chromitites in oceanic lithosphere.

Diamonds in metamorphic rocks discovered in different regions of the World. Early Archean diamonds discovered in the inclusions in zircon from Jack Hills metasedimentary belt of the Yilgarn craton, Western

Australia (Menneken et al., 2007). These highly-frayed zircons are dated at 3-4 Ga (U-Pb dating). Diamond inclusions with size 3-50 μm were identified in 45 zircon in association with graphite, apatite and quartz. These diamonds are oldest found in terrestrial rocks.

Diamond microcrystals (size 15-700 μm, cubic, skeletal and spheroid habit) have been also discovered in: felsic gneisses (age 374-378, 408-425 Ma) in the area of continental collision in Fjørtoft, Western Gneiss region, Norway (Dobrzhinetskaya et al., 1993); the garnet-kyenite schists and eclogite samples from Rhodope Metamorphic Massif (age 186-42 Ma) in Bulgaria and Greece (Mposkos, Kostopoulos, 2001), in gneisses (age 340 Ma) of Erzgebirge, Saxony, Germany (Massonne, 1999); metasediments including garnet-biotite gneisses and schists, garnet-phengite-kyanite schists, garnet-pyroxene rocks and dolomitic marbles (530 Ma) of Kokchetav massif (Dobrzhinetskaya et al., 1994); and (220-240 Ma) at eclogite, garnet-pyroxenite and jadeitite of Dhabi Shan and Su-Lu Metamorphic rocks, China (Xu et al., 1993). Scattered UHP rocks are preserved mainly in eclogites and garnet peridotites enclosed as pods and slabs within metamorphic rocks.

Diamonds in calc-alkaline lamprophyres (minettes) discovered in Wawa subprovince of the Southern Superior Craton, Canada (Lefebvre, 2005). They are dated at 2.67–2.7 Ga and comprise part of a calc-alkaline volcanic sequence of the Michipicoten Greenstone Belt. Minettes represented by dikes with average diamond grade 0.2-1 ct/t. This is alkaline ultra-potassic rock (amount of alkali - 9-13%) with low silica content (40-45%). Holocrystalline massive black rock consists of mainly three minerals K-feldspar (55%), biotite (35%), and apatite (10%). The average size of diamond crystals is 0.5 mm. Habit of crystals is different: round dodecahedron, tetrahexahedron, cubes, and combination forms with rare octahedron and octahedra spinel-twins. Almost all of the crystals are colored: yellow-green, yellow-brown, green, black and other colors. Carbon isotopic composition of diamonds ranges: $\delta^{13}C$ = -2,0 ‰ and -18,0 ‰ at two maxims -5,0 ‰ and -10,0 ‰.

Diamonds in komatiites are discovered Dachine region in French Guiana for which the host rock is volcaniclastic komatiite (age 1.9 Ga) - an unusual type of volcanic rock whose composition and origin are quite unlike those of kimberlite and lamproite. (Capdevila, 1999). The quantity of diamonds in samples is varying from 1 to 77 per kg. Most grains are microdiamonds, but there are some larger (> 1 mm) crystals. The appearance of crystals (the presence of a cube-octahedra), as well as low ratio of carbon isotopes ($\delta^{13}C$ is generally -23-27 ‰) suggest their genesis in typical eclogite formation conditions.

Diamonds in carbonatites have been discovered in Chagatai trachyte-carbonatite complex of Southern Nuratau, Western Uzbekistan (Divaev, 2000). The Triassic age complex formed by a swarm of carbonatites dikes associated with volcanic diatremes. More than 200 grains of diamonds (size 0.02-0.1 mm) extracted from matrix of melanocratic carbonatite. Diamonds are mostly presented by yellowish-greenish octahedrons often distorted.

After consideration of different genetic types of diamonds it is possible to conclude: there are typical spatial and timing scales of these diamond genesis.

According to the spatial scale there are: 1. Diamonds with genesis associated with evolution of cosmic space (cosmic, meteoritic and impact diamonds); 2. Diamonds with genesis associated with geodynamical processes of the Earth evolution (the whole range of diamonds from mantle, kimberlites, lamproites, metamorphic rock, lamprophyres, komatiites and carbonatite complexes).

Accordingly it is possible to suggest a timing scale for these spatial groups: 1. Giant cosmic diamonds (11 Ga) → diamonds from meteorites (4-5 Ga) → impact diamonds (37 Ma – Popigay structure age); 2. Mantle diamonds (4 Ga – diamonds) → metamorphic diamonds (4-0.42 Ga, limited by the residential time of crustal rocks within mantle depths) → diamonds from kimberlites and lamproites (3.3-0.02 Ga) → diamonds from lamprophyres (2.67–2.7 Ga) → diamonds from komatiites (1.9 Ga) → diamonds from carbonatite complexes (0.25-0.2 Ga).

Undoubtedly, this is approximate assessment, but we are going to estimate a timing scale of different diamond types genesis with the improvement of our knowledge about the processes of different rocks formation, their composition, Pt-conditions and other parameters more and more closer to the time of formation, which can be proven accurately.

References:

1. Capdevila, R. Diamonds in volcaniclastic komatiite from French Guiana. Nature, 06/1999. Vol. 399 (6735). 456-458 pp.

2. Deller, A.T., et al. VLBI Astrometry of PSR J2222-0137: A Pulsar Distance Measured to 0.4% Accuracy. The Astrophysical Journal. 2013. Vol. 770.

3. Divaev, F. Chagataisky trachyte-carbonatite complex of Southern Nuratau. PhD thesis. Tashkent. 2000. 27 p.

4. Dobrzhinetskaya, L., et al. A microdiamond from eclogite-gneiss area of Norway. In Proceedings, International Eclogite Conference, 4th, Terra Nova Abstract Supplement: Oxford, Blackwell Scientific. 1993. Vol. 5. P. 9.

5. Dobrzhinetskaya, L., et al. Geology and structure of diamond bearing rocks of the Kokchetav massif (Kazakhstan). Tectonophysics. 1994. Vol. 233. 293-313 pp.

6. Garai, J., et al. Infrared Absorption Investigations Confirm the Extraterrestrial Origin of Carbonado-Diamonds. The Astrophysical Journal Letters. 2006. Vol. 653, L153

7. Kaplan, D.L., et al. A 1.05 M□ companion to PSR J2222-0137: the coolest known white dwarf? The Astrophysical Journal. 2014. Vol. 789.

8. Lefebvre, N., et al. Archean calc-alkaline lamprophyres of Wawa, Ontario, Canada: Unconventional diamondiferous volcaniclastic rocks. Precambrian Research, 2005. Vol. 138. 57–87 pp.

9. Massonne, H.-J. A new occurrence of microdiamonds in quartzofeldspathic rocks of the Saxonian Erzgebirge, Germany, and their metamorphic evolution. Proc. VIIth Int. Kimberlite Conf., Cape Town. 1999. P.H. Nixon Vol., 533-539 pp.

10. Menneken, M., et al. Hadean diamonds in zircon from Jack Hills, Western Australia. Nature. 2007. Vol. 448, 917-920 pp.

11. Mposkos, E.D., Kostopoulos, D.K. Diamond, former coesite and supersilicic garnet in metasedimentary rocks from the Greek Rhodope: a new ultrahigh-pressure metamorphic province established. Earth Planet. Sci. Lett. 2001. Vol. 192, 497-506 pp.

12. Xu, S., et al. Diamond from the Dabie Shan metamorphic rocks and its implication for tectonic setting. Science, 1992. Vol. 256. 80-82 pp.

13. Yang, J. S. et al. Diamonds in Ophiolites. Elements, April 2014. Vol. 10, p. (2): 127-130 pp.

Kimberlite emplacement temperatures: insights from interaction between carbonate-evaporite xenoliths and kimberlites of various volcanic facies

Gaudet M.A.*, Kopylova M.G.*, Kostrovitsky S.I.**, Polozov A.G.***
*The University of British Columbia, Vancouver, Canada, mkopylov@eos.ubc.ca
**Institute of Geochemistry, Irkutsk, Russia
***Institute of Geology of Ore Deposits, Petrography, Mineralogy and Geochemistry, Moscow, Russia

Temperatures of the near-surface emplacement of kimberlites is poorly constrained due to lack of observable kimberlite eruptions and impossibility to reproduce kimberlite crystallization experimentally. One of the indirect ways to have some insights on the temperature of kimberlite melt at the surface is to study how the melt interacts with country rock xenoliths. We studied interaction of carbonate-evaporite xenoliths and the Udachnaya East kimberlite of hypabyssal (HK) and pyroclastic (PK) volcanic facies.

The Late Devonian Udachnaya kimberlite, located in the Yakutian kimberlite province, was emplaced through Late Neoproterozoic- Silurian carbonate and evaporite sequences of the Siberian Platform. Udachnaya HKs contain moderately to strongly serpentinized olivine macrocrysts and phenocrysts in a fine-grained coherent, crystalline groundmass of calcite, phlogopite and lesser serpentine with uniformly distributed spinel, perovskite and magnetite. Udachnaya PKs contain very fresh, angular, deformed olivine macrocrysts, and olivine phenocrysts, in an interclast matrix of irregularly distributed phlogopite, Na-carbonate and lesser spinel, perovskite, magnetite, chromite, +/- crustal chloride xenocrysts, with late deuteric calcite and minor serpentine. PKs show significant heterogeneity in the distribution and mineralogy of the interclast matrix, showing strong correlation with the mineralogy of crustal xenoliths on a local millimeter scale. When salt-bearing xenoliths are not present in the PK, halite is absent from the local interclast matrix. It is therefore suggested to be derived from the disaggregation of crustal xenoliths during emplacement, controlled by abundances of xenolith types.

Four types of upper crustal xenoliths are common in both hypabyssal and pyroclastic kimberlites. These are 1). limestone xenoliths (with minor silicates and Na-carbonates), which may be fossiliferous, bedded or massive;

2). Phlogopite+Na-carbonate - dominated xenoliths; 3). Massive halite-dominated xenoliths; and 4). Dolomite xenoliths with calcite + barian-celestine rims. Halite-dominated xenoliths show 1-3 mm reaction rims in HKs but not in PKs. The margins of the xenoliths show textures typical of salt recrystallization (Grishina et al., 2014), with round sylvite blebs in monomineral halite. Broken fragments of these xenolith margins are present in PKs. Limestone xenoliths show a widely varying mineralogy interpreted as progressive development of silicates and alkaline carbonates due to interaction with kimberlite melt. The development leads to crystallization of Na-carbonates, wollastonite, diopside, phlogopite and kalsilite. The reaction rim consists of zones of halite + sylvite, calcite, anhydrite + iowaite and Ba-celestine. Additionally, olivine macrocrysts and phenocrysts in HK's, proximal to chloride-bearing xenoliths, record a progressive enrichment of Cl in serpentine during serpentinization of olivine from rim to core. These observations suggest a higher temperature of interaction between HK and the carbonate-evaporite xenoliths than between PK and the xenoliths. The higher

temperature enabled incorporation of Cl in the structure of late deuteric serpentine only in coherent kimberlite, but not in colder pyroclastic kimberlite. We also confirm the previous conclusion (Kopylova et al., 2013) that chlorides and alkalis were not a significant component of the primary kimberlite melt, as they do not form halides or alkali-carbonate mineral assemblages in the groundmass of HK.

The study is supported by an NSERC Discovery Grant to Maya G Kopylova.

References:

Grishina, S. N. Polozov A. G., Smirnova, S. Z., Mazurova M. P., and. Goryainov, S. V., 2014. Inclusions in Chloride Xenoliths from the Udachnaya East Kimberlite. Geochemistry International, 52, 7, 595–603.

Kopylova M.G., Kostrovitsky, S.I., Egorov, K. N., 2013. Salts in Southern Yakutian kimberlite and the problem of primary melt composition of the Udachnaya East. Earth Science Reviews, 119, 1-16.

European REE resources: alkaline magmatism and beyond

Goodenough K.M.*, Deady É.A**, Shaw R.A.**, and the EURARE WP1 Team
*British Geological Survey, West Mains Road, Edinburgh EH9 3LA
**British Geological Survey, Environmental Science Centre, Keyworth, Nottingham, NG12 5GG
kmgo@bgs.ac.uk

Europe has resources of many of the critical metals, particularly the rare earth elements (REE); yet economic, environmental and accessibility issues have combined to slow progress toward the exploitation of these resources. The EURARE project, funded by the EU's Seventh Framework programme, brings together a number of partners from across Europe to assess Europe's REE resources and to set the basis for an European REE industry. This talk will describe new research on some of the wide range of potential REE resources within Europe and showcase the diversity of resources available.

The most well-known REE resources in Europe are associated with alkaline magmatism and carbonatites. Recent research and exploration have focused on: 1) agpaitic syenites, including Mesoproterozoic intrusions of the Gardar Province in south Greenland and Norra Kärr in southern Sweden, and the Devonian plutons of the Kola Province; and 2) Palaeozoic to Mesozoic carbonatites across Scandinavia and west Greenland.

However, reviews of European REE resources show that a range of alternative deposit types are also of interest for their REE enrichment. In many cases, the REE in these localities could be produced as a by-product of another commodity, and these might therefore represent important opportunities to diversify European REE supply. Such deposit types include hydrothermal mineralisation associated with alkaline magmatism; placers associated with alkaline magmatism; and bauxites.

Hydrothermal mineralisation associated with alkaline magmatism

The largest REE deposits known in Europe are associated with large bodies of agpaitic syenite. However, many alkaline intrusions across Europe are miaskitic in composition and thus REE minerals are limited within the main body of the intrusion. Such intrusions commonly include late-stage pegmatitic sheets and/or hydrothermal veins that may be enriched in REE minerals. A classic example is the Triassic Ditrău Alkaline Complex in Romania, which has late-stage REE-rich mineral veins that include minerals such as bastnäsite, parisite, synchysite, apatite, allanite, monazite and xenotime in association with sulfides, carbonates and a wide range of other minerals. Our ongoing research is investigating the origin of these mineral veins and their relationship to the host alkaline magmatism.

Placers associated with alkaline magmatism

Intraplate, alkaline magmatism has developed throughout much of Europe during the Cenozoic, particularly around the margins of the Alpine collisional zone and along the Mediterranean. The surface expression of this alkaline magmatism commonly includes volcanic rocks of basanitic and alkali basaltic composition, and associated pyroclastic rocks. In many areas these eruptive products contained a range of heavy minerals that have been concentrated into fluvial and marine sediments: a well-known example is the Nettuno placers in Italy. In Turkey, heavy minerals derived from the Gölcük alkaline volcano are thought to have been concentrated in the placer deposit at Çanakli, which has been explored by AMR Mineral Metal Inc. for a range of metals. Our ongoing research looks at the link between the placer and the volcano, in order to assess the potential for low-grade REE enrichment in the wider areas around alkaline volcanoes.

Bauxites

Large resources of bauxite are well known across Europe, particularly in the Mediterranean region. Karst-type bauxites typically contain elevated concentrations of REE, in the form of authigenic REE-bearing minerals formed during the process of bauxitisation. The processing of bauxite to alumina, through the Bayer Process, produces a vast quantity of waste material known as red mud, which is stored in large onshore tailing ponds

across Europe. REE originally in the bauxite ore are transferred to these red muds and hence represent a potential unexploited REE resource for Europe. Our ongoing research is investigating the potential low-grade, high-tonnage REE resources found in red mud, with a particular focus on deposits in Turkey and Greece.

Petrogenesis of EL-Kahfa Ring Complex Eastern Desert, Egypt

Hegazy H.A.
Geology Department - Assiut University, Egypt
E.mail: hhegazv4451@vahoo.com
Mobile: +201227831604

El kahfa Ring Complex (ERC) is a member of an alkaline province including complexes of similar size, structure and composition which crop out along the western margin of the Red Sea in Egypt. ERC (5x6 km) occurs as oval intrusion, rising up to 1018 m.a.s.l. at the intersection of latitude 24° 08′ 18″and longitude 34° 38′55″ belongs to the youngest group of Phanerozoic ring complexes having an emplacement age of 92±5 Ma (Serecsists et al. 1981; lutz et. al. 1988). It is related to structural lineament trending N 30 W parallel to the Red Sea and was controlled by pre-existing deep crustal lines of weakness in the basement complex.

Field investigation revealed that ERC is composed of two intrusive phases, i.e. oldest one represented by essexite gabbros, intruded later by syenitic rock. The latter formed of inner zone of undersaturated syenites (i.e. Litchlleldite and cancrinite syenites), while the outer ring massif is composed of silica oversaturated syenites. The extrusive rocks of trachyte, basalt and rhyolite form plugs, sheets and ring dykes.

The mineralogical and chemical features show that these rocks belong to anorogenic interplate A-type alkaline suite (i.e. enriched in alkalis and HFS elements, Nb, Ta, Zr, Hf, Y, HREE). The Y/Nb and Ce/Nb ratios suggest fractional crystallization of primary source of picritic-like basaltic magma in the asthenospheric mantle. Oversaturated liquid is an excellent demonstration of the strong fractionation of saturated magma, while undersaturated magma may evolve in a rather similar way dominantly by fractionation of feldspar until the nepheline feldspar coetectic is reached. Later iron-rich sodic (amphibole and pyroxene) and potassic (micas) minerals are of intercumulus origin and the result of magmatic differentiation; they appear often as subsolidus assemblages, sensitive to oxygen fugacity and to the water content of vapor phase. Simplified modeling of magma evolution within Petrogeny's Residue System demonstrates the ability of ACF processes to cause a critically undersaturated magma to evolve across the feldspar join and produce oversaturated rocks.

The gemstone (diamond and sapphire) potential of lamprophyres in the North Atlantic Craton – examples from Northwest Scotland

Hughes J.W.*, Faithfull J.**
*University of St Andrews, Fife, United Kingdom
**The Hunterian Museum, University of Glasgow, United Kingdom
Author E-mail: josh_hughes25@hotmail.com

In recent decades there has been a realisation that lamprophyres are associated with a variety of mineral deposits including diamond, gold, sapphire and possibly even PGE (e.g. Rock and Groves, 1988). The occurrence of diamond in any other rock than kimberlite was for many years treated as a mineralogical oddity rather than of any commercial importance. This was finally laid to rest by discovery of the diamondiferous Argyle lamproites in Australia, a classic example of an obscure and largely ignored rock type jumping to prominence after being found to have major economic significance. In the last 30 years, further discoveries of diamond in other host rocks, including lamprophyres, has highlighted that there is a substantial lack of research into determining how far the field of diamondiferous rocks extends and what implications this has on traditional exploration techniques.

This is further complicated by the confused classification of lamprophyres; the result of nearly two centuries of misunderstanding in which the term lamprophyre was applied to any porphyritic mafic igneous rock that could not be easily classified. This resulted in a proliferation of locality-specific rock types. In part this is due to each individual craton having its own "flavour", whereby its magmatism is a combination of the cratons

metasomatic history, along with additions from the surrounding asthenospheric mantle. The North Atlantic Craton (NAC) is typified by the predominance of aillikite (the carbonate-rich endmember of the ultramafic lamprophyre clan), which macroscopically resembles kimberlite and is commonly associated with, and grading into carbonatite. Despite aillikite not being a conventional primary diamond host rock, there are numerable examples of aillikite-hosted diamond deposits within the NAC, some of which host sub-economic grades, for example in West Greenland (e.g. Hutchison and Frei, 2009) and Labrador (e.g. Digonnet et al., 2000), demonstrating that aillikite magmatism has the potential to sample diamondiferous portions of the SCLM. Tappe *et al.* (2011) coined the term the '*Greenland-Labrador Diamond Province*' (or GLDP), on account of both diamondiferous regions representing fragments of the NAC.

The **Glen Gollaidh aillikite dyke** has intruded psammites of the Moine Supergroup a few km east of the Moine Thrust at Glen Gollaidh in the NW Highlands of Scotland. Trending ESE-WNW, the dyke ranges from 0.2 – 1 metre in width and is exposed in a series of meandering stream cuts over a distance of nearly 300 metres. Although not strictly "on-craton", the location of the dyke within the marginal cratonic cover sequences rationally implies that it is underlain by Archaean SCLM. The dyke represents the closest analogue to a potentially diamond-bearing intrusion described from the United Kingdom (UK) to date. With further exploration the potential exists for an extension of the GLDP, to include the Scottish fragment of the NAC, hence the '*Greenland-Labrador-Scotland Diamond Province*'.

We have shown unambiguously, based upon geochemistry, mineralogy and mineral chemistry, the dyke classifies as an aillikite permitting to the strict criteria defined in the recently proposed ultramafic lamprophyre classification scheme of Tappe *et al.* (2005). It is a composite and shows considerable internal variation in mineralogy and texture along strike, from carbonate-poor lithologies with fresh olivine macrocrysts, grading into silico-carbonatite. The mineralogy encompasses of serpentinised and carbonated (occasionally unaltered) olivine macrocrysts and phenocrysts, primary carbonate, phlogopite zoned to tetraferriphlogopite, apatite, magnesiochromite-magnetite spinels, diopsode, perovskite, ilmenite, barite, pyrite and various other opaque phases some of which are Ti, REE and Zr-rich. The dyke also contains abundant spinel lherzolite xenoliths, up to 3 cm in width and in various stages of disaggregation. Although REE geochemistry indicates the dyke may have originated from within the garnet stability field. Ar-Ar dating of phlogopite has yielded a plateau age of 357±7Ma (Carboniferous), which does not match any currently reported dates for similar rocks from Greenland or Labrador, or for any Scottish alkaline intrusions, but may suggest an association with the early Carboniferous Birrenswark lavas in the Scottish Borders, and perhaps with altered ultramafic/carbonate-rich rocks reported from western Ireland. Sr and Nd isotopes suggest source mantle similarities to those recorded in the younger Streap Comhlaidh and Loch Roag dykes of NW Scotland.

The **Loch Roag monchiquite dyke** intruded Archaean Lewisian gneisses near Carishader on the Isle of Lewis, Scotland. Trending ENE-WSW, the dyke ranges from 0.5 to 1.5 metres in width. The marginal portions of the dyke are fine-grained and aphanitic while the axial zone is crowded with xenoliths of assorted petrology and a diverse suite of xenocryts (Menzies *et al.*, 1987). The Loch Roag has been shown to contain xenocrysts of euhedral sapphire, generally ranging from 1-3 cm of mostly gem quality although their colour can be variable. Generally the smaller crystals are of the desired fine blue colour, becoming more variable through increasing size with regions of green, blue and occasionally yellow. The largest sapphire recorded was 39 carats, producing a 9.6 carat cut stone of fine blue colour known as the '*Saltire Sapphire*', which in 1995 sold for a reported £65,000.

Menzies *et al.* (1989) report a biotite K-Ar age of 46.9 Ma (Eocene), rendering it the youngest onshore igneous intrusion in the UK. The age has been contested on account of the composition and orientation being more typical of Permian dykes that are prevalent through the NW Highlands of Scotland. However the age has been confirmed by recent re-dating (Faithfull *et al.*, *in press*). This demonstrates that enriched SCLM was able to survive beneath NW Scotland unaffected by the magmatism of the British Palaeogene Igneous Province during the opening of the Atlantic. The sapphires have also been dated and shown to be broadly coeval with the dyke itself, implying that they crystallised from a peraluminous precursor melt at, or shortly before, their entrainment by the monchiquite magma. Etching and resorption textures indicate that the sapphires were out of equilibrium with the carrier melt. The Loch Roag and Glen Gollaidh dykes, along with other lamprophyres in northwest Scotland are typically enriched in Nb. This is in contrast to the calc-alkaline Caledonian lamprophyres (Silurian - early Devonian) of Scotland that have negative Nb anomalies typical of subduction zone settings.

Meyer and Mitchell (1987) describe a similar lamprophyre-hosted sapphire deposit at Yogo Gulch, Montana, U.S.A. hosted in ouachitite (a biotite-rich monchiquite lamprophyre). This occurrence is one of the few igneous rocks from which sapphire is mined; the majority of the world's sapphire production is from alluvial deposits. However the Yogo sapphires are attributed to the re-crystallisation of aluminous mudstones incorporated into the melt at depth, analogous to the formation of the Loch Scridain sapphires from Mull, Scotland that formed from the contact metamorphism of alumina-rich shales. Unlike Yogo Gulch and Loch Scridain, the Loch Roag sapphires are believed to originate from the break up of peraluminous pegmatites in the upper mantle or lower crust (Upton et al., 2009).

References:

Digonnet, S., Goulet, N., Bourne, J., Stevenson, R., and Archibald, D. (2000) Petrology of the Abloviak aillikite dikes, New Québec: evidence for a Cambrian diamondiferous province in northeastern North America. *Canadian Journal of Earth Sciences*, v. 37, pp. 517-533.

Menzies M. A., Halliday A. N., Palacz Z., Hunter R. H., MacIntyre R. M., and Upton B. J. G. (1986) The age, composition and significance of a xenolith-bearing monchiquite dike, Lewis, Scotland. In: Ross J., Jaques A. L., Ferguson J., Green D. H., O'Reilly S. Y., Danchin R. V., and Janse A. J. A. Kimberlites and related rocks (Vol. 2). Proceedings of the IVth International Kimberlite Conference, pp. 843-852.

Meyer H. O. A., and Mitchell R. H. (1988) Sapphire bearing ultramafic lamprophyre from Yogo, Montana: an ouachitite. *Canadian Mineralogist*, v. 26, pp. 81-88.

Rock N. M. S., and Groves D. I. (1988) Do lamprophyres carry gold as well as diamonds? *Nature* v. 332, pp. 253-255.

Upton B. G. J., Finch A. A., and Slaby E. (2009) Megacrysts and salic xenoliths in Scottish alkali basalts: derivatives of deep crustal intrusions and small-melt fractions from the upper mantle. *Mineralogical Magazine*, v. 76 (6), pp. 943-956.

Hutchison, M. T., and Frei, D. (2009) Kimberlite and related rocks from Garnet Lake, West Greenland, including their mantle constituents, diamond occurrence, age and provenance. *Lithos*, v. 112, pp. 318-333.

Tappe, S., Foley, S. F., Jenner, G. A., and Kjarsgaard, B. A. (2005) Intergrating ulramafic lamprophyres into the IUGS classification of igneous rocks: rationale and implications. *Journal of Petrology*, v. 46, pp. 1893-1900.

Tappe, S., Pearson, D. G., Nowell, G., Nielsen, T., Milstead, P., Muehlenbachs, K. (2011) A fresh look at Greenland kimberlites: cratonic mantle lithosphere imprint on deep source signal. *Earth and Planetary Science Letters*, v. 305, pp. 235-248.

Geology and mineralisation of the Jurassic (165 Ma) Qeqertaasaq Carbonatite Complex, West Greenland

Hughes J.W.*,**, Goodenough K.M.***, Finch A.A.*
*University of St Andrews, Fife, United Kingdom
**NunaMinerals A/S, Nuuk, Greenland
***British Geological Survey, Edinburgh, United Kingdom
Author E-mail: josh_hughes25@hotmail.com

The Qeqertaasaq (formerly "Qaqarssuk") carbonatite complex is located 135 km NE of the Greenlandic capital, Nuuk near the town of Maniitsoq. The complex is situated within the Fiskefjord Block of the Archaean (3.8 – 2.55 Ga) West Greenland North Atlantic Craton (WG-NAC; Windley and Garde, 2009). The NAC is also exposed in the Nain Province of Labrador and the Lewisian of North West Scotland. The WG-NAC has been subject to extensive and prolonged, yet episodic alkaline magmatism, this includes several large carbonatite complexes and extensive ultramafic lamprophyre (var. aillikite) and rare kimberlite (*sensu stricto*). From North to South, the carbonatite complexes comprise **Sarfartôq** (564 Ma; Secher *et al*., 2009), **Tupertalik** (3 Ga; Bizzarro, 2002), **Qeqertaasaq** (165 Ma; Secher *et al*., 2009) and **Tikiusaaq** (158-155 Ma; Tappe *et al*., 2009). Tupertalik is acknowledged as the world's oldest known carbonatite (Bizzarro, 2002) and is broadly coeval with the Maniitsoq impact structure (Garde et al., 2012).

The Jurassic Qeqertaasaq and Tikiusaaq complexes are thought to result from continental rifting prior to the opening of the Labrador Sea (Secher *et al*., 2009; Tappe *et al*., 2009) with evidence that both complexes were emplaced in zones of active deformation. Qeqertaasaq was emplaced at the boundary between Archaean TTG basement gneisses and the younger Finnefjeld Domain which was recently interpreted as the remains of the world's oldest (2975 Ma) and most deeply eroded impact structure (Garde *et al*., 2012). The Greenland Norite

Belt (GNB) and post-kinematic diorites form a 75 x 15 km curvilinear belt east of the impact centre of crustally contaminated mantle melts considered to have been triggered by impact (Garde *et al*., 2012). The GNB is currently the focus of Ni-Cu-PGE exploration by North American Nickel Inc. The GNB appears to have been emplaced into a magma conduit system that followed deep seated structures, which were likely induced by the impact event. These deep seated structures were later reactivated during extensional tectonics in the Jurassic and exploited by the carbonatite magmas at Qeqertaasaq.

Since 2009, Greenlandic exploration company NunaMinerals A/S and exploration partner Korea Resources Corporation, have been exploring Qeqertaasaq for rare earths elements (REE) and niobium (with phlogopite mica, phosphorous, tantalum, strontium and zirconium as important potential by-products).

Original mapping of Qeqertaasaq by Knudsen (1991) indicated that the 3 x 5 kilometre complex was formed of arcuate to subcircular intrusions of carbonatite in a composite quasi-ring dyke pattern focussed upon two intrusive centres situated in the SE and NW of the complex with varying amounts of alkali metasomatism (fenitisation) of the screens of basement gneiss between the carbonatite dykes. Knudsen (1991) advocated that all silicate rocks within the complex represented variably fenitised basement. The complex is relatively poorly exposed in comparison to the surrounding gneisses, with the carbonatite lithologies weathering to form a thick soil profile that tends to be highly vegetated due to the high phosphorous content. Recent mapping by the authors suggests that the individual units cannot be mapped out with the level of certainty inferred by Knudsen (1991), and the complex is transected by major faults that were not previously recognised by earlier workers. The whole of the complex is cut by late faults which form major lineaments, in places clearly observed offsetting geological units. The dominant trend is ENE-WSW, which is typical for this part of the WG-NAC and represents a set of faults and shear zones that have been reactivated multiple times. The most significant faults in the complex (namely the "Banana Lake North" & "Banana Lake South" faults) are considered to be an important control on the migration of later magmas and fluids through the complex.

The reappraisal has also shown that the carbonatites can be divided into two principal suites. The central part of the complex is dominated by banded and foliated calcite-phlogopite carbonatites and silicocarbonatites, and ultramafic rocks dominated by phlogopite and/or alkali amphiboles. Together these are termed the "*early-carbonatite suite*". This suite forms a major sill (or set of sills) intruded into the basement gneisses forming a broad dome with its core on the north shore of Banana Lake. The banding dips away from the core in all directions and in some areas the banding is folded with the development of a second cleavage indicating that the early carbonatite suite was deformed during and after emplacement, probably due to uplift on the ENE-WSW faults. Intensely sheared carbonatites around the margins of the complex form sheets cutting through the basement gneiss and enclosing abundant basement xenoliths, these are termed the "*xenolithic carbonatite suite*". The xenolithic suite is considered to represent pathways through which the carbonatite magma rose to higher levels in the crust yielding the early carbonatite suite. Marginal selvages around basement xenoliths indicate crustal assimilation occured. All of the lithologies are cut by a series of discreet sheets and veins. The earliest of these are the "*actinolite-magnetite-calcite (AMC) carbonatite sheets*", themselves commonly strongly foliated and containing appreciable concentrations of niobium with coarse grained visible pyrochlore group minerals (PyGM). The AMC sheets are concentrated along the Banana Lake South Fault, broadly parallel with the fault but with shallower dips. Later undeformed sheets that are observed cutting earlier carbonatites, include coarse-grained calcite carbonatites (late sövites) and lastly vuggy carbohydrothermal REE veins. An undeformed xenolith-rich lamprophyre dyke is observed cutting the xenolithic carbonatite at a high angle in the NW of the complex and clearly post-dating all deformation. The late stage sövites host a titanomagnetite-apatite-phlogopite-alkali amphibole-PyGM-zircon-carbonate rock that resembles phoscorite (locally up to 15 wt% Nb_2O_3, 35% P_2O_5 and 4.7 % Zr).

The REE-veins are predominantly focused to the north of the Banana Lake Faults within the core of the complex, and trend parallel or perpendicular to the ENE-WSW faults clearly exploiting existing structural weaknesses. The REE-rich fluids are thought to have migrated from the Banana Lake faults, rising up to the core of the complex into the early carbonatite suite and trapped below a cap of basement gneiss forming REE veins. The REE veins occur as steeply dipping veins up to several metres in width (rarely swell to tens of metres) and can be traced in drill core several hundred metres in strike, with a maximum grade of 13.2% total rare earth oxides (TREO) recorded. The REE-veins are thought to represent the transition from late-stage magmatic to hydrothermal, typically characterised by the following assemblage: **[i]** a tetraferriphlogopite reaction selvedge when in contact with fenitised gneiss (generally absent where cutting earlier phases of carbonatite); **[ii]** texturally variable, coarse grained calcite-dolomite carbonatite representing the inferred magmatic component of the mineralisation, with accessory quantities of the rare earth minerals (REM) ancylite-(Ce) and donnayite-(Y); **[iii]** transition of the calcite-dolomite carbonatite into a rose-pink, vuggy, predominantly massive LREE-dominated carbohydrothermal product, consisting chiefly of intimately intergrown paralstonite and ancylite-(Ce) forming irregular, porous aggregates with accessory qaqarssukite-(Ce) [BaCe(CO$_3$)$_2$F], alstonite, strontianite, barite and a later generation of calcite, markedly enriched in Ba and Sr. SEM analysis reveals botroyoidal clusters of paralstonite in **[iii]** suggesting rapid precipitation from a fluid dominated system. The calcite-dolomite

carbonatite component **[ii]**, commonly contains 'dogstooth' calcite up to 10cm in length, with fan-shaped extinction and occasional exsolution blebs of the REM, ancylite-(Ce) and burbankite. The crystals form perpendicular to the margin of the veins (reminiscent of unidirectional solidification textures observed in granitic pegmatites) indicating crystallisation from a volatile-rich melt. The REE-veins also contain variable concentrations of pyrite, galena, sphalerite, pyrrhotite, chalcopyrite and hessite [Ag_2Te] with some unidentified sulphides. The Qeqertaasaq carbonatite complex is the type locality for the REM, qaqarssukite-(Ce) first described by Grince *et al.* (2006). Zonation of qaqarssukite-(Ce) records the geochemical evolution of the carbohydrothermal fluids, with a MREE-enriched core and LREE-rich, MREE-poor rim. However ancylite-(Ce) is the principal REM at Qeqertaasaq. REE-veins are porous and possess an increased susceptibility to weathering in comparison to earlier carbonatite lithologies, hence outcropping REE-veins are interpreted to grossly underestimate the true volume of REE mineralisation.

References:

Bizzarro M., Simonetti A., Stevenson R.K., and David J. (2002) Hf isotope evidence for a hidden mantle reservoir. Geology, v. 30, pp. 771-774.

Garder A.A., McDonald I., Dyck B., and Keulen N. (2012). Searching for giant, ancient impact structures on Earth: The Mesoarchaean Maniitsoq structure, West Greenland. Earth and Planetary Science Letters, v. 337-338, pp. 197-210.

Grince J.D., Gault R.A., and Rowe R. (2006). Qaqarssukite-(Ce), a new barium cerium flurocarbonate mineral species from Qaqarssuk, Greenland. The Canadian Mineralogist, v. 44, pp. 1137-1146.

Knudsen C. (1991). Petrology, geochemistry and economic geology of the Qaqarssuk carbonatite complex, southern West Greenland. Monograph Series on Mineral Deposits 29. Berlin: Gebrüder Borntraeger

Secher K., Heaman L.M., Nielsen T.F.D., Jensen S.M., Schjoth F., and Creaser R.A. (2009) Timing of kimberlite, carbonatite, and ultramafic lamprophyre emplacement in the alkaline province located 64º – 67º N in southern West Greenland. Lithos, v. 112S, pp. 400-406.

Tappe S., Steenfelt A., Heaman L.M. and Simonetti A. (2009) The newly discovered Tikiusaaq carbonatite-aillikite occurrence, West Greenland, and some remarks on carbonatite-kimberlite relationships. Lithos, v. 112S, pp. 385-399.

Windley B.F. and Garde A.A. (2009) Arc-generated blocks with crustal sections in the North Atlantic Craton of West Greenland: Crustal growth in the Archaean with modern analogues. Earth Science Reviews, v. 93, pp. 1-30.

The first results of the melt inclusion study of phonolite dykes from Kovdor massif (Kola Peninsula)

Isakova A.T.*, Arzamastsev A.A.**, Rokosova E.Yu.*
*V.S. Sobolev Institute of geology and mineralogy SB RAS, Novosibirsk, Russia,
**Institute of Precambrian Geology and Geochronology, RAS, Saint-Petersburg, Russia
atnikolaeva@igm.nsc.ru

The Paleozoic dykes within Kovdor massif are located in the exocontact aureole of fenites and are confined to the system of ring and conical faults, dipping towards the intrusion at steep angles (Arzamastsev et al., 2009). The object of our study is the phonolite dyke. At the present time, the methods of the thermobarogeochemistry (melt inclusion study) are widely used to obtain information about the genesis of rocks and the physico-chemical conditions of crystallization.

This type of information has been received for the first time for the dyke phonolite of the massif, which are composed of phenocrysts of clinopyroxene, nepheline, apatite, mica and groundmass, including predominantly these minerals as well as potassium feldspar and ore minerals. The chemical composition of the rock varies and contains 47.5-52.4 wt.% SiO_2, 0.5-0.8 wt.% TiO_2, 16-18.3 wt.% Al_2O_3, 4.8-4.9 wt.% FeO, 0.1-0.2 wt.% MnO, 1.5-2.8 wt.% MgO, 3.7-6.6 wt.% CaO, 9.1-9.7 wt.% Na_2O, 3.4-4.2 wt.% K_2O, and 0.5-1.1 wt.% P_2O_5. This variation in the chemical composition is explained by the different proportion of the same minerals in analyzed samples. The clinopyroxene phenocrysts in the considered rock has an elongated prismatic form, varying composition from diopside (Mg/Mg+Fe 62-64), and augite (Mg/Mg+Fe 55-67) to aegirine-augite (Mg/Mg+Fe 47-54, 17-21 % aegirine and 6-9 % jadeite components). Phenocrysts of nepheline are less common in the rock, their composition is 76.5-79 % Ne, 19.5-23.4 % Ks, 0.1-1.5 % Q. Mica is represented by biotite with Mg/Mg+Fe 49-54 in the rock. Apatite comprises 0.7-0.9 wt.% SrO and 1.7-2.1 wt.% F.
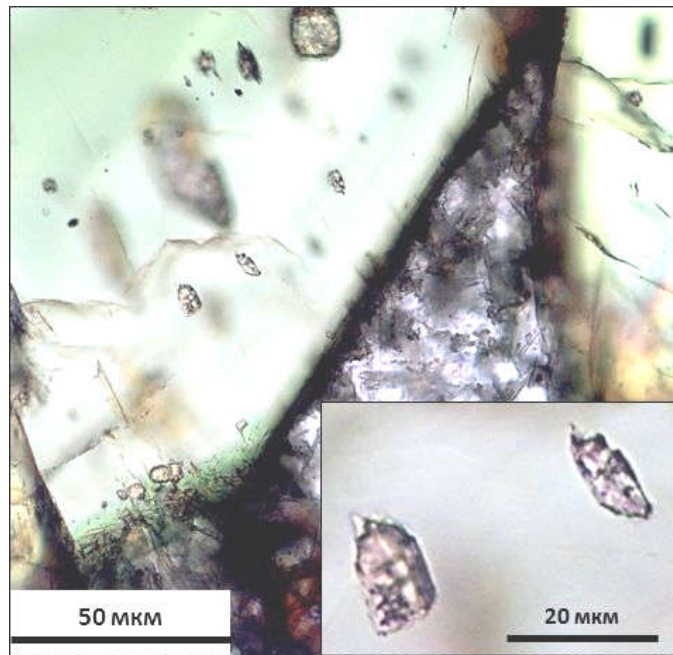
Figure 1. The primary melt inclusions in the clinopyroxene phenocrysts. Transmitted light image.

Phenocrysts of clinopyroxene contain primary melt inclusions, which are found singly and within the growth zones of the host mineral (fig. 1). They are studied by us in order to obtain the information about initial melts. The size of melt inclusions is about 10-20 μm, the form is close to the elongated oval (fig. 1). The melt inclusions in clinopyroxene are crystallized. The scanning electron microscope identified the following crystalline daughter phases in inclusions: biotite, nepheline, potassium feldspar, and apatite.

During heating experiments at 550-650 °C the contents of the inclusions begin to melt. At 700-750 °C the gas phase is transformed into a bubble, which begins to shrink at 1050-1100 °C. At higher temperatures (1100-1150 °C) the heating experiment is stopped because of the possibility of the inclusion decrepitation. Hence, the crystallization of clinopyroxene phenocriysts occurred at obviously higher temperatures.

The chemical composition of the homogeneous glasses quenched at the mentioned temperature varies and contains (wt.%) 50.2-58.5 SiO_2, 0.4-0.8 TiO_2, 14.1-20.2 Al_2O_3, 4.4-7.7 FeO, 0.7-2.1 MgO, 2-5.4 CaO, 6.3-10.1 Na_2O, 1.6-4.8 K_2O, as well as up to 0.3 MnO, up to 0.5 BaO, up to 0.3 P_2O_5, up to 0.3 SO_3, up to 0.3 Cl. This composition corresponds to that of the average nepheline-bearing phonolite (Andreeva et al., 1883). This is clearly seen in the binary diagram (fig. 2), where the content of the main components in the glasses with low SiO_2 is consistent with that of the considered rock. In addition, the amount of Al_2O_3 and CaO increases and that of TiO_2 and K_2O decreases in the chemical composition of glasses with an increase in SiO_2. This reflects the fractional crystallization processes in the melt.

It should be noted that phenocrysts of clinopyroxene contain secondary melt inclusions, which are trapped during the healing of the fractures. Their chemical composition compared to that of primary melt inclusions contains similar Na_2O (4.7-10.8 wt.%), more SiO_2 (59.8-67.6 wt.%), Al_2O_3 (17.4-21.8 wt.%), K_2O (2-6.8 wt.%), and less FeO (0.4-1.5 wt.%), MgO (0.5-0.7 wt.%), and CaO (0.7-2.3 wt.%). Hence, the composition of melt inclusions is obviously much more differentiated.

Therefore, melt inclusion study suggest that the clinopyroxene crystallized at temperatures higher than 1100-1150 °C from phonolitic melt. The composition of initial melt varies during crystallization with increasing of SiO_2, Al_2O_3, and K_2O contents and decreasing FeO, MgO и CaO contents.
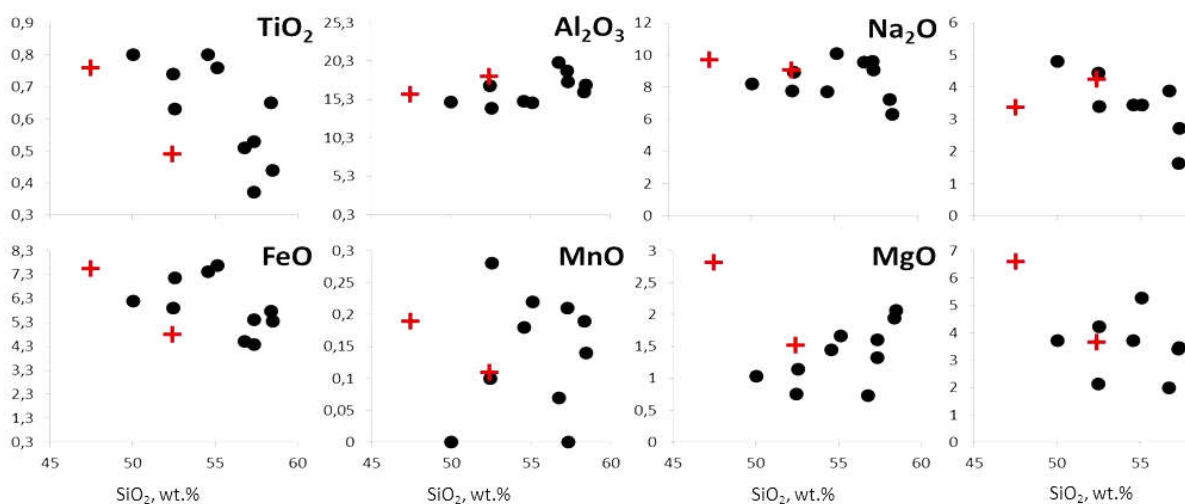
Figure 2. Relationship between the concentrations of SiO$_2$ and major oxides in glasses of heated melt inclusions of clinopyroxene (circles) and considered dyke phonolite (crosses) of the Kovdor massif.

References:

Andreeva E.D., BaskinaV.A., Bogatikov O.A. et al. Igneous rocks: V. 1. The classification, nomenclature, petrography. M.: Nauka, 1983. 767 p.

Arzamastsev A.A., Fedotov A.A., Arzamastseva L.V. Dyke magmatism of the north-eastern part of the Baltic Shield. SPb.: Nauka, 2009. 383 p.

Deep carbon connection to long-term enrichment of rare earth elements in the Earth's crust

Jones A.P.

Dept. of Earth Sciences, University College London, Gower St, London WC1E 6BT UK

adrian.jones@ucl.ac.uk

The mobility of carbonatitic melts and fluids in the mantle has been linked to metasomatism, alkaline magmatism and the transport of incompatible elements including the REE, and Nb. For example, residual low-temperature carbonatite melts become enriched in volatiles, and can have a high solubility for rare earth elements (REE), enabling precipitation of primary magmatic REE phases. A brief review of the Earth's deep carbon will draw attention to the international effort being made to quantify the fluxes and reservoirs for carbon through time (The Deep Carbon Observatory, DCO). At a planetary perspective there is growing evidence for heterogeneous accretion of the Earth and a complex delivery of volatiles, which now include newly recognised hydrous phases like shocked-clay minerals in meteorites. The complicated geological processes recorded in the lithosphere and crust are widely explained by internal endogenic processes and mantle geodynamics related to plumes, but the survival of impact heterogeneities from the late heavy bombardment also need to be considered, including the role of impact structures in the formation of some giant economic deposits (eg: Sudbury, Canada). Major geological exploration programs which combine radiometric age-dating with mineralogical and geochemical observations of natural systems are very important to identify significant regional events, and to establish global correlations in Earth history, which ultimately must connect with Earth system models.

A brief description of Greenland alkaline magmatism in the Gardar Province provides an important comparison with Kola peninsula, and the detailed geological processes which lead to lujavrites and economic mineralization. In Greenland, a supra-crustal sequence of contemporary alkaline volcanism suggests development of an ancient alkaline rift with many similarities to modern continental rifts. However, we may question if it is sufficient to understand only a petrogenetic model for the development of economic mineralization, or whether new techniques might be developed to determine whether or not such regional mineralization might also be relics of more ancient lithospheric heterogeneities?

New models for kimberlite parental melts: composition, temperature, ascent and emplacement

Kamenetsky V.S.*, Golovin A.V.**, Maas R.***, Yaxley G.M.****, Kamenetsky M.B.*
*University of Tasmania, Hobart, Australia, Dima.Kamenetsky@utas.edu.au
**V.S. Sobolev Institute of Geology and Mineralogy, Novosibirsk, Russia
***University of Melbourne, Melbourne, Australia
****Australian National University, Canberra, Australia

Kimberlites represent magmas derived from great mantle depths and are the principal source of diamonds. Kimberlites and their xenolith cargo have been extremely useful for determining the chemical composition, melting regime and evolution of the subcontinental mantle. Significant effort has gone into characterizing styles of emplacement, ages, petrography, mineralogy, textural and compositional characteristics, and the tectonic setting of kimberlites. However, a full understanding of kimberlite petrogenesis has been hampered by effects of pre-emplacement contamination, syn-emplacement stratification and syn/post-emplacement alteration of kimberlite rocks, all of which tend to hinder recognition of primary/parental kimberlite magma compositions. The prevailing practice of using bulk kimberlite compositions to derive parental compositions has been challenged by research on the Devonian Udachnaya-East pipe and other relatively fresh kimberlites worldwide.

Since its discovery in 1956, the Udachnaya kimberlite pipe has become a "type locality" for geochemists and petrologists studying mantle rocks and mantle physical-chemical conditions. Apart from hosting a diverse suite of extremely well-preserved mantle xenoliths, the host kimberlite (East body) is the only known occurrence of fresh kimberlite, with secondary serpentine almost absent and uniquely high Na_2O and Cl (up to 6.2 wt.%) and low H_2O (< 1 wt.%) contents. The discovery of such compositional features in the only unaltered kimberlite has profound implications for models of parental kimberlite magma compositions, and the significance of the high Na and Cl abundances in the Udachnaya-East pipe has therefore been subjected to vigorous criticism. The main argument against a primary magmatic origin of high Na - Cl levels involves the possibility of contamination by salt-rich sedimentary rocks known in the subsurface of the Siberian platform, either by assimilation into the parental magma or by post-intrusion reaction with saline groundwaters.

The main evidence against crustal contamination of parental kimberlite magmas is that the serpentine-free varieties of the Udachnaya-East kimberlite owe their petrochemical and mineralogical characteristics to a fortuitous lack of interaction with syn- and post-magmatic aqueous fluids. The groundmass assemblage of this kimberlite, as well as earlier-formed melt inclusions, contains alkali carbonate, chloride and other Na- and Cl-bearing minerals. This mineralogy reflects enrichment of the parental melt in carbonate, chlorine and sodium. The combination of low H_2O, high alkali-Cl abundances, lack of serpentine, and the presence of alteration-free mantle xenoliths all indicate that the Udachnaya-East kimberlite preserves pristine compositions in both kimberlite and mantle xenoliths. Evidence for broadly similar chemical signatures is found in melt inclusions from kimberlites in other cratons (South Africa, Canada, Finland and Greenland). We demonstrate that two supposedly "classic" characteristics of kimberlitic magmas - low sodium and high water contents - relate to postmagmatic alteration. The alkali- and volatile-rich compositions of melt inclusions is responsible for low-temperature phase transformations during heating experiments, melting at <600°C, carbonate-chloride liquid immiscibility and homogenisation temperatures at ~650-800°C, well below the solidus of the high-Mg melt that is traditionally inferred to be primary kimberlite composition. Notably, records of heating stage experiments with melt inclusions from different kimberlites are broadly similar.

Previously inferred high liquidus temperatures (>1400°C) are inconsistent with geological evidence (e.g., absence of thermometamorphic effects), temperatures in the potential mantle source and melt inclusion data. We consider the protokimberlite liquid to be low temperature near the surface (<800°C), virtually anhydrous, aluminosilicate-poor, Na-Ca carbonate, enriched in lithophile trace elements, halogens, and sulphur. Although kimberlite magmas are dense in crystals and deeply-derived rock fragments, they ascend to the surface extremely rapidly, enabling diamonds to survive. The unique physical properties of kimberlite magmas depend on the specific compositions of their parental melts. We explain exceptionally rapid ascent of kimberlite magma from mantle depths by combining empirical data on the essentially carbonatite composition of the kimberlite primary melts and experimental evidence on interaction of the carbonate liquids with mantle minerals. Our experimental study shows that orthopyroxene is completely dissolved in a Na_2CO_3 melt at 2.0 to 5.0 GPa and 1000-1200°C. The dissolution of orthopyroxene results in homogeneous silicate-carbonate melt at 5.0 GPa and 1200°C, and is followed by unmixing of carbonate and carbonated silicate melts and formation of stable magmatic emulsion at lower pressures and temperatures. The dispersed silicate melt has a significant capacity for storing a carbonate component in the deep mantle (13 wt% CO_2 at 2.0 GPa). This component reaches saturation and is gradually released as CO_2 bubbles, as the silicate melt globules are transported upwards through the lithosphere by the carbonatite magma. The globules of unmixed, CO_2-rich silicate melt are continuously produced upon further reaction between the natrocarbonatite melt and mantle peridotite. On decompression the dispersed silicate melt phase ensures a continuous supply of CO_2 bubbles that decrease density and increase buoyancy and promote

rapid ascent of the magmatic emulsion, and ultimately drives crack propagation and emplacement of kimberlite with its load of entrained ultramafic and crustal material into the crust. The melt saturation in olivine at low pressure prompts olivine crystallisation, which drives the residual melt towards the initial (protokimberlite) carbonatite composition.

The solubilities of H_2O and CO_2 in the model (ultramafic/ultrabasic) kimberlite melt at emplacement pressures are not as high, as measured abundances of these volatiles in kimberlite rocks. The low H_2O content of the kimberlite melt, as at least during emplacement in the crust, do not support fluidisation mechanism (i.e., rapid degassing and expansion of magmatic volatiles in an open system) of the kimberlite emplacement. Furthermore, a number of studies have convincingly demonstrated that kimberlite explosions were unexpectedly powerful for such small magma volumes. The evidence was interpreted as excavation and even emptying of pipes from top down to significant depths (up to 1 km), prior to filling with juvenile material and pulverised country rocks. Notably, eruptive activity was shown to be polyphase and span considerable time with intermittent episodes of violent venting out and periods of quiescence and sedimentation in crater lakes. Moreover, as manifested by the presence at significant depths in some pipes of relatively fresh, often uncharred wood fragments, plant leaves, animal and fish parts, the venting juvenile material was likely cold and even solid.

If the kimberlite magma does not experience H_2O and CO_2 degassing and is disrupted at subsolidus conditions, what causes the kimberlite explosive eruption? We hypothesise that emplacement of the kimberlite magma as subsurface dykes is followed by gravitational separation and sinking of dense olivine and xenoliths, whereas the buoyant carbonatitic liquid is squeezed to the top of intrusive bodies. Olivine-rich cumulates with interstitial carbonate-rich melt form the "root zones" of hypabyssal kimberlites, whereas the upper parts of dykes are composed of the carbonatite with scattered silicate minerals. The olivine-rich rocks worldwide are prone to intensive serpentinisation and associated production of H_2 and CH_4 through the Fischer-Tropsch synthesis. The amount of hydrogen produced is ~10% of the volume of serpentinised olivine. thus the serpentisation may explain spontaneous outgassing of the UE kimberlite (~10^5 m^3/day at 50-70 atm; 52% H_2) recorded in the boreholes at the level of the lower aquifer.

We envisage that degrading water-soluble carbonatite in the upper parts of kimberlite intrusions was turned into a cavernous system that provided initial storage to the hydrogen- and methane-rich gases derived from serpentinisation of olivine cumulates in the kimberlite "root zone". The oxidation of these flammable gases and/or their pressurisation in a single spot resulted in a powerful detonation and destruction of surrounding rocks, and possibly caused "chain reaction" by sending shock waves through the cavernous system and thus triggering numerous explosions. Subsequent detonation activity resulted in vertical and lateral explosive boring, and further fragmentation inside the dyke system and surrounding country rocks. This was followed by collapse of rocks from the top and walls and related growth of a carrot-shaped "diatreme" by excavation from top down and fragmentation on the contacts between the kimberlite and country rocks (i.e. in-situ "contact breccia"). While the idea of post-magmatic brecciation of kimberlite rocks is not entirely new, the role of combustible gases in the formation of kimberlite diatremes and their pyroclastic and volcaniclastic kimberlite facies is proposed for the first time.

We invite collaborations on microanalysis of individual mineral phases and phenocryst-hosted melt inclusions in the least altered kimberlite samples from different localities. It is important to maintain an open mind, to not doggedly stick to increasingly untenable orthodox views, and to analyse emerging evidence on merit.

Metasomatic processes in peridotite xenoliths, Grib pipe, Arkhangelsk province, Russia

Kargin A.V., Sazonova L.V., Nosova A.A., Kovalchuk E.V., Minevrina E.A.
Institute of Geology of Ore Deposits, Petrography, Mineralogy and Geochemistry Russian Academy of Sciences (IGEM RAS), Moscow, Russia, kargin@igem.ru

The Arkhangelsk diamond province is situated in the northern East European craton. Several fields of kimberlites and related rocks were distinguished within the province. The Grib pipe is located in the central part of the Arkhangelsk diamond province. The Grib kimberlite was dated at 374 ± 1.3 Ma (Rb–Sr isotope methods) (Lebedeva et al., 2014). They are assigned to the Fe–Ti series (1.0–2.0 wt. % TiO_2) with strongly fractionated REE pattern, $(La/Yb)_n$ = 38-87 and have $\varepsilon Nd_{(T)}$ is from –0.4 to +1.8, and $(^{87}Sr/^{86}Sr)_T$ is 0.7042–0.7069 (Kononova et al., 2007).

The geochemical (Jeol JXA-8200 electron microprobe; SIMS; LA-ICP-MS) composition of clinopyroxene and garnet from mantle-derived xenoliths (19 samples) of the Grib kimberlite pipe was studied to provide new insights into metasomatic processes in the mantle beneath the Arkhangelsk diamond province.

Petrography. Xenoliths have a size from 0.5 to 10 cm and consist Gar (3-5 to 15%); Ol (60-85%); Opx (5-15%); Cpx (0-25%). Majority of Griba peridotite xenoliths are garnet lherzolites. Textural and structural characteristics were described in detail by. (Sazonova et al., 2015).

Garnets commonly form zoned porphyroblasts. Rim zones have are uneven, often maculose shapes and consist of garnet with metasomatic origin. Often, garnets become overgrown the later aggregate of garnet, phlogopite, Cr-spinel, carbonate and amphibole. Clinopyroxene mainly form an anhedral phase between the crystals of olivine and orthopyroxene, sometimes altered the latter. Less common clinopyroxene forms fine-grained crystals up to 1-3 mm in size. Sometimes clinopyroxene was altered by a later aggregate of clinopyroxene and phlogopite.

P-T estimates. The mineral assemblage of peridotites was in equilibria with T - 730-841°C and P - 22-44 kbar, except for the sample deformed peridotite (T - 1160-1200°C and P - 55-62 kbar) (Sazonova et al., 2015).

Based on both major (Ca and Cr) and trace element (REE, Ti, Zr-Hf) data, five geochemical groups of peridotitic garnet were distinguished.

Major elements composition. Garnet. In general garnets are presented by Cr-pyrope (the proportion of the pyrope member is from 63 to 76%) with large range of Cr_2O_3 (1.30-12.20 wt. %), CaO (2.82-7.92 wt. %), TiO_2 (up to 0.94 wt. %) content and Mg-number. In the G-number nomenclature of the classification scheme (Fig. 1) the majority of garnets are plotting within the lherzolite field (G9). In contrast, two samples form group III are plotting within the harzburgitic field (G10); one sample from V group have an intermediate composition between lherzolite and harzburgitic fields (G9-G10). Garnet of I group have intermediate composition between lherzolite and wehrlitic fields (G9-G12).
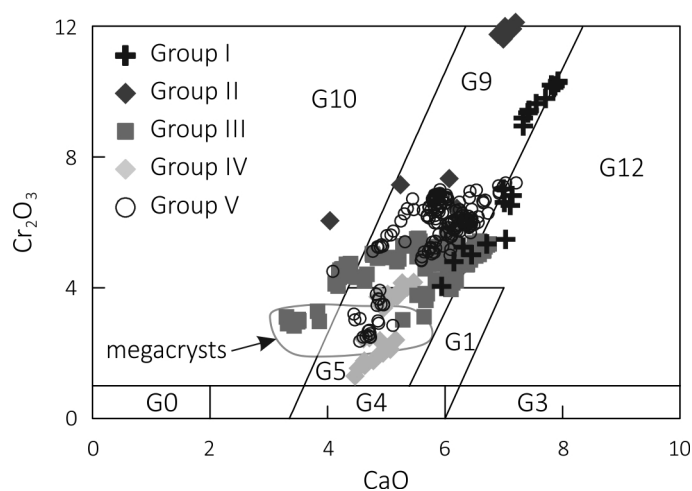
Fig. 1. G-number nomenclature of the classification scheme (Grutter et al., 2004). G1 – low-Cr megacrysts (are separated from G4, G5, G9 by high-TiO_2 composition); G3 – eclogitic garnets; G4, G5 – pyroxenitic garnets (Group G5 garnets are separated from G9 garnets by a Mg-number < 0.7 threshold); G9 – lherzolitic garnets; G10 – harzburgitic garnets; G12 – wehrlitic garnets; G0 – unclassified category. Cr_2O_3 and CaO in wt. %

Clinopyroxene from Grib peridotite xenoliths are presented by diopside with the jadeite member content up to 14 mol. %. The Mg-number is range from 0.89 to 0.95 within the wide variation of Cr_2O_3 (0.69-3.93 wt. %), TiO_2 (0.06-0.84 wt. %) and Al_2O_3 (0.47-5.61 wt. %) contents.

Garnet trace elements composition. Garnet central zones are distinguish by C1-normalized REE patterns and the level of enrichment trace elements (Fig. 2a-c):

(i) – garnets that have "normal" (like as megacrysts) C1-normalized REE profiles with increasing values from La to Lu (II and IV groups);

(ii) garnets that have "sinusoidal" C1-normalized REE profiles enriched in LREE-MREE with a maximum at Nd-Sm and Yb-Lu and with a minimum at Dy (III and V groups);

(iii) garnets that have high enriched in LREE (up to 10xC1) with C1-normalized profiles for MREE and HREE typical for megacrysts (I group Fig. 2a).

In additional garnets are distinguish by Ti, Zr, Hf contents (Fig. 2d-f): enriched in these HFSE elements like as megacrysts (II group and some garnets from V group) and garnets with poor Ti, Zr, Hf contents (III-IV-V groups).

56
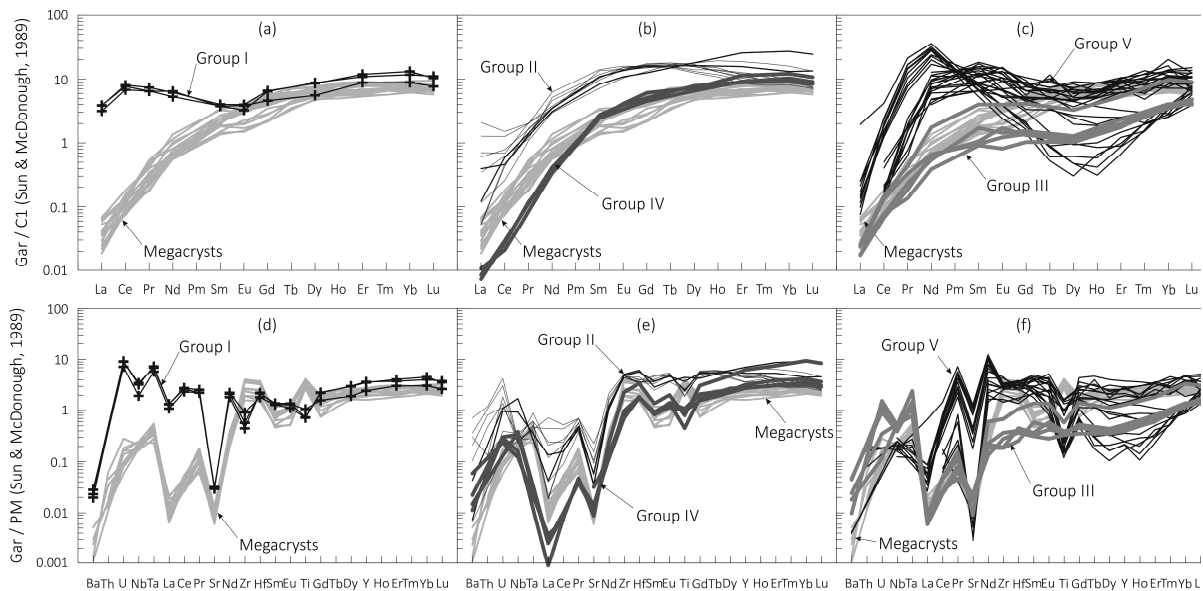
Fig. 2. C1-normalized REE patterns and PM-normalized (Sun & McDonough, 1989) trace element patterns for garnets and megacrysts garnets from Griba pipe.

Discussion. The interpretation of the major and trace elements composition of garnet and clinopyroxene from Grib peridotite xenoliths based on the garnet-clinopyroxene equilibria and the theoretical composition of metasomatizing melts led to next conclusions:

1) Mantle garnet peridotites were in equilibria as minimum with two metasomatic melts that were presented different protokimberlitic melts:

a) early melt had enriched in REE and Fe-Ti (HFSE) content and had mostly carbonate composition (the high carbonate/silicate ratio). This protokimberlitic melt was existed until the crystallization of the megacrysts assemblage (garnet, clinopyroxene, olivine, spinel, ilmenite) within the evolutionary increasing in silicate components. This melt was metasomatic agent for peridotite xenoliths of I, II groups and some sample of V group;

b) later, Fe-Ti-depleted melt with low carbonate/silicate ratio. This protokimberlitic melt was existed after the crystallization of the megacrysts assemblage. This melt was metasomatic agent for peridotite xenoliths of III, IV, V groups.

2) The different C1-normalized REE patterns ("sinusoidal" and "normal") in garnet of III, IV, V groups peridotite xenoliths may be explained by the model of melt injection and percolation through a refractory mantle column. In this model, the melt progressively changes its composition owing to chromatographic ion exchange, fractional crystallization and assimilation of peridotitic minerals, under decreasing melt/rock ratios (Ziberna et al., 2013). In the proximity to the source of protokimberlitic melt, the peridotite garnet has C1-normalized REE patterns close to megacrysts (II and IV groups). Respectively, at a distance from the source the peridotite garnet has C1-normalized "sinusoidal" REE patterns (III and V groups).

References:

Lebedeva N.M., Larionova Yu.O., Sazonova L.V. Rb-Sr isotopic age of phlogopite from Griba and Karpinskogo-1 kimberlite pipes // Abstract of IV Scientific Youth School «New in the knowledge of the processes of ore formation». Moscow, IGEM RAS. 2014. P. 190-192. *In Russian.*

Kononova V.A., Golubeva Yu.Yu., Bogatikov O.A., Kargin A.V. Diamond resource potential of kimberlites from the Zimny Bereg Field, Arkhangel'sk oblast, Geol. Ore Dep. 2007. V. 49. N. 6. P. 483–505.

Sazonova L.V., Nosova A.A., Kargin A.V. et al. Olivine from the Pionerskaya and V. Grib Kimberlite Pipes, Arkhangelsk Diamond Province, Russia: Types, Composition, and Origin // Petrology. 2015. V. 23. N. 3. Pp. 227-258.

Grutter H.S., Gurney J.J., Menzies A.H., Winter F. An updated classification scheme for mantle-derived garnet, for use by diamond explorers // Lithos. 2004. V. 77. P. 841–857.

Sun S., McDonough W.F. Chemical and isotopic systematics of oceanic basalts: implications for mantle composition and processes // Geological Society Special Publication. 1989. N. 42. Pp. 313-345.

Ziberna L., Nimis P., Zanetti et al. Metasomatic Processes in the Central Siberian Cratonic Mantle: Evidence from Garnet Xenocrysts from the Zagadochnaya Kimberlite // J. of Petrology. 2013. V. 54. N. 11. Pp. 2379-2409.

Geochemical models of superlarge deposits of strategical metals in alkaline rocks (Eastern Fennoscandia)

Kogarko L.N.

V.I. Vernadsky Institute of Geochemistry and Analytical Chemistry, Russian Academy of Sciences, Moscow, Russia

kogarko@geokhi.ru

The world's largest deposits of REE, Nb, Ta, Sr, Al, P are related to alkaline rocks and carbonatites. The interest to alkaline rocks and carbonatites has grown significantly due to the increasing consumption of strategic metals in industry most especially of REE. In the center part of Kola Penunsula (Russia) there is ultramafic alkaline province comprising carbonatites, ultramafic rocks and two largest of the Globe layered peralkaline intrusion Khibina and Lovozero (370 Ma age [1,2] (fig. 1)).
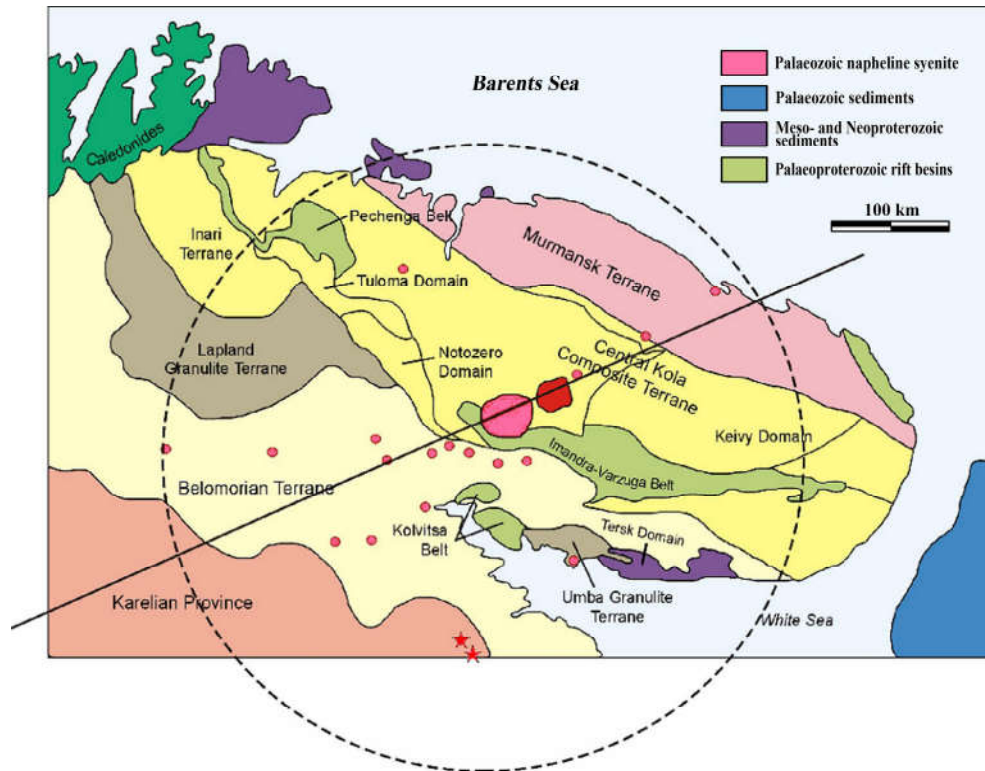
Fig. 1. Kola Alkaline Province Paleozoic nepheline syenite-Khibina. Lovozero massifs.

The Lovozero massif, contains super-large loparite rare-metal (Nb, Ta, REE) deposit (fig. 2) and eudialyte ores (fig. 3) the valuable source of zirconium, hafnium and rare earth. (fig. 4,7). Khibina apatite and Lovozero loparite had been mined during many years and constitute a world class mineral district.
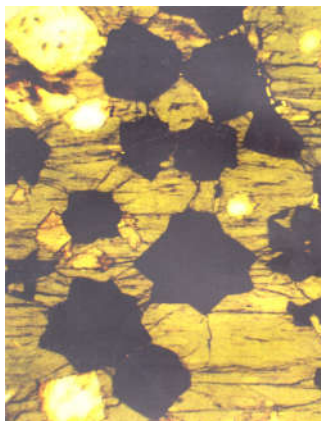
Fig. 2. Loparite ore x12.

Fig. 3. Eudialite ore x4.
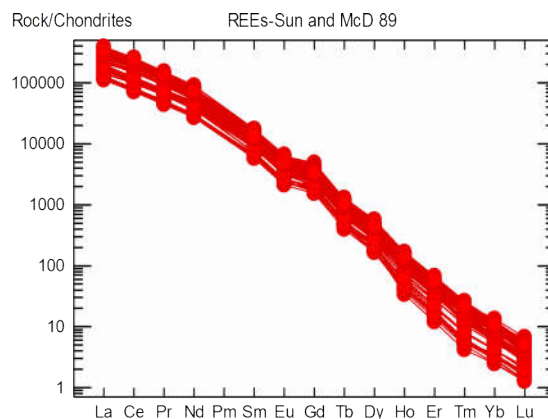
Fig. 4. REE pattern Lovozero loparite.

The main ore mineral is loparite (Na, Ce, Ca)$_2$ (Ti, Nb)$_2$O$_6$, (fig. 2). In the deepest zone of the intrusion loparite forms anhedral grains confined to interstitial spaces. Above 800m in stratigrafic section loparite makes up euhedral crystals which were formed at the early stage of crystallization. Therefore the initial magma was undersaturated with loparite. After the formation of approximately one-third of the volume of the Lovozero intrusion, the melt became saturated with loparite and this mineral accumulated in ore layers. The composition of cumulus loparite changed systematically upward through the intrusion with an increase in Na, Sr, Nb, Th, U and decrease in REE, Zr, Y, Ba and Ti. Our investigation indicates that the formation of loparite ore was the result of several factors including the chemical evolution of high alkaline magmatic system and mechanical accumulation of loparite as a heaviest phase at the base of convecting unit.

Zirconium-hafnium-rare-earth deposit is situated in the upper part of Lovozero intrusion as horizontal lenticular bodies.

The amount of Zr in eudialyte is very hight -up to 14 wt % and total REE up to 4 wt %. (fig. 7) Morfology of eudialyte grains is changed with depth of Lovozero intrusion. In the lower part of the intrusion eudialyte forms anhedral interstitial crystals (fig. 5) and crystallised when rock-forming minerals generated well-developed framework when convection ceased and accumulation of eudialyte is impossible. In the upper part of Lovozero stratigrafic section eudialyte forms euhedral grains which were formed at the early stage of crystallization. Thus the initial magma of Lovozero complex was undersaturated with this mineral. The melt became saturated with eudialyte after the approximately two-third of the volume of the massif solidified.

There is hidden layering in eudialyte in the crossection of the intrusion. The composition of cumulus eudialyte changed systematically upward through the eudialyte intrusion with an increase in Na, Sr, Nb, Th, Mn/Fe, Nb/Ta, U/Th and decrease in REE, Zr, V, Zn, Ba and Ti. The specific gravity of eudialyte is much higher then initial alkaline melt. Nevertheless eudialyte accumulated in the very upper zone of Lovozero intrusion. We suggest that eudialyte formed very small crystals (nanoctystals) (fig. 6) which were stirred in melt and under the conditions of steady-state convection eudialyte emerged upward. Later eudialyte crystals recrystallized and increased in size (fig. 6).
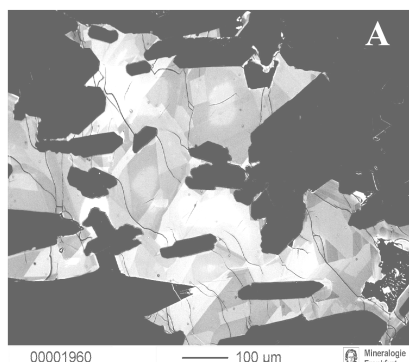
Fig. 5. Interstitial eudialyte.

Fig. 6. Recrystallized eudialyte. 200μm.
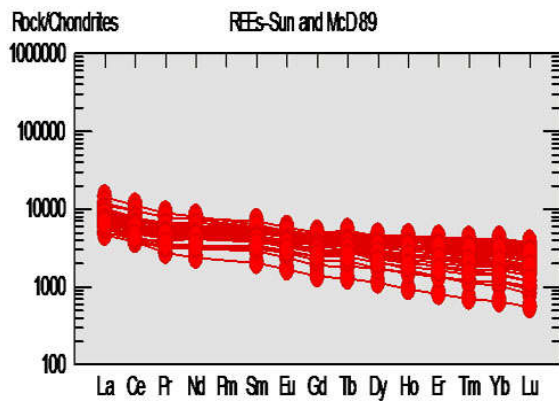
Fig. 7. REE pattern of eudialyte.
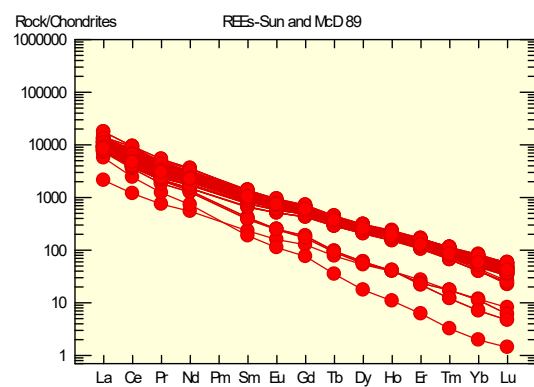
Fig. 8. REE pattern Khibina apatite.

The Khibina alkaline massif (Kola Peninsula, Russia) hosts the world's largest and economically most important apatite deposit. The Khibina massif is a complex multiphase body built up from a number of ring-like and conical intrusions. The apatite bearing intrusion is ring-like and represented by a layered body of ijolitic composition with a thickness of about 1-2 km. The upper zone is represented by different types of apatite ores. This rocks consists of 60-90% euhedral very small (tenths of mm) apatite crystals. The lower zone is mostly ijolitic composition. The lower zone grades into underlying massive urtite consisting of 75-90% large (several mm) euhedral nepheline. Our experimental studies of systems with apatite demonstrated the near-eutectic nature of the apatite-bearing intrusion, resulting in practically simultaneous crystallization of nepheline, apatite and pyroxene. Khibina apatite is rich in REE fig. 8.
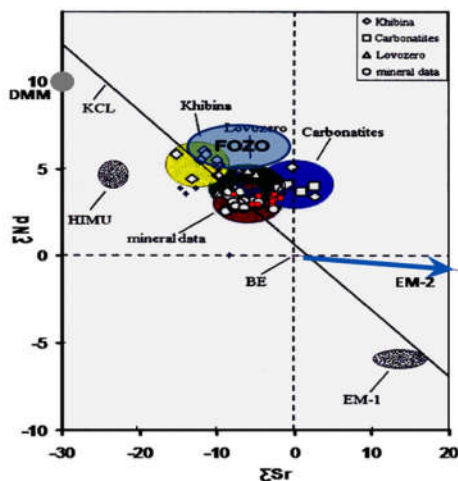
Fig. 9. εNd versus εSr isotopic composition of Lovozero and Khibina rocks.
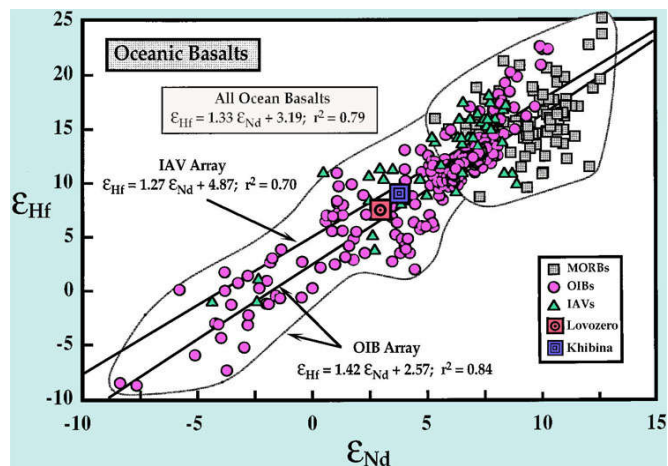
Fig. 10. εNd versus εHf isotopic composition of the Lovozero and Khibina ore minerals.

The mathematical model of the formation of the layered apatite-bearing intrusion based on the processes of sedimentation under the conditions of steady state convection taking account of crystal sizes is proposed. Under the conditions of steady-state convection large crystals of nepheline continuously had been settling forming massive underlying urtite when smaller crystals of pyroxenes, nepheline and apatite had been stirred in the convecting melt. During the cooling the intensity of convection decreased causing a settling of smaller crystals of nepheline and pyroxene and later very small crystalls of apatite in the upper part of alkaline magma chamber.

References

1.   Kogarko L.N., Kononova V.A., Orlova M.P., Woolley A.R., 1995. Alkaline rocks and carbonatites of the world: Part 2. Former USSR. Chapman and Hall, 225 p. (London)

2.   Kramm U., Kogarko L.N., 1994. Nd and Sr isotope signatures of the Khibina and Lovozero agpaitic centers, Kola Alkaline Province, Russia. Lithos. v. 32, p. 225-242.

3.   Kogarko L. N., Lahaye Y. & Brey G. P., 2010. Plume-related mantle source of super-large rare metal deposits from the Lovozero and Khibina massifs on the Kola Peninsula, Eastern part of Baltic Shield: Sr, Nd and Hf isotope systematic. Miner. Petrol. v. 98, p. 197-208.

Use of RHA language for ordering rocks on their mineral composition

Krasnova N.I.*, Burnaeva M.Yu.**
* St.-Petersburg State University, Russia
** FGUP "BNIIOkeangeologia", St.-Petersburg, Russia
nataly_krasnova@rambler.ru

The geology deals with high variety of objects, having different composition, among which are minerals, rocks, formation complexes, and waters, gases, soils, etc. Between these objects, it is possible to designate the general features. 1) All these geological objects consist of atoms, molecules and their various associations. 2) Between chemical, and other compositions of "different" objects, do not exist natural borders, in particular, between compositions of different species in isomorphic rows of minerals, and between compositions of rocks. Therefore, in one classification family, the limits of fluctuations of different components usually overlap, and in this connection, definition of separate species is mostly difficult. In addition, different classifications of rocks often are based on various principles: on mineral and-or chemical composition, on texture and structure, genetically definition, that gives some miscellaneous results sometimes complicating even simple diagnostics of studied object. 3) Motion of a substance, its transformation and the different processes occurring in it, depend to the certain laws, which knowledge, obviously, is very important. 4) On objective representation of our terrestrial object's composition, and also the laws operating their evolutionary processes depends not only understanding of the various natural phenomena, but also an opportunity of use of our knowledge for the most various needs of mankind.

An actual problem of prompting of the uniform order in data of chemical and mineral composition of geological objects, in particular, in petrography exists up to now. The order, which would not depend on genesis, forms of individuals or their aggregates, a degree of their transformation, a priori allocated components and other specific properties of objects and their composition. Earlier based on method RHA, the principle of ordering of any objects [1] on their chemical composition has been worked out: rocks [2], minerals [3], and crystalline and holocrystalline rocks and on modal and normative mineral to composition [4]. Use of this method allows identifying any rocks more definitely. The collection for chemical composition of rocks (Rchem) for today totals more than 7000 inputs.

At work with rocks, it is important to consider their mineral composition, and then the components are minerals. Ranging them (or their abbreviations) on decrease molecular (or, more often – volumetric) percents, we shall receive the rank formula of mineral composition (Rmin). Rank formulas of mineral composition of geological objects – Rmin – settle down under "alphabet". Here the sequence of minerals – R – we accept to "word", ordered in decreasing of their quantities, where "letters" are names of minerals. As the «alphabet», the sequence of these minerals received in their chemical R-classification, or the R-catalogue of composition of all minerals [4] serves. The rank formula represents distribution of components on their importance; in other words, it is the formula of component's rating. Other parameters of the RHA method (entropy and anentropy) reflect character of distribution of content of components. The entropy (H) reflects a degree of complexity, or uniformity of distribution of content, and anentropy (A) – a degree of composition purity, a degree of the smallness of small components, "admixtures" in the rank formula. The RHA-system is a way for curtail of the information on rather full analyses, i.e. which sum is close to 100 %. Rank formulas – Rmin's – are convenient for creation of names of rocks and specification of their nomenclature. If we will limit only to the first mineral in Rmin for rocks of, e.g., phoscorite-carbonatite series, we shall have names forsteritite, magnetitite, apatitite, calcititite, etc. For more detailed name of any rock, it is possible to use two and more symbols of the minerals in decreasing order of their quantity in corresponding Rmin (unlike the IUGC recommendations). For the decision of a specific target, the classification of mineral composition of any group of objects the R-catalogue can be made of rank formulas of all composing it minerals. As a result of such ordering for mineral composition of rocks, the rank formulas – sequences of minerals, such as OlivBiotDipsMagt can be received, that corresponds to volume fractions (Vol. %) minerals in rock: Oliv> Biot> Dips> Magt.

We had composed the RHA-table for mineral composition of crystalline rocks for more than 900 modal analyses, using the data published mainly up to 80th of the last century (fragment see in Tab. 1). Now the problem to receive such data considerably facilitates an opportunity of automatic scanning of polished thin sections under an electronic microscope. As a result, it is possible to receive the ready rank formula for everyone thin section, ordering their modal composition in decreasing of the mineral's content. The problem of ordering of such results and their comparisons to the data received the last years, will give us greater opportunities. Among them are: 1) the identification of some not named rock; 2) finding the analogues of rock on their mineral composition; 3) revealing of new species of rocks with unique mineral composition; 4) finding of synonyms of some local and rare rock names and use this method for the discontinuing of them; 5) composition of the simple (monosemantical) classifications of mineral rock compositions. It is possible to draw the borders between rock varieties on the presence of some changes in their R (for example, by appearance of new components in the rank formulas, or by rearrangement of components in R).

RHA_Modal Min.Comp.different rocks_Vol%						Description
1	2	3	4	En	An	No in DB,rock name
Oliv=	Augt	Hypr=	Labr	0.895	0.034	6-2218-t5_peridotite
Oliv	Augt	Magt	Apat	0.215	0.354	11-960-t21_olivinite
Oliv	Augt	Magt	Chrt	0.561	0.278	23-960-t21_wehrlite
Oliv=	Hypr	Augt	Chrt	0.743	0.096	21-960-t21_lherzolite
Oliv	Hypr	Augt	Chrt	0.520	0.156	17-960-t21_harzburgite
Qutz=	Albt=	Ortc	Biot	0.817	0.114	395-960-t21_leucogranite 2Fsp
Qutz=	Ortc	Albt	Biot	0.629	0.167	384-960-t21_granite alkaline
Neph	Aegn	Ortc	Apat	0.437	0.181	2-2219-t2-p38_urtite
Neph=	Aegn	Titn	Ortc	0.761	0.085	18-2219-t2-p38_ijolite
Neph	Ortc	Aegn	Hbld	0.631	0.107	15-2219-t9-p115_juvite
Neph	Ortc=	Aegn	Apat	0.784	0.055	3-2219-t9-p118_Ap-Ne rock ???
Augt	Neph	Biot	Magt	0.479	0.144	89-960-t21_jacupirangite
Augt	Neph	Magt	Phlg	0.667	0.217	92-960-t21_melteigite
Augt=	Hypr	Oliv	Labr	0.905	0.038	5-960-t21_picrite
Hypr	Titn	Augt	Oliv	0.095	0.396	141-960-t21_orthopyroxenite
Olig	Qutz	Musc	Epid	0.702	0.090	347-960-t21_plagiogranite
Olig	Qutz	Biot	Ortc	0.753	0.067	282-960-t21_diorite subalk.Qtz
Ortc	Qutz=	Albt	Musc	0.808	0.110	357-960-t21_leucogranite
Ortc	Qutz	Albt	Biot	0.937	0.019	387-960-t21_granite Mic Ab
Ortc	Neph	Albt	Biot	0.855	0.046	320-960-t21_miaskite
Ortc	Neph	Aegn	Biot	0.609	0.170	311-960-t21_foyaite
Labr	Hypr	Oliv	Augt	0.754	0.082	170-960-t21_norite Ol
Labr	Hypr	Qutz	Biot	0.596	0.127	252-960-t21_diorite
Labr	Ortc	Qutz	Hbld	0.840	0.058	285-960-t21_monzodiorite Qtz
Mell	Oliv	Perv	Magt	0.678	0.097	77-960-t21_kugdite
Apat	Neph	Aegn	Ortc	0.623	0.113	2-2219-t9-p118_Ap-Ne rock

Table 1. Fragment of the **RHA** table for some rock types.
Note: The alphabet for the Rmin's ordering corresponds to the order of minerals in their R-catalogue [3].

There exist some more difficulties in the diagnostic and ordering of porphyritic rocks with non-completely crystalline, or a glassy matrix, in comparison with the same tasks for crystalline rocks. Minerals of phenocrysts, as a rule, we define or optically, or by some exact methods on their chemical composition. The mineralogical diagnostics by optical methods of the composition of matrix is often impossible because of the small sizes of individuals. The proposed resulting classification is based on the mineral composition of porphyritic phenocrysts and norm mineral composition of the matrix. The last we can calculate from the data on scanning of matrix in the form of areas under an electronic microscope [4]. Rocks are ordered first on R composition of phenocrysts, and in case of their coincidence – on R derived from normative composition of a matrix. Our results we compared with the rank formulas received for 92 mineral compositions of the porphyritic rocks resulted in work [5]. It has been established, that studied dike rocks from Spitsbergen show the most similarity on their R to composition of picrites [4]. Presentation of results and unambiguity of ordering of mineral compositions of rocks an offered method facilitates identification complex for definition of not holocrystalline rocks.

Let us note, that most close to our decision of this problem offered R.H. Mitchell who had "suggested to change historical rock names (in his case – lamproites) not reflecting the material composition by the composite names based on prevalence" in rock of some rockforming minerals. The members of a Subcommission on the Systematics of Igneous Rocks of the IUGS, however, had not accept this offer, as giving excessively complicated description [6, p. 153]. Our method formalizes the standard, traditionally developed principles at rock nomenclature: to give the rock names on main (leading) minerals (the R – rank formula), with the account of complexity of rock (using H). The most simple of rocks (with low H, i.e. – monomineral) it is possible to name using the slightly changed title of a predominant mineral, for example, apatitite, olivinite, magnetitite, etc. Use these suggested method allows making determinants of crystalline rocks – on their mineral composition, glassy – on their normative composition, and of non-completely crystalline rocks – on a combination of these of two. Among preliminary tasks is the creation of the list of name abbreviations of rockforming minerals for all spectrums of rocks. Creation of the representative RHA-catalogue of such full data for all rocks will provide an opportunity of their identification on real mineral composition. Such catalogue is opened for addition of new, before unknown rock types. Such rank formulas, in our opinion, are especially actually to use for the rock groups, which have no accepted and approved nomenclature, as, for example, for phoscorites. For rocks which have the traditional and standard names, such as: "granite", "gabbro", "diorite", etc., it will be rational to use the rank formulas such as granite muscovite (OrtQutzAlbtMusc), in difference, for example, from a granite biotite

(OrtQutzAlbtBiot). In the simplified variant: granite (Musc) and a granite (Biot), if, parities of three other main minerals in their composition have the same succession: Ort>Qutz>Albt in R. This attempt is quite easy and does not much differ from creating of traditional rock names. In the future, such classification of all rocks on RHA method can become a perspective theme for different groups of geologists. For these purposes, possibly, it will be convenient to create on the Internet a site, that could be similar to the site: mindat.org. The function and problems of such web site could be developed and approved by the International union of geological sciences (IUGS).

References

[1] Petrov T.G. Substantiation of a variant of the general classification of geochemical systems. // Vestnik LGU. 1971. Ser. 18. No 3. 30-38. (In Russian).

[2] Krasnova N.I., Petrov T.G., Balaganskaya E.G., Garcia D. and Moutte J. An introduction to phoscorites. // In: Phoscorites and carbonatites from Mantle to Mine: the Key Example of the Kola Alkaline Province (Eds. F. Wall, A.N. Zaitsev) Publishing House of Mineralogical Society Series, London. 2004. Chapter 2. 45-74.

[3] Petrov T.G., Krasnova N.I. R-dictionary-catalogue of chemical compositions of minerals. S.-Petersburg: Nauka Press. 150 p. (In Russian).

[4] Burnaeva M.J., Krasnova N.I. Presentation of mineral composition of non-completely crystalline rocks using the RHA information language. // In: Ore potential of alkaline, kimberlite and carbonatite magmatism. XXX Int. Conf. School "Alkaline magmatism of the Earth". Abstr. Vol. Moscow, Sept. 16-17-2013. P. 19.

[5] Bogatikov O.A., Kosareva L.P., Sharkov E.V. (1987) Average chemical composition of magmatic rocks. Moscow: Nedra Press. 153 p. (In Russian).

[6] Petrographic code of Russia. St. Petersburg. VSEGEI Press. 2012. 196 p.

Minerals and sources of rare-earth elements in Karelia

Kuleshevich L.V., Dmitrieva A.V.
IG KarRC RAS, Petrozavodsk, Russia
kuleshev@krc.karelia.ru; dmitrievaa-v@yandex.ru

In the last few years rare-earth elements (REE) have been widely used in various industries. Their production and application are growing. In Russia, the prospecting of rare and rare-earth elements as strategic raw materials is a priority. Analysis performed in Karelia shows that the highest REE concentrations are associated with alkaline and metasomatic rocks, apatite ore and some other ore types [1-6].

Examples are: 1 – ultramafic alkaline4 rocks and titanite-apatite ores of the Elisenvaara complex ($\sum$REE 0.22-1.7 %); 2 – ultramafic alkaline rocks, carbonatites and apatite ores of the Tiksheozero complex ($\sum$REE~0.36 %); 3 – moderately alkaline gabbro-pyroxenites, monzonites and titanite-apatite ores of the Syargozero complex, Central Karelia; 4 – apatite-magnetite ores (West Rybozero occurrence); 5 – subalkaline granites, pegmatites and metasomatic rocks of Archean (0.13-0.41 %) age; 6 – Riphean rapakivi granites and alkaline metasomatic rocks in their halo (northern Lake Ladoga area, 0.12-0.63 %); 7 – alkaline metasomatic rocks and associated Pd-Cu-Se-U and Cu-Se-U-V ores (PR_1, Srednyaya Padma, Svetloye); 8 – quartz gravelstones with Y-U-Th-mineralization (Cherny Navolok, Tedrilampi).

High REE concentrations are associated with ladogalites, toensbergites and Ba-Sr-P-Ti ores of the Elisenvaara massif of PR_1-age (Kaivomäki and Raivimäki occurrences (local names are used after [5-6]). REE are concentrated in monazite, orthite, epidote, apatite and titanite and lesser in more recent carbonates such as lantanite, bastnaesite and Ca-Sr-Ce-carbonates which are separated with chlorite, sulphides, Sr-barite and celestine [4]. $\sum$REE in rocks is as high as 0.22-1.04 %; $\sum$REE in titanites is 1-1.7 % and in apatite concentrates is 0.45-1.36 %. The rocks of the Elisenvaara complex contain 0.13-1.3 % Ba, 0.5-1.2 % Sr, 220-940 ppm Zr, 2-14 ppm Hf, 190-346 ppm Ga, 36-170 ppm Y, 10-28 Nb, less commonly up to 128 ppm, and 10-77 ppm Th (ISP-MS analysis). Apatite contains 1.2-1.7 % Sr, which is its isomorphic constituent, and strontiobarite and celestine microinclusions. Apatite is cross-cut and is overgrown by orthite and monazite. The light cores of zonal apatites and titanites contain up to 1.3-1.63 % Ce. Apatite and apatite-titanite ores are most enriched in REE. REE resources are estimated at 15 Mt, their average concentration in ladogalites being 0.25 % [4, 6].

Phosphates and carbonates (monazite, xenotime, bastnesite and parisit), apatite, titanite and more scarce Sr-Ce minerals in the carbonatites of the 1.8 Ga Tiksheozero massif, North Karelia, are REE concentrates. REE minerals and elevated lanthanide concentrations are confined to apatite ores; $\sum$REE in disseminated

mineralization in carbonatites is 600-1260 ppm. Carbonatites contain 0.24-0.44 % Sr, 200-626 ppm Ba, 14, to 411-930 ppm Nb, 1-14 ppm Ta, 14-48 ppm Y, 8-143 ppm Zr and 3-30 ppm Th.

The West Rybozero apatite-magnetite ore occurrence (AR_2) in carbonate-tremolite schist, overprinted by disseminated-veilet Pd-Cu-Ni-S mineralization, is an unusual representative of REE mineralization. It, in turn, is cross-cut by more recent REE-carbonate veinlets dominated by bastnaesite and parisite associated with monazite and lesser xenotime.

The moderately alkaline intrusives of the Syargozero complex (AR_2), Central Karelia, are differentiated from gabbro-pyroxenites to monzonites and syenites (Panozero, Syargozero, Torosozero and Sharavalampi massifs). They contain elevated REE concentrations up to 1314 ppm, Zr, Ba, Sr [1]. REE are concentrated in monazite, orthite-epidote, apatite, titanite, Ce-thorite (up to 7 % Ce), parisite and bastnaesite.

The rapakivi granites of the Salmi massif (~1.5 Ga), northern Lake Ladoga area, metasomatic rocks in them and greysens in their halo display elevated REE concentrations. In phase-1 porphyraceous rapakivi granitesB ∑REE (218-432 ppm) increases in altered rock zones to 1046 ppm, Ba concentration varies from 65 to 1400 ppm, Sr is 21-100 ppm, Rb 240-314 ppm, Y 58-96 ppm, Zr 51-250 ppm and Nb 24-90. Y concentration in phase-2 granites rises to 325 ppm (up to 0.1 %, after [5]). They are accompanied by greysens with W-Bi-Te-As mineralization, Y-Ce-U mineralization is well-developed in the Lypikko occurrence (uraninite, monazite, xenotime and bastnesite), and Be increases to 413-1327 ppm. REE carbonatites are encountered in the weathering crust of the Salmi massif and in overlying rocks in the Karku uranium deposit.

Alkaline and associated Fe-Mg metasomatic rocks with Cu-S, Cu-Se-U and Cu-Se-U-V ores with noble metals (Svetloye, Srednyaya Padma and other occurrences of the Padma group) are formed in late faulting-folding zones in Proterozoic units of PR_1jt-ld age such as basalts, carbonate rocks and at their contacts with gabbro-dolerite sills. The Pd-Cu-Se-U ores of the Svetloe occurrence contain ∑REE 457-660 ppm, 210-400 ppm Y and their concentrate minerals such as REE-carbonates, monazite, xenotime and and thoritophosphates. Elevated Zr, Y and Th concentrations are encountered in the quartz conglomerates and gravelstones (PR_1jt$_1$) of some occurrences in Central Karelia such as Cherny Navolok and Tedrilampi. These elements are concentrated in zircon, thorite, thoritophosphates and monazite. At low REE concentrations the strata-bound extensive pattern of quartz gravelstone deposits with local deformation zones could be of interest in prospecting.

References
1. Dmitrieva A.A. Geochemistry of the ore mineralization of the Syargozero moderately alkaline complex, Central Karelia // Uchenye zapiski PetrGU. 2013. No. 6. P. 45-50.
2. Kuleshevich L.V. The Rybozero gold deposit, South Vygozero greenstone belt, East Karelia // Geology and commercial minerals of Karelia. Petrozavodsk. 2013. No. 16. P. 89-101.
3. Kuleshevich L.V., Dmitrieva A.V. Minerals and sources of rare-earth minerals in Karelia // Uchenye zapiski PetrGU. No. 4. 2012. Vol. P. 62-66.
4. Kuleshevich L.V., Dmitrieva A.V., Khazov R.A. Ba-Sr-P-Ti-TR-feldspar of the Elisenvaara alkaline complex, Karelia: geochemistry and mineralogy of rare-earth elements // Uchenye zapiski PetrGU. 2014. No. 4. P. 67-70.
5. Mineral resources of the Republic of Karelia / V.P.Mikhailov & V.N.Aminov, Eds. Petrozavodsk: Karelia Publishers. 2005. Book 1. 278 p.
6. Khazov R.A., Popov M.G., Biske N.S. Riphean potassic alkaline magmatism of the southern Baltic Shield. S-Pb.: Nauka. 1993. 218 p.

Monzogabbro "Uborok"of the south-east of Belarus (Voronezh crystalline massif)

Kuzmenkova O.*, Ryborak M.**, Tolkachikova A.*, Taran L.*, Al'bekov A.**, Levy M.*
*State Enterprise "Research and Production Center for Geology", Minsk, Belarus
**Voronezh State University, Voronezh, Russia
e-mail: kuzmenkovaof@mail.ru, maximm.r@gmail.com, tolk@geology.org.by, taran@geology.org.by, sashaalb@list.ru

The positive magnetic anomaly "Uborok" (Dobrush district, Gomel region) was verified by drilling (well 785, depth 544 m) in 2013 - 2014. An anomaly-forming body is represented by the elongated northeast stock of monzogabbro with size of 1.1 x 2.2 km. The intensity of the magnetic anomaly in the epicenter is of 2203 nT (ground verification of the aeromagnetic survey 1:25 000). Crystalline basement of the area lies at a depth of about 500 m and it is overlaped by the terrigenous sediments of Riphean, Triassic, Jurassic, Cretaceous and Quaternary.

The stock of monzogabbro "Uborok" is located at the junction of the northeast trending strike structures -

Gremyachsky Entombed ledge and Klintsovsky graben of the Voronezh Anteclise. The deep northeast trending faults are dominated here. The stock is interesting for its position on the border between Belarus and Russia where in the crystalline basement are distinguished the following structures: the Bragin Granulite Massif in Belarus [1], the Bryansk granulite gneissic megablock - in Russia [4, 5]. Obviously, these structures are mutually connected in the space, and form the Bragin-Bryansk Granulite block (BBGB) because composed of the similar types of intensively migmatized high-alumina garnet-biotite gneisses sometimes sillimanite- and cordierite-bearing. They belong to the Kulazhin series in Belarus and to Oboyansky complex in Russia. The gneisses of the Kulazhin series also are fragmentary distributed to the west of BBGB where they form a rare blocks among the Central Belarus suture zone and Osnitsk-Mikashevichy volcanoplutonic belt which have been formed on the northwest edge of Sarmatia about 2.0 billion years ago.

Migmatite, plagioclase granites and granites of the Saltykovsky complex as well as the moderately-alkaline granites of the Atamansky complex [4, 5] are distributed in the Bryansk megablock. Migmatite and granites of the Barsukovsky complex and also granodiorites of the Kopansky complex compose the Bragin block [6]. In addition, within of the BBGB a lot of small bodies, presumably basic-ultrabasic composition, are highlighted from the geophysical data. The stock of the moderately-alkaline monzogabbro "Uborok" is the first such body in the area that has been opened by drilling.

Rocks belonging to moderately-alkaline series are defined by the total content of alkalis ($Na_2O + K_2O$ = 4.42 -6.30%), significant contents of Ba and Sr (Sr = 1212.00 ppm, Ba = 1090.00-1559.00 ppm). Barium is mostly included in biotite while strontium isomorphically enters into the crystal lattice of plagioclase. The chemical composition of rocks is SiO_2 = 47.00 - 50.06 %, TiO_2 = 1.23 - 1.70 %, Al_2O_3 = 19.05 - 19.69 %, Fe_2O_3t = 7.11 - 12.40 %, MnO = 0.06 - 0.14 %, MgO = 3.70 - 4.76 %, CaO = 8.09 - 8.80 %, Na_2O = 2.90 - 3.40 %, K_2O = 1.22 - 2.90 %, P_2O_5 = 1.16 - 1.54 %. Total REE content varies from 231.01 ppm in montzogabbro-norite to 291.100 ppm in monzogabbro and a significant predominance of LREE over the medium and heavy ratios of La_n/Sm_n = 4.44 - 4.48, La_n/Yb_n – 30.22 - 30.63) respectively (figure).

The unusual geochemical features of the rocks studied are a high alumina content and low – titanium with a high content of phosphorus which is probably defined by the significant presence of apatite (up to 2 %). Absence of the orthoclase in montzogabbro-norite do not manifested by the lowering of the potassium relativelly the monzogabbro because it is likely explained by higher potassium content in biotite from montzogabbro-norite (K_2O = 9.24 - 9.33 %) if compare to monzogabbro (K_2O = 7.80 - 8.40 %).

The biotite is rather chemically close to biotite from charnockites by the content of iron, titanium and potassium, but contain more titanium (TiO_2 = 4.50 - 5.82 %) that is compatible biotite from alkaline rocks. Moreover, there is positive correlation betwen titanium and potassium.

Compositionally clinopyroxene is similar to that from shonkinites. Its composition varies from salite in the center of large grains to ferrosalite in the marginal part and ferroavgite in small grains. The most magnesian salite is fixed in the center of the grains and contains more calcium.

The plagioclase contains in 50 – 55 % in the montzogabbro-norite, 45 – 50 % in monzogabbro, and forms two generations. The porphyry normally-zoned grains of the first generation has the tabular form (1.5 - 3.0 mm) namely the basic labrador $An_{69-70}Ab_{30-31}Or_1$ is founded the central parts of the grains (FeO = 0.18 - 0.39 %), while acid labrador $An_{52-63}Ab_{36- 47}Or_1$ forms the marginal parts of the grains (FeO = 0.43 - 0.87 %). The short-prismatic grains of the second generation (0.2x0.1 mm) forms the clusters That plagioclase has the more acidic composition which is similar to those composing boundary parts of the grains of porphyry allocations – andesine $An_{48-50}Ab_{48}Or_{2-3}$-acid labrador An_{44-52}. suggesting a simultaneous crystallization. The plagioclase is idiomorphic in association with the biotite and pyroxene while it is always idiomorphic relatively the orthoclase.
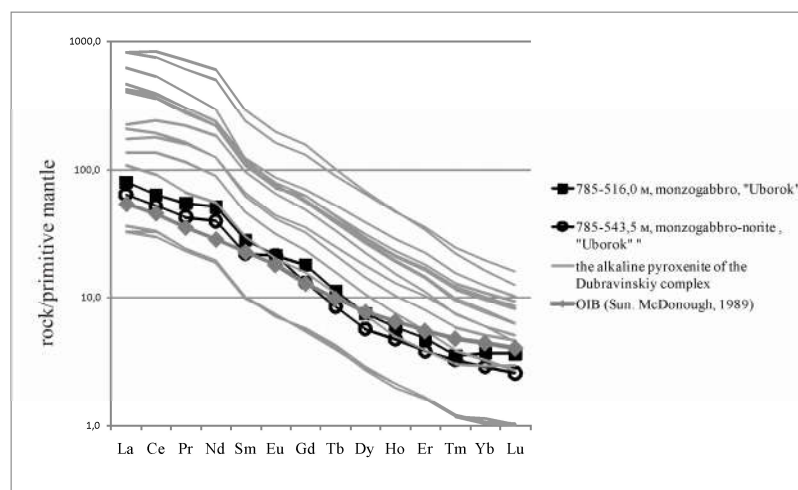
Figure – Primitive mantle normalised REE distribution in "Uborok" and the Dubravinsky rocks (primitive mantle by Sun, McDonald, 1989).

The irregular form of grains of orthoclase $An_{0-5}Ab_{6-11}Or_{88-93}$ (0.4x0.5 mm to 3.0x4.0 mm) is strongly pronounced in monzogabbro. It defines the monzonite structure of the rock. The mineral is distributed unequally in rocks. The host rock "engorged" by the orthoclase in areas where it often forms aggregates. The content of orthoclase $An_{0-1}Ab_{7-12}Or_{87-93}$ in pegmatites is about 40 – 60 %. Increasing of the iron content is characteristic feature of the marginal parts of grains of orthoclase. Orthoclase with MgO up to 0.62% is fixed in the central part of the grains of orthoclase in monzogabbro.

The magnetite and the ilmenite of the monzogabbro and monzogabbro-norite contain up to 1.16 % of V_2O_5 which is characteristic feature of basic rocks. High contents of chromium and nickel in the ore minerals of pegmatite indicate on the common source of the pegmatite forming fluids connecting with the basic-ultrabasic melts.

Geochemical data suggest that the fractional crystallization occurred on the melt consolidation inside the magmatic chamber. This led to the bundle of the intrusion and formation of the two petrographic varieties of rocks: orthoclase-containing (10 - 15%) monzogabbro in the upper part of the body and orthoclase pure monzogabbro-norite in the low part of the body. The pegmatite veins were probably formed by the residual melts rising from the basitic magma chamber.

Analogs of the studied monzogabbro has not still established in Belarus as in adjacent areas of the Ukraine and Russia within Paleoproterozoic complexes. The studied monzogabbro show the geochemical similarities with the alkaline pyroxenite of the Dubravinskiy complex of the Voronezh Crystalline Massif that has been formed on the final stage of the Early Paleoproterozoic stabilization phase of the Kursk block of the Sarmatia [2, 3, 6].

References:

1. Aksamentova N., Naidenkov I. Geological map of the crystalline basement of Belarus and the surrounding areas in scale 1: 1 000 000. Minsk, 1990.

2. Albekov A., Ryborak M., Kuznetsov V., Kolesnikova E., Choline V. Age and geodynamic position of Dubravinskiy alkaline-ultramafic-carbonatite massif of Kursk block of Sarmatia: U-PB isotopic data for sphene // Reports of the Academy of Sciences. Title: Geochemistry.

3. Bagdasarov Yu., Voronovskiy S. Ovchinnikov L. The features of the geological situation and the radiological manifestations of the new age of the carbonatites in the area KMA // Reports of the Academy of Sciences of the USSR. 1985. T.282. №2. pp. 404-408.

4. Molotkov S., Kostjukov V., Lositsky V., Krivtsov I., Zolototrubova E., Potomareva R. Geological map of the Voronezh crystalline massif in scale of 1: 500 000. Voronezh, 1999.

5. Tolkachikova A. Petrology of the Bragin granulite massif //Abstract of cand. of geol.-min. sciences. Minsk, 2004.

6. Chernyshev N., Albekov A., Ryborak M. About the present state of the Circuit of the Stratigraphy and Magmatism in the Early Precambrian of the Voronezh crystalline massif // Herald of the Voronezh State University, Series: Geology, 2009. № 2. pp 33-40.

Evolution of carbonatites and associated rare-earth mineralization in the Lugiin Gol complex, Mongolia

Kynicky J.*, Chakhmouradian A.R.**, Smith M.P.***, Xu Ch.****, Galiova V.M.*****,******, Brtnicky M.*

*Mendel University in Brno, Zemedelska 1, CZ-613 00 Brno, Czech Republic
**Department of Geological Sciences, University of Manitoba, Winnipeg, Manitoba, Canada
***School of the Environment and Technology, University of Brighton, Brighton, BN2 4GJ, United Kingdom
****School of Earth and Space Sciences, Peking University Beijing 100871, China
*****Department of Chemistry, Faculty of Science, Masaryk University, Kotlarska 2, CZ-611 37 Brno, Czech Republic
******Central European Institute of Technology (CEITEC), Masaryk University, Kamenice 5, CZ-625 00 Brno, Czech Republic

A large suite of fresh and metasomatically modified carbonatites from the Lugiin Gol complex in South Gobi, Mongolia, was examined. The carbonatite samples were sampled from outcrops and drill-core material (down to a depth of 1000 m). The carbonatites are represented predominantly by coarse-grained sövite, consisting of magmatic calcite, minor to accessory Na-Sr-REE-bearing apatite, and a paragenetically diverse suite of rare-earth carbonates whose modal content locally reaches 30 vol.%. The latter group includes both

primary carbonates (burbankite–calcioburbankite series and fluorocarbonates of rare-earth elements, REE) and hydrothermally or metasomatically formed phases associated with strontianite, fluorite, barite, celestine and quartz. The primary fluorocarbonates are represented by zoned synchysite-(Ce) (synchysite I) with lamellae of bastnäsite-(Ce) and röntgenite-(Ce). Some samples contain phenocrysts of euhedral parisite-(Ce) which is also present as cores overgrown by a zone of synchysite I forming an hour-glass microstructure. The primary textures and parageneses are partially modified and overprinted by recrystallization of calcite, alteration of apatite, breakdown and replacement of burbankite and other early-crystallized carbonates, followed by the precipitation of secondary carbonate parageneses.

Several carbonatites are zoned and exhibit a pegmatoid texture. The selvage of these zoned bodies comprises fine-grained calcite and fluorite and is practically devoid of fluorocarbonates. This zone grades to a medium- to coarse- grained (locally extremely so) burbankite-bearing zone also containing primary fluorocarbonate crystals. Somewhat similar, but even more spectacular textures were found recently in drill-core, where carbonatites contain very coarse-grained Sr-bearing calcite forming intimate symplectitic intergrowths with fluorite. These textures, not previously reported in carbonatites, are interpreted as evidence for melt immiscibility. This process could have contributed to the development of REE mineralization at Lugiin Gol.

The Lugiin Gol carbonatites have a recognized, although largely unexplored economic potential because of their overall enrichment in REE, coupled with the lack of understanding of lithologic and structural controls over mineralization. The deposit is currently undergoing re-evaluation. All of the examined carbonatites exhibit chondrite-normalized REE profiles with a steep negative slope and lacking any anomalies. In addition, these carbonatites are characterized by extremely high abundances of Ba and Sr, coupled with low levels of Nb, Ta, Ti, K, Rb and Cs. Their age of emplacement has been determined by U-Pb dating of zircon as Triassic (ca. 240 Ma). Thus, in the context of regional geodynamics, these rocks are interpreted as post-orogenic, which is consistent with their geochemical signature. The carbonatites have an average $\delta^{13}C_{\text{V-PDB}}$ value of -8.6‰ and $\delta^{18}O_{\text{V-SMOW}}$ of 10.4‰, indicating contamination of their mantle source by subducted crustal material.

Rare metals – the first step to richest ore complex of massif Tomtor

Lapin A.V.*, Tolstov A.V.**
*IMGRE, lapin@imgre.ru, *Moscow, Russia*
**IGM SB RAS, tols61@mail.ru, *Novosibirsk, Russia*

Tomtor massif that located in the north of Yakutia is one of the biggest carbonatite complex in the world (S ≈ 250 км^2) and containing the most significant carbonate body (более 30 км^2). Massif has a rounded shape on plane and concentric zoned structure with carbonatites in core surrounded by alkaline and nephelinitic syenite rocks. Carbonatized ijolites are less developed comparing to syenites present as semilunar body that divide syenites and carbonatites. Massif Tomtor is an example of high productivity of carbonatite complexes that includes exogenous and endogenous deposits of wade spectra ores of metallic and nonmetallic mineral resources and is the main source of REE resources. Tomtor is characterized by well developed supergene zone and up to 400m thick weathering crust. Geological exploration of carbonatite weathering crust has revealed the unique complex rare metals ores that parameters significantly exceeds the ores of well known deposits such as Araha ? and Mount-Weld? (Lapin, Tolstov 1995).

The unique features of Tomtor deposit and its anomaly high concentrations of ore components could be explained by complex history of carbonatite weathering crust formation and two successive episodes of gypergenesis comparative to other deposits of such types. At the first stage under the oxidation environment of near-surface weathering the common profile of laterite weathering was formed. At this stage the main ore-concentration processes were residual concentration of inert metals along with Fe and Mn by dissolution and removal of carbonates and formation of secondary P-enrichment zone by accumulation of P on the deep horizons of laterite profile. Second stage is epigenetic that starts to operate after crust overlapping by coal-bearing sediments and is connected with influence of reduced anoxic water that percolated through coal sediments. At this stage the strong ore-concentration effect is due to the reducing of inert at the first stage Fe and Mn which became mobile and washed out making sharp repeated concentration of rare metals and other inert components.

As the result, a total degree of concentration of rare metals in the ores increases up to 15-20 times compared to parent carbonatites. Typical carbonatitic ore components such as Nb, La and Ce are becames anomalously high concentrated like rock-forming oxides. Concentrations of range of trace components that usually do not have a practical interest (P, Ti, V, Sc, Y, Sr, Ba, Ga, Pb, Zn ans others) are increased up to economically valuable level. Overall, successive operation of two stages of gypergenesis and their summary ore-

concentrating effect determine the unique parameters of Tomtor rare-metal ores and complex character of the deposit. Average concentrations of main and associated components in the ores in wt.% are as follow: Nb_2O_5-6,71;TR_2O_3-12,48;Y_2O_3-0,75;Sc_2O_3-0,06;TiO_2-7,0;V_2O_5-1,0;P_2O_5-13,5;Al_2O_3-13,0;$ZrO2$-0,65;SrO-3,0;BaO-3,7. Total amount of useful components is over than 50% of ore weight. Tompor ore resources can upload the rare-metals processing enterprise for 500 years of works.

On the state balance resources of Nb, Y, Sc, La, Ce, Pr, Nd, Eu, Sm are registered. Excepts those components in the contour of Nb ores resources of Ti, V, Al, P, Zr, Sr, U, TRY (Gd, Tb, Dy, Er, Tm, Yb, Lu) are evaluated. However, for the number of associated components only author estimation of average contents and resources that based on geochemical data and needs in detailization is present. The new geochemical works can increase potential of unique Tomtop ore complex by inclusion of new component in the estimated resources. Moreover, it is clear that possibility to obtain one or another component as economical products depends on the technologies of ore processing that must be oriented to maximum extraction of ore components. The technological process that developed by (VIMS,GIREDMET) suggests two stages of hydro-metallurgical processing: 1- alkaline decomposition with P extraction; 2- dissolution by hydrochloric acid with chlorination of hard residue and extraction of REE group. This technology suggests obtaining of Nb_2O_5 (extraction 83,1%); TiO_2 (87,8); Y_2O_3 (60); Sc_2O_3 (71,3); La_2O_3 (72,5); CeO_2 (72,5); Pr_2O_3 (72,5); Nd_2O_3 (72,5); Eu_2O_3(73); Sm_2O_3(72,5) as economical products. Additionally, this technology allows to extracts P, Al, Sr and Ba.

The ore potential of Tomtor massif is not restricted to discussed above unique rare metal ores therefore an investment to this ores exploration is only first step to Tomtor complex (Tolstov et al, 2014). First of all, the unique Tomtor rare metal ores is underlayered by Nb-P-Fe ores in carbonatite weathering crust and their siderite enriched varieties. Resources of those ores are significantly higher than that of explored rare-metal ores. Average contents of Nb_2O_5 is 0,7-0,8% and P_2O_5 is 16,5% with resources of P_2O_5 approximately 500 mln tons. In addition, rare metal ores is overlayered by Permian age sediments that contain significant resources of kaoline rocks and 10 m sick layers of brawn coal with resources approximately 20 Mln tons. To the north from Burannyi area the big deposit of magnetite ores that genetically related to carbonatites and are analogue to phoscorite or camaforite is located. Prognostic resources of these ores that by 80% composed by magnetite is estimated as 1 Bln tons. And finally, there is high probability to find economical Pt group element resources connected with alkaline and ultramafic rocks of Tomtor massif (Tolstov, 2014). All those factors multiple perspectives of Tomtor ore filed.

As a conclusion we emphasize that investments to exploration of unique Tomtor ores with first of all stimulated by interest to their REE contents not only provide access to this rare-metal ore complex but opens a new perspectives for other rich deposits of Tomtor massif. Thus we at the beginning point of new stage in the history Tomtor ore field exploration. Some goals of this new stage can be formulated as follow: At first it is necessary to conduct the detailed mineralogical and geochemical investigation of ultrarich rare metal Tomtor ores for full identification and evaluation of all associated components complex and identification and contouring of ore blocks that rich in Y, Sc and heavy REE. Secondly, perform the exploration of rare-metal deposit flanks with the purposes to follow the ore layer spread and increasing known resources. In third, to develops ore processing industrial technology for most full extraction of all ore components. As the result those steps will allow to estimate all Tomtor are filed potential including rocks that underlie and overlie unique rare-metal deposit and the flanks of ore field.

References

Lapin A.V., Tolstov A.V . Deposits of carbonatite weathering crust// Moscov, Nayka.1995, 208 c.

Tolstov A.V., Pokhilenko N.P., Lapin A.V., Kryukov V.A., Samsonov N. Yu. Investment attraction of Tomtor deposit and perspectives to its increase// M Razvedka i okhrana nedr. 2014, №9. c. 25-30.

Tolstov A.V. Platinum prospects of alkaline Rocks of Udzha Province (Northwest of Yakutia). 30-th International Conference on "Ore Potential of Alkaline, Kimberlite and Carbonatite Magmatism" 29 September - 02 October 2014 Antalya - Turkey Abstrakt Book Akdeniz Univercity-Antalya \ UCTEA Chamber of Turkish Geological Engineers-Ankara \ 2014, p 196-197.

On the problem of Y-mineralization of complex Nb-TR-Sc Tomtor deposit ores

Lapin A.V.*, Tolstov A.V.**, Kulikova I.M.*
IMGRE, lapin@imgre.ru, Moscow, Russia*
**IGM SB RAS, tols61@mail.ru*, Novosibirsk, Russia*

The unique rare-metal ores of Tomtor deposit are characterized by common for carbonatite weathering crust domination Ce-group in REE composition and contents of Y and Sc are connected with total concentrations of TR in carbonatites (Lapin and Tolstov 1992, Tolstov 2006). However, recently conducted detailed analysis

reveal significant variations of TR composition in terms of Ce/Y ratio (2.4-81, average 10-12) within the ore body. In some parts of ore body Ce/Y ratio drops up to 1-2 and concentrations of light REE and heavy REE became comparable. It is known that prices of individual TR elements are different by 1-2 orders of magnitude and heavy REE, Y and Sc are much expensive than light REE. Bearing that price difference in mind, the investment attraction of Tomtor ores strongly depends on contents of most valuable components first of all middle and heavy REE, Y and Sc (Tolstov et al, 2014).

Within the Tomtop deposit a significantly enriched in Y, Sc and HREE units can be divided. Parameters of one of those units are provided in table 1, where average contents of components in three 10 meters thick drill interceptions of ore body are shown. The average contents of Y oxide in the interceptions rich up to 2 wt% and more and have Ln_2O_3/Y_2O_3 ratios of 4.8-8 comparing to 20-30 in the main Tomtor ore body. The ratios Ce/Y are also decreases to 2-6 that indicates increasing role of HREE in ore composition. This fact in turn make up new principal situation under with the extraction of most deficite and expensive HRE and Y became economically profitable and may strongly influence the price of mining production.

Table 1.

№№	Parameters	Hole 5655	Hole 5755	Hole 5855	Average
1	H, м	30,4	23,8	31,5	28,6
2	M, м	12,6	12,4	10,1	11,7
3	$Nb_2O_5\%$	9,47	9,08	5,85	8,13
4	$Y_2O_3\%$	2,223	2,067	1,668	2,00
5	$Sc_2O_3\%$	0,136	0,150	0,108	0,13
6	$Ln_2O_3\%$	10.65	14,28	13,41	12,78
7	Ln_2O_3/Y_2O_3	4,79	6,91	8,04	6,44

Notes: H – depth of position of ore body top below the surface

M – sickness of ore body

Ln_2O_3- sum of light REE contents

In the enriched Y and HREE units a common correlation between Y, Sc and TR are disturbed. On the correlation plot the field of points with high concentration of Y and Sc that not correlate with LREE is appeared. This feature points to presence in the ore of additional REE-bearing phase with different REE composition. The presence of additional phase is also confirmed by correlation between Y,Sc and Zr contents that unusual for main ore body. Mineralogical and geochemical study revealed the presence of late epigenetic Y-Zr mineral- Zr xenotime with domination of middle and heavy REE in its composition. Position of xenotime in the rocks structure indicates its relation to one of latest stages of rocks epigenetic alteration. This stage is accompanied by their recrystallization and development of Al-phosphate and Ti- minerals (mostly ilmenorutile) rich zones around of fluidal and banded xenotime allocations.

The features of textural and structural position of xenotime in the ores and clearly late stage character of Y-mineralization allows to define specific stage of Y-mineralization within the prolonged in time period of epigenetic alteration of carbonatite weathering products (Lapin and Tolstov, this issue). The processes of this late stage led to significant shift in ores REE composition toward Y, middle and heavy REE and enrichment in Sc and Th. Overall, comparing to residual enrichment geochemical behavior of LREE in epigenetic alteration of carbonatite weathering products, for Y, Sc, HREE and Th the important role plays their introduction to ores by epigenetic solutions. Firstly epigenetic generation of monazite and florensite increase Y, Sc, HREE and Th concentrations and at the late epigenetic stage the Y-mineral Zr-xenotime is appeared in the ores.

The final result of evolution of TR composition in the epigenetic process is appearance of HREE, Y, Sc enriched blocks within mostly LREE-rich ore body. This stage of Y- epigenetic mineralization are important for economical evaluation of complex TR ores and determine the needs to more detailed study of ores compositional variations, mapping and contouring the ore blocks rich in Y, Sc and HREE on the preliminary explored Burannyi area as well as on the North and south parts of ore field that are under exploration in present time.

References

Lapin A.V., Tolstov A.V. New unique deposits of rare metals in the carbonatites weathering crust// Razvedka i okhrana nedr.1993. № 3. с. 7–11.

Tolstov A.V. The main ore formation of the North of Siberian Platform. M.: IMGRE. 2006. 212 c.

Tolstov A.V., Pokhilenko N.P., Lapin A.V., Kryukov V.A., Samsonov N. Yu. Investment attraction of Tomtor deposit and perspectives to its increase// M.: Razvedka i okhrana nedr. 2014, №9. с. 25-30.

Rare beryllium silicates - meliphanite and leucophanite - from nepheline-feldspar pegmatite, Sakharjok massif, Kola Peninsula

Lyalina L., Zozulya D., Selivanova E., Savchenko Ye.

Geological Institute, Kola Science Centre RAS, Apatity, Russia, lialina@geoksc.apatity.ru

Meliphanite $Ca_4(Na,Ca)_4Be_4AlSi_7O_{24}(F,O)_4$ and leucophanite $NaCaBeSi_2O_6F$ are studied from pegmatite body on the contact between alkaline gabbro and nepheline syenite, and from micaceous rim of the same pegmatite. The pegmatite body outcrops up to 30 m^2 in area and exhibits a complex internal structure and consists mainly of blocky nepheline, albite and analcime, and of intersticious aggregates of leucocratic (analcime, thomsonite, albite, nepheline) and melanocratic (phlogopite-annite series, aegirine-augite) minerals (Batieva and Bel'kov, 1984). The characteristic feature of pegmatite is the development of micaceous rock at the contact to host rock. Pegmatite is remarkable for abundant Be, REE and chalcophile mineralization. It is represented by meliphanite, leucophanite, behoite, gadolinite, britholite group minerals, REE bearing apatite, mimetite, nickeline, molybdenite and unidentified phases of lead (Lyalina et. al., 2010).

Meliphanite from pegmatite forms as independent crystals and grains, and irregularly oriented and radiating aggregates. The subidiomorphic platy crystals of meliphanite reach of 2-3 cm size with thickness up to 5 mm. Coarse grains are transparent and of different yellow colors. Numerous mineral inclusions are characteristics of meliphanite, the most abundant of them are biotite, pyroxene, amphibole, apatite, britholite, fluorite. Often meliphanite grains have poikilitic texture. Thus, it can be suggested that meliphanite crystallizes on the late stages of pegmatite formation.

Meliphanite from micaceous rock exibits the poikilitic crystals and grains up to 5 cm size. Meliphanite is non-transparent and semi-transparent, of grayish-green color. Often the grains are resorbed and have the uneven boundaries. These grains are often intergrown with leucophanite. The last one forms outer zones of poikilitic meliphanite. Both minerals are not visually distinguishable. Leucophanite was identified by microprobe and X-ray analysis. The boundary between meliphanite and leucophanite is uneven and, somewhere, sutural (Fig. 1).
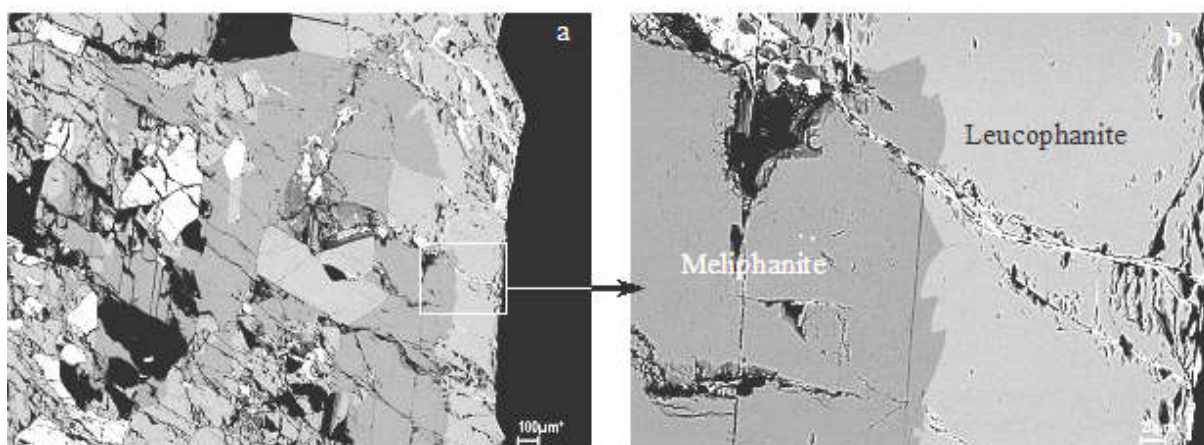
Fig. 1. Fragment of poikilitic meliphanite crystal with outer zone, composed of leucophanite (a), morphology of boundary between meliphanite and leucophanite (b). BSE images.

The chemical compositions of minerals are similar to those from other occurrences, early published in literature.

Meliphanite from pegmatite is characterized by average composition (N=7, wt. %): Na_2O=8.55, CaO=28.83, BeO_{calc}=8.91, FeO=0.05, SiO_2=43.30, Al_2O_3=5.07, F=5.41. Meliphanite from micaceous rock is of similar composition (N=3): Na_2O=8.38, CaO=28.80, BeO_{calc}=9.66, FeO=0.07, SiO_2=43.62, Al_2O_3=4.06, F=5.40.

Leucophanite is characterized by average composition (N=3, wt. %): Na_2O=12.17, CaO=23.39, BeO_{calc}=9.03, FeO=0.00, SiO_2=49.67, Al_2O_3=0.00, F=5.74.

The data obtained encourage us for further search of REE-bearing leucophanite, taking into account the development of Y-REE mineralization in pegmatite studied.

Of great interest is the fact that both meliphanite and leucophanite are established not only in the same occurrence but also as intergrowth. Earlier, the coexistence of both minerals was abandoned due to different geochemical media for their crystallization. According to J.D. Grice and F.C. Hawthorne (2002) "differences in the activity of Al in the environment of growth of these minerals seem critical in their paragenesis".

References

Batieva I.D., Bel'kov I.V. The Saharjok alkaline intrusion: rocks and minerals. Kola Branch, USSR. Acad. Sci., Apatity, 1984, 133 p. [in Russian].

Grice J.D., Hawthorne F.C. New data on meliphanite, $Ca_4(Na,Ca)_4Be_4AlSi_7O_{24}(F,O)_4$ // Canadian Mineralogist, 2002, V 40, pp. 971-980.

Lyalina L.M., Savchenko Ye.E., Selivanova E.A., Zozulya, D.R. (2010) Behoite and mimetite from the Saharjok alkaline pluton, Kola Peninsula // Geology of Ore Deposits, V 52, pp. 641-645.

The rare earth metals resource potential of the Kola Peninsula
Masloboev V.A.

Kola Science Center of the Russian Academy of Sciences
masloboev@ksc.ru

Rare-earth metals belong to the group of strategic mineral resources in all developed countries. These metals are being actively applied in high-tech industries; they are irreplaceable in contemporary military equipment. Their consumption grows 8-10 % per year abroad and in some high-tech fields – up to 30% per year. The unique structure of their electron shell makes them irreplaceable in many spheres; any substitution will deteriorate the quality of the final product. For example,   one of conventional filed of their application is oil catalytic cracking where lanthanum is used and not only sustains the catalyzer, but increases the efficiency of the cracking device on 7%, thus sparing the oil as the initial non-renewable resource.

Russia possesses no less than 20% of the world reserves of rare earth metals, though their extraction is about 2% and their application in production is less than 1%. The peculiar feature about the mineral resource base of our country is that it is mainly represented by complex ores containing the rare earth metals in particular.

The reserves of the rare earth metals in Russia are registered in the ores of 14 deposits, and their main part (60,2 %) is found in apatite-nepheline ores of the Kola Peninsula. The rare earth metals are not extracted during the processing of these ores. The licenses belong to Fosagro Company. The company develops 6 deposits: Kukisvumchorr, Yukspor, Apatity Circus, Rasvumchorr Plateau, Koashva and Nyurkpah. In situ reserves of apatite-nepheline ores in the deposits under development were 2 085 040 tons at 01.01.2011. Regarding the current level of production of the apatite concentrate the company is supplied by the resources for over 75 years. The deposits are worked out at 4 mines (Kirovskiy, Rasvumcjorr, Central and Eastern mines). Their total ore production capacity is 27 mln. tons per year. The company is planning to produce new products based on rare earth metals in the medium term.

Large reserves of rare earth metals are found in loparite ores of the Lovozero deposit containing about 1% of the oxides of the rare earth metals. The produced loparite concentrates contain 30% of oxides of the REM represented mainly by cerium group. The production volume of the loparite concentrate in Lovozerskiy GOK (mining and processing company) is 10 thous. tons per year and is limited by production capacity of the Solikamsk magnesium production plant. In recent years the plant has been producing about 6 thous. tons of the loparite concentrate per year and has been producing about 2,5 thous. tons of the rare-earth metal based products (carbonates of the rare earth metals) in the amount of about 1 billion rubles. About 98 % of the products were exported.

The rest reserves belong to rare-earth-apatite ores of the Seligradskoe deposit in the Republic of Sakha Yakutia (22,8%) and in the form of by-components are found in rare-metal ores of the Ulug-Tanzeksk deposit and oil-bearing sandstones of the Yaregskoe deposit. Recently the Tomtorskoe deposit, which is the largest in RF rare-metal deposit, was discovered and preliminarily explored in the North of the Republic of Sakha Yakutia. The deposit is represented by re-deposited crust of weathering of pyrochlore-monacite-crandallite ores and is remarkable for the highest concentrations of rare earth metal oxide (13-14%).

In the presentation is analysed the rare earth metals resource potential of the Kola Peninsula, including such promising deposits and mineral occurrences as eudialute ores of the Lovozero alkaline massif, yttrium-briolite ores of the Sakhar-jok deposit, etc.

Using noble gas isotope signatures to unveil the origin of carbon from the Cape Verde oceanic carbonatites

Mata J.*, Mourão C.*, Moreira M.**, Martins S.*

**Instituto Dom Luiz, Faculdade de Ciências, Universidade de Lisboa, 1749-016 Lisboa,
Portugal*
**Institut de Physique du Globe de Paris, France

It is consensual that carbonatites are rocks formed by crystallization of carbonate-rich mantle melts. Less clear is the origin of carbon and a debate exists between those invoking the involvement of crustal carbon recycled to the mantle and those proposing that carbon at the origin of carbonatite melts is "primordial" and has been stored at the deepest levels of the mantle. Probably these hypotheses are not mutually exclusive and *there are carbonatites and carbonatites*.

The Cape Verde archipelago is a plume-related hotspot located on ≈140 Ma Atlantic oceanic crust, west of the West African craton and at 600 km of the Senegal coast. It is the most important of the very few occurrences of oceanic carbonatites, with outcrops of these types of rocks being recognized in 5 islands and two islets. Calcium-carbonatites, magnesium-carbonatites, intrusive and extrusive occurrences have been described (Assunção et al., 1965; Silva et al., 1981; Mourão et al., 2010; Hoernle et al., 2002; Kogarko et al, 1993) and interpreted as the result of nephelinitic-carbonatitic magma immiscibility (Mourão et al., 2010; 2012). Evidence for sub-Cape Verde lithosphere carbonatite metasomatism is portrayed by the geochemistry of silicate lavas from Santiago Island, as described by Martins et al. (2010).

We review noble gas and carbon isotope signatures of the Cape Verde carbonatites in order to discuss the origin of carbon.

Cape Verde calcium-carbonatites are characterized by $\delta^{13}C$ (-7.8 to -4.2 ‰) and $\delta^{18}O$ values (usually < 8.5‰) typical of mantle rocks, while magnesium-carbonatites present significantly heavier carbon and oxygen isotope signatures (up to -0.5‰ and 21‰, respectively) suggesting that these rocks were affected by secondary processes (Hoernle et al., 2002; Mata et al., 2010). For this reason we will restrict the discussion to noble gas analyses performed for calcium-carbonatites.

The studied carbonatites, are characterized by low $^4He/^3He$ ratios (down to 46,700; R/Ra up to 15.5) which are considered to be primary, given that there are no evidences supporting significant cosmogenic ^3He additions. Such low ratios reflect sampling by carbonatite magmas of a reservoir characterised by low time-integrated $(U+Th)/^3He$, which we interpret as being localized in the deepest levels of the lower mantle. Considering that, according to experimental work, crustal carbonates are unlikely to be transported by subducting slabs to deep lower mantle depths, as a consequence of their removal by melting reactions, the above mentioned He isotope signatures point to a non-recycled origin for carbon (Mata et al., 2010; Mourão et al., 2012)

In the Cape Verde carbonatites ^{129}Xe anomalies ($^{129}Xe/^{130}Xe$ up to 6.84), relatively to the present day atmosphere ($^{129}Xe/^{130}Xe$ = 6.50), also cannot be explained by carbonate recycling. Indeed, if crustal carbonates could be characterised by high concentrations of Te and Ba, these would simultaneously increase with time both the ^{129}Xe and ^{130}Xe. This allows the interpretation of these anomalies as produced by decay of the now extinct ^{129}I (Mata et al., 2010).

The studied oceanic carbonatites would be characterized, before degassing, by $^4He/^{40}Ar^*$ ratios ($\leq$ 0.3) which are significantly lower than the instantaneous $^4He/^{40}Ar^*$ mantle production ratio (around 4 to 5) or the long-term (>1 Ga) accumulated $^4He/^{40}Ar^*$ (1 to 2; e.g. Yamamoto et al. 2009). This reflects the involvement of a mantle domain evolving under very high K/U which is not compatible with models invoking the recycling of crustal carbonates to explain the origin of carbonatites. In fact, a model invoking the recycling of altered (carbonated) oceanic crust at circa 1.6 Ga would imply the need of an evolution under K/U ratios of some 110,000. This value is two orders of magnitude higher than the K/U ratio of deeply recycled subducting slabs (see for example Becker et al., 2000; Lassiter, 2004). Interestingly such value is also more than 8 times higher than the estimated for the Bulk Silicate Earth thus endorsing the idea of the sampling by carbonatites of a long-term isolated "primordial" reservoir probably located at the base of mantle in the D" layer (Mourão et al., 2012)

In conclusion, despite that some models for the genesis of Cape Verde carbonatites invoke the necessity of the involvement of crustal carbonates recycled to the mantle (Hoernle et al., 2002; Doucelance et al., 2010; Doucelance et al., 2014), the conjugated use of several noble gas isotopic systems deny such hypothesis and lend support to an important role of carbon which remained isolated at an infra-mantle reservoir since the earliest stages of the Earth's history.

References:

Assunção, C.F.T., Machado, F., Gomes, R.A.D., 1965. On the occurrence of carbonatites in the Cape Verde Islands. Boletim da Sociedade Geológica de Portugal 16, 179–188.

Becker, H., Jochum, K.P., Carlson, R.W., 2000. Trace element fractionation during dehydration of eclogites from high-pressure terranes and the implications for element fluxes in subduction zones. Chemical Geology 163, 65-99.

Doucelance, R., Hammouda, T., Moreira, M., Martins, J.C., 2010. Geochemical constraints on depth of origin of oceanic carbonatites: The Cape Verde case. Geochimica et Cosmochimica Acta 74, 7261-7282.

Doucelance, R., Bellot, N., Boyet, M., Hammouda, T., Bosq, C., 2014. What coupled cerium and neodymium isotopes tell us about the deep source of oceanic carbonatites. Earth and Planetary Science Letters 407, 175–186.

Hoernle, K., Tilton, G., Le Bas, M., Duggen, S., Garbe-Schönberg, D., 2002. Geochemistry of oceanic carbonatites compared with continental carbonatites: mantle recycling of oceanic crustal carbonate. Contributions to Mineralogy and Petrology 142, 520-542.

Kogarko, L., 1993. Geochemical characteristics of oceanic carbonatites from the Cape Verde Islands. South African Journal of Geology 96, 119-125.

Lassiter, J.C., 2004. Role of recycled oceanic crust in the potassium and argon budget of the Earth: Toward a resolution of the "missing argon" problem. Geochemistry, Geophysics and Geosystems 5, Q11012, doi:11010.11029/12004GC000711.

Martins, S., Mata, J., Munhá, J., Mendes, M.H., Maerschalk, C., Caldeira, R., Mattielli, N. 2010. Chemical and mineralogical evidence of the occurrence of mantle metasomatism by carbonate-rich melts in an oceanic environment (Santiago Island, Cape Verde). Mineralogy and Petrology 99, 43-65.

Mata, J., Moreira, M., Doucelance, R., Ader, M., Silva, L.C., 2010. Noble gas and carbon isotopic signatures of Cape Verde oceanic carbonatites: Implications for carbon provenance. Earth and Planetary Science Letters 291, 70-83.

Mourão, C., Mata, J., Doucelance, R., Madeira, J., Silveira, A.B.d., Silva, L.C., Moreira, M., 2010. Quaternary extrusive calciocarbonatite volcanism on Brava Island (Cape Verde): A nephelinite-carbonatite immiscibility product. Journal of African Earth Sciences 56, 59-74.

Mourão, C., Mata, J., Doucelance, R., Madeira, J., Millet, M.-A., Moreira, M., 2012a. Geochemical temporal evolution of Brava Island magmatism: Constraints on the variability of Cape Verde mantle sources and on carbonatite-silicate magma link. Chemical Geology 334, 44-61.

Silva, L.C., Bas, M.J.L., Robertson, A.H.F., 1981. An oceanic carbonatite volcano on Santiago, Cape Verde Islands. Nature 294, 644-645.

Yamamoto, J., Nishimura, K., Sugimoto, T., Takemura, K., Takahata, N., Sano, Y., 2009. Diffusive fractionation of noble gases in mantle with magma channels: Origin of low He/Ar in mantle-derived rocks. Earth and Planetary Science Letters 280, 167-174.

Native lamproitic melts and their evolution: a study of subglacial glasses from Gaussberg volcano (West Antarctica)

Migdisova N.A., Portnyagin M.V., Suschshevskaya N.M.
Vernadsky Institute for Geochemistry and Analytical Chemistry, Russian Academy of Sciences Moscow, Russian Federation, nat-mig@yandex.ru

Extinct Gaussberg volcano on the West Antarctic ice sheet coast is composed by lamproites of the late Cenozoic age (56±5 ky [Tingey et al., 1983]). The origin and evolution of these continental alkaline melts is under discussion since 80th [Foley et al., 1987; Foley, Venturelli, 1989; Mitchell, Bergman, 1991; Foley, 2008]. Gaussberg volcano is a unique object to study alkaline continental magmatism due to its subglacial eruptions and excellent preservation of rocks often containing volcanic glass. Several pulses of such eruptions are expressed by terraces building a 370 m high volcanic edifice.

We present here the results of study of 20 quenched glasses from Gaussberg rock samples collected during the 2nd Soviet Antarctic Expedition in 1957-1958. The samples are fragments of glassy rims of pillow lavas [Vyalov & Sobolev, 1959]. We present also the results of analysis of melt inclusions (MI) in olivine (Ol) and leucite (Lc) phenocrysts. Major elements and volatile components (S, Cl, F) in the glasses were analyzed by electron microprobe at Max-Plank Institute für Chemie (Mainz, Germany) and GEOMAR Helmholtz Centre for Ocean Research (Kiel, Germany). Trace elements were obtained by LA-ICP-MS in the Institute for Geosciences at the Christian-Albrecht University (Kiel, Germany).

Mineral phenocryst assemblage of the Gaussberg lamproites is represented by 20-40% Lc, 10% Ol, and 5% Cpx. Leucite, diopside, phlogopite and apatite microliths are present in glassy matrix (Fig. 1A). Sample #464 (trachy-andesite) contains ortho- and clinopyroxene, magnetite, ilmenite, olivine, pyrrhotite sulfur globules and rare large rounded grains of ilmenite, apatite and zircon in glassy matrix (Fig.1B).
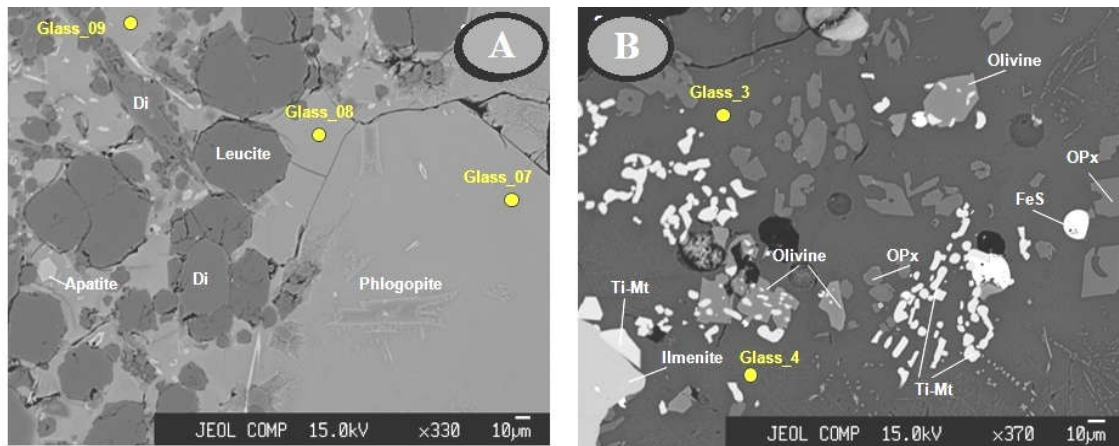
Fig. 1. Microphotographs of Gaussberg pillow lavas quenched rims fragments.
A – prevalent lamproitic type. B – trachy-andesite sample #464.

The composition of the Gaussberg glasses comprise two groups (Fig. 2): (1) predominating group of lamproitic glasses, and (2) high-Si evolved glasses from sample #464. MgO in group 1 varies from 5.5 to 1.5 wt%. With decreasing of the MgO content, SiO_2 (50-55 wt%), TiO_2 (5.5-7.8 wt%), Na_2O (3-5 wt%) increase; K_2O (11-12 wt%) remains nearly constant, and Al_2O_3 (5-7 wt%), CaO (1-7 wt%), P_2O_5 (0.3-1.6 wt%) decrease. FeO content (7.5-9 wt%) increases in the most MgO-rich glasses and then remains constant. Cl (0.13-0.27 wt%) and S (0.05-0.11 wt%) concentrations increase as MgO decreases due to their incompatibility with the liquidus crystal phases. In contrast to S and C, F content (0.17-0.45 wt%) drops in more evolved glasses, likely due to phlogopite and apatite crystallization. H_2O content does not exceed 1-2 wt%. The most primitive glasses have low Cl (0.13 wt%), S (0.05-0.1 wt%) and high F (0.5 wt%) and P (1.5-2 wt%), which may be characteristic of primary lamproitic melts. Group 2 glasses from sample #464 are remarkably evolved and heterogeneous. The glasses have trachyandesitic (SiO_2 = 57-72, Na_2O = 2.5-4, K_2O = 5-7.5 wt%), high-Al_2O_3 (10-20 wt%) compositions, which fall off the main fractionation trend of the lamproite melts (Pic.2).
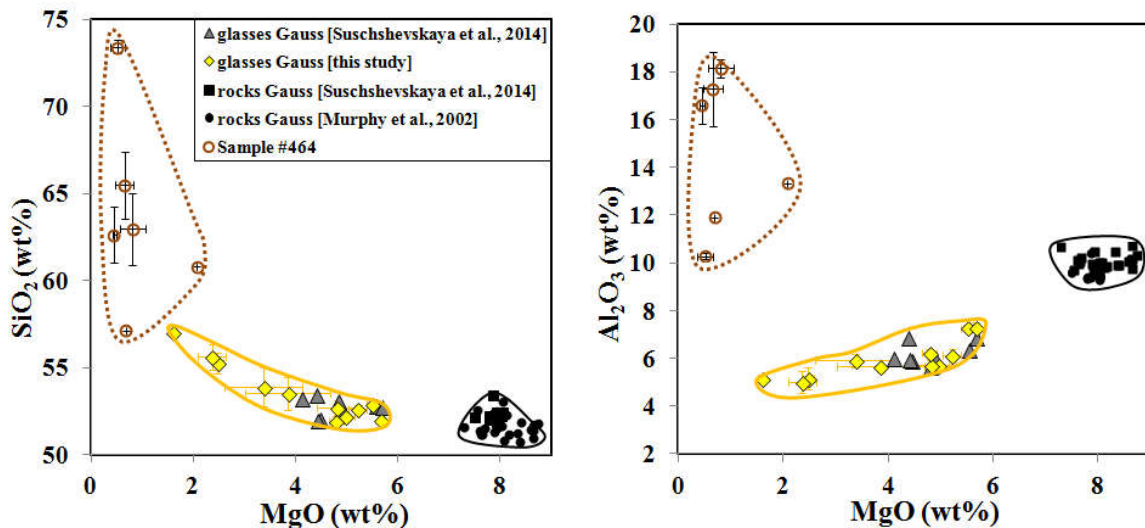
Fig.2. Major elements in quenched glasses and bulk rocks from Gaussberg volcano.

Gaussberg lamproites exhibit highly enriched in LREE, strongly fractionated spectra (La/Yb_n = 80, $Dy/Yb_n \approx 2.2$, Sm/Nd_n = 0.4). Characteristic features of the lamproites are also Zr, Hf, Ba and Pb maxima and K (not shown), Rb, U, Nb, Ta minima relative to REE on the PM-normalized patterns. Sample #464 has distinctively lower LREE, higher HREE, low Ba, Sr, Ti and Eu, and no Zr-Hf maximum compared to more mafic samples (Pic.3).

74
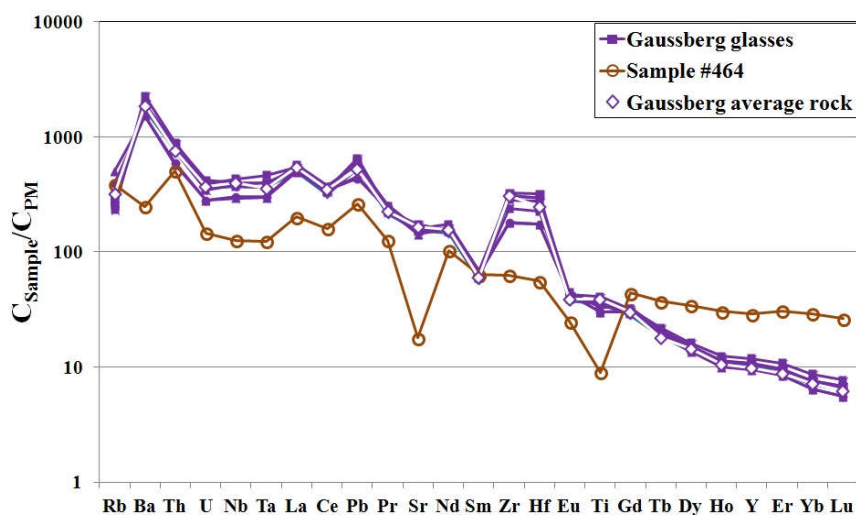
Fig.3. Lithophile element patterns of Gaussberg glasses. PM after Sun & McDonough [1989].

Major conclusions of the study are:

1. Major elements in the Gaussberg glasses main elements form continuous series ranging from 6 to 2 wt% MgO and reflecting ~50% crystal differentiation of olivine, leucite, clinopyroxene, phlogopite, and apatite from the primary lamproite melts having presumably ~8.5wt% MgO (similar to WR samples). Sample #464 has likely a hybrid origin via assimilation of sedimentary bedrocks (sandstones) by mafic lamproitic melts.

2. Gaussberg lamproitic primary melts are enriched in volatiles (H_2O, Cl, F, S) compared with typical oceanic basalts. F concentrations are however significantly lower than in the West Australian lamproites, similar in major, trace element and isotope composition to those from Gaussber volcano [Sobolev et al., 1989]. The lack of sulfide phases in Gaussberg mafic lamproites suggests a deep magma origin in the garnet stability field or possible oxidation of lamproites during their ascent to the surface [Mavrogenes, O'Neil, 1999].

References:

1. Foley S.F., Venturelli G., Green D.H., Toscani L. The ultrapotassic rocks: characteristics classification and constraints for petrogenetic models // Earth-Science Reviews. 1987. V.24. P. 81–134.

2. Foley S. F., Venturelli G. High K_2O rocks with high MgO, high SiO2 affinities // In Boninites and Related Rocks (ed. A. J. Crawford) Unwin Hyman. London. 1989. P. 72–88.

3. Mitchell R.H., Bergman S.C. Petrology of Lamproites // Plenum Press, New York. 1991. 408 p.

4. Foley S.F. Rejuvenation and erosion of the cratonic lithosphere // Nature Geoscience. 2008. V. 1. P. 503–510.

5. Сущевская Н.М., Мигдисова Н.А., Антонов А.В., Крымский Р.Ш., Беляцкий Б.В., Кузьмин Д.В., Бычкова Я.В. Геохимические особенности лампроитовых лав четвертичного вулкана Гауссберг (Восточная Антарктида) - результат влияния мантийного плюма Кергелен // Геохимия. 2014. №12. С.1-21.

6. Vyalov O.S. and Sobolev V.S. Gaussberg, Antarctica // International Geology Review. 1959. № 1 (7). P. 30-40.

7. Tingey R.J., McDougall I., Gleadow A.J.W. The age and mode of formation of Gaussberg, Antarctica // Journal of the Geological Society of Australia. 1983. № 30. P.241-246.

8. Gupta Alok K., Kenzo Yagi. Minerals and Rocks 14 // Springer-Verlag. Berlin Heidelberg New York, 1980. Editor in Chief P. J. Wyllie, Chicago, IL.

9. Prelevic D., Foley S.F., Romer R., Conticelli S. Mediterranean Tertiary lamproites derived from multiple source components in postcollisional geodynamics // Geochimica et Cosmochimica Acta, 2008, 72, pp. 2125-2156.

10. Foley S.F. Petrological characterization of the source components of potassic magmas: geochemical and experimental constraints // Lithos. 1992a. V.28. P. 187–204.

11. Sobolev, A.V., Gurenko, A.A., Sobolev, N.V. 1989. Petrology of ultrabasic ultrapotassic magmas of continental lithosphere: results of inclusions studies in olivine from lamproites, kimberlites, and kamafugites, 28th IGC, Washington, D.C. USA, pp. 146-147.

12. Mavrogenes, J.A., O'Neill, H.S.C. 1999. The relative effects of pressure, temperature and oxygen fugacity on the solubility of sulfide in mafic magmas. Geochim. Cosmochim. Acta 63, pp.1173-1180.

13. Murphy D.T., Collerson K.D., Kamber B.S. 2002. Lamproites from Gaussberg, Antarctica: Possible Transition Zone Melts of Archaean Subducted Sediments. J.Petrol., 43. pp. 981-1001.

14. Sun S.-S., McDonough W.F. Chemical and isotopic systematic of ocean basalts: implications for mantle composition and processes/ Magmatism in the ocean basins. (Eds.Suanders A.D., Norry M.J.). Geol.Soc.Spec.Publ. 1989. V.42. P. 313-345.

Compositional variation in the pyroxenes and amphiboles of the Abu Khruq ring complex, Egypt

Mogahed M.M., Rashwan A.A.
Department of Geology, Faculty of Science, Benha University, Benha, Egypt.
MUSTAFA.AHMED01@fsc.bu.edu.eg

Alkaline ring complexes display many paradoxical characteristics. Some tend to have mantle origin, indicated by the presence of alkaline rocks in an oceanic environment and confirmed by their association with basic lava. While other complexes, display crustal isotopic signatures in hydrothermally altered and mineralized zones.

The Abu Khruq alkaline ring complex (ARC) is one of about fifteen alkaline ring complexes intruding Precambrian rocks of the Arabo-Nubian shield in the south Eastern Desert of Egypt (Fig. 1) and ranging in age from Silurian to Late Cretaceous (Serencsits et al.,1979). ARC is an epizonal, multi –intrusion alkaline ring complex that exhibit the association of silica saturated, under- and oversaturated rocks. We are undertaking more detailed mineralogical and chemical studies, and present here an electron microprobe investigation of the pyroxenes and amphiboles of the intrusion. The country rocks immediately surrounding the ARC are mainly consist of a series of highly grade metamorphic rocks which grades gradually from hornblende gneisses into greenish actinolite schists that were subsequently intruded by granite.
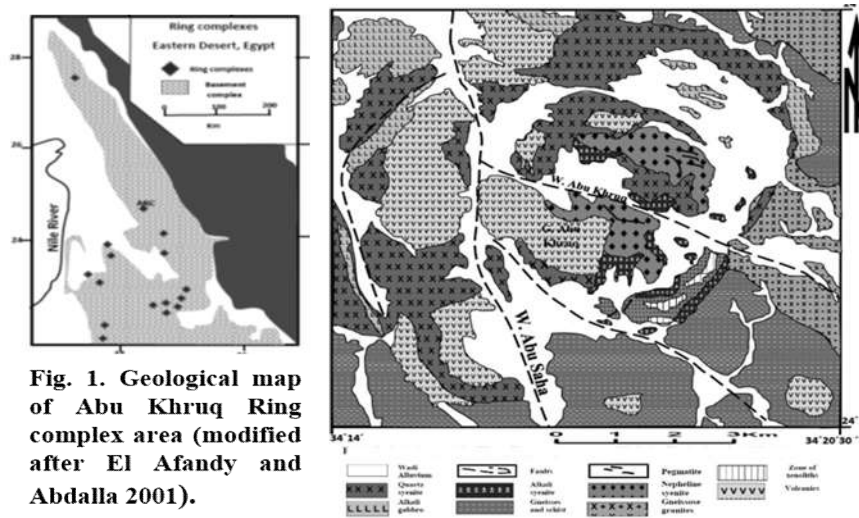
Fig. 1. Geological map of Abu Khruq Ring complex area (modified after El Afandy and Abdalla 2001).

At the scale of the handspecimen and thin section, most **volcanic rocks** have a porphyritic texture with variable modes of phenocrysts (and rare xenocrysts in some samples) in an aphanitic groundmass. Phonolite represents the dominant volcanic rock unit in the AKC and it is mainly massive and varies from dark grey to greenish grey. **Alkali gabbro** is massive, medium to coarse-grained, and characterized by dark to light grey colours consisting predominantly of plagioclase (ranging from oligoclase to labradorite), perthitic orthoclase, aegirine-augite, calcic amphibole and Fe-Ti oxides. Biotite, nepheline and apatite occur in variable accessory amounts. **Quartz syenites** are medium to coarse grained, white-yellow to light brown rocks and composed mainly of zoned grey euhedral perthitic orthoclase laths and interstitial quartz in clusters with sodic-calcic amphiboles, aegirine-augite and accessory magnetite, ilmenite, titanite, apatite and zircon. **Alkali syenites** are pinkish gray, medium- to coarse-grained nepheline bearing alkali feldspar syenites. They consist mainly of euhedral to subhedral perthitic orthoclase, interstitial, zoned amphibole, biotite, light green aegirine-augite, and titanite. **Nepheline syenites** are medium-grained grey rocks with euhedral to subhedral, coarse perthitic alkali feldspar with many minute inclusions, euhedral to subhedral nepheline, sodalite, aegirine-augite and melanite garnet with subordinate biotite and alkali amphibole. The late magmatic evolution of ARC is represented by the formation of nepheline syenitic **pegmatitic veins** that cut the nepheline syenite at the east and northeastern part of the complex and trending NNW-SSE. They contain the same mineral assemblages as the enclosing nepheline syenite.

The chemistry of the pyroxene can be illustrated using diagrams of the figures 2 through 4. Both core and rim of the pyroxene for the alkali gabbro and nepheline syenite are calcic-sodic aegirine-augite while alkali syenite and quartz syenite are scattered between augite and aegirine-augite (Fig. 2). The analysed pyroxene form a trend from the augite to the pigeonite fields (Fig. 3). Pyroxene trend is characterized by a progressive enrichment in Na towards the aegirine corner, with no significant enrichment in hedenbergite (Fig. 4). The overall pyroxene trend is suggestive that fractionation involved a late, progressive increase in Na. Microprobe analysis shows that

76

the earliest-formed pyroxenes in most units are much less acmitic in composition. Mg-number pyroxenes increase markedly from the Alkali syenite to quartz syenite to nepheline syenite and get the highest value in alkali gabbro.

The amphiboles distribution in the ARC rock units are restricted mainly to syenite and quartz syenite while it is less common in nepheline syenite. The rim`s Mg-number of zoned amphiboles is consistently lower than the cores. The amphibole are ranging from calcic in alkali gabbro to sodic calcic and sodic in both syenite and quartz syenite. All analysed amphiboles are characterized by high SiO_2, low Al_2O_3 and TiO_2 contents, and low MgO/FeO^* ratios. The composition of the analysed amphibole samples are compositionally similar to amphiboles from typical differentiated peralkaline suites, such as those from the Rallier-du-Baty Peninsula, Kerguelen (Giret *et al.* 1980). According to Leake's classification (1978), ARC amphiboles from syenite and alkali gabbro are ranging from arfvedsonite to ferro-eckermannite, to winchite, to katophorite, to hastingsite and lastly to pargasite, involving (K,Na), Fe^{2+}, Fe^{3+} substitution, under reducing conditions (Giret *et al.* 1980). These authors noted that there is a close relationship between amphibole compositional trends and agpaitic coefficient of their host rocks: the more differentiated the magma, the more silica-rich the amphiboles. According to them, these silica- and alkali-rich amphiboles crystallize only in a very late magmatic stage, usually later than alkali feldspar, or during hydrothermal stages. Amphiboles from gabbro display limited $Ca+Al^{iv}$ versus $Si+Na+K$ substitution and plot next to the fields of amphibole from gabbro with normative nepheline defined by Bedard (1988; fig.5). This amphibole is richer in $Ca+Al^{IV}$ than that from syenite and quartz syenite amphibole.
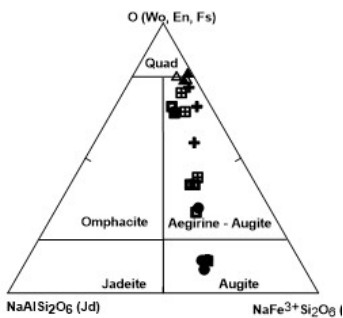
Fig. 2. Compositional variation of clinopyroxene of the ARC in the Jd-Q- diagram. Fields and nomenclature after Morimoto (1988). Symbols: □-quartz syenite; ●-alkali syenite; nepheline syenite (⊞-rim, +-core); alkali gabbro (△-rim, ▲-core).
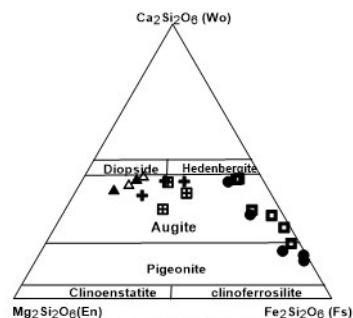
Fig. 3. Compositional variation of clinopyroxene of the ARC in the quadrilateral of pyroxenes. Fields and nomenclature are the one adopted by Deer et al. (1978).Symbols as in figure 2.
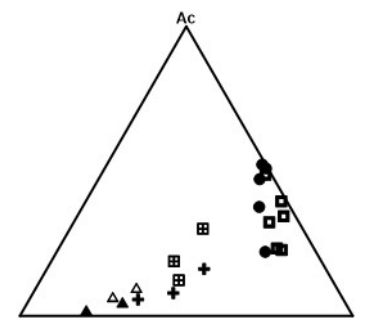
Fig. 4. Compositional variation of pyroxenes of the ARC in the Di-Ac-Hd diagram. Symbols as in figure 2
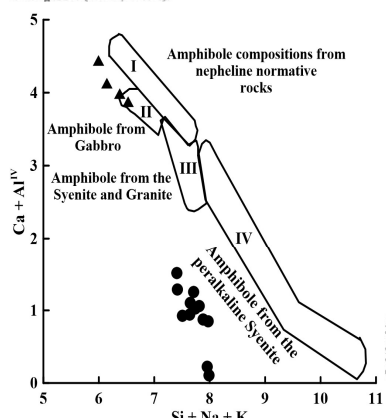
Fig. 5. Diagram of Ca + Al^{iv} vs. Si + Na + K after Giret et (1980). Fields are adopted after Bedard (1988). Symbols: ▲-amphiboles from alkali gabbro; ●- amphiboles of syenit and quartz syenite.
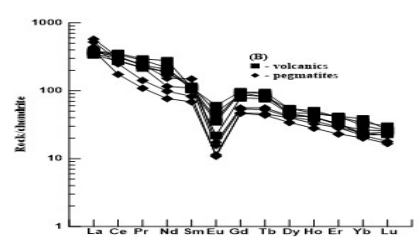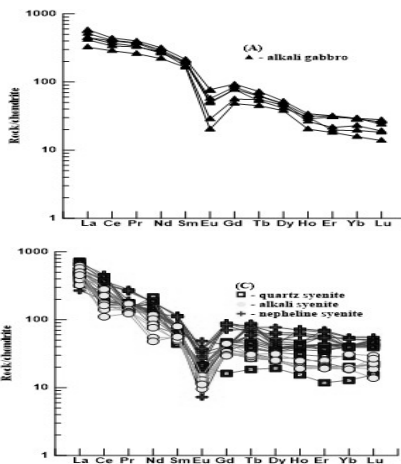
Fig. 6. Chondrite-normalized rare-earth-element plots, with chondrite values of McDonough and Sun (1995). (A) Alkali gabbro, (B) volcanics and pegmatite, and (C) syenite

The REE patterns of ARC rocks (Figs. 6A to 6C) show overall enrichment of the REE contents from alkali gabbro and nepheline syenite with intermediate contents of alkali syenite and volcanics. Almost all samples showed similar REE patterns suggesting that they have a cogenetic relationship. The chondrite-normalized REE distribution patterns (Figure 6) illustrate that ARC rocks are characterized by enrichment in LREE and depletion in HREE with well-defined Eu-negative anomaly which may be related to the later formation of this intrusion body and strong differentiation during crystallization. The enrichment of LREE relative to HREE for all the rocks from ARC is significantly different from the REE distribution pattern in normal mantle-derived rocks (e.g. MORB), which should usually be enriched in HREE. This indicates that the magma sources of ARC are not derived from normal primitive mantle. Also it is shown from the REE pattern that this pluton is high in REEs, with enrichment of LREE and depletion of HREE, suggesting that the mantle source of the rock is either enriched or juvenile.

Conclusions

Abu Khruq ring complex represents alkaline mafic-felsic intrusion formed of cogenetic alkaline rocks, ranging from alkali gabbroic and intermediate compositions to syenites, quartz syenite and nepheline syenites. All samples are enriched in LREE with moderate to steep fractionated patterns and possess a Eu negative anomaly. The whole complex is inferred to have originated from alkali basaltic to basanitic magmas of OIB-like character. The general increasing of the amphibole and biotite among the different rocks of the complex reflects the hydrous nature of ARC magmas. The phonolitic magmas from which the nepheline syenites crystallised were produced as fractionation residues from basanitic parent magmas which experienced insignificant crustal assimilation. Crustal contamination led to the formation of the quartz syenite at the expense of the silica-undersaturated syenitic magma.

References:

Serencsits, C.M., Faul, H., Foland, K.A., El Ramly, M.F. & Hussein, A.A. Alkaline ring complexes in Egypt: their ages and relationship to tectonic development of the Red Sea. // Ann. Geol. Serv. Egypt. 1979. Vol. 9. pp. 102–116.

Giret, A., Bonin, B., & Léger, J. Amphibole compositional trends in oversaturated alkaline plutonic ring-complexes. // The Canadian Mineralogist. 1980. Vol. 18. pp. 481–495.

Bedard, J.H. Comparative amphibole chemistry of the Monteregian and White Mountain alkaline suites, and the origin of amphibole megacrysts in alkali basalts and lamprophyres // Mineralogical Magazine. 1988. Vol. 52. pp. 9l-103.

McDonough, W. F. & Sun, S.-s. The composition of the Earth. // Chemical Geology. 1995. Volume. 120. pp. 223-253.

LEAKE, B.E. Nomenclature of amphiboles. // Candian mineralogist.1978. Volume. 16. pp., 501-520.

Rb-Sr, Sm-Nd, Pb-Pb, Lu-Hf isotope systems as a signature of sources of alkaline-carbonatite magmatism (by the example of Urals and Timan complexes, Russia)

Nedosekova I.L.

Zavaritsky Institute of Geology and Geochemistry UB RAS, Ekaterinburg, Russia vladi49@yandex.ru

Various isotope systems (Rb-Sr, Sm-Nd, U-Pb, Pb-Pb, C-O, Lu-Hf) in the rocks and minerals of the Urals and Timan alkaline-carbonatite complexes are investigated. They are also compared to alkaline-carbonatite magmatism types existing in various structures of the Earth: (a) with the carbonatite complex cratons and platforms framing Na-ultramafic-alkaline-carbonatite formation (UAC) – by the example of the complexes of Maimecha-Kotui, East Sayan, East Aldan, Sette-Daban (Siberian Platform and its framing), Karelian-Kola and the East African Provinces; (b) with K-alkaline-carbonatite complexes of rift zones of shields (by the example of the Aldan Shield complexes); (c) with the carbonatite complex fold zones (by the example of the Altai-Sayan, South Tien Shan, Himalayan fold regions).

We have obtained isotopic parameters for the rocks of Ilmeno-Vishnevogorsky alkaline-carbonatite complex (IVAC), Urals fold belt: $^{87}Sr/^{86}Sr_{440}$ = 0.70336-0.70380, εNd_{440} (+ 2.9 ... + 5.8), εHf_{440} (+ 4.7 ... + 11.4), $^{206}Pb/^{204}Pb_{440}*$ = 18.54 -20.6, $^{207}Pb/^{204}Pb_{440}*$ = 15.53-15.66 (Vishnevogorsky carbonatite-miaskite massif) and $^{87}Sr/^{86}Sr_{440}$ = 0.70421-0.70470, εNd_{440} (+ 0.7 ... -2.8), $^{206}Pb/^{204}Pb_{440}*$ = 18.04-19.91, $^{207}Pb/^{204}Pb_{440}*$ = 15.65-15.93 and εHf_{440} (0 ... -2) (Buldym carbonatite-ultrabasic massif). These values correspond to moderately depleted mantle compositions (Vishnevogorsky carbonatite-miaskite massif) and moderately enriched mantle EM1 (Buldym carbonatite-ultrabasic massif). Similar isotopic compositions are typical for ultramafic-alkaline-carbonatite complexes located on the edge of the platform and the Precambrian cratons (Fig. 1).
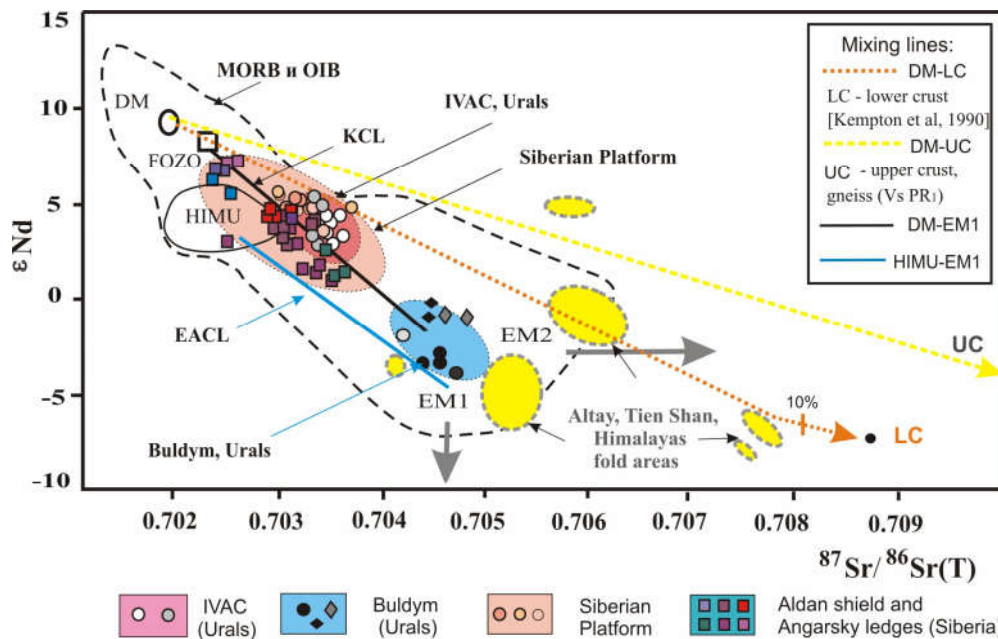
Fig.1. Diagram εNd vs. ^{87}Sr/^{86}Sr$_i$ of carbonatites and alkaline rocks of the IVAC and Buldym (Urals) in respect to the mantle sources DM, HIMU, FOZO, EM1, EM2, MORB and OIB [8], as well as Kola (KCL) [7], Eastern African (EACL) [4], Siberia [1, 3], Aldan [1] carbonatite complex of platforms and shields and Himalayas, Tian Shan, Altai, Mongolia collision carbonatite complex of fold regions [1, 2, 5].

On the εNd vs. ^{87}Sr/^{86}Sr (T) diagram the data points of of the IVAC miaskites and carbonatites fit the mantle array along the line connecting depleted (DM) and enriched (EMI-like) mantle. A similar evolution line is marked for the carbonatite complex of Karelia-Kola Province and shows mixing of two mantle reservoirs FOZO and EM1 in the processes of magma generation [6, 7]. Carbonatite complexes on the edge of the Siberian Platform (Maimecha-Kotuiskaya and Eastern Aldan provinces) also have similar isotopic compositions [1, 3]. Sr-Nd isotopic compositions of Buldym carbonatites correspond to the enriched mantle EM1 and the carbonatite complexes of rift zones of shields with the deepest mantle sources (complexes of the East African Rift, the Aldan and Angarsk shields), formed with a substantial contribution of the HIMU component [4]. It should be noted that the IVAC differs by Sr-Nd-isotopic composition from the collision carbonatite complexes with mixed mantle-crustal source EM2 (Himalayas, Tien Shan, Altai, Mongolia fold areas) [1, 2, 5] (see fig. 1).

On the ^{206}Pb/^{204}Pb vs. εNd diagram, compositions of IVAC rocks are on a three-component mixing line with DM-, EM1- and HIMU-components (similar composition is marked for platform ultramafic-alkaline-carbonatite complexes of Karelia-Kola-Scandinavian province) and on the mixing line HIMU-EM1 (which is similar to the carbonatite isotopic compositions of the East African Rift). It should be noted in this diagram that the isotopic compositions of collision carbonatite complexes are outside of the «mantle triangle DM-EM1-HIMU». Thus, Pb-Nd-systematic of IVAC illustrates the absence of the two-component mixing DM-EM1 in the IVAC rocks and the need of participation enriched component, which usually correlates with the plume (HIMU or others). The nature of the enriched component needs further studies, but at the moment we can say that the IVAC constitutes lines of Pb-Nd isotopic evolution, which are similar to platform ultramafic-alkaline-carbonatite complex.

Hf-Nd systematic also confirms a mantle source of the IVAC magma. Early zircon compositions of the IVAC plot in the field of moderately depleted mantle and lower crust rocks. Considerable variations in the initial Hf isotope ratios in these zircons are likely to reflect the heterogeneity of primary magmatic source and may be indicative of the participation in the crystallization of IVAC zircon new portions of melts with different isotopic composition determined by mixing materials at their source. The Hf isotopic composition of later metamorphic zircons shows that they were formed during recrystallization of the early zircon without substantial additional supply of trace elements. Thus, Hf-isotope data of IVAC confirm the participation of DM and more enriched nonradiogenic Hf source (probably representing a lower crustal component LC) in the magma generation. It should be noted that Nd-Sr-isotopic mixing lines DM-LC also shows the presence of the lower crust components in the IVAC rocks (see fig. 1).

Isotopic parameters for Chetlassky dyke alkaline-ultramafic-carbonatite complex (Timan): initial isotopic ratio of carbonatites ((^{87}Sr/^{86}Sr)i = 0.70336-0.70369, εNd = 5.07-5.71) are close to lamprophyres and picrites ((^{87}Sr/^{86}Sr)i = 0.7037-0.7043, εNd = 5.42-6.19), which may indicate "primary" carbonates and single mantle source of the Chetlassky complex rocks with a small addition of crustal component (probably metamorphic fluid). The source of crustal fluid could be Riphean host sedimentary carbonate series, having the radiogenic

isotope composition Sr (^{87}Sr / ^{86}Sr)i = 0.7138 and "heavy" isotope composition of C and O – δ^{13}C (from -4.5 to 0.5 ‰) and δ^{18}O (from 18.1 to 25.7 ‰). Nd-Sr-isotope mixing line DM-UC (upper crust, Riphean host sedimentary carbonate rocks) shows, that the Chetlassky carbonatites have more, than 95% of the mantle component and less, than 5% of the upper crust component.

Thus, the study of Sm-Nd, Rb-Sr, Lu-Hf, Pb-Pb-isotopic systems of Urals and Timan alkaline-carbonatite complexes and their comparison to alkaline-carbonatite magmatism types, existing in various structures of the Earth, showed that the Urals and Timan alkaline-carbonatite complexes are similar to those carbonatite complexes, localized on the edge of the platform (with moderately depleted sources) and Precambrian cratons (with the deepest mantle sources such as EM1 and HIMU), and differ from the carbonatite complexes of consolidated fold regions (usually with mixed mantle-crustal source such as EM2).

References:

1. Vladykin NV. Sr and Nd isotope geochemistry of alkaline carbonatite complexes of Siberia and Mongolia and some geodynamic consequences // Problems of sources of deep magmatism and plumes. Publ. Institute of Geography RAS. 2005. P. 13–29.

2. Vrublewsky VV, Gertner IF. Nature carbonatite complexes of fold regions: isotopic evidence of mantle-crust interaction // Problems of sources of deep magmatism and plumes. Publ. Institute of Geography RAS. 2005. P. 30-49.

3. Kogarko LN et al. Evolution and isotopic sources of Guli ultrabasic alkaline massif // DAN. 1999. V. 364. № 2. P. 235–247.

4. Bell K, Petersen T. Nd and Sr Isotope Systematics of Shombole Volcano, East Africa, and the Links between
Nephelinite, Phonolites and Carbonatites // Geology. 1991. 19. P. 582–585.

5. Hou Z., Tian S., Yang Z. et al. The Himalayan collision zone carbonatites in western Sichuan, SW China: Petrogenesis, mantle source and tectonic implication // Earth and Planet. Scie. Letter. 2006. V. 244. P. 234–250.

6. Kogarko LN, Lahaye Y, Brey GP Plume-related mantle source of super-large rare metal deposits from the Lovozero and Khibina massifs on the Kola Peninsula, Eastern part of Baltic shield: Sr, Nd and Hf isotope systematics // Miner Petrol. 2010. 98. P. 197–208

7. Kramm U Mantle components of carbonatite from the Kola Alkaline Province, Russia and Finland: a Nd-Sr study // Eur J Mineral. 1993. 5. P. 985–989.

8. Zindler A, Hart SR Chemical geodynamics // Ann Rev Earth Planet Sci. 1986. 14. P. 493–571.

Major, minor and trace element and oxygen isotopic composition of olivine from kimberlites of the Arkhangelsk Diamond Province, Russia

Nosova A.A.*, Sazonova L.V.**, Kargin A.V.*, Borisovsky S.E.*, Khvostikov V.A.**, Burmiy J.P.*, Kondrashov I.A.*
*Institute of Geology of Ore Deposits, Petrography, Mineralogy, and Geochemistry (IGEM), Russian Academy of Sciences, Moscow, Russia
**Institute of Microelectronics Technology and High Purity Materials (IMT), Russian Academy of Science, Chernogolovka, Russia

This study presents the first systematic petrographical, geochemical and stable isotopic investigations on different textural varieties of olivine (olivine from peridotite xenoliths, macrocryst-type (Ol-I), and phenocryst-type zoned (Ol-II) from two diamondiferous kimberlite pipes (V. Grib and Pionerskaya) of the Arkhangelsk diamond province (ADP), which differ in geologic setting, geochemical and isotopic characteristics, and diamond content.

The problem of the origin of olivine in kimberlite is hotly debated. The main unsolved question is whether large rounded or subrounded crystals (Ol-I) are xenocrystic (i.e. mantle-derived) or represent phenocrysts cognate to the kimberlite melt. Smaller euhedral or subhedral often zoned grains (Ol-II) may consist of xenocrystic core and rim crystallized from kimberlite melt. Some recent studies (Arndt et al., 2010; Brett et al., 2009; Kamenetsky et al., 2008; Pilbeam et al., 2013; Bussweiler et al 2015; Sazonova et al., 2015) demonstrated a complex crystallization history of the kimberlitic olivine. Our results support a diversity of olivine origin in the kimberlites and show that there is no single mechanism of olivine formation.

Geological setting and samples. The Arkhangelsk diamond province is situated in the northern East European Craton. Several fields of kimberlites and related rocks were distinguished within the province. The Pionerskaya pipe is located in the Zolotitsa kimberlite field and, together with the Arkhangelsk, Karpinsky-1,

Karpinsky-2, and Lomonsov pipes, assigned to the Lomonosov diamond deposit. The V. Grib pipe is located in the central part of the Arkhangelsk diamond province, 30 km northeast of the Pionerskaya pipe, and belongs to the Verkhotina or Chernoozerskoe kimberlite field.

Deep borehole no. 1490 in the northwestern part of the Pionerskaya pipe penetrated porphyritic kimberlites (perhaps, dikes) with fresh olivine at depths of 1040–1050 m (Mahotkin et al., 2000). We studied olivine from this depth interval. Some boreholes (nos. 106 and 1) drilled in the V. Grib pipe penetrated autolithic breccia or porphyritic kimberlite at depths of 600–750 m; these rocks contain almost unserpentinized or weakly altered olivine, which was used in our study. Olivines (partly or completely preserved) were also analyzed in five peridotite xenoliths from the V. Grib kimberlites. Four xenoliths are garnet lherzolites, including one deformed peridotite, and one sample is a garnet harzburgite.

The presence of two olivine types (generations) in the Pionerskaya kimberlites was noted previously (Mahotkin et al., 2000; Parsadanyan et al., 1996), but they were not studied in detail; in the V. Grib kimberlites, olivine was studied only in peridotite xenoliths and inclusions in diamond (Malkovets et al., 2011).

Methods. Analyses of major and minor element compositions of olivines were performed on polished thin sections of kimberlites and xenoliths and on epoxy mounts with olivine grains separated from crushed kimberlite samples and deformed peridotite xenolith.

Olivine (approximately 550 grains) was analyzed by the electron microprobe (EPMA) technique using the high precision method developed by Sobolev et al. (2007) and adapted at the IGEM RAS (Moscow) by Kargin et al. (2014). This method was designed for the high precision analysis of both major and minor elements in olivine. Our results of the measurements of the San Carlos olivine standard (Jarosewich et al., 1980) during the investigation of olivine from the kimberlites of the ADP are consistent with published data, and the error for the Mg# value of olivine is smaller than 0.1% relative (2σ). Laser ablation inductively coupled plasma mass spectrometry (LA-ICP-MS) was performed to determine the trace element compositions of olivines (65 analyses for macrocryst-type olivine (Ol-I)) using the New Wave Research UP266 MACRO laser ablation system coupled to an Thermo Scientific XSeries II plasma-mass spectrometer equipped with a quadrupole mass analyzer at the IMT RAS (Chernogolovka). The oxygen isotope composition of olivine was analyzed in 10 olivine microsamples at the Laboratory of Isotopic Geochemistry and Geochronology of the IGEM RAS by fluorination using laser heating. The reproducibility of $\delta^{18}O$ was ±0.1‰ (1σ).

Results. A significant portion of *Ol-I from the V. Grib kimberlites* with Mg# = 92.9±0.005, high Cr (132±28 ppm) and Ca (157±45 ppm) and low Ti (under 70 ppm) contents falls within the field of olivine megacrysts (macrocrysts) from the Udachnaya pipe (Mg# = 92.7 ± 0.8; Sobolev et al., 2009). They are characterized by high Ni (2825±243 ppm) concentration. Nb и Zr show wide variations, with Nb/Zr ratio from 0.2 to 3.6. A distinctive feature of FRTE (Zn, Ni, Cu, V, etc.) distribution is elevated Cu (up to 10 ppm) and moderate Zn (~ 50 ppm) concentrations and the low Zn/Cu ratio (average 9.1). The olivine is also characterized by high Na concentration (up 220 ppm) and the lowest Li concentration among all studied olivines. The value of $\delta^{18}O$ in olivine is 5.6‰. Such olivines account for ~70% of the V. Grib kimberlites dataset.

The second group of Ol-I grains from the V. Grib kimberlites is characterized by high Ti (181±28 ppm) and low Cr and Ca contents. These olivines account for ~20% of the dataset and fall within the fields of olivine porphyroclasts and neoblasts from deformed peridotite sample.

The *Ol-I grains from the Pionerskaya kimberlites* (~60%) are subdivided into two groups, one of which consists of colorless low-Ti (31±28 ppm) crystals and other group includes yellow high-Ti (177±28 ppm) ones. Colorless olivine shows Mg# = 92.1±0.01 and high Ni and Cr concentrations. Yellow olivine is characterized by Mg# = 91.7±0.01 and high B, Li, Nb and Zr concentrations, and Nb/Zr ratio from 0.2 to 3.6. They differ from the *Ol-I in the V. Grib kimberlites* in high Zn/Cu ratio (averages of 15 colorless olivines and 28 yellow olivines). The values of $\delta^{18}O$ in olivine are 5.3‰.

The *deformed peridotite* shows porphyroclastic textures. Olivine porphyroclasts (~50%) are embedded in a mosaic matrix of small olivine neoblasts. The latters have high Ti concentration (241±46 ppm) and very narrow Mg# variations around 89.5. As compared with olivines from kimberlite, the neoblasts are enriched in Mn, Zn, V and are depleted in B, Li, Nb, Zr, Ni and Cr. The values of $\delta^{18}O$ in olivine are 5.0-5.1‰.

In *harzburgite*, Mg# of olivine is almost always within the range 92.3–92.4; olivines from the *garnet lherzolites* are different: their Mg# values are strongly variable from 89.0 to 93.0 with a maximum at the most magnesian compositions (92–93). The values of $\delta^{18}O$ in peridotitic olivine are 5.3-5.4‰.

The *cores of Ol-II* from kimberlites of V. Grib and Pionerskaya pipes are chemically very similar to Ol-I, which is supported by statistical analysis. A characteristic feature of Ol-II from the V. Grib pipe is the absence of cores corresponding to high-Ti Ol-I.

The *outer zones of Ol-II* from the V. Grib kimberlites, as well as small groundmass olivines, are different from the cores of these crystals in, first, lower and almost constant Mg# values, averaging 90.5 ± 0.3; second, higher Ti, Mn, and Cr and lower Ni contents at almost invariant Ca contents; and, third, strong variations in trace element contents within a narrow Mg# range. In the V.Grib kimberlites the ranges of minor element contents in the cores of Ol-II outer zones and neoblasts from deformed peridotite are either identical or very close.

We used the V-in-olivine oxybarometer (Mallmann, O'Neill, 2013) in order to estimate oxygen fugacity for V. Grib and Pionerskaya kimberlites. Calculations give QFM-0.5 to olivines from former and QFM-2.1 to olivines from latter.

Discussion and Conclusions. FRTE distribution in olivines is an indicator of such petrogenetic processes as partial melting of peridotite or pyroxenite source, presence of sulfide phase (mss or sulfide liquid), and oxygen fugacity.

It was found that the generation and compositional evolution of olivine types identified in the studied kimberlites was controlled by the following processes: 1) Formation of xenocrysts via fragmentation of peridotites metasomatized by melts from a pyroxenite source (as follows from Cu-Zn-Ni relations) is important for low-Ti Ol-I macrocrysts and some cores of Ol-II from the Pionerskaya kimberlites. 2) Macrocrystic olivines and cores of Ol-II from the V. Grib pipe represent protoxenocryst recrystallized under a carbonate rich protokimberlite melt contaminated by orthopyroxene. 3) The sharp difference of outer zones of Ol-II from the cores of Ol-II and Ol-I grains in minor element contents and distribution indicates their different nature. It can be suggested that the high-Ti rim zones of olivine and groundmass olivine crystallized from evolved, probably water-bearing kimberlite melts enriched in Ti. 4) The composition of the high Ti neoblastic olivines in deformed peridotite and the high Ti rim zones of Ol-II is identical except Mg#. One can assume that neoblasts were crystallized from a protokimberlite melt at the early stage of kimberlite formation after wall peridotites were deformed probably by ascending melts. Oxygen isotope composition of all studied olivines fall within ranges typical of mantle olivines. There is no single mechanism of olivine formation in kimberlites.

References:

Arndt N.T., Guitreau M., Boullier A.M. et al. Olivine and the origin of kimberlite // J. Petrol. 2010. V. 51. Pp. 573–602.

Brett R.C., Russell J.K., and Moss S. Origin of olivine in kimberlite: phenocryst or imposter // Lithos. 2009. V. 112S. Pp. 201–212.

Bussweiler Y., Foley S.F., Prelević D., Jacob D.E. The olivine macrocryst problem: New insights from minor and trace element compositions of olivine from Lac de Gras kimberlites, Canada // Lithos. 2015. V. 220–223. Pp. 238-252.

Jarosewich, E., Nelen, J.A., Norberg, J.A., Reference samples for electron microprobe analysis // Geost. Geoanal. Res. 1980. vol. 4. Pp. 43–47.

Kamenetsky V., Kamenetsky M., Sobolev A. et al. Olivine in the Udachnaya-East kimberlite (Yakutia, Russia): types, compositions and origins // J. Petrol. 2008. V. 49. Pp. 823–839.

Mallmann G., O'Neill H.S.T.C. Calibration of an Empirical Thermometer and Oxybarometer based on the Partitioning of Sc, Y and V between Olivine and Silicate Melt // J. Petrol. 2013. V. 54. Pp. 11–17.

Mahotkin, I.L., Gibson, S.A., Thompson, R.N., et al. Late Devonian diamondiferous kimberlite and alkaline picrate (proto-kimberlite?) magmatism in the Arkhangelsk region, NW Russia // J. Petrol. 2000. vol. 41. no. 2. Pp. 210–227.

Malkovets, V.G., Zedgenizov, D.A., Sobolev, N.V., et al. Contents of trace elements in olivines from diamonds and peridotite xenoliths of the V. Grib kimberlite pipe (Arkhangel'sk Diamondiferous Province, Russia) // Dokl. Earth Sci. 2011. vol. 436. no. 2. Pp. 219–223.

Pilbeam L.H., Nielsen T.F.D., Waight T.E. Digestion fractional crystallization (DFC): an important process in the genesis of kimberlites. Evidence from olivine in the Majuagaa Kimberlite, southern West Greenland // J. Petrol. 2013. V. 54. No. 7. Pp. 1399–1425.

Magmatism and metallogeny of the western Anatolia, Turkey, associated with subduction rollback and trench retreat: a comparison with the Basin and Range province, USA - Mexico

Öztürk H.

İstanbul University, Department of Geology, Avcılar Campus, Avcılar, İstanbul, Turkey email:
ozturkh@istanbul.edu.tr

Calc alkaline and alkaline magmatic activity in the western Anatolia has been associated with extensional tectonic regime in relation with subduction retreat and rollback in the Aegean Sea, especially in the Miocene which resulted in formation of a specific type of mineral deposits. Bimodal magmatic rocks of this rifted arc setting of the Aegean Sea and the western Anatolia are composed of hypabyssal stocks, dykes, lava or eruption products of andesite, basalt, tephrite, phonolite, basanite, kulaite, nefelinite, even carbonatites. These alkaline - calc alkaline rocks are associated with the Oligocene - Miocene age world class mineral deposits including B, Au, Ag, Hg, Cu, (REE + Ba + Th + F), Ba, Sr and trona.

Very recent radiometric studies have been made especially in the western Anatolian ore deposits namely the carbonatite - hosted Kızılcaören REE +Ba +F + Th deposit and the shale - basanite- hosted Şekeroba barite deposit , porphyry -type Kışladağ gold deposit and the Kütahya silver deposit. Age determinations by both Sr/Nd and K / Ar and Ar/Ar methods gave age of 24- 25 Ma for the Kızılcaören (Nikoforov et al. 2014a-b) and age of 13 - 15 Ma (Öztürk at al. 2014) for the Şekeroba Ba deposit. The porphyr - type Kışladağ Au deposit in western Anatolia which is associated mainly with extrusive caldera complex, indicated 11 Ma age by K / Ar method (Oyman and Dyar, 2007).

The Basin and Range province is another extension - related metamorphic core complex region in the world like to the western Anatolia and includes more or less similar type bimodal magmatic rocks and similar type mineral deposits to the western Anatolia, such as REEs + B+ trona+ Au + Ag + Hg (California - Nevada - Arizona region) Ag +Au+ F+ Ba+ Sr deposits (Encantada - Buenavista Region, Northern Mexico).

Formation of these mineral deposits of the incompatible elements both in the western Anatolia and the Basin and Range province in a short period of time during the Oligocene and the Miocene indicates a) mantle related metallogeny for both Anatolia and the Basin and Range province under a N - S and E-W extensional regime, respectively b) a metamorphic core complex development associated with rollback of the Create and Pacific subduction, and c) migration of the arc volcanism from the north to the south, west to east, respectively and d) passing from calc alkaline to alkaline magmatic products.

The alkaline - calc alkaline magmatism and coeval mineral depositions are associated with an extensional tectonic episode both in the western Anatolia and the Basin and Range province should have been formed related to subduction rollback triggered core complex mechanism instead of a slab break off. Ancient equivalents of such back arc rift basins can define provided that the three distinctive features together; association of Au, Ag, Cu, REE deposits, strong extensional tectonic – metamorphic core complex generation and bimodal volcanics.

References:

Nikiforov, A.V, Öztürk, H., Altuncu S. and Lebedev V.A, Kızılcaören Ore and Carbonatite- Bearing Complex: Formation Time, Mıneralogy and Sr-Nd Isotope Geochemistry of the Rocks (Northwestern Anatolia, Turkey). 30th International Conference on Ore Potential of Alkaline, Kimberlite and Carbonatite Magmatism, Turkey, 2014a v.1 p. 122-123.

Nikiforov, A. V, Öztürk, H., Altuncu, S. and Lebedev, V. A. Kizilcaören Ore-bearing Complex with Carbonatites (Northwestern Anatolia, Turkey): Formation Time and Mineralogy of Rocks, Geology of Ore Deposits, 2014b, 56, p. 35-60.

Oyman, T. and Dyar, M. D., Chemical substitutions in oxidized turmaline in granite – related mineralized hydrothermal systems, western Turkey, Canadian Min. 2007 p. 1397- 1413.

Öztürk H., Cansu Z., Nikiforov A.E. and Zhukovsky V.M., K-Ar and SEM Results of the Alkaline Porphyritic Stocks in the Şekeroba Barite Deposit, Kahramanmaraş, Turkey, 30th International Conference on Ore Potential of Alkaline, Kimberlite and Carbonatite Magmatism, Antalya, Turkey, 2014, v.1, p.126-126

New data about the genesis of potassic lamprophyre of the Tomtor massif based on melt inclusions

Panina L.I., Rokosova E.Yu., Isakova A.T., Tolstov A.V.

Sobolev Institute of Geology and Mineralogy SB RAS, Novosibirsk, Russia

panina@igm.nsc.ru

The Tomtor massif (north of the Siberian Platform) refers to volcano-plutonic complexes of central type and is the largest rare-metal Sc-TR-Y-Nb deposits of the world. Geophysical data evidence that it is about 10 km in depth and about 300 km^2 in the area. The shape of the massif is isometric. Its peripheral zone is composed of nepheline and alkaline syenites represented by predominantly potassium (rischorite) and more rarely sodium (khibinite) types, whereas the center is composed of carbonatite stock, with a ring intrusion of jacupirangite-urtites between them (Lapin, Tolstov, 1993). The dike series of alkaline-ultrabasic rocks intrude the carbonatite stock as well as alkaline rocks of the massif and form difficult carbonate-silicate alternation (Kravchenko, 2003). Among dyke rocks there occur alkaline picrites, augitite-limburgites, melanephelinites, monchikites, phonolites, alkaline trachytes. Entin and coauthors (1990) report that the time interval of the formation of the Tomtor massif is 800-240 Ma, and the data of Vladykin et al. (2014) suggest two stages of formation of magmatic rocks of the massif – 701-675 Ma and 414-387 Ma.

Previously the main attention was paid to the investigation of the massif geology, its rocks and, first of all, the evaluation of its unique hypergene ores. The most poorly studied are the genetic problems concerning the physicochemical conditions of formation of rocks, composition of their initial melts, fluid saturation, evolution, enrichment in trace elements, PT-parameters of crystallization and magma sources.

To obtain genetic information, we have studied a virtually unaltered pyroxene amphibole dyke rock with analcime, orthoclase, and phlogopite from the drill-hole cores No.1625 (depth 114 m), localized in the body of jacupirangite-urtites. The rock is inequigranular, porphyric, glomeroporphyric, due to the accumulations of clinopyroxene and amphibole. Phenocrysts are represented by diopside, kaersutite, analcime, less often by phlogopite and ore minerals.Groundmass is fine-crystallized and consists of small (10-50 μm) grains of clinopyroxene, phlogopite, amphibole, potassium feldspar, ore minerals, and carbonate. Phenocrysts of clinopyroxene are typically zoned in composition. There are high-manganic (0.53-0.43 wt.% MnO) clinopyroxene varieties with a low (1-1.9 wt.%) content of TiO$_2$ and high (6-7%) content of jadeite component as well as low-manganic (0.07-0.1 wt.% MnO) clinopyroxene varieties with high (3-6 wt.%) TiO$_2$ and low (1-2%) content of jadeite component. A great number of intermediate clinopyroxene varieties were observed between them. The cores of phenocrysts are represented by high-manganic clinopyroxene varieties and rarely by Mn-free diopside. Alternation of zones in the phenocrysts is typically multiple, often unsystematic. Apatite phenocrysts are well faceted and contain 2-3 wt.% F, to 0.2 wt.% Cl and most of them are rich in SrO (1.3-1.7 wt.%). In mineral and chemical composition (wt.%: 39.4 SiO$_2$, 3.6 TiO$_2$, 11.9 Al$_2$O$_3$, 12.6 Fe$_2$O$_3$, 0.26 MnO, 5.8 MgO, 11.5 CaO, 3.4 Na$_2$O, 3.8 K$_2$O, 1.05 P$_2$O$_5$, 0.7 BaO, 0.5 SO$_3$) the rock corresponds to lamprophyre of potassium type of alkalinity. It is worth noting that the rocks of the same composition and from the same drill-hole cores No.1625 and drill-hole cores No.7264 are referred by some researchers (Kravchenko, 2003; Vladykin, Torbeev, 2005) to lamproites.

Primary melt inclusions were found in the phenocrysts of clinopyroxene, apatite, and sphene. The inclusions are scarce, occur as single or, less often, by 2-3 inclusions in the field of microscope. All the inclusions in the phenocrysts of diopside and apatite are crystallized. The daughter phases of inclusions in diopside of most phenocrysts are dominated by analcime, biotite, apatite, calcite, and ore minerals. Low-manganic diopsides contain crystallized inclusions with such daughter phases as potassium feldspar, pseudoleucite, ankerite, amphibole, biotite, and albite. In Sr-bearing apatite the inclusions contain analcime, aegirine, calcite, and magnetite. In Sr-free apatite, inclusions contain potassium feldspar, biotite, amphibole, ilmenite, and pyrite. Inclusions in sphene consist of residual glass, leucite and potassium feldspar. The homogenization temperature of inclusions in clinopyroxene is slightly higher than 1200 ºC, and in apatite is about or somewhat higher than 1060-1090 ºC.
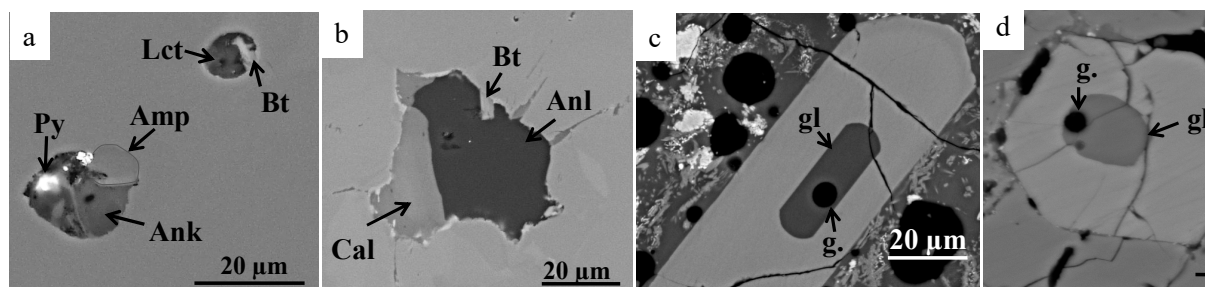
Fig. Primary melt inclusions: a, b - unheated inclusions in clinopyroxene; c, d - heated inclusions in apatite. Back-scattered electron images. Amp, amphibole; Ank, ankerite; Anl, analcime; Bt, biotite; Cal, calcite; Lct, pseudoleucite; Py, pyrite; gl - glass; g. - gas bubble.

Table. 1. Chemical composition of homogenized melt inclusions, wt.%

Host minerals	Clinopyroxene							Apatite					Sphene	
№№	1	2	3	4	5	6	7	8	9	10	11	12	13*	14**
SiO_2	49,50	51,34	52,85	54,00	55,64	53,21	54,32	50,80	53,02	46,92	52,87	53,25	58,39	53,85
TiO_2	2,39	2,14	1,44	1,37	1,79	1,58	1,43	1,07	1,53	2,54	1,33	1,00	1,03	3,15
Al_2O_3	15,17	16,57	16,69	16,93	18,62	16,89	16,33	17,52	18,14	17,06	16,49	17,82	18,01	17,33
FeO	6,92	6,93	5,24	5,13	4,39	4,30	5,07	4,74	5,67	7,92	5,81	2,98	2,87	4,35
MnO	b.d.l.	0,31	b.d.l.	b.d.l.	0,23	b.d.l.	b.d.l.	b.d.l.	b.d.l.	0,17	b.d.l.	b.d.l.	b.d.l.	0,32
MgO	1,49	0,95	0,61	0,60	0,61	0,95	1,84	0,60	0,78	3,23	1,59	1,14	0,18	0,22
CaO	8,07	5,99	2,39	2,52	2,98	4,03	4,27	7,51	3,89	8,86	2,54	4,91	2,34	4,31
Na_2O	5,76	5,90	7,36	7,33	6,89	5,24	7,00	7,88	7,53	6,48	7,35	5,61	4,72	8,86
K_2O	3,90	4,20	5,59	5,75	5,63	5,10	6,81	5,50	5,29	4,83	7,29	6,30	9,29	5,54
P_2O_5	b.d.l.	b.d.l.	b.d.l.	b.d.l.	0,32	b.d.l.	b.d.l.	2,19	0,85	2,61	2,45	1,72	b.d.l.	b.d.l.
Cl	0,37	0,35	0,34	0,35	0,34	0,37	b.d.l.	b.d.l.	0,24	b.d.l.	b.d.l.	b.d.l.	b.d.l.	0,31
Total	93,58	94,69	92,48	93,97	97,43	91,66	97,06	97,78	96,92	100,92	96,65	94,73	96,81	98,23
Na_2O/K_2O	1,48	1,40	1,32	1,27	1,22	1,03	1,03	1,43	1,42	1,34	1,00	0,89	0,51	1,60

Note. * - in inclusion are also present leucite and potassic feldspar. ** - inclusion from sphene of ijolites of Tomtor massif. Also take into account the presence of SO_3: №5 – 0,22 wt.% и №9 – 0,24 wt.%. B.d.l. = below detection limit.

The chemical composition of heated inclusions in all analyzed minerals is alkaline-basic. In diopside phenocrysts it is mainly of Na-type of alkalinity. In high-manganic diopsides the Na_2O/K_2O value varies from 1.5 to 1.2, whereas in Mn-free diopsides it is close to 1 (Table 1, ans. 1-5 and 6, 7, respectively). In Sr-bearing apatite the composition of melts conserved in inclusions is also high sodium ($Na_2O/K_2O = 1.42$-1.43), and in Sr-free apatite, it is highly potassium: $Na_2O/K_2O = 0.89$ (Table 1, ans. 8-10 and 11, 12, respectively). Residual glass from inclusions in sphene is also highly potassium: $Na_2O/K_2O = 0.5$ (Table 1., an. 13). On the whole, compared to the potassium melts, the conserved melts of Na-type of alkalinity have higher iron and alumina contents, lower silica content and are enriched in Mn, Cl, SO_3, CO_2, and P. Melt inclusions of such chemical composition were also found in the sphene of ijolites from the Tomtor massif (Table 1, an. 14). The obtained data suggest that the phenocrysts of diopside in the studied potassium lampropyres began to crystallize from Na alkaline-basic deep melts, with the composition similar to the melts from which ijolites of the Tomtor massif crystallized. As it is known, the chemical composition of primary inclusions in the early crystallized minerals must be consistent with the composition of melt from which a rock crystallized, and the type of alkalinity depends on the type of magma. However, in our case, this composition is similar to the composition of magma with a Na-type of alkalinity, from which at early stages, in addition to diopside, analcime, calcite and ores crystallized. Potassium melts appeared at late crystallization stages of diopside and their mixing with Na melts led to crystallization of amphibole, biotite and leucite.

This produces an impression that lamprophyres of Tomtor massif formed from hybrid magma in the conditions of ascending movements caused by tectonic activity. Crystallization of diopside phenocrysts started with high-manganic varieties in depth (which is suggested by the presence of jadeite component in the mineral) from Na alkaline-basic melt. At the later crystallization stage of diopside, during the rise of melt to the surface, inflow of higher-Mg K-magma into the chamber took place. Most likely, the inflow was multiple and mixing of melt was irregular.

References:

Vladykin N.V., Kotov A.B., Borisenko A.S., Yarmolyuk V.V. et al. Age boundaries of formation of the Tomtor alkaline-ultramafic pluton: U-Pb and 40Ar/39Ar geochronological studies // Doklady Earth Sciences. 2014. v. 454, Issue 1, p.7-11.

Vladykin N.V., Torbeeva T.S. Lamproites of the Tomtor massif (eastern Anabar area) // Geology and Geophysics. 2005. № 10. p. 1024-1036.

Kravchenko S.M. Porphyritic potassium-rich alkaline-ultrabasic rocks of the central Tomtor massif (Polar Siberia): carbonatized lamproites // Russian Geology and Geophysics. 2003. v. 44. №. 9. p. 870-883.

Lapin A.V., Tolstov A.V. New unique deposits of rare metals in the weathering crusts of carbonatites // Razvedka I Okhrana Nedr. 1993. № 3. p. 7-11, (in Russian).

Entin A.R., Zaitsev A.I., Nenashev N.I. On the sequence of geologic events related to the emplacement of the Tomtor massif ultrabasic-alkaline rocks and carbonatites // Geology and Geophysics. 1990. № 12. p. 42–51 (in Russian).

The crystal chemistry and origin of alexkhomyakovite, a new potassic chlorocarbonate from the Khibiny alkaline complex, Kola peninsula, Russia

Pekov I.V.*,***, Zubkova N.V.*, Lykova I.S.*,***, Turchkova A.G.*, Yapaskurt V.O.*, Chukanov N.V.****,
Belakovskiy D.I.***, Britvin S.N.*****,******, Pushcharovsky D.Yu.*

[1]Faculty of Geology, Moscow State University, Moscow, Russia
[2]Vernadsky Institute of Geochemistry and Analytical Chemistry RAS, Moscow, Russia;
[3]Fersman Mineralogical Museum of Russian Academy of Sciences, Moscow, Russia
[4]Institute of Problems of Chemical Physics, Russian Academy of Sciences, Chernogolovka, Russia
[5]Department of Crystallography, St Petersburg State University, St Petersburg, Russia
[6]Nanomaterials Research Center, Kola Science Center of Russian Academy of Sciences, Apatity,
Russia

Unlike sodium carbonates that are numerous in nature and some of them form large deposits, carbonate minerals with species-defining potassium were until recently represented by only seven very rare species, namely baylissite $K_2Mg(CO_3)_2 \cdot 4H_2O$, bütschliite $K_2Ca(CO_3)_2$ (trigonal), fairchildite $K_2Ca(CO_3)_2$ (hexagonal), kalicinite $KHCO_3$ and three uranyl-bearing species: agricolaite $K_4(UO_2)(CO_3)_3$, grimselite $K_3Na(UO_2)(CO_3)_5 \cdot H_2O$ and línekite $K_2Ca_3[(UO_2)(CO_3)_3]_2 \cdot 7H_2O$.

A new structurally unusual natural potassic chlorocarbonate alexkhomyakovite, ideally $K_6(Ca_2Na)(CO_3)_5Cl \cdot 6H_2O$ (IMA2015-013), was discovered at Mt. Koashva, Khibiny, Kola peninsula, Russia, and named in honour of the Russian mineralogist Alexander Petrovich Khomyakov (1933–2012), a well-known specialist in the mineralogy of peralkaline rocks who made a great contribution to the mineralogy of the Khibiny and Lovozero alkaline complexes. It was found in significant amount in a hyperagpaitic pegmatite together with villiaumite, natrite, potassic feldspar, pectolite, sodalite, biotite, lamprophyllite, titanite, wadeite, yuksporite, fluorapatite, burbankite, *etc*. The most commonly alexkhomyakovite occurs as colourless to white or grey fine-grained aggregates forming intimate intergrowths with others minerals inside the pseudomorphs after large (up to 3 x 5 x 15 cm) delhayelite crystals. It was also found as grains, sometimes abundant, included in massive natrite in natrite-villiaumite nests closely associated with the pseudomorphs after delhayelite. The empirical formula of the new mineral, based on 9 cations *pfu* [EMPA data, H_2O is calculated by stoichiometry], is: $K_{5.90}Ca_{2.07}Na_{1.03}(CO_3)_5(SO_4)_{0.01}O_{0.05}Cl_{0.95} \cdot 6H_2O$.

The crystal structure of alexkhomyakovite was studied using the single-crystal XRD data. The mineral is hexagonal, $P6_3/mcm$, $a = 9.2691(2)$, $c = 15.8419(4)$ Å, $V = 1178.72(5)$ Å^3, $Z = 2$. The structure was solved by direct methods and refined to $R = 0.0578$ on the basis of 555 independent reflections with $I > 2\sigma(I)$. The structure of alexkhomyakovite (Figure 1) is unique. It is based on the (001) heteropolyhedral layers of the (Ca,Na)-centred pentagonal bipyramids $(Ca,Na)O_5(H_2O)_2$ connected with each other *via* common O vertices shared with the triangular carbonate groups $C(2)O_3$ and $C(3)O_3$. These groups play different role in the construction of the heteropolyhedral layer: the C(2)-centred triangle shares all three edges with three (Ca,Na)-centred pentagonal bipyramids while the C(3)-centred triangle shares with the (Ca,Na)-centred polyhedra only three vertices (Figure 2a). H atoms of H_2O molecules involved in the formation of the (Ca,Na)-centred polyhedra are oriented to the interlayer space where the $C(1)O_3$ triangles are located. Thus the system of hydrogen bonds O(4)-H.....O(2) is formed [O(4)–O(2) distance is 2.624(4) Å] is formed (Figure 2b). K cations occur between the H_2O molecules located in the vertices of the (Ca,Na)-centred polyhedra from both sides of the heteropolyhedral layers and occupy the ten-fold polyhedra $KO_6Cl(H_2O)_3$.

a)   b)
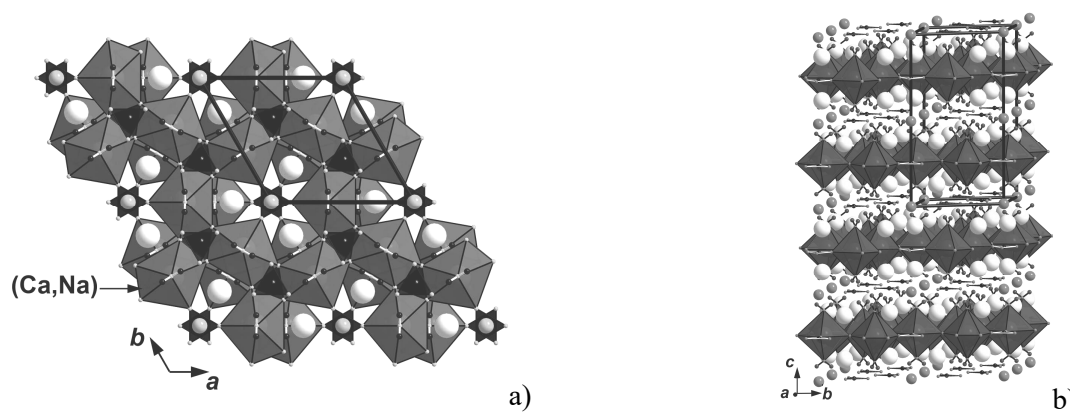
Figure 1. The crystal structure of alexkhomyakovite. CO_3 groups are black triangles, K cations are big light-grey spheres, Cl anions are medium-grey spheres, O anions are small grey circles and H atoms are small grey circles. The unit cell is outlined.

86
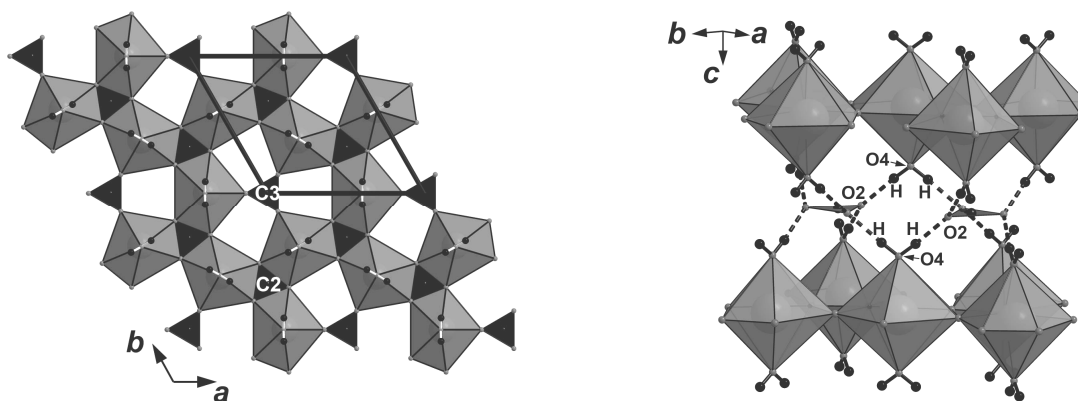
Figure 2. Heteropolyhedral layer formed by the $(Ca,Na)O_5(H_2O)_2$ pentagonal bipyramids and the $C(2)O_3$ and $C(3)O_3$ triangles (a) and the system of hydrogen bonds (shown as dashed lines) ($C(1)O_3$ triangles located in the interlayer space are shown) (b) in alexkhomyakovite.

In spite of the great diversity of carbonates, from one hand, and of potassium minerals, from other hand, in peralkaline postmagmatic assemblages of Khibiny, no potassic carbonate was known here before the discovery of alexkhomyakovite. This obviously hydrothermal mineral was formed at late stage of evolution of a potassium-rich peralkaline pegmatite, probably under very specific conditions when K^+ was not too mobile. Alexkhomyakovite mainly occurs inside pseudomorphic polymineralic aggregates after completely altered crystals of delhayelite (that are easily recognized by their typical morphology and mineral association). In some areas (up to 2 x 4 cm) of the pseudomorphs its share is 30–40 vol.%. Delhayelite $K_4Na_2Ca_2(AlSi_7O_{19})F_2Cl$ is widespread in K-rich hyperagpaitic pegmatites at Khibiny. In the hydrothermally altered bodies, partial to complete pseudomorphs after delhayelite are common and are diverse in mineral composition. In the discussed pegmatite, early, high-temperature, anhydrous mineral delhayelite most likely underwent an influence of peralkaline hydrothermal solutions strongly enriched in Na, CO_2, and F and was altered to aggregates of alkali/calc-alkali silicates, alkali/calc-alkali carbonates and villiaumite. The natrite-villiaumite nests saturated with alexkhomyakovite were formed probably in the same stage between altered crystals of delhayelite and aggregates of unaltered, more stable primary pegmatitic minerals: potassic feldspar, sodalite, biotite, lamprophyllite and coarse-crystalline pectolite. The process of the hydrothermal alteration of delhayelite in this pegmatite can be schematically presented as follows: delhayelite $K_4Na_2Ca_2(AlSi_7O_{19})F_2Cl$ + [H_2O, Na^+, CO_3^{2-}, F^-] → alexkhomyakovite $K_6(Ca_2Na)(CO_3)_5Cl•6H_2O$ + pectolite (secondary, fibrous) $NaHCa_2(Si_3O_9)$ + potassic feldspar (secondary, fine-grained) $K(AlSi_3O_8)$ + villiaumite NaF + natrite Na_2CO_3. Metal cations and chlorine for alexkhomyakovite could be directly inherited from delhayelite.

New data on metallogeny of rare metals occurences in Romania

Popescu G.C., Neacşu A., Petrescu L.
Dept. of Mineralogy, Faculty of Geology and Geophysics, University of Bucharest, 1 N. Bălcescu Blvd., 010041 Bucharest, Romania; ghpop@geo.edu.ro

According to the geological structure of Romanian territory, its metallogeny is different as forming and organisation. Geologic and metallogenic characteristics of the Romanian territory offer many arguments in order to understand the rare metal forming processes and their spread, and also to discovery new ore deposits. This kind of accumulation was formed both intracontinental rift stage - case of the Ditrău Massif, East Carpathians, whith some rare and radioactive metal occurences (Nb, Zr, Y, Th, U), and during the collision between the Getic Unit and the Danubian Realm, when conditions for generating RMs (Nb, Y, Zr) and radioactive metals in the shear zone of Getic „blocks" from the South Carpathians have been developed.

RM deposits in relationship with the intracontinental rift stage. There is a well-known metallogenesis only in the Ditrău Alkaline Massif zone, consisting of Mo and carbonatite-type REE concentrations. There is an

intrusive alkaline massif with a quasi-ring structure, where central part is represented by foidic rocks, followed discontinuously to the periphery by syenites, monzonites, monzodiorites, granites and alkaline-granites (Pál-Molnár et al., 2010) (Fig. 1).

New petrological studies revealed that the formation of the Ditrău Alkaline Massif can be related to a continental magmatic activation started in the Middle Triassic at the southern passive edge of the European continent in an extensional tectonic environment by the uplift of mantle-origin magma.

Two metallogenic sectors are drawn (Fig.1): the northern Jolotca-Tarniţa Sector, and the southern Aurora-Hereb Sector.

-*The Jolotca-Tarniţa* Sector includes "primary" Fe, Ti, P, V, Ta mineralization, related to ultramafites, mafites and diorites, represented by disseminations and nests of vanadiferous magnetite, ilmenite, sphene, apatite; it includes also postmagmatic mineralization of Mo, REEs, Ti, Nb, Pb, Zn, spatially associated to vein rocks (lamprophyres, albitites, carbonatites). Last mineralization contains a quasiparalel system veins, but also disseminations and net veinlets with molybdenite, xenotime, loparite, monazite, ilmenite, pyrite, sphalerite and galena;

- *The Aurora field* contains Th, V, REE, Zr, F, and Mo vein mineralization, spatially associated to lamprophyre veins, syenites, granites and crystalline schists. Mineralization includes pyroclor, bastnaesite, thorite, xenotime, niobiotantalite, zircon, fluorine, and Pb, Zn sulphides.

Metallogenesis associated to the Ditrău Alkaline Massif is complex, its main characteristic being the presence of RMs (*e.g.,* Zr, Ti, Nb, Th, Mo), and REEs. From the genetic point of view, primary concentrations formed by magmatic segregation are seen, related to the Tarniţa Complex magmatites, represented by Fe, Ti, P, V, Ta, and postmagmatic mineralization related to syenites and foidite syenites, *e.g.,* Zr, P, Nb, Th, REEs, Mo, Pb, Zn.

A modern and detailed mineralogical study of RMs from the Ditrău Massif is published by Hârtopanu et al., 2010. On this occasion, more than 100 new minerals were described for the first time in Romania, and were added to the 85 already described REE, Y, and also Th, U, Nb, Ta, Zr minerals.
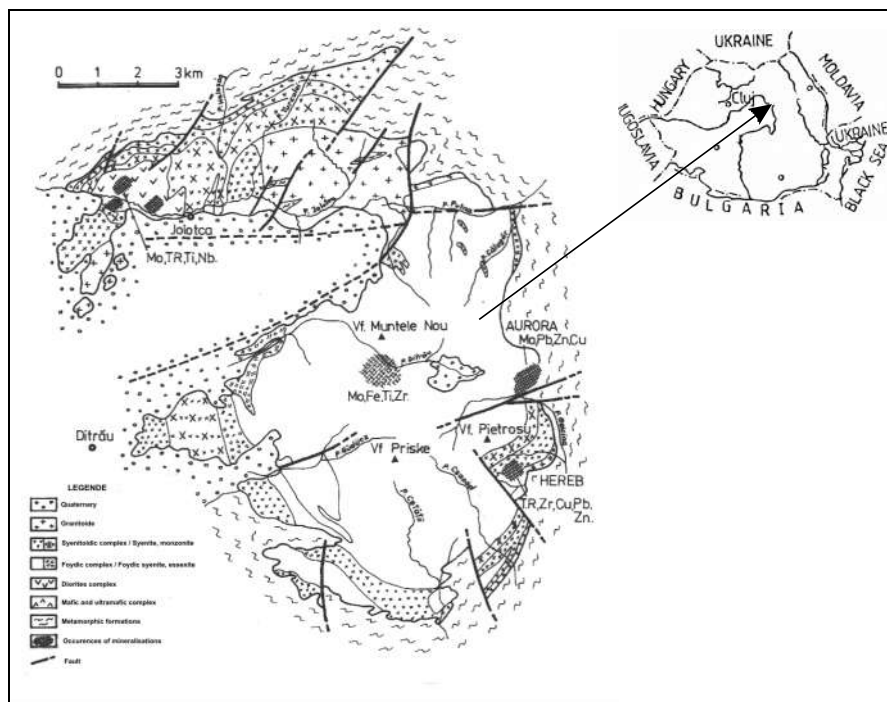
Fig. 1. Geological sketch of the Ditrău Massif and associated metallogenesis (according to Constantinescu et al., 1983, with additions).

Occurrences of RMs and minor elements, Grădiştea de Munte along the Cioclovina-Şugag shear zone, in the northern part of the Sebeş Mountains (Fig. 2A). Evidences of the dismembering of the pre-Alpine metallogeny are observed in the South Carpathians, in the Sebeş Mountains, *i.e.* Grădiştea de Munte area, as a result of the collision between the Getic Unit and the Moesian Platform. The most significant metallogenic result is the dismembering of the Pre-Alpine metallogenic unit related to the Getic crystalline rocks (manganese and iron metallogenic unit), so relicts of manganese metallogenesis are found within the Getic „blocks", created as a result of the collision process (Fig. 2). The motion of the Getic blocks has been realised alternatively on E-W and NE-SW directions, resulting strike-slip faults, which prolonged within some blocks as shear zones,

88

having a metallotect role, especially for Au-Ag mineralization, but also for RMs, all these forming new Alpine metallogenic units, with a liniamentary disposition (Fig. 2B). Another result is the presence of Au-Ag mineralization and some rare and radioactive metal occurences (Li, Nb, Zr, Y, Th, U).

Mineralization of Grădiştea de Munte is included within one of this body, having a tabular-like aspect, a thickness between 5-6 m and till 35 m long. Ore deposit is concordant with surrounded formations, having E-W trending and 75-80^0 dips, sometimes vertically disposed. The exploration activity evidentiated RMs (Zr, Nb, Th, U, Rb, Sn) and REEs (Y, Ce, La). These elements form their own minerals, but they are also included as isomorphic substituents in other mineral network structures. RM and REE minerals have been identified (Popescu et al., 2003) *e.g.*, zircon, monazite, xenotime, allanite, törnebohmite, pyroclor, fergusonite, thorite, cassiterite, *etc*., as hypidiomorphic to xenomorphic grains, with very small sizes, even microscopic ones, extremely difficult to detect. Genesis of mineralization is due to pneumatolitic process, as a consequence of rich in potassium supracritic solutions transport along the Subcetate-Căpâlna shear zone, and with regional development in the northern part of the Sebeş Mountains (Popescu et al., 2003).

In sum, there are two RMs metallogenesis in Romania: related to alkaline magmatites, *i.e.* Ditrău Massif, Eastern Carpathians, and related to shear zones, *i.e.* Grădiştea de Munte, South Carpathians.
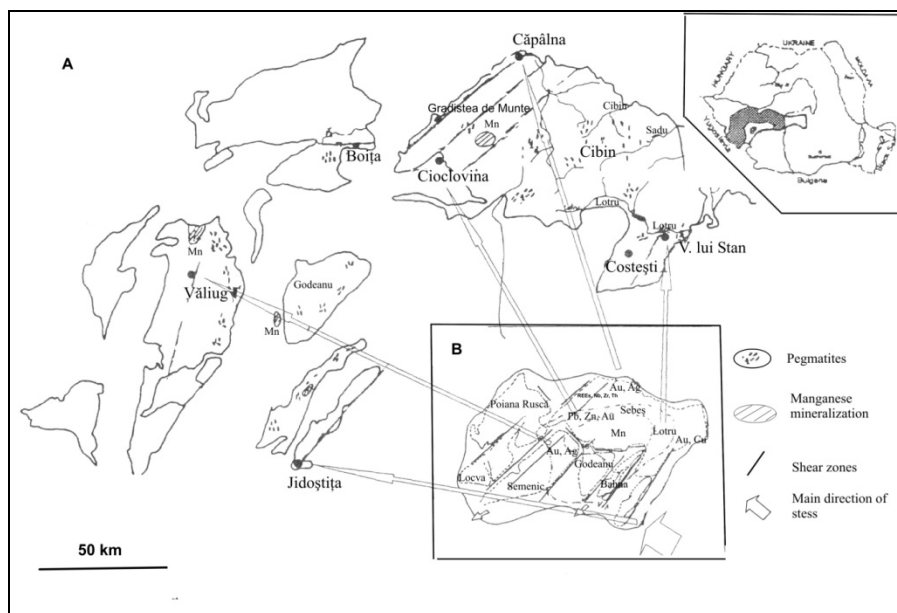
Fig.2A. Getic „blocks" resulting by collision process between the Getic Domain and the Moesian Platform, and share zone mineralization. **2B**.The Getic Domain before the collision process with the Danubian Domain (strike slip faults who facilitate the Getic Domain dismembering are observed) (Popescu, Tămaş-Bădescu, 1998 with additions).

References:

Constantinescu E., Anastasiu N., Garbaşevschi N., Pop N., 1983. Contribution à la connaisance des aspects paragénétiques de la minéralisation associée au Massif alcalin de Ditrău. An. Inst. Geol. LXII Bucureşti, 91-101.

Hârtopanu Paulina, Andersen J., Fairhurst R., 2010. Nb, Ta, REE(Y), Ti, Zr, Th, U and TR element minerals within the Ditrău alkaline intrusive complex, Eastern Carpathians, Romania: Mineralogy of Székelyland, Eastern Transylvania, Romania. Ed. by S. Szakáll and F. Kristály, 89-128.

Pál-Molnár E., 2010. Rock-Forming Minerals of the Ditrău Alkaline Massif: Mineralogy of Székelyland, Transylvania, Romania. Ed. by S. Szakáll and F. Kristály, 63-88.

Popescu C.Gh. and Tămaş-Bădescu S., 1998. Shear zones and mineralization. Romanian J. of Mineral Deposits, IGR, Bucureşti, Vol. 78, Supp. Nr 1, 21-27.

Popescu C.Gh., Luduşan N., Cioacă Mihaela Elena, 2003. RMs and REE mineralization in Grădiştea de Munte – Sebeş Mountains (in Romanian) in Gheorghe C. Popescu: From Mineral to Metallogenic Province, Ed. Focus-Petroşani, 409-417.

Temporal variations of hydrogen emission in the Lovozero rare-metal deposit (Kola Peninsula, NW Russia)

Pukha V.V., Nivin V.A.

Geological Institute of the Kola Science Centre of the Russian Academy of Sciences, Apatity, Russia;
puha.vyacheslav@mail.ru

Recently an interest is growing for the problem of the lithosphere molecular hydrogen emission, being, in particular, stipulated by the necessity to understand its role in the earthquake preparation conditions and its occurrence, in the stratosphere ozone layer depletion, as well as by the perspectives to use the gas release variations as precursors of unfavourable natural processes. The Lovozero alkaline massif is one of few localities known for its relatively concentrated hydrogen release and is the second in significance (after methane), sometimes even dominating, component in the gas phase composition [Nivin, 2006]. It is also important to understand the dynamics of combustible H_2 and CH_4 because of the necessity to secure gas safety in mining operations carried out within the deposit.

The paper reports the results of the analysis of a continuous temporal series of the hydrogen concentrations structure in the atmosphere in the blind part of a horizontal underground working (crosscut) separated by a brick dam with a door. The measurements were performed with a portable hydrogen analyzer VG-3B (Nikolayev et al., 2007). The resolution ability of the device is 0.0001 vol. %, a relative error is ±5 %. The measurements were performed within the discretization interval of 5 minutes. The relative increments mV measured with the device were transformed to the corresponding increments of the volume concentration, ppm.

Figure 1 shows the temporal series of the hydrogen concentrations obtained within the time interval from June 1, 2008 till November 7, 2012 (the measurements were not performed in the period from September 28 till November 2, 2010 due to technical reasons).
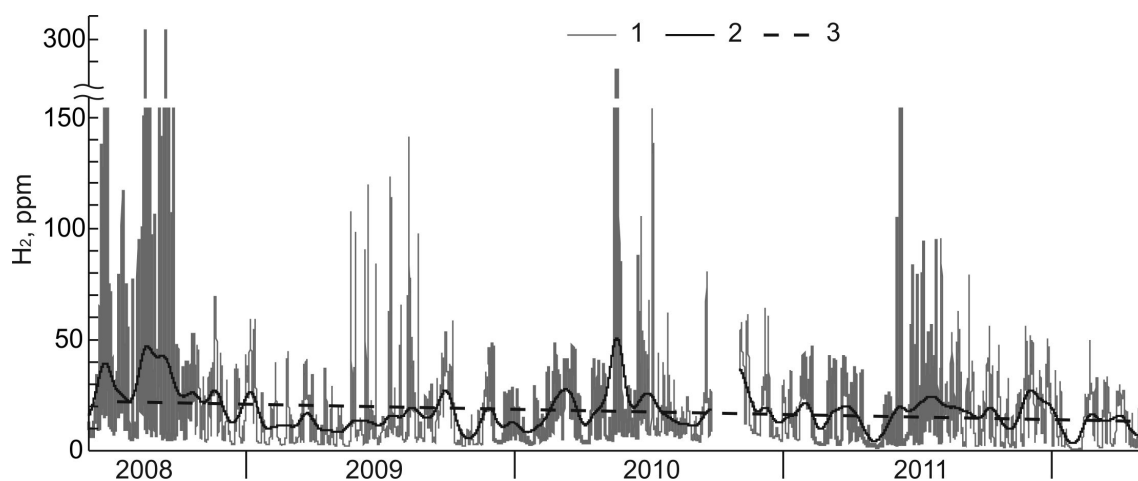
Fig.1. The temporal series of the molecular hydrogen concentrations
1 – concentration H_2; 2 – smoothing the set by the local moving weighed means by the Gaussian kernel with the width of a window of one day; 3 - the trend regression line.

In a general view the H2-concentration variations are a curve with alternating regions of two types: those presented by subhorizontal lines corresponding to low (background) levels of concentration, which, as a rule, exceed several times the H2-content in the atmosphere, and those of spikes against the background often presented by a combination of convexities, peaks and concavities.

The analysis has shown the inconsistence between the empirical distribution of the data obtained and any classical distribution function. So to verify various statistical hypotheses, non-parametric tests were carried out.

The temporal series is characterized by the following descriptive statistics (ppm): the mean value is 17.15, a median is 10.98, the geometric average is 10.52, the minimum value is 0.72, the maximum value is 303.6, the interquartile range is 18.45.

The hypothesis of temporal series stationarity has been verified by the augmented Dicke-Fuller test applied to a version when the series has a constant and a linear trend. The test has revealed the presence of the series stationarity of 1 % of significance. The established property of stationarity allows us not to be surprised with the inadequate results obtained from the Fourier analysis, taking these as normal in future.

Established in the series structure is a common tendency to decrease (Fig. 1), a random noise component, a seasonal and other cyclic components.

The noise component is expressed by a set of extremely minor abrupt changes of a signal near some average level within the corresponding local interval. The amplitude of the abrupt changes never exceeds the specified resolution capability of the gas analyzer. Due to the negligible contribution of the noise to a common signal, we do not take it into account and use a decimated series with the interval of discretization equal to one hour.

The temporal gas release series clearly reveals a seasonal component. The greatest contribution made by gas release falls approximately at the period from June till November.

The Cox-Stuart test revealed the trend (the final and initial values of the trend are 11.98 and 21.96 ppm, respectively) in the temporal series with the significance level being equal to 0.1 %. The trend can be determined by the influence exerted by man-made factors and likely by some tendency of the gas analyser susceptibility to change.

In order to detect other, but seasonal, regular components, the spectral analysis methods based on the fast Fourier transformation algorithm were used. The linear trend has been preliminary eliminated and the data sequence gained has been centred. The periodograms were smoothed by the Blackman-Tukey method, with the Hanning window. The periodograms smoothed with the smoothening degree parameter 0.1N, are shown in Fig. 2.
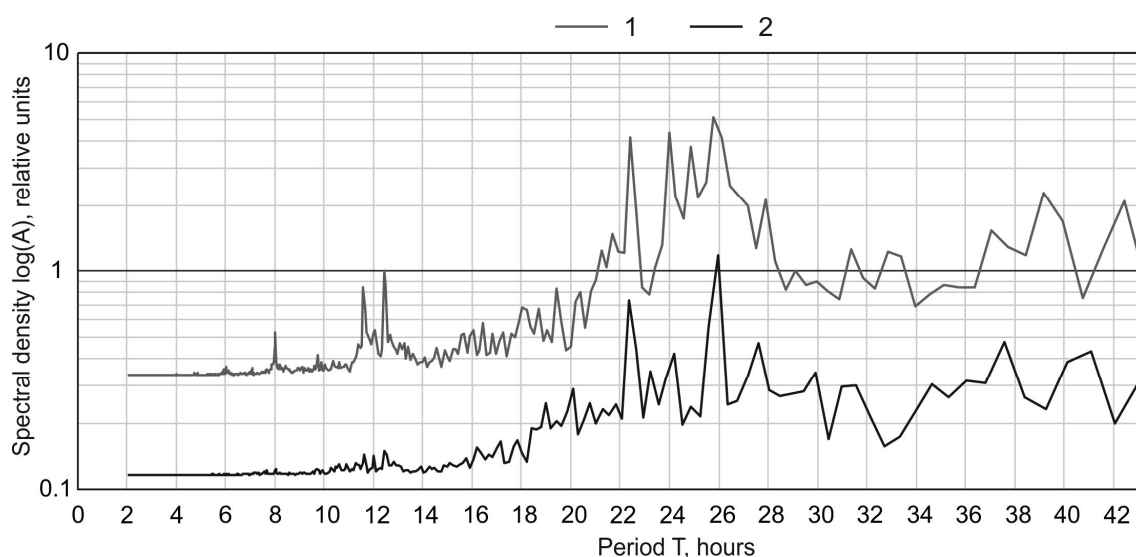
Fig. 2. The smoothed periodograms for the harmonics periods not exceeding two days.

According to the spectral analysis results there is a set of the different periods (shown in bold are the most distinctive ones): 8.0, **11.6, 12.4**, 18.0, 18.7, 19.4, 20.4, **22.4, 24.0, 24.8, 25.8** of an hour, 1.2, 1.3, 1.4, 1.5, 1.6, 1.8, 1.9, 2.3, 2.5, 3.3, 4.7, 5.3, 5.5, 6.5, 7.1, 28.3 of a day - for the first part of the set; 11.6, 12.0, 12.4, 17.1, 17.8, 19.0, 20.1, **22.3**, 24.2, **25.9** of an hour, 1.1, 1.6, 1.7, 2.5, 3.5, 3.7, 4.3, 5.1, 5.4, 6.9, 29.4 of a day - for the second part of the set. The distinguishing of harmonics, multiple of the basic daily harmonics, is likely to be the result of the resolution into sinusoids with frequencies multiple of the basic frequency of the periodic rather than the harmonic component of the signal [Dikanev T.V., 2011]. The presence of several subday peaks seems to testify the quasiperiodicy of the process inducing the peaks.

The Fourier transformation is the tool to be used to study the periodic processes in the frequency field whose properties do not change in the course of time. Therefore to further study the hydrogen dynamics, it is necessary to use the frequency-and-temporal analysis based on the Wavelet transformations.

References:

Dikanev T.V. The spectral analysis of signals. The text-book for students of the Faculty of nano-and biomedical technologies. Saratov, 2011. 24 pp.

Nivin V.A. The free phase hydrocarbon gases in nepheline-syenites magmatic complexes as a product of natural abiogenic synthesis // The genesis of hydrocarbon fluids and deposits M.: GEOS. 2006. P. 130-138.

Nikolayev I.N., Litvinov A.V., Yemelin E.V. The availabilities of MDC-sensors applying as sensitive elements of gas analyzers // Sensors and systems. 2007. №5. P. 66-73.

Phoscorites-carbonatite relations in the Kovdor complex

Rass I.T., Kovalchuk E.V.

Institute of the Geology of Ore Deposits, Petrography, Mineralogy, and Geochemistry (IGEM), Russian Academy of Sciences, Moscow, Russia

rass@igem.ru

The crustal differentiation of primary magmas that had been derived from mantle material at low-degree partial melting is known to be able produce mineral deposits of such strategically important metals as Zr, Nb, REE, and Sr [Kogarko, 1977; Kogarko et al., 1988]. According to Rayleigh's differentiation model of primary magmas, fractional crystallization in closed systems at more or less constant bulk distribution coefficients of trace elements can be described by the equation $C^L = C_0(M^L/M)^{k-1}$, where C_0 is the initial concentration of an element, C^L is the concentration of this elements in the liquid phase, k is its bulk distribution coefficient, and (M^L/M) is the degree of differentiation, which is evaluated as the ratio of the weight concentration of the liquid phase to the total mass of the system [McIntire, 1963]. Since the distribution coefficients of incompatible elements are very small, $K_{Nb,Zr,La,Ce}$ Ol/silicate melt < 0.0001 [Green, 1994], these elements progressively enrich successive derivatives.

Alkaline ultramafic massifs containing alkaline rocks that are derivatives of mantle magmas are genetically related to carbonatites, which are characterized by a vast ore-bearing potential. It was thought until lately that the uniquely high concentrations of Nb, Zr, and REE of carbonatites in alkaline-ultramafic complexes are produced by liquid immiscibility between carbonate and silicate magmas at a high enough degree of differentiation of the primary alkaline ultramafic melts. However, recent experiments aimed at evaluating the distribution coefficients of elements between immiscible silicate magma and magmas of other composition [Veksler et al., 2012] have proved that these elements are preferably concentrated in the silicate liquid compared to the carbonate one and also that these elements can be concentrated in fluorite and phosphate (but not carbonate) melts as compared to the silicate ones. Experimental data on the distribution of REE in the course of partial melting in the peridotite-carbonate-phosphate system have discovered immiscibility between the silicate and phosphate-bearing carbonatite melts at high pressures (20-30 kbar) and temperatures 950-1000°C [Ryabchikov et al., 1989, 1993] and concentration of REE and Ti(?) in the latter.

The Kovdor massif is a typical (and one of the most thoroughly studied) ring complexes of alkaline-ultramafic rocks, carbonatites, and phoscorites; it hosts a unique magnetite-apatite-rare-metal deposit. Complex Ti, Nb, and Zr oxides and minerals of the perovskite, pyrochlore, and ilmenite groups are the principal REE concentrators [Chakhmouradian, Williams, 2004; Chakhmouradian, 2006], and their contents in the phoscorites are higher than in the carbonatites.

We have analyzed seven phoscorite and six carbonatite samples by XRF and ICP. These rocks crystallized during successive evolutionary stages of the Kovdor phoscorite-carbonatite complex that were distinguished in [Krasnova et al., 2004]. The highest Sr concentrations were found in the calcite carbonatite. The Zr and Nb concentrations in the phoscorites are notably higher than in the coeval carbonatites. The REE concentrations in the rocks of both types are comparable.

The plots of logarithmic concentrations of pairs of incompatible elements (for example, of Zr and Y) in these rocks show two different evolutionary trends, none of which follows the trends in silicate alkaline-ultramafic rocks.

According to the hypothesis of local equilibrium [Korzhinskii, 1973], thermodynamic equilibrium is reached at any point of a system at any given moment of time in the course of an irreversible process if the rate of this process (such as fractional crystallization, solution filtration, or diffusion of a component) is lower that the rate of establishing equilibrium between the outermost portion of the solid phase and the liquid (either melt or solution). The sequence of equilibria established between the outermost part of the solid phases and liquid is "recorded" in the zoning of the minerals. This zoning provides information on the evolution of the physicochemical conditions under which the mineral crystals grew. Data on the zoning of equilibrium minerals and the principle of phase coexistence [Perchuk and Ryabchikov, 1976] provide insight into relations between the zoning of minerals, physicochemical parameters of the mineral-forming processes (P, T, fO_2, pCO_2 αSiO_2), and their kinetic characteristics in magmatic and metasomatic rocks.

Differences in the compositions and zoning of equilibrium rock-forming magnetite, apatite, calcite, and dolomite (and, where possible, also accessory ilmenite, baddeleyite, and pyrochlore) were examined by using microprobe analyses of these minerals from carbonatites and phoscorites. The Ti concentration decreases from the cores to their margins of magnetite grains in carbonatites. The Al_2O_3 concentrations are at a maximum (>2 wt %) in magnetite from some phoscorites and decrease from the cores to margins of the crystals. The very high contents of the magnesioferrite component, up to 7.5 wt.% MgO, are fixed in magnetites from phoscorites whereas MgO concentrations in magnetites from carbonatites are < 2.6 wt.%. The ilmenite-magnetite [Spencer and Lindsley, 1981] crystallization temperature is 647°C at log fO_2 = -18 for the older phoscorite and 474°C for the younger one. Some of the analyzed ilmenite grains were rejected from the set used to determine the parameters because of their anomalously high concentrations of MgO (up to 25%) or MnO (13.6%).

The apatite of the phoscorites and carbonatites is F-apatite, and its F concentrations vary from 1.09 to 2.12 wt % in the phoscorites and from 1.35 to 2.00 wt % in the carbonatites. Practically all apatite grains are

zoned, with their F concentrations increasing from cores to margins. The SrO concentrations of these minerals are practically equal and vary within the range of 0.20-0.44 wt %, except only for two samples with a zonal SrO distribution: 0.23 in the cores and 0.37 wt % in the margins. The concentrations of this component slightly decreases from older to younger phoscorites. The Ce_2O_3 concentration of apatite in the phoscorites and carbonatites are also closely similar and mildly increase from older to younger rock varieties. This seems to be consistent with the fact that Kd Sr Ap/carbonatite melt = 2.4 and Kd Ce_2O_3 Ap/ carbonatite melt = 0.49 [Klemme and Dalpe, 2003]. Compared to the coexisting apatite, the calcite is poorer in REE and richer in Sr. The apatite/calcite distribution coefficients of SrO and Ce_2O_3 are equal in the older phoscorites and carbonatites: 0.43-0.46 and 1.95-2.11, respectively. The magnetite/calcite distribution coefficients of MnO and MgO are also equal in the older phoscorites and carbonatites: 5.60-5.00 and 2.79-2.77, respectively.

Geology of the Kovdor magnetite-apatite-rare metal deposit [Rimskaya-Korsakova and Krasnova, 2002; Krasnova et al., 2004], data on pyrochlore zoning in the Sokli phoscorite-carbonatite complex, Finland [Lee et al., 2006], and our petrochemical data suggest liquid immiscibility between the phosphate-magnetite and carbonatite liquids at lower temperatures, likely slightly above the solidus temperature of carbonatite magma. A seeming immiscibility between phosphate and carbonatite liquids was first detected in melt inclusions [Andreeva, Kovalenko, 2003] within the likely temperature range of 500 < T < 900ºC. Experimental data on the maximum Zr solubility in fluorite complexes [Migdisov et al., 2011] provide support for the hypothesis of possible liquid immiscibility between phosphate and carbonate melts, and our data on zoning of equilibrium magnetite, apatite and calcite in the Kovdor phoscorites and carbonatites are also consistent with this hypothesis.

Refrences

Andreeva I.A., Kovalenko V.I. Magma compositions and genesis of the rocks of the Mushugai-Khuduk carbonatite-bearing alkaline complex (southern Mongolia): evidence from melt inclusions // Per. Mineral., 2003, vol. 72, special issue:

Chakhmouradian A.R., Williams C.T. Mineralogy of high-field-strength elements (Ti, Nb, Zr, Ta, Hf) in phoscoritic and carbonatitic rocks of the Kola Peninsula, Russia // Phoscorites and carbonatites from mantle to mine: the key example of the Kola alkaline province. Zaitsev A., Wall F. – Eds., 2004: 293-340.

Chakhmouradian A.R. High-field-strength elements in carbonatitic rocks: Geochemistry, crystal chemistry and significance for constraining the sources of carbonatites // Chemical geology, 2006, vol.235: 138-160.

Green T.H. Experimental studies of trace-element partitioning applicable to igneous petrogenesis – Sedona 16 years later // Chemical geology, 1994, vol. 117: 1-36.

Klemme S., Dalpe C. Trace-element partitioning between apatite and carbonatite melt // American Mineralogist, 2003, vol. 88: 639-646.

Kogarko L.N. Genesis of agpaitic magmas, Moscow: Nauka, 1977, 294 p. (*in Russian*)

Kogarko L.N., Lazutkina L.N., Krigman L.D. Conditions of Zr concentrating in magmatic processes, Moscow: Nauka, 1988, 121 p. (*in Russian*)

Korzhinskii D.S. Theoretical fundamentals of analysis of mineral assemblages, Moscow: Nauka, 1973. (*in Russian*)

Krasnova N.I., Balaganskaya E.G., Garcia D. Kovdor – classic phoscorites and carbonatites // Phoscorites and carbonatites from mantle to mine: the key example of the Kola alkaline province. Zaitsev A., Wall F. – Eds., 2004: 99-132.

Lee M.J., Lee J.I., Garcia D., Moutte J., Williams C.T., Wall F., Kim Y. Pyrochlore chemistry from the Sokli phoscorite-carbonatite complex, Finland: Implications for the genesis of phoscorite and carbonatite association // Geochemical Journal, 2006, vol. 40: 1-13.

Migdisov A.A., Williams-Jones A.E., van Hinsberg V., Salvi S. An experimental study of the solubility of baddeleyite (ZrO_2) in fluoride-bearing solutions at elevated temperature // Geoch. Cosmoch Acta, 2011, vol. 75: 7426-7434.

Perchuk L.L., Ryabchikov I.D. Phase equilibria in mineral systems, Moscow: Nedra, 1976. (*in Russian*)

Rimskaya-Korsakova O.M., Krasnova N.I. Geology and mineral deposits of the Kovdor Massif, St.-Petersburg University: St.-Petersburg, 2002, 146 p. (*in Russian*)

Ryabchikov I.D., Baker M, Wyllie P.J. Phosphate-bearing carbonatite melts in equilibrium with mantle lherzolite at 30 kbar // Geokhimiya, 1989, no. 5: 725-729.

Ryabchikov I.D., Orlova G.P., Senin V.G., Trubkin N.V. Partitioning of rare earth elements between phosphate-rich carbonatite melts and mantle peridotites. // Mineral. Petrol., 1993, vol. 49: 1-12.

Spencer K.J., Lindsley D.H. A solution model for coexisting iron-titanium oxides // Amer.Mineral., 1981, vol.66:1189-1201.

Veksler I.V., Dorfman A.M., Dulski P, Kamenetsky V.S., Danyushevsky L.V. Jeffries T., Dingwell D.B. Partitioning of elements between silicate melt and immiscible fluoride, chloride, carbonate, phosphate and sulfate melts, with implications to the origin of natrocarbonatite // Geoch. Cosmoch Acta, 2012, vol. 79: 20-40.

The 'malignite-hornblende syenite-nepheline syenite-quartz syenite' association of Purimetla alkaline complex, Prakasam alkaline province, Andhra Pradesh, India

Ratnakar J.
*Department of Geology, University College of Science, Osmania University Main Campus,
Hyderabad-500 007, Telangana, India
Emai: jrtnkr@yahoo.com*

Ratnakar and Leelanandam (1989) and Ratnakar (2006a) have shown the distribution of Precambrian alkaline rocks and carbonatites in the eastern and southern peninsular India. The locations of these alkaline plutons have eventually provided clues to identify a major *Precambrian suture* which coincides with the 'Great Indian Proterozoic fold belt' (Leelanandam, et al., 2006). A Proterozoic igneous province called 'Prakasam alkaline province' (Leelanandam, 1989) marks a segment of this Precambrian suture in the GIPFOB. The suture marks boundary *zone* between low-grade (amphibolie-greenschist facies) Eastern Dharwar craton on the west and high-grade (granulite facies) Eastern Ghats belt on the east. The Purimetla alkaline complex (Leelanandam and Ratnakar, 1983; Ratnakar and Leelanandam, 1989) is located in the Prakasam alkaline province and it occupies an area of ~ 7 sq km. The alkaline intrusion is situated 25 km SSW of Elchuru alkaline complex and 35 km NNE of Uppalapadu alkaline complex (Ratnakar, 2006a). The Rb-Sr isochron age of the Purimetla alkaline complex is 1369±33 Ma with initial ratio Sr_i is 0.70409 (Sarkar et al., 1994).

The Purimetla alkaline complex is chiefly composed of nepheline syenite with minor hornblende syenite and quartz syenite, and rare malignite. The complex is traversed by a few ocellar lamprophyre dykes of camptonite-sannite clan. Nepheline is the sole foid; clinopyroxene is *not* ubiquitous, amphibole is the most abundant ferromagnesian silicate, and biotite is *ubiquitous*. Calcite, zircon, sphene, apatite and opaques are the conspicuous accessories in the complex. This mineralogy reflects *miaskitic* character of the nepheline syenites (Ratnakar, 2006b). Major and trace element variations in the rock types of the complex are consistent with those normally expected for a differentiated alkaline magmatic suite. The rocks of the complex define a reciprocal relationship between CaO and (Na_2O+K_2O) suggesting their igneous origin. Excepting the quartz syenites, all other rocks have normative *ol* and *ne*. The Peacock's alkali-lime index of this comagmatic alkaline series is 47. The peralkaline index ($Na_2O+ K_2O$) / Al_2O_3 (mol. prop.) of the nepheline syenites ranges from 0.69 to 0.75 suggesting *miaskitic* character that is acquired by unscrambled main trend of differentiation which is considered to have been modulated by thickened continental crust (Ratnakar, 2006b). The FeO^t-MgO-(Na_2O+K_2O) and CaO-Na_2O-K_2O variation in the *malignite-hornblende syenite-nepheline syenite-quartz syenite series* of Purimetla complex resembles that of *basanite-trachyte-phonolite series with additional rhyolite.*

The parental magma of basanitic composition, upon differentiation, followed two lineages: a main *undersaturated trend* forming malignite, hornblende syenite and nepheline syenite in that order, and another *oversaturated (offshoot) trend* emerging from the hornblende syenitic stage leading to quartz syenite. The hornblende syenitic liquids, which were developed near the critical plane of undersaturation in the basalt tetrahedron, remained critically undersaturated throughout the low temperature regime, and delivered residual liquids with a broad range of silica saturation, from undersaturated to oversaturated compositions, from which nepheline syenite and quartz syenite were formed (Ratnakar and Vijaya Kumar, 1995). The main trend of Si-undersaturation (malignite-hbl.syenite-ne.syenite) is considered to be controlled by fractionation of mafic phases at an early stage of differentiation followed by fractionation of Si-saturated K-feldspar that depleted silica in the residues. The offshoot trend of Si-oversaturation (hbl.syenite-qz.syenite) is considered to be achieved by 'assimilation fractional crystallization' (AFC). In the Ne-Ks-Qz system, the passage of undersaturated hornblende syenitic liquids to oversaturated portion through the thermal barrier -the Ab-Or join, may have been largely favoured by an increase in P_{H2O} which depressed the *liquidus temperature* as well as the *thermal minimum of the feldspar s*ystem. Thus, the silica undersaturated and -oversaturated syenites of the Purimetla are formed from a middle stage hornblende syenitic magma by branching differentiation mechanism aided by crustal contamination.

References

Leelanandam, C. (1989) The Prakasam alkaline province in Andhra Pradesh, India. Jour. Geol. Soc. India, v. 34, pp. 25-45.

Leelanandam, C., Burke, K., Ashwal, L. D. and Webb, S. J. (2006) Proterozoic mountain building in Peninsular India: an analysis based primarily on alkaline rock distribution. Geol. Mag., v. 143 (2), pp. 195-212.

Leelanandam, C. and Ratnakar, J. (1983) The Purimetla alkaline pluton, Prakasam District, Andhra Pradesh. Quart. Jour. Geol. Min. Met. Soc. India, v. 55, pp.14-30.

Ratnakar, J. (2006a) Precambrian alkaline complexes of southern India. International Symposium on *"Montreal 2006 : Alkaline igneous systems: dissecting magmatic and hydrothermal mineralizing processes"*, Montreal, Canada. Abstracts, p. 126.

Ratnakar, J. (2006b) Lithosphere control of the character of the Proterozoic alkaline magmatism: the miaskitic nepheline syenites from thickened crust of southern India. DST Group Discussion on *The evolution of the Indian continental crust and upper mantle: Recent advances and future thrust.* Osmania University, Hyderabad. Abstracts, p. 67.

Ratnakar, J., and Leelanandam, C. (1986) A petrochemical study of the Purimetla alkaline pluton, Prakasam District, Andhra Pradesh, India. Neues Jahrbuch Mineral Abh., v. 156, pp. 99-119.

Ratnakar, J. and Leelanandam, C.(1989) Petrology of the alkaline plutons from eastern and southern Peninsular India. *In :* C. Leelanandam (Ed.) *Alkaline Rocks*, Mem. Geol. Soc. India, No. 15, pp. 145-176.

Ratnakar, J. and Vijaya Kumar, K. (1995) Petrogenesis of quartz-bearing syenite occurring within nepheline syenite of the Elchuru alkaline complex, Prakasam province, Andhra Pradesh. Jour. Geol. So. India, v. 46, pp. 611-618.

Sarkar, A., Rao, K.N., Bishui, P.K. and Gupta, S.N.(1994) Rb-Sr geochronology of the Kotappakonda charnockites and the Purimetla alkaline complex, Andhra Pradesh sector, Eastern Ghats belt(abstracts). Workshop on *Eastern Ghats Mobile Belt,* Visakhapatnam, India, pp. 74-75.

Sr-Nd isotope data for carbonatite and related UHP rocks from Tromso nappe, Northern Scandinavian Caledonides

Ravna E.J.K.*, Zozulya D.R.**, Kullerud K.*, ***, Serov P.**
*Department of Geology, University of Tromsø, N-9037 Tromsø, Norway
**Geological Institute, Kola Science Centre, 184209 Apatity, Russia
***Norwegian Mining Museum, N-3602 Kongsberg, Norway
e-mail: zozulya@geoksc.apatity.ru

The carbonatite is associated with eclogite and its retrograde products, garnet clinopyroxenite (Cr-rich) and glimmerite, country-rock marble and garnet-phengite schist. It penetrates the country rock as veins and small dikes, locally cross-cutting the UHP fabric in eclogite and causing local metasomatism. Carbonatite also occurs in direct contact with marble, with a sharp boundary. The country-rock marble is strongly foliated and folded, and locally contains trains of numerous pods and lenses of retrograded eclogite. The carbonatite also appears interlayered with Cr-rich (locally garnet-bearing) clinopyroxenite. Eclogite associated with carbonatite is commonly metasomatized (phlogopite-rich) and carbonated.

Carbonatite generally have a coarse-grained isotropic fabric with clusters of mafic silicates. Primary minerals in the carbonatite-like rock are Mg-Fe-calcite ± Fe-dolomite + ternary garnet + omphacitic pyroxene + phlogopite + apatite + rutile + ilmenite. Carbonatite occurs as two different types. The major type, C1, is silicate-rich. Type C2 is silicate-poor and occurs as veins and patches within type 1.

The field relations, overall texture, presence of different types exsolution textures suggest that the carbonatitic rock crystallized from a melt.

The carbonatite-like rocks are strongly enriched in Ba, Sr and LREE. Their chondrite-normalized incompatible elements' and REE patterns are similar to common carbonatite.

Here we present the Sr-Nd isotope data for carbonatite and related rocks (carbonated and metasomatized eclogites, marble). The radiogenic isotope signature of the type C1 carbonatite is similar to that of the country-rock marbles with values mostly around 0.705-0.708 for $^{87}Sr/^{86}Sr$ and -1 to -2 for ε_{Nd}, but there are values -11 to -13 for ε_{Nd}. One sample of type C2 carbonatite has similar Sr but a more negative Nd value (3.3). Eclogite has the most radiogenic Sr (0.708-0.710) and unradiogenic Nd (-2.4 to -3.3). The carbonated eclogite has a similar Sr value as the carbonatite but ε_{Nd} is closer to the eclogite values, the relative abundances of Sr and Nd suggesting that carbonation added Sr but essentially no Nd to the eclogite. The metasomatized eclogite is distinct in having most radiogenic ε_{Nd} value (0.1) and 0.7067 for Sr. This implies that the metasomatic fluid was compositionally more primitive than the carbonatitic-like magmas, or that the latter have been isotopically modified by interaction with the crust. Overall the compositions of the Tromsø occurrence falls close to those of some of the orogenic occurrences such as northern Pakistan, west-central India and Qinling, northern China (Tilton et al, 1998; Simonetti et al, 1995; Xu et al, 2011) and fit at the crustal end of the general trend defined by carbonatites. The latter is commonly explained in terms of extraction of the carbonatitic melt from enriched mantle domains (HIMU, EM1 and EM2; e.g. Bell and Simonetti (2010)).

Noteworthy, that carbonatites and carbonated and metasomatised eclogites form the Rb-Sr errorchrone with age (ca. 470 Ma) which is closed to the U-Pb zircon age of both carbonatite and eclogite. This apparently confirms that the rocks are isotopically homogenous (another word, carbonatites and altered eclogites are of the

same source and genetically related). The petrogenetical model for carbonatite by partial melting of carbonated eclogite is suggested.

References

Bell K., Simonetti A. Source of parental melts to carbonatites-critical isotopic constraints // Mineralogy and Petrology, 2010, v.98, pp.77–89.

Simonetti A., Bell K., Viladkar S.G. Isotopic data from the Amba Dongar carbonatite complex, west-central India: evidence for an enriched mantle source // Chemical Geology, 1995, v.122, pp.185–198.

Tilton G. R., Bryge J. G., Mateen A. Pb-Sr-Nd isotope data from 30 and 300 Ma collision zone carbonatites in Northwest Pakistan // Journal of Petrology, 1998, v.39, pp.1865-1874.

Xu C., Taylor R.N., Kynicky J., Chakhmouradian A.R., Song, W., Wang, L. The origin of enriched mantle beneath North China block: Evidence from young carbonatites // Lithos, 2011, v.127, pp.1-9.

Major and trace elements in calcite and dolomite from carbonatites and the stories they tell

Reguir E.P., Chakhmouradian A.R.
Department of Geological Sciences, University of Manitoba, Winnipeg, Manitoba, Canada

Carbonate minerals are the principal constituent of intrusive carbonatites; their content ranges from 50 modal %, which is accepted as a nominal threshold for this rock type, to well over 90% in some varieties interpreted as cumulates (e.g., Xu et al., 2007). Approximately 60% of intrusive carbonatites worldwide are predominantly calcitic; most of the remaining 40% comprise members of the dolomite-ankerite series. The latter cover a compositional range from nil to ~23 wt.% FeO or 70 mol.% $CaFe(CO_3)_2$, i.e. approach the solubility limit established for these minerals empirically (Reeder and Dollase, 1989). Notably, ankerite sensu stricto [> 18 wt.% FeO or 50 mol.% $CaFe(CO_3)_2$] is restricted to late-stage postmagmatic parageneses. The Ca content of igneous dolomite does not deviate from the ideal stoichiometric value by more than 0.04 atoms per formula unit (apfu) in ~90% of the published and our own data. This amount of variation is consistent with the width of the dolomite intersolvus field in the binary system $CaCO_3$-$MgCO_3$. At the same time, the proportion of $MgCO_3$ that can be incorporated in calcite is much greater. Our data show that up to 4.3 wt.% MgO (~11 mol.% $MgCO_3$) can be present in early calcite associated with subsolvus dolomite in some carbonatites (e.g., Goldray, Canada). Based on these considerations, it is obvious that exsolution of dolomite from Mg-rich calcite will be a much more common phenomenon in carbonatites than exsolution of calcite from Ca-rich dolomite. In both calcite and dolomite, the divalent cations are coordinated by six atoms of oxygen, but the Ca site is more spacious in the latter, which accounts for complete miscibility between $CaMg(CO_3)_2$ and $SrMg(CO_3)_2$ in synthetic systems (Brice and Chang, 1973), but only limited incorporation of Sr in calcite. Under experimental conditions, equilibrated dolomite and calcite appear to have comparable Sr contents. The highest levels of Sr and Ba (up to 13 mol.% $SrCO_3$ and 1.5 mol.% $BaCO_3$) occur in the so-called "strontium-barium" carbonatites, where calcite formed by exsolution of an unknown ternary Ca-Sr-Ba carbonate (Wall et al., 1993; Konev et al., 1996). Lead is low in primary calcite (≤ 140 ppm: Xu et al., 2007), but reaches 370 ppm in late-stage calcite formed in an oxidizing environment at Eh levels too low to stabilize Pb^{4+}. Consistently lower Sr, Ba and Pb levels in dolomite (including that associated with calcite) appear to be at variance with experimental data (see above), because the Ca site in the dolomite structure is 2-3% larger than in calcite (Reeder and Dollase, 1989). There are three possible explanations for this discrepancy: (1) dolomite crystallizes from melts impoverished in Sr, Ba and Pb relative to their Ca-rich counterparts; (2) dolomite co-crystallizes with other minerals that are more efficient at scavenging large-ion lithophile elements than dolomite; or (3) partitioning of these elements between calcite (dolomite) and a carbonate melt differs significantly from experimental results based on solid-state reactions.

The incorporation of non-divalent cations in igneous carbonates is problematic because it requires coupled substitutions in proximal sites to avoid under- or overbonding of oxygens in carbonate groups. In this work, the highest levels of REE (1840 ppm) were detected in primary calcite from Aley, Canada. About 98% of analyses contain ≤ 1400 ppm REE. The lowest levels of REE (60-90 ppm) are observed in the Magnet Cove carbonatite (USA). This sample contains a large proportion of cumulus andradite, which probably accounts for early depletion of the parental carbonatitic magma in REE. The patterns of REE distribution in calcite normalized to the chondrite composition vary from extremely steep negatively sloping with a high $(La/Yb)_{cn}$ ratio (up to 1740 at Turiy Mys, Kola) to nearly flat (1-5 at Cinder Lake, Canada). The highest recorded REE contents in dolomite are close to 600 ppm, and are commonly observed in the products of calcite dolomitization. For a given locality, dolomite is appreciably poorer in REE relative to cogenetic calcite. The chondrite-normalized patterns range from negatively sloping light-REE-enriched to flat in the LREE range, but sloping either down (prevalent type) or up toward HREE. The available analyses cover a $(La/Yb)_{cn}$ range of 0.3 to 303,

but ~80% of the data fall within a much smaller range (20-150). Positive correlation between $(La/Yb)_{cn}$ and REE, clearly expressed in rock-forming carbonates from some localities (e.g., Aley, Canada) , results from preferential partitioning of REE into fractionating apatite, which is a common cumulus mineral in carbonatites. The greater affinity of apatite for light REE relative to heavy lanthanides and Y drives the composition of rock-forming carbonates to progressively lower $(La/Yb)_{cn}$ ratios. Early crystallization of other minerals capable of scavenging REE will change the vector of geochemical evolution. Fractionation of monazite or fluorocarbonates, for example, will yield an even steeper REE evolutionary trend with respect to the $(La/Yb)_{cn}$ axis.

Despite their extensive variation in the content of individual trace elements, early-crystallizing calcite and dolomite from carbonatites exhibit fairly consistent ratios between some of the elements, especially those sensitive to redox conditions (Ce/Ce*, Eu/Eu*). The Y/Ho value, controlled by cation complexation in aqueous systems or volatile-rich melts, is somewhat less consistent, but in common with the redox-sensitive parameters, is typically within the error of the primitive-mantle values. An important telltale sign of hydrothermal reworking is deviation from the primary, chondrite-like REE ratios, accompanied by a variety of other compositional changes depending on the redox state of the fluid (e.g., depletion of carbonates in Mn owing to its oxidation and sequestration by secondary oxides). Hydrothermal processes do not produce a unique geochemical fingerprint, leading instead to a variety of evolutionary trends that range from light-REE-Sr-Ba enrichment (Turiy Mys) to heavy-REE enrichment and Sr-Ba depletion (Bear Lodge, USA). Supergene oxidation is typically manifested in extreme depletion of rhombohedral carbonates in Mn and Ce, ultimately leading to a strong negative Ce anomaly and very high Mg/Mn ratios.

A number of important questions regarding the crystal chemistry of calcite and dolomite from carbonatites (and in general), and their trace-element characteristics remain outstanding. These include: (1) structural mechanisms of REE uptake by these minerals; (2) partitioning of REE, Sr, Ba and Pb between cogenetic calcite and dolomite; (3) the effects of apatite, phlogopite and pyrochlore fractionation on the compositional evolution of magmatic carbonates; and (4) the relations between fluid chemistry and compositional changes in hydrothermal carbonates.

References:

Brice, W.R., Chang, L.L.Y. (1973) Subsolidus phase relations in aragonite-type carbonates. III. The systems $MgCO_3$-$CaCO_3$-$BaCO_3$, $MgCO_3$-$CaCO_3$-$SrCO_3$, and $MgCO_3$-$SrCO_3$-$BaCO_3$ // American Mineralogist. Volume 58. Pages 979-985.

Konev, A.A., Vorob'ev, E.I., Lazebnik, K.A. (1996) Mineralogy of the Murun alkaline massif // Siberian Branch of the Russian Academy of Sciences press, Novosibirsk, Russia, 221 pages.

Reeder, R.J., Dollase, W.A. (1989) Structural variation in the dolomite-ankerite solid-solution series: An X-ray, Mössbauer, and TEM study // American Mineralogist. Volume 74. Pages 1159-1167.

Wall, F., Le Bas, M.J., Srivastava, R.K. (1993) Calcite and carbocernaite exsolution and cotectic textures in a *Sr,REE-rich* carbonatite dyke from Rajasthan, India // Mineralogical Magazine. Volume 57. Pages 495-513.

Xu, C., Campbell, I.H., Allen, C.M., Huang, Z., Qi, L., Zhang, H., Zhang, G. (2007) Flat rare earth element patterns as an indicator of cumulate processes in the Lesser Qinling carbonatites, China // Lithos. Volume 95. Pages 267-278.

Formation conditions of potassium mafic rocks from Yllymakh, Ryabinovy and Inagli Massifs, Central Aldan

Rokosova E. Yu., Sokolova E.N.
V.S. Sobolev Institute of Geology and Mineralogy SB RAS, Novosibirsk, Russia
rokosovae@gmail.com

Yllymakh, Ryabinovy and Inagli alkaline massifs (Central Aldan) of Mesozoic age belong to an intricate volcano-plutonic structures. These massifs consist of intrusive, volcanic and dike rocks of potassic series. They are about 20-50 km² in area. In these massifs, almost the entire range of rocks was found, from the potassic alkaline ultrabasic rocks through basic and intermediate ones to alkaline granosyenites and granites. The formation of massifs related to the activity of the Mesozoic rift structure of the Aldanian Shield. Melt inclusions in clinopyroxenes and olivines were studied to find out the formation conditions of potassium mafic rocks.

Primary completely crystallized silicate-carbonate-salt inclusions were studied in diopside of the olivine shonkinites from INAGLI massif. It was found that, diopside crystallized from homogeneous carbonate-salt silicate melt at 1170-1190°C. Homogeneous carbonate-salt silicate melt was separated into silicate and carbonate-salt fractions at cooling to 1150-1160ºC. The composition of silicate fraction evolves from alkali-basalt to alkali-trachyte. Carbonate-salt fraction has an alkali-carbonatite composition and were enriched in SO_3, Cl.

At the crystallization stage of diopside (1120-1190ºC) of the biotite shonkinites from RYABINOVYJ

massif the melt was heterogeneous and consisted of immiscible silicate, carbonate-salt, and carbonate fractions. The composition of silicate fractions evolves from alkali-basalt to melaphonolite-alkali trachyte. The carbonate-salt and carbonate melts separated from silicate magma were enriched in Ca, alkalies, CO_2, S, Cl.

By studying the glassy and partly crystallized melt inclusions in in diopside and olivine of the alkaline-basic dike rock of the YLLYMAKH massif, it was found that, diopside crystallized from homogeneous tephri-phonolite melt at 1200-1240°C. The tephri-phonolite melt were enriched in Cl, S, F, Ba, and then evolved to phonolite melt.

It is important that silicate melts from inclusions in olivine shonkinites of the Inagli massif, biotite shonkinites of the Ryabinovyj massif and alkaline-basic dike rocks of the Yllymakh massif evolve in the same direction and form a single trend with decreasing temperature and crystallization minerals (Fig. 1). It is seen that crystallization of the melts was accompanied by the decrease in the contents of calcium, iron, magnesium, and increase in aluminum, silica, alkalis, which is typical of the fractional crystallization of alkaline-basaltoid melts. The chemical compositions of igneous rocks that form Yllymakh and Inagli massifs, as well as the compositions of biotite shonkinites, alkaline picrites and minettes of the Ryabinovyj massif are also plotted in the trend. Such a trend may indicate that studied rocks of the Yllymakh, Ryabinovy and Inagli massifs were formed as a result of fractional crystallization of parental alkali-basalt-like magmas.

Besides, all studied rocks have similar trace elements and significant enrichment relative to primitive mantle. Incompatible trace element distributions normalized to the primitive mantle of Sun and McDonough (1989) show almost identical patterns for all studied rocks and negative slope (Fig. 2a). High LILE content, the relative overweight of LREE over HREE and marked negative HFSE (Ta, Nb, Hf, Zr), Ti anomalies are characterized for all studied rocks.

Homogenized melt inclusions in minerals of alkaline-basic dike rocks of the Yllymakh massif and olivine shonkinites of the Inagli massif are significantly enriched in trace elements relative to primitive mantle. Incompatible trace element distributions normalized to the primitive mantle of Sun and McDonough (1989) show almost identical patterns for all glass inclusions (Fig. 2b). The enrichment of the LILE, the relative overweight of LREE over HREE and marked negative Nb, Ti anomalies and positive Sr anomaly are characterized for all glass inclusions.

Rare earth elements distributions normalized to the chondrite of Anders and Grevesse (1989) show almost identical patterns for clinopyroxenes from studied rocks (Fig. 2c). REE patterns of clinopyroxenes display the relative overweight of LREE over HREE.

Almost identical trace elements patterns for all studied rocks, glass inclusions and clinopyroxenes indicates that parental magmas were generated from sources with similar compositions. High concentrations of LILE (K, Rb, Ba) and LREE, probably indicates to enriched mantle sources. The relative overweight of LREE over HREE for studied rocks, glass inclusions and clinopyroxenes indicates that the sources of magma apparently located in the mantle at depths of existence of garnet-bearing associations.
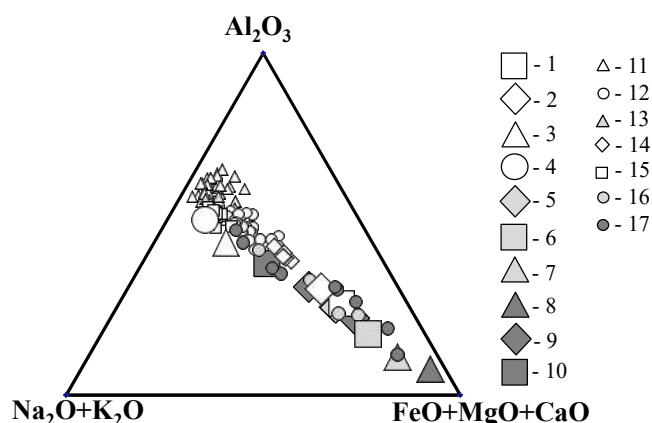
Fig. 1. Compositions of rocks and glass inclusions in minerals of studied rocks in the system
Al_2O_3 - (FeO + MgO + CaO) - (Na$_2$O + K$_2$O).
1-10 - rocks: 1-4 - Yllymakh massif (1 – alkaline-basic dike rocks, 2 – malignites*, 3 – pseudoleucite phonolites*, 4 – pulaskites*); 5-7 - Ryabinvy massif (5 – minettes, 6 – alkaline picrites**, 7 – biotite shonkinites); 8-10 - Inagli massif (8 – olivine shonkinites, 9 – alkaline gabbroid rocks*, 10 – pulaskites*).
* - composition of rocks by V.P. Kostyuk et al (1990); ** - composition of rocks by V.V. Sharygin (1993).
11-17 - glass inclusions: 11-15 – in alkaline-basic dike rocks of the Yllymakh massif (11 – secondary unheated inclusions in olivine, 12 – secondary heated inclusions in olivine, 13 – primary unheated inclusions in clinopyroxene, 14 – primary heated inclusions in core of the clinopyroxene, 15 – primary heated inclusions in rim of the clinopyroxene; 16 – primary heated inclusions in clinopyroxene of biotite shonkinites of the Ryabinvy massif; 17 – primary heated inclusions in clinopyroxene of olivine shonkinites of the Inagli massif.
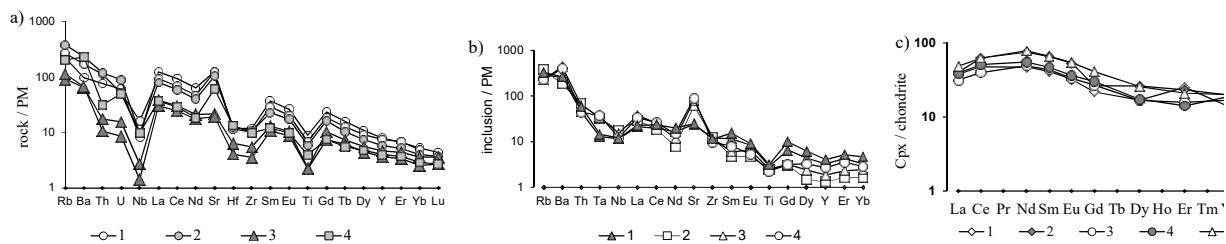
Fig. 2. a) Primitive mantle-normalized (по Sun, McDonough, 1989) trace element diagrams for studied rocks of Central Aldan: 1 – biotite shonkinites of the Ryabinvy massif, 2 – minettes of the Ryabinvy massif, 3 – olivine shonkinites of the Inagli massif, 4 – alkaline-basic dike rocks of the Yllymakh massif.

b) Primitive mantle-normalized (по Sun, McDonough, 1989) trace element diagrams for glass inclusions: 1 – from olivine shonkinites of the Inagli massif, 2-4 – from minerals of the alkaline-basic dike rocks of the Yllymakh massif (2 - from intermediate zone of the clinopyroxene, 3 – from rim of the clinopyroxene, 4 – from olivine).

c) Chondrite-normalized (по Anders, Grevesse, 1989) REE diagrams for clinopyroxenes of the studied rocks: 1-2 - Yllymakh massif, 3-4 - Ryabinvy massif, 5 - Inagli massif.

References:

Anders E., Grevesse N. Abundances of the elements: meteoric and solar // Geochimica et Cosmochimica Acta. 1989. v. 53. p. 197-214.

Kostyuk V.P., Panina L.I., Zhidkov A.Ya., Orlova M. P., Bazarova T. Yu. Potassium alkaline magmatism of Baikal-Stanovoy rifting system. 1990. Novosibirsk "Nauka", (in Russia).

Sharygin V.V. Potassic alkaline picrites of the Ryabinovyi Massif, Central Aldan // Geology and Geophysics. 1993. v. 34. № 4. p. 51-61.

Sun S. S., McDonough W. F. Chemical and isotopic systematics of oceanic basalts: implications for mantle composition and processes // Magmatism in Ocean Basins. Geological Society Special Republication. London. 1989. p. 313-345.

Carbonatite magmas in Lower Mantle

Ryabchikov I.D.
Russian Academy of Sciences, IGEM RAS
iryab@igem.ru

It has been experimentally demonstrated that at PT-parameters of sublithospheric zones substantial part of ferrous iron in peridotitic material must be disproportioned with the formation of Fe_2O_3 and iron-rich metallic alloy. Under these conditions carbonate components should be reduced with the formation of diamond or carbides. Nonetheless, the presence of carbonate-rich melts in lower mantle is confirmed by the studies of mineral inclusions in the diamonds of lower-mantle source [1]. It demonstrates that lower mantle is heterogeneous with respect to redox characteristics.

In order to assess redox-potential of lower mantle mineral-forming systems I performed thermodynamic analysis of phase equilibria of rock-forming minerals of pyrolitic lower mantle with carbon-bearing crystalline compounds demonstrated that the field of diamond stability is separated from that of Fe-rich metallic alloy by the field of co-existence of iron carbides with prevailing silicates and oxides (Fig. 1). It implies that the formation of diamond in lower mantle requires more oxidizing conditions by comparison with the predominant part of this geosphere.

The absence of metallic phase among the minerals of low-mantle diamond-bearing paragenesis is consistent with the high (about 1% - Fig. 2) Ni contents in ferropericlases trapped by diamond (Ni should be intensely extracted by Fe-rich alloy). The elevated redox potential is corroborated by the measurements of $Fe3+/\Sigma Fe$ values in ferropericlases included in diamonds transported from lower mantle [2].
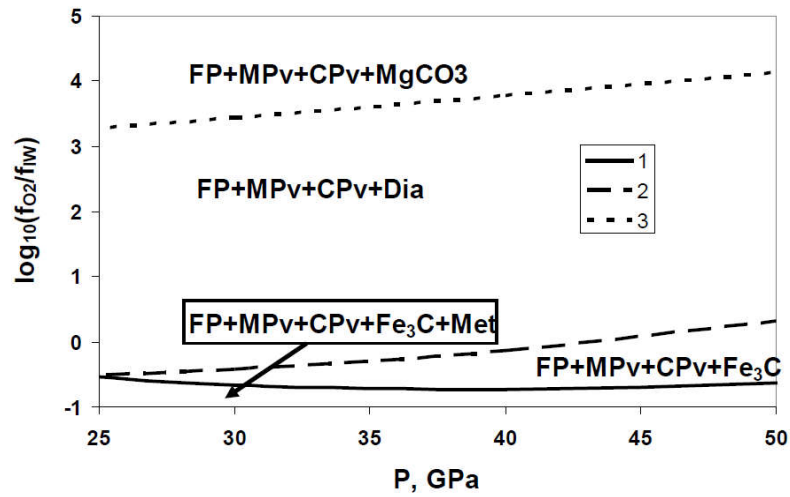
Fig. 1. Stability fields of lower mantle mineral assemblages (oxygen fugacity is normalized by iron wuestite buffer). FP is ferropericlase, MPv is Mg-rich silicate perovskite, CPv is Ca-rich silicate perovskite, Dia is diamond and Met is Fe-rich metallic alloy.
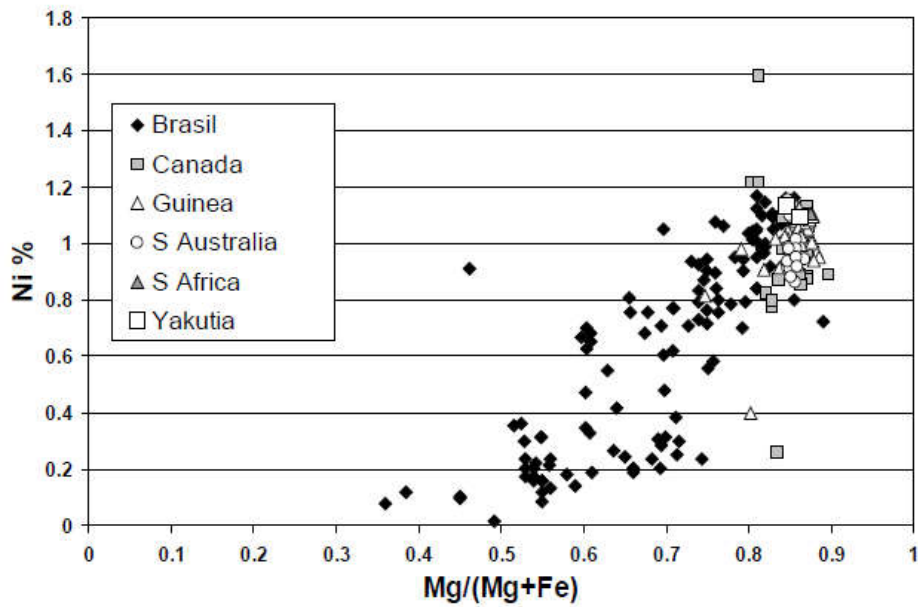
Fig. 2. *FP* inclusions in diamonds of lower mantle origin with Mg-numbers appropriate for metaperidotite bulk composition all cluster around 1 % of Ni. Some outliers may correspond to lower f_{O2} values.

The most likely cause of increasing oxygen fugacities is the displacement of redox equilibria with the growing temperature towards the decreasing amount of Fe-rich alloy and finally its complete disappearance (Fig. 3). An important role in the genesis of diamonds may be played by the appearance of carbonate-phosphate and silicate melts their migration and interaction with the surrounding rocks.

100
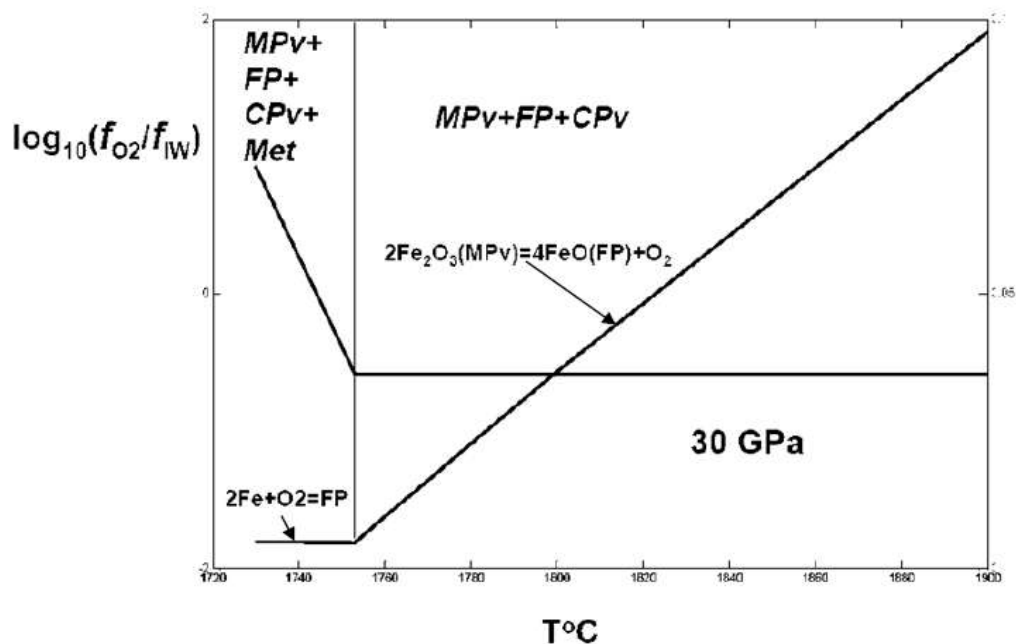
Fig. 3. Effect of temperature on redox equilibria in lower mantle of pyrolitic composition. Left vertical axis is logarithm of oxygen fugacity normalized to IW buffer, right vertical axis is a number of Fe^{3+} atoms in *MPv* per one oxygen.

The link of sublithospheric diamond formation with high temperature conditions follows from the confinement of such processes and to mantle plumes. Kimberlites are also related to the mantle plume environment.

Relatively oxidizing conditions related to mantle plumes are also manifested in the high level of oxygen fugacitiy typical for some ultramafic-alkaline magmatic rocks such as meimechites and intrusive rocks of the Maimecha-Kotuy Province (Polar Siberia).

References

1. Kaminsky F.V., Ryabchikov I.D., Wirth R., 2015. A primary natrocarbonatitic association in the Deep Earth // Mineralogy and Petrology. V. P. DOI 10.1007/s00710-00015-00368-00714.

2. Kaminsky F.V., Ryabchikov I.D., McCammon C.A., Longo M., Abakumov A.M., Turner S., Heidari H., 2015. Oxidation potential in the Earth's lower mantle as recorded by ferropericlase inclusions in diamond // Earth Planet. Sci. Lett. V. 417. P. 49-56.

Findings related the project of Turkey Ophiolite Inventory of Geological Survey of Turkey

Sarifakioglu E.*, Timur E.*, Dilek Y.**
*The General Directorate of Mineral Research and Exploration (MTA), Geological Research Department, Ankara, Turkey
**Department of Geology & Env. Earth Science, Miami University, Oxford, OH, 45056, USA

Turkey, in Alp-Himalaya-Tibet orogenic belt, contains alots tectonic units and ophiolitic rocks among them. The studies related inner structure, stratigraphical sequence, chemical features and tectonic evolution of ophiolitic rocks because of determination of their ages of emplacement and formation is very important to propound the geodynamic evolution of tectonic units and ophiolites. The ophiolites in Turkey are mainly classified in four suture zones. These are Intra-Pontide Suture Zone (IPSZ), Izmir-Ankara-Erzincan Suture Zone (IAESZ), Inner-Tauride Suture Zone (ITSZ) and Bitlis-Zagros Suture Zone (BZSZ) from North to South. Two objectives are

defined for the project of "Turkey Ophiolite Inventory" belonging to the Geological Research Department of the General Directorate of Mineral Research and Exploration (MTA). One is to collect the information gathered from the MTA project in digital data base of Geographic Information Systems (GIS) in order to be associated with each other. Other is to prepare a report summarizing all information related to ophiolite in Turkey (lithology, paleontological age, radiometric, geochemistry, mineralization).

In previous studies, most of ophiolites in Turkey were reported to be late Cretaceous SSZ (suprasubduction zone)–type characteristics (Parlak et al. 2013) while some of those was emphasized as MORB (mid ocean ridge basalt)–type ophiolitic blocks within ophiolitic mélanges ranging from late Triassic to late Cretaceous (Göncüoğlu et al. 2001). However, in recent years, some SSZ–type ophiolitic rocks along Izmir–Ankara–Erzincan Suture Zone (IAESZ) were determined as Jurassic age of their formation representing the remnants of the northern Neotethys (Dilek and Thy, 2006; Sarifakioglu et al. 2014; Uysal et al. 2015) (Figure 1).

Here, it will be summarized the findings obtained during the studies related "Turkey Ophiolite Inventory", especially along IAESZ. It extends from west to east, connecting Vardar Suture in west and Sevan–Akera Suture Zone to Tethyan Himalaya Belt in east representing the suture of a Tethyan ocean from Late Palaeozoic to earliest mid–Eocene. The presence of late Permian (256.9±8.0 Ma) amphibole–epidote schist blocks within the ophiolitic mélange, and late Triassic (201–204Ma from Ar–Ar age dating) gabbro, Lias plagiogranite (180Ma from U–Pb zircon age dating) and Cretaceous (135.9±3.1 Ma to 118.3±3.4Ma from Ar–Ar age dating) diabase and basalt within various ophiolite sequences along IAESZ may indicate the existence of northern Neotethyan ocean in late Permian at least, and southward retreating of subduction zone in the intra–oceanic environment of northern Neotethyan ocean during Mesozoic era. These ophiolite sequences contain ultrabasic–basic–leucocratic rocks and are covered by deep sea sedimentary rocks (chert, radiolarite, pelagic limestone, mudstone etc.) (Figure 2). Also, these ophiolitic rocks sometimes are found together with island-arc rocks, oceanic plateau volcanics and seamount volcanics.

Some findings, especially Jurassic and Cretaceous ophiolitic rocks were obtained in Balkan Peninsula along Vardar Zone and in Armenia along Sevan–Akera Suture Zone (Koglin, 2008; Hässig et. al. 2013).

References:

Dilek, Y. and Thy, P. Age and petrogenesis of plagiogranite intrusions in the Ankara Mélange, central Turkey. 2006. Island Arc 15, 44–57.

Hässig, M., Rolland, Y., Sosson, M., Galoyan, G., Müller, A., Avagyan, A. and Sahakyan, L. New structural and petrological data on the Amasia ophiolites (NW Sevan–Akera suture zone, Lesser Caucasus): Insights for a large-scale obduction in Armenia and NE Turkey. 2013. Tectonophysics 588, 135–153.

Koglin, N. Geochemistry, petrogenesis and tectonic setting of ophiolites and mafic–ultramafic complexes in the Northeastern Aegean Region: New trace–elements, isotopic anda ge contraints. 2008. Ph.D thesis, Gutenberg Universty, Mainz, Germany.

Sarifakioglu, E., Dilek, Y. and Sevin, M. Jurassic–Paleogene Intra–Oceanic Magmatic Evolution of the Ankara Mélange, North–Central Anatolia, Turkey. 2014. Solid Earth 5, 77–108.

Göncüoğlu, M.C., Tekin, U.K. and Turhan, N. Late Carnian radiolarite-bearing basalt blocks within the Late Cretaceous Central Sakarya Ophiolitic Mélange, NW Anatolia: Geological constrains. 54th Geological Congress of Turkey. 2001. Proceedings CD-format, 54-61.

Parlak, O., Çolakoğlu, A., Dönmez, C., Sayak, H., Yıldırım, N., Türkel, A. and Odabaşı, İ. Geochemistry and tectonic significance of ophiolites along the Izmir–Ankara–Erzincan Suture Zone in northeastern Anatolia. In: Robertson, A.H.F., Parlak, O. and Ünlügenç, U.C. (eds), Geological Development of Anatolia and the Easternmost Mediterranean Region. Geological Society, London, 2013, Special Publication 372, 75–107.

Uysal, I., Ersoy, E.Y., Dilek, Y., Escayola, M., Sarifakioglu, E., Saka, S. and Hirata, T. Depletion and refertilization of the Tethyan oceanic upper mantle as revealed by the early Jurassic Refahiye ophiolite, NE Anatolia–Turkey. 2015. Gondwana Research 27, 594-611.

Figure 1. The representative geochronological and paleontological data from opiolitic rocks and methamorphic sole rocks along the IAESZ.
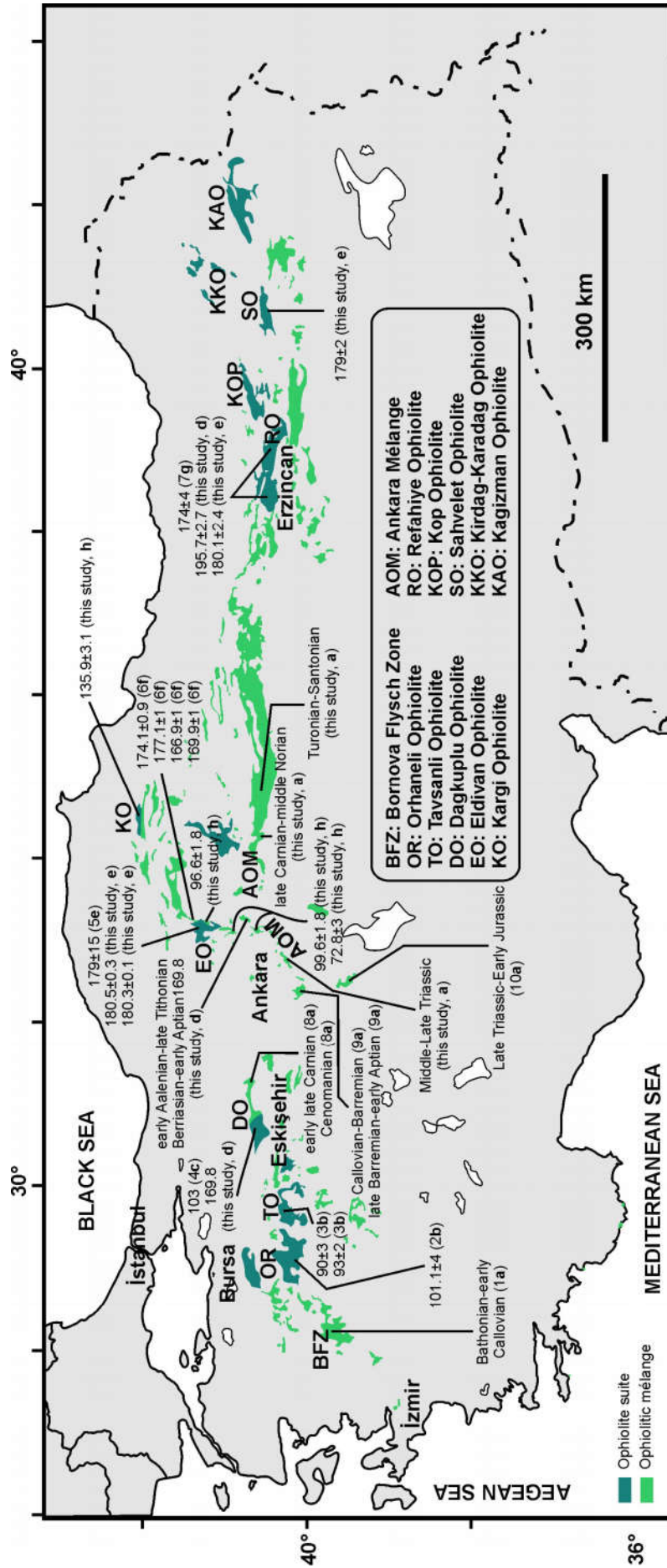
(1) Tekin & Göncüoğlu (2009), (2) Harris et al. (1994), (3) Onen & Hall (2000), (4) Sarıfakıoğlu et al. (2009), (5) Dilek & Thy (2006), (6) Çelik et al. (2011), (7) Topuz et al. (2013), (8) Göncüoğlu et al. (2001, 2010), (9) Rojay et al. (2004), (10) Uğuz et al. (1999)

(a) Paleontological data, (b) ^{40}Ar/^{39}Ar amphibole ages from metamorphic sole, (c) Sm-Nd garnet ages from metamorphic sole, (d) ^{40}Ar/^{39}Ar hornblende ages from pegmatitic gabbro, (e) U-Pb zircon ages from plagiogranite, (f) ^{40}Ar/^{39}Ar hornblende ages from amphibolites within AOM, (g) ^{40}Ar/^{39}Ar hornblende ages from foliated gabbros, (h) ^{40}Ar/^{39}Ar ages from basic rocks within AOM

103

Figure 2. The ophiolitic rocks along IAESZ (a: TO; b: OR; c–d–e: EO; f: RO; g–h: EO; du: dunite; gb: gabbro; db: diabase; pg: plagiogranite; dss: deep sea sedimentary rocks).

New discoveries of REE-mineralization in the Ilimaussaq intrusion, South Greenland

Schonwandt H.K.V.

Tanbreez Mining Greenland A/S

A decade of continuous exploration on the Ilimaussaq intrusion, South Greenland has revealed several new styles of mineralization within the intrusive complex. The type of mineralization is not unusual for mineralization associated with alkaline to peralkaline complexes. Three new types of mineral occurrences from the southern part (south of Tunulliarfik Fjord) of the complex is described. (1) A U-REE deposit of similar type as the Kvanefjeld deposit in the northern part of the Ilimaussaq complex. Aerial geophysical program showed an 80-hectar uranium anomaly associated with arfvedsonite lujavrite. 250 grab samples returned an average of 340 ppm U3O8 and 1.3% TREO. (2) Eudialyte dominated pegmatite associated with lujavrite sill's intruding naujaite. The eudialyte pegmatite is enveloping the lujavrite sills and at the same time replacing the naujaite. The nearly mono-mineral eudialyte mineralization assayed 9.3% ZrO2 and 2.7% TREO. (3) A large hydrothermal deposit was intersected by drilling. The hydrothermal system has a vertical extent of more than 300 m and a grade of 0.9% TREO of which 20% is heavy REE.

Some of these deposits have potential for hundreds of million tons of ore and are significant discoveries and possibley relevant to other similar intrusions.

Silicate-salt inclusions in diopside of Oldoinyo Lengai ijolites, Tanzania

Sekisova V.S., Sharygin V.V.

Novosibirsk State University, Novosibirsk, Russia

V.S. Sobolev Institute of Geology and Mineralogy SB RAS, Novosibirsk, Russia, vikasekisova@mail.ru

Ijolites sometimes occur as xenoliths in the Oldoinyo Lengai pyroclastic rocks of nephelinite composition [Dawson, 1962; Dawson et al., 1995]. Diopside is one of the main minerals in these rocks. It forms euhedral crystals (up to 2 mm in size) and shows pronounced oscillatory zoning. Its chemical composition strongly varies (in wt.%): SiO_2 (49.3-54.6), FeO_t (4.8-20.0), MgO (6.8-15.9), Na_2O (0.6-3.8) and CaO (18.2-24.3). The marginal zones of diopside contain numerous crystal inclusions, represented by nepheline, fluorapatite, Ti-magnetite, perovskite, titanite and phlogopite.

Primary melt inclusions with silicate-carbonate immiscibility are most common in nepheline and Ti-magnetite of ijolites. Other minerals (clinopyroxene, etc.) rarely contain primary inclusions with the immiscibility; fluorapatite bears primary natrocarbonatite inclusions. Majority of nepheline-hosted inclusions (5-100 µm) has the following phase composition: silicate glass + vapor-carbonate globule ± daughter/trapped crystals ± sulphide bleb. Some inclusions may also contain numerous micron-sized carbonate globules in silicate glass. Vapor-carbonate globule (up to 20 µm) consists of gas bubble (60 vol.%) and nyerereite-rich carbonate aggregate (40 vol.%) [Sekisova et al., 2013].

Diopside rarely contains primary silicate melt inclusions (size 10-30 µm), which usually occur in the core of the host. Their phase composition is silicate glass + gas bubble $\pm$ daughter crystals, represented by Ti-rich magnetite, fluorite and baryte. Primary inclusions with silicate-carbonate immiscibility are scarce.

In addition to primary silicate-melt inclusions diopside also contains secondary silicate-salt and sulphide inclusions. They form trails, crossing the central zones in the host mineral. Sulphides are represented pyrrhotite, rarely pentlandite, chalcopyrite, djerfisherite, galena, bornite (?) and Ag-bearing phases. Silicate-salt inclusions are completely crystallized (Fig. 1).
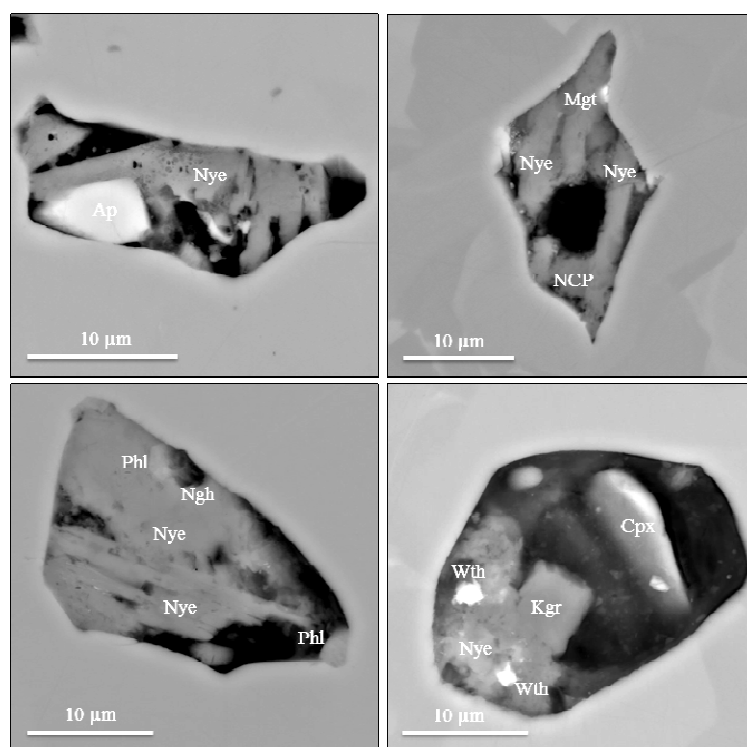
Figure 1. **Backscattered electron images (BSE) of secondary silicate-salt melt inclusions in diopside.**
Symbols: Nye – nyerereite; Ap – fluorapatite; Ngh – neighborite, Wth – witherite, Phl – phlogopite,
Kgr – kogarkoite, Mgt – Ti-magnetite, NCP – Na-Ca-phosphate, Cpx - clinopyroxene.

Their sizes vary from 10 to 40 μm. Their phase composition strongly varies and silicate constituent is minor in respect to other phases (carbonates, sulphates, phosphates, etc.). Silicate-salt inclusions contain nyerereite, fluorapatite, nepheline, phlogopite, thenardite, sylvite, Ti-magnetite, neighborite, leucite (?), baryte, witherite, kogarkoite, Na-Ca-rich sulphates and phosphates. Identification of the daughter phases within inclusions was supported by EDS, elemental mapping and Raman spectra.

Nyerereite of the secondary diopside-hosted melt inclusions is a dominant phase (Fig. 1); its chemical composition is shown in Table 1. In general, it is similar in composition to nyerereite from the Lengai natrocarbonatite [Zaitsev et al., 2009]. Rare alkali sulphate, kogarkoite $Na_3(SO_4)F$, was identified in some diopside-hosted inclusions. It is close to the ideal composition. Its Raman spectrum is characterized by the presence of the strong peak at 997 sm[-1], which corresponds to $(SO_4)^{2-}$-group. Earlier kogarkoite was detected only in inactive natrocarbonatite hornitos at Oldoinyo Lengai [Mitchell, 2006].

It should be noted that secondary silicate-melt inclusions with similar phase composition were previously found in the Lengai ijolite forsterite. However, in the case of forsterite silicate part of the inclusions is more essential [Sekisova et al., 2014].

Table 1. Chemical composition (EDS, wt.%) of some daughter phases from secondary silicate-salt inclusions in diopside.

	CaO	Na$_2$O	K$_2$O	MgO	MnO	FeO	P$_2$O$_5$	SO$_3$	Cl	F	SrO	BaO	SiO$_2$	Сумма
1	21.84	18.18	3.95	-	0.50	0.87	1.54	1.90	0.79	-	1.67	0.83	-	52.07
2	21.79	19.20	3.96	0.22	0.31	1.17	1.26	2.35	0.43	-	1.56	1.09	-	53.34
3	21.56	20.14	6.41	0.22	0.40	1.09	2.82	4.25	0.76	-	2.03	1.25	-	60.93
4	24.36	15.26	6.05	-	0.18	0.44	0.76	1.10	0.49	0.98	1.53	0.56	-	51.71
5	0.39	53.16	0.14	-	-	-	0.25	42.55	-	11.41	-	-	-	107.90
6	50.72	1.47	-	-	-	-	38.56	0.37	2.01	2.18	1.56	-	1.41	98.29

1 – 4 – nyerereite, 5 – kogarkoite, 6 – fluorapatite.

The study of secondary silicate-salt inclusions in diopside is evidenced that carbonate-salt (natrocarbonatite) portions of melt existed up to late stages of ijolite crystallization. Such melt inclusions in diopside were completely crystallized into fine-grained aggregate of carbonates, sulphates, halogenides and silicates with temperature decreasing.

References:

Dawson J.B. The geology of Oldoinyo Lengai // Bulletin of Volcanology. 1962. V 26. p. 349–387.

Dawson J.B., Smith J.V., Steele I.M. Petrology and mineral chemistry of plutonic igneous xenoliths from the carbonatite volcano, Oldoinyo Lengai, Tanzania // Journal of Petrology. 1995. V 36. p. 797-826.

Mitchell R.H. Mineralogy of stalactites formed by subaerial weathering of natrocarbonatite hornitos at Oldoinyo Lengai, Tanzania // Mineralogical Magazine. 2006. V 70. p. 437-444.

Sekisova V.S., Sharygin V.V., Zaitsev A.N. Carbonates in olivine-hosted inclusions from ijolite at Oldoinyo Lengai, Tanzania: microprobe data and Raman spectroscopy // ACROFI-V, Xi'an, China. 2014. CD abstract volume. Abstract 84.

Sekisova V.S., Sharygin V.V., Zaitsev A.N. Silicate-natrocarbonate immiscibility in ijolites at Oldoinyo Lengai, Tanzania: melt inclusion study // Goldschmidt – 2013 Conference Abstracts. Mineralogical Magazine. V 77(5). p. 2175.

Zaitsev A.N., Keller J., Spratt J., Jeffries T.E., Sharygin V.V. Chemical composition of nyerereite and gregoryite from natrocarbonatites of Oldoinyo Lengai volcano, Tanzania // Geology of Ore Deposits. 2009. V 51(7). p. 608-616.

Mid-Paleoproterozoic titaniferous Elet'ozersky complex of ultramafic-mafic-alkaline rocks in Northern Karelia (Russia) as transitional chamber of Fe-Ti-alkali basaltic magmatic system

Sharkov E.V.*, Shchiptsov V.V.**, Chistyakov A.V.*, Bogina M.M.*
*Institute Geology of Ore Deposits, Petrography, Mineralogy and Geochemistry RAS, Moscow'
** Institute of Geology, Karelian Scientific Center RAS, Petrozavodsk

The Elet'ozero complex in Northern Karelia is one of the largest (about 100 km^2) layered mafic-ultramafic intrusions with alkaline core, as the Gremyakha-Vermes Complex at the Kola Peninsula. These intrusive complexes belong to the Mid-Paleoproterozoic Jatulian-Ludicovian large igneous province in the eastern Fennoscandian Shield, which additionally contains alkali Fe-Ti basalts and tholeiitic basalts with variable Ti-content (Sharkov, Bogina, 2006). However, the tholeiitic basalts are predominant rocks, whereas alkaline volcanics were found only in the Kuetsjarvi Group, Pechenga structure (Kola Peninsusula).

The periphery of the Elet'ozrsky complex is mainly made up of fine-grained marginal gabbros, while prevailing inner portion (Layered Series) is represented by alternation of ferroclinopyroxenite, ferrogabbros (olivine gabbro, gabbro, gabbro-anorthosite, as well as orthoclase gabbro, phlogopite gabbro, etc) and their ore-bearing varieties (Bogachev et al., 1963; Kukharenko et al., 1969; Shchiptsov et al., 2007). All rocks of the layered series are variably enriched in Fe-Ti-oxides (magnetite, titanomagnetite and ilmenite), amounting up to 30-40 vol.% and more in ore varieties, averaging 10 vol.%. The core of the massif (about 10% of the area) consists of alkaline rocks: nepheline syenites and Ne-bearing syenites which cross-cut ferrogabbros. Carbonatite veins and diatreme with xenoliths of the massif's rocks also occur there. During the Svecofennian orogeny (1900-1800 Ma), the complex was unevemy deformed and metamorphosed under the amphibolites-facies conditions.

According to our data (Sharkov et al., 2015), the alkaline and mafic rocks of the complex contain two major types of zircon: oscillatory zoned magmatic zircon and porous zircon (hydrozircon) partly or completely developed after the former. Isotopic-geochronological data show that mafic and alkaline rocks were formed almost simultaneously, at about 2080±30 Ma (zircon U-Pb method, SHRIMP-II data); $\varepsilon_{Nd(2100)}$ = +3.4; the formation of hydrozircon was presumably related to the amphibolite metamorphism of the complex during Svecofennian orogeny.

Thus, the Elet'ozero Complex is the oldest manifestation of the intrusive high-Ti mafic-alkaline magmatism at the Karelian Craton. At the same time, there are no any volcanics of such composition and age in Karelia. On the other hand it was found that the Elet'ozero cumulates are close in REE pattern to the alkali basalts of the Kuetsjarvi Group, but strongly differ from tholeiitic volcanics of the Central Karelia (Fig. 1). However, their spidergrams are different, in particular, the Ti, Eu, and Ba contents in the cumulates are higher than those in lavas, and U, Th, Nb, Eu, Sr, lower.
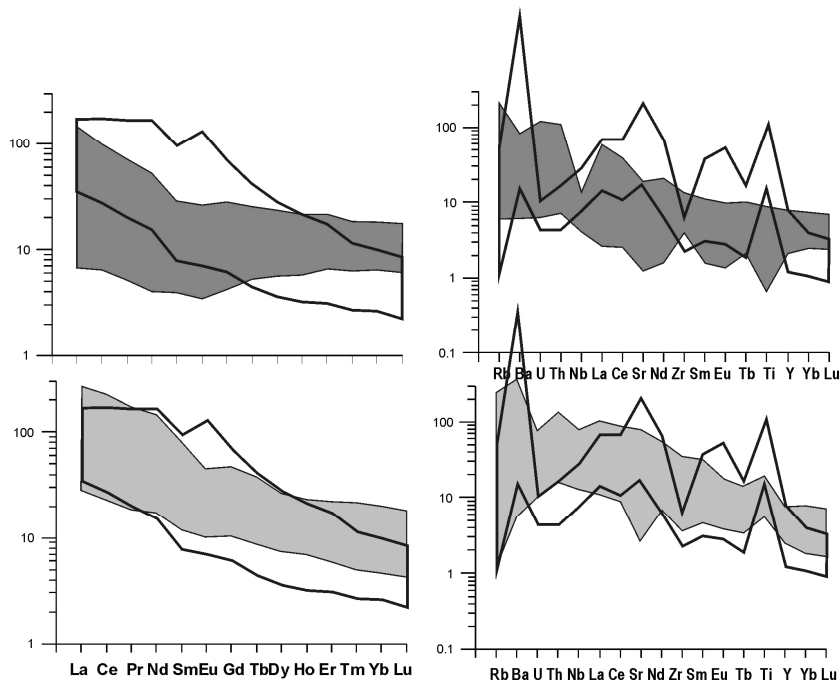
Fig. 1. Trace element patterns for the rocks of Elet'ozero complex (contour) as compared to those of tholeiitic volcanics from the Central Karelia (upper plots) and Fe-Ti alkali basalts of the Kuetsjarvi Group (Pechenga structure, Kola Peninsula, lower plots).

These differences are presumably related to the retention of some components in transitional chamber in cumulates and transportation of others to the surface with lavas. For example, cumulates are often enriched in Ba, Sr, and Eu, as well as Nb and Ta, which led to the depletion of lavas in these components; at the same time cumulates are depleted in U, Th, Nb, and REE, which led to the enrichment of lavas in these elements. So, it is highly probable that the Elet'ozero complex and Fe-Ti alkali were derived from a common source, representing, correspondingly, a transitional magma chamber and volcanic counterpart of a single magmatic system.
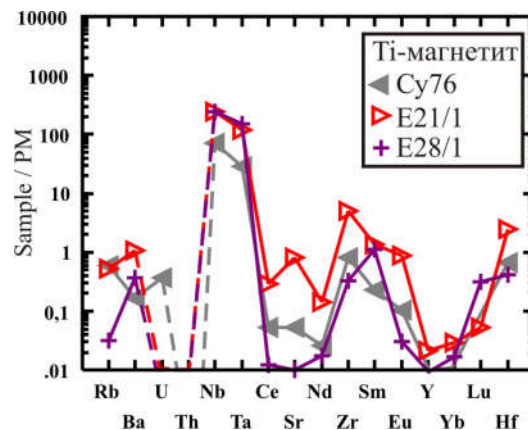
Fig.2. Trace-element distribution patterns of Ti-Mt from the Elet'ozero's ferrogabbros.

The Elet'ozero complex is an important source of Fe-Ti-oxide ores. The analysis of these oxides showed that they are enriched in Nb and Ta (Fig. 2) and may be also considered as Nb-Ta ores. Besides, independent rare-metal and REE mineralization was found in the veins of alkaline pegmatites, associated with Fe-Ti-oxide ores.

108

References

Bogachev, A.I., Zak, S.I, Safronova, G.P., and Inina, K.A., Geology and petrology of the Elet'ozero gabbroid massif of Karelia // Moscow—Leningrad: AN SSSR, 1963. 158 P.

Kukharenko, A.A., Orlova, M.P., and Bagdasarov, E.A., Alkaline gabbroids of Karelia. Elet'ozero Massif - petrology, mineralogy, and geochemistry) // Leningrad: Izd-vo LGU, 1969. 183 P.

Shchiptsov, V.V., Bubnova, T.P., Garanzha, A.V., et al., Geological--technological and economic assessment of resource potential of the carbonatites of the Tiksheozero Massif: formation of ultramafic--alkaline rocks and carbonatites // Geol. Polezn. Iskop. Karelii. 2007. Vol. 10. PP. 159-170.

Sharkov, E.V. and Bogina, M.M. Evolution of the Paleoproterozoic magmatism: geology, geochemistry, and isotopic constraints // Stratigraphy and Geological Correlations, 2006. Vol. 14. N 4. P. 345-367

Sharkov, E.V., Belyatsky, B.V. Bogina, M.M. Chistyakov, A.V., Shchiptsov, V.V., Antonov, A.V. Lepekhina, E.N. Genesis and age of zrrcon from alkali and mafic rocks of the Elet'ozero Complex, North Karelia // Petrology. 2015. № 3 (in press).

Silicate-carbonate liquid immiscibility in melilitolite from Pian di Celle volcano (Umbria, Italy)

Sharygin V.V.

V.S. Sobolev Institute of Geology and Mineralogy SB RAS, Novosibirsk, Russia, sharygin@igm.nsc.ru

Melilitolites represent the final event in the activity of the late Pleistocene Pian di Celle tuff ring and lava flow volcano (Stoppa, 1996). They form a 1-m-thick sill and dykelet swarm in the NE flow-front of the Le Selvarelle venanzite lava. The rocks contain phenocrystal melilite (up to 5 cm), olivine, leucite, phlogopite and Ti-magnetite as essential minerals that resemble in moda to fine-grained groundmass of the country venanzites. The fine-grained groundmass consists of Ti-magnetite, fluorapatite, fluorophlogopite, nepheline, kalsilite, clinopyroxene, Zr-cuspidine, götzenite, umbrianite, khibinskite, Co-Ni-rich westerveldite, sulphides (pyrrhotite, bartonite-chlorobartonite, galena), Fe-monticellite - Mg-kirschsteinite, ilmenite, Na-rich pyroxene and amphibole (Zr-bearing aegirine, arfvedsonite), bario-olgite, bafertisite, and brown or green glass (Sharygin et al. 1996; 2013; Stoppa et al. 1997; Sharygin, 2012). Numerous irregular vugs (up to 3 cm) with well-faceted crystals of the above minerals are observed in this rock. The glassy blebs sometimes occur on the surface of crystals in the vugs. The groundmass glass commonly contains Ca-rich carbonate ocelli with high Sr, Ba and REE (Stoppa, Woolley, 1997) or carbonate-fluorite globules. In addition the presence of carbonate globules is fixed in mineral-hosted inclusions (see Figure 1).

Melt inclusions (5-70 μm) have been identified in both phenocrystal and groundmass minerals of the Pian di Celle melilitolite (Sharygin et al., 1996; Stoppa et al., 1997; Sharygin, 1999, 2001). In phenocrysts (melilite, olivine, leucite), the silicate-melt inclusions are mainly localized in the outer zones, whereas, in the groundmass minerals (nepheline, kalsilite, fluorapatite and others), they are situated in the central zones. Their phase composition is green glass + shrinkage fluid bubble ± carbonate globule ± trapped/daughter crystals. Carbonate globule ($CaCO_3$ or $CaCO_3+CaF_2$) was identified in melt inclusions from all melilitolite minerals, but it is clearly fixed in olivine-, melilite- and kalsilite-hosted inclusions (see Figure 1).
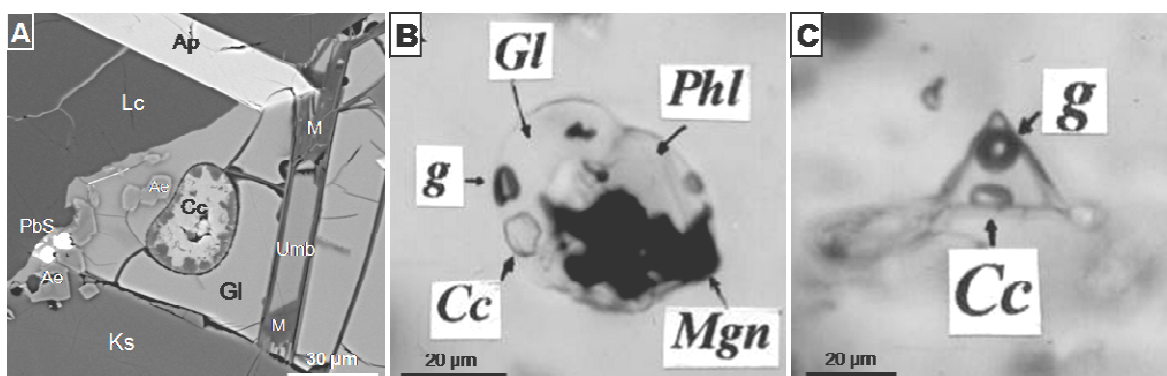
Figure 1. Calcite-fluorite globule in groundmass glass (**A**, BSE image) and silicate-melt inclusions with carbonate globule in the outer zones of melilite (**B**, ordinary light) and olivine (**C**, ordinary light) from the Pian di Celle melilitolite. Symbols: Lc - leucite; Ks – kalsilite; Umb – umbrianite; M – macdonaldite ?; Ap – fluorapatite; Ae – aegirine; Gl – glass; Phl – fluorophlogopite; Mgn - Ti-magnetite; Cc - carbonate or carbonate-CaF_2 globule; g - low-density fluid bubble.

Homogenization temperatures of inclusions are higher than 1000°C in phenocrysts and 830-870°C in groundmass kalsilite, nepheline and cuspidine (Stoppa et al., 1997; Sharygin, 1999, 2001). The heating experiments with melilite- and kalsilite-hosted inclusions have shown the following main events: melting of silicate glass occurred at 560-620°C; carbonate globule began fusing at 600-650°C; sulphides, westerveldite and one of colourless phases (umbrianite ?) melt at 730-800°C. In melilite-hosted inclusions, the colourless phases (cuspidine, kalsilite, nepheline) disappear at 850-900°C, melting of phlogopite occurs at 950-1050°C (Stoppa et al., 1997; Sharygin, 1999, 2001) and over 900°C additional carbonatitic liquid droplets separate immiscibly from silicate liquid and clinopyroxene crystals appear inside inclusions. Thus, the existence of carbonate-silicate liquid immiscibility observed in the melilitolite minerals has been fixed in the 670-1000°C range.

Recent geological and petrological data for the Pian di Celle volcano (Stoppa, 1996; Stoppa et al., 1997; Stoppa, Cundari, 1998) show that initial melilitolite melt represents a residual venanzite liquid enriched in volatiles (mainly in CO_2, F, Cl) and trace elements (REE, Nb, Zr, Ba, Sr, B, Li, Be). In general, the evolution of the initial melilitolite melt had a phonolitic peralkaline character and was directed towards gradual increase of SiO_2, FeO_t, alkalis, light elements (B, Be, Li), Ba, S, F, Cl, possibly H_2O, and decrease of Al_2O_3, MgO, CaO (Sharygin, 1999, 2001). Crystallization of early minerals, separation of carbonatite liquid and possible CO_2 degassing seem to be responsible for the accumulation of trace elements and volatile components in residual peralkaline melts with (K+Na)/Al>5. These factors stimulated the decrease of solidus temperature of the melt (down to 500-600°C) and resulted in formation of specific phases (umbrianite, westerveldite, bartonite-chlorobartonite, bario-olgite, bafertisite, etc.) during the latest stage. However, crystallization of Ca-rich silicates (melilite, Zr-cuspidine, götzenite, clinopyroxene) probably prevented abundant separation of carbonatitic liquid at high temperatures. The modal abundance of carbonate globule in silicate-melt inclusions suggests that widespread separation of carbonatite occurred at lower temperatures after crystallization of kalsilite (approximately at 800°C). In addition to inclusions the extraction of carbonatite liquid and CO_2 degassing in the Pian di Celle melilitolite are also based on some mineralogical data: the appearance of rim of Fe-monticellite - Mg-kirschsteinite around olivine; the existence of westerveldite instead of arsenopyrite; the presence of K-sulfides.

It should be mentioned that mechanism of separation of carbonate-salt liquid from silicate melt for the Pian di Celle melilitolites is very similar to that for other peralkaline volcanic rocks, in particular for nephelinites of the Gregory Rift, Tanzania (Sharygin et al., 2012; Zaitsev et al., 2012 and other works).

References:

Sharygin V.V. Boron-rich glasses in melilitolite from Pian di Celle, Umbria, Italy // Terra Nostra. 1999. No. 6. P. 268-270.

Sharygin V.V. Silicate-carbonate liquid immiscibility in melt inclusions from melilitolite minerals: the Pian di Celle volcano (Umbria, Italy) // Memórias. 2001. No. 7. P. 399-402.

Sharygin V.V. Magnesian kirschsteinite in melilitolites of the Pian di Celle volcano, Umbria, Italy // in Abstracts of 29th International conference ''Ore potential of alkaline, kimberlite and carbonatite magmatism'', School ''Alkaline magmatism of the Earth'', Sudak-Moscow. 2012. P.154–155.

Sharygin V.V., Kamenetsky V.S., Zaitsev A.N., Kamenetsky M.B. Silicate-natrocarbonatite liquid immiscibility in 1917 eruption combeite-wollastonite nephelinite, Oldoinyo Lengai volcano, Tanzania: melt inclusion study // Lithos. 2012. V. 152. P. 23-39.

Sharygin V.V., Pekov I.V., Zubkova N.V., Khomyakov A.P., Stoppa F., Pushcharovsky D.Y. Umbrianite, $K_7Na_2Ca_2[Al_3Si_{10}O_{29}]F_2Cl_2$, a new mineral species from melilitolite of the Pian di Celle volcano, Umbria, Italy // European Journal of Mineralogy. 2013. V. 25. P. 655-669.

Sharygin V.V., Stoppa F., Kolesov B.A. Zr-Ti-disilicates from the Pian di Celle volcano, Umbria, Italy // European Journal of Mineralogy. 1996. V. 8. P. 1199-1212.

Stoppa F. The San-Venanzo maar and tuff ring, Umbria, Italy: eruptive behaviour of a carbonatite-melilitite volcano // Bulletin of Volcanology. 1996. V. 57. P. 563-577.

Stoppa F., Cundari A. Origin and multiple crystallization of the kamafugite-carbonatite association: the SanVenanzo - Pian di Celle occurrence (Umbria, Italy) // Mineralogical Magazine. 1998. V. 62. P. 273-289.

Stoppa F., Sharygin V.V., Cundari A. New mineral data from the kamafugite-carbonatite association: the melilitolite from Pian di Celle, Italy // Mineralogy and Petrology. 1997. V. 61. P. 27-45.

Stoppa F., Woolley A.R. Italian carbonatites: field occurrence, petrology and regional significance // Mineralogy and Petrology. 1997. V. 59. P. 43-67.

Zaitsev A.N., Marks M.A.W., Wenzel T., Spratt J., Sharygin V.V., Strekopytov S., Markl G. Mineralogy, geochemistry and petrology of the phonolitic to nephelinitic Sadiman volcano, Crater Highlands, Tanzania // Lithos. 2012. V. 152. P. 66-83.

Delhayelite-group minerals from Sadiman nephelinite (Tanzania) and Saghro phonolite (SE Morocco)

Sharygin V.V.*, Zaitsev A.N.**, Berger J.***
*V.S. Sobolev Institute of Geology and Mineralogy SB RAS, Novosibirsk, Russia, sharygin@igm.nsc.ru
**Saint Petersburg State University, Saint Petersburg, Russia
***Université de Toulouse, Toulouse, France

Double-layered (delhayelite) and triple-layered (umbrianite) alkali-halogen-rich silicates are sometimes formed in young K-rich peralkaline volcanic and subvolcanic rocks and in large peralkaline plutonic complexes (Khibiny). They commonly occur as late-magmatic groundmass minerals (Sahama, Hytönen, 1959; Pekov et al., 2009; Andersen et al., 2014; Sharygin et al., 2012; 2013). However, some volcanic rocks may also contain other minerals, which can be structurally related to delhayelite or umbrianite. The phases close to $KNa_2Ca_2[AlSi_7O_{17}(OH)_2]F(Cl,OH)$ were recently described in K-rich peralkaline rocks in Morocco and Tanzania (Berger et al., 2009; Zaitsev et al., 2012) and seem to be intermediate between delhayelite and hydrodelhayelite. Our short communication is devoted to a more chemical and structural information about these minerals from Morocco and Tanzania.

At the Sadiman volcano, Tanzania, a delhayelite-group mineral was found as a principal groundmass phase in sanidine-poor nephelinite (II type, Zaitsev et al., 2012). It seems to be a primary phase within the groundmass and also occurs as a daughter phase of primary completely crystallized inclusions in nepheline phenocrysts. It is closely associated with aegirine (or aegirine-augite) and potassic arfvedsonite (Fig. 1). Other minerals in groundmass and inclusions are presented by wollastonite, sanidine, nepheline, sodalite, götzenite, canasite, sulfides (pyrite, pyrrhotite, djerfisherite), lamprophyllite, fluorapatite, titanite, pectolite, Ba-Sr-phospates and zeolites.

Sanidine-rich lava-flow phonolite (sample BAG-2) from Sahgro, SE Morocco, contains small grains of a delhayelite-group mineral (Berger et al., 2009). It is related to groundmass association also consisting of sanidine, aegirine-augite, nepheline, fluorapatite, REE-rich götzenite-hainite, titanite, eudialyte and its Ti-analogue, pyrite, pyrrhotite, cancrinite (?), lorenzenite and zeolites. The relations of mineral in the groundmass have shown that delhayelite-like phase is a later mineral and commonly contain inclusions of other minerals (Fig. 1).
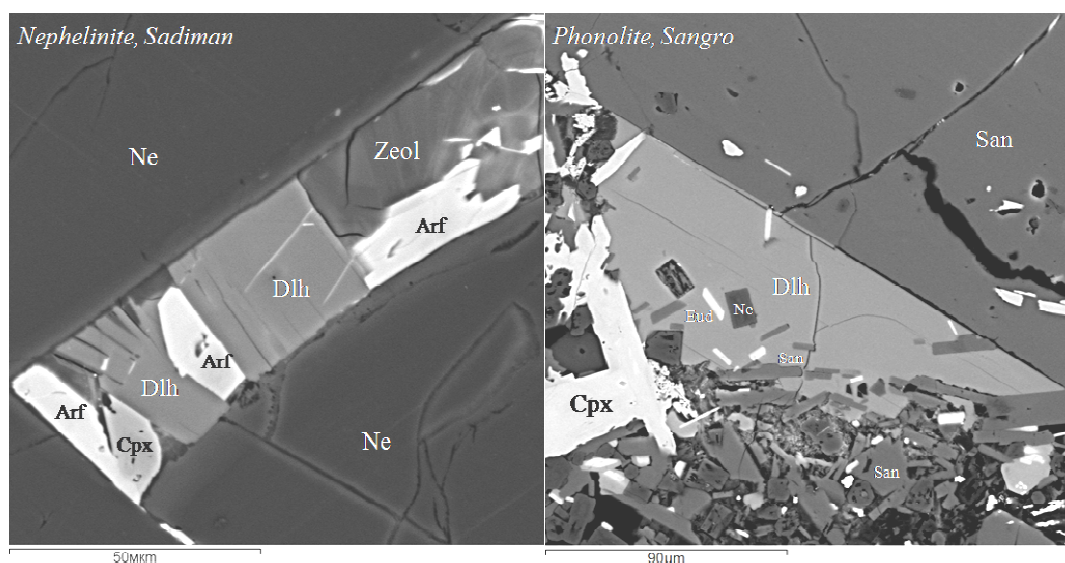
Figure 1. Delhayelite-group minerals in groundmass of peralkaline rocks from Tanzania and Morocco (BSE images).
Dlh – delhayelite-group mineral; Ne – nepheline; Arf – potassic arfvedsonite; Cpx – aegirine-augite; Zeol – zeolite (former glass ?); San – sanidine; Eud – eudialyte.

In chemical composition both delhayelite-like minerals drastically differ from delhayelite in lower K_2O, F and Cl and higher CaO, Na_2O and SiO_2 (Table 1). In general, the Sadiman mineral is compositionally similar to the Sahgro sample, but contains lower alkalis and higher CaO, H_2O and Fe_2O_3. Of course, chemical data do not give any severe grounds to relate these minerals to delhaylite- (double-layer) or umbrianite- (triple-layer) structural type of Si-Al tetrahedral blocks. However, the HRTEM data for the Sadiman sample have shown that *b* parameter is ≈ 24.1 Å (Sharygin et al., 2013) what is very close to that of delhayelite (Pekov et al., 2009). In addition the Raman spectra for the Khibiny delhayelite and the Sadiman mineral (Fig. 2) show the identity in the

200-1200 cm^{-1} region (vibration modes in tetrahedral and octahedral sites) differing only in band suite for the 2500-4000 cm^{-1} region (vibration modes for OH-group and H$_2$O). Assuming the data above, the formulae for the Sadiman and Sahgro minerals may be written as delhayelite-based [AlSi$_7$O$_{19}$]: K$_{1.20}$Na$_{1.98}$Ca$_{2.30}$[Fe$^{3+}_{0.10}$Al$_{0.90}$Si$_{7.00}$O$_{18.0}$(OH)$_{1.0}$]F$_{1.09}$Cl$_{0.43}$(OH)$_{0.31}$S$_{0.02}$ and
K$_{1.37}$Na$_{2.21}$Ca$_{2.17}$[Fe$^{3+}_{0.03}$Al$_{0.92}$Si$_{7.05}$O$_{18.5}$(OH)$_{0.5}$]F$_{1.09}$Cl$_{0.46}$(OH)$_{0.38}$S$_{0.02}$.

Table 1. Chemical composition (EMPA+SIMS, wt.%) of delhayelite-group minerals from Tanzania (**1**) and Morocco (**2**) and delhayelite from Khibiny (**3**).

	1	**2**	**3**		**1**	**2**	**3**
Sample	Sd-11	BAG-2	Khib		Sd-11	BAG-2	Khib
n	*11*	*14*			*Formula based on (Si+Al+Fe^{3+})=8*		
SiO$_2$	54.72	55.05	47.12	Si	7.00	7.05	6.91
TiO$_2$	0.03	0.04	0.04	Al	0.90	0.92	1.06
B$_2$O$_3$ SIMS	0.001	0.006	0.04	Fe^{3+}	0.10	0.03	0.02
Al$_2$O$_3$	5.95	6.09	6.14	B	0.000	0.000	0.01
Fe$_2$O$_3$	1.00	0.31	0.17	Be	0.000	0.000	
MnO	0.08	0.17	0.13	*Sum T*	*8.00*	*8.00*	*8.00*
MgO	0.06	0.00	0.04	Ti	0.003	0.004	0.005
CaO	16.75	15.81	13.44	Mn	0.01	0.02	0.02
BaO	0.17	0.02	0.01	Mg	0.01	0.001	0.01
SrO	0.52	0.67	0.28	Ca	2.30	2.17	2.11
Na$_2$O	7.96	8.91	6.84	Sr	0.04	0.05	0.02
K$_2$O	7.37	8.38	19.91	Ba	0.01	0.001	0.000
Rb$_2$O SIMS		0.014	0.27	Na	1.98	2.21	1.95
Li$_2$O SIMS	0.07	0.15	0.000	K	1.20	1.37	3.73
BeO SIMS	0.007	0.008		Rb		0.001	0.025
F	2.69	2.68	4.38	Li	0.003	0.007	0.000
Cl	1.98	2.11	3.78	*Sum K*	*5.55*	*5.84*	*7.86*
S	0.08	0.08	0.16	*Sum cat*	*13.55*	*13.84*	*13.86*
H$_2$O SIMS	1.53	1.04	0.86	F	1.09	1.09	2.03
Sum	100.96	101.54	103.60	Cl	0.43	0.46	0.94
O=F,Cl,S	1.62	1.65	2.70	S	0.02	0.02	0.04
Sum	99.35	99.90	100.83	H$^+$	1.31	0.88	0.84

Data for delhayelite-like phases are given for grains shown in Figure 1. Composition of the Khibiny delhayelite is quoted from Sharygin et al. (2013).
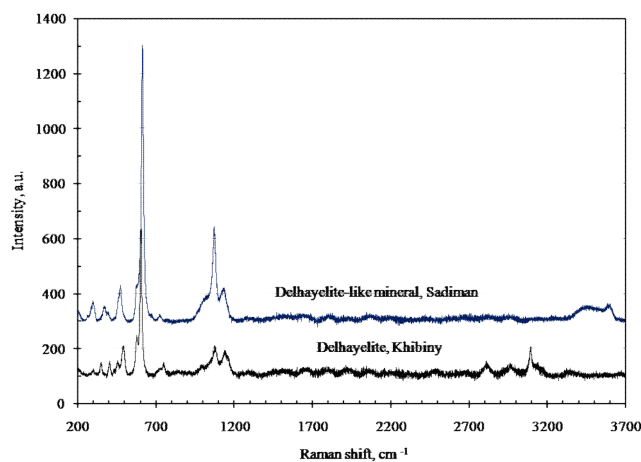
Figure 2. Raman spectra for delhayelite-group mineral from Tanzania and delhayelite from Khibiny.

Delhayelite, K$_4$Na$_2$Ca$_2$[AlSi$_7$O$_{19}$]F$_2$Cl, is very unstable in post-magmatic aqueous solutions, especially under weakly alkaline conditions, and alters to fivegite, K$_4$Ca$_2$[AlSi$_7$O$_{17}$(O$_{2-x}$OH$_x$)][(H$_2$O)$_{2-x}$OH$_x$]Cl, and further to hydrodelhayelite, KCa$_2$[AlSi$_7$O$_{17}$(OH)$_2$]•(6-x)H$_2$O, which is accompanied by leaching of alkali cations and halogen anions and hydration. In the course of these transformations, the CaAlSiO motif remains stable (Pekov et al., 2011). In summary, the mineral from Sadiman and Sahgro with generalized formula K$_2$Na$_2$Ca$_2$[AlSi$_7$O$_{18}$(OH)]F(Cl,OH) is a new potential mineral species, which is intermediate between delhayelite and hydrodelhayelite. This mineral may be crystallized directly from a silicate melt slightly rich in H$_2$O like nephelinite or phonolite peralkaline melt.

112

References:

Andersen T., Elburg M.A., Erambert M. Extreme peralkalinity in delhayelite- and andremeyerite-bearing nephelinite from Nyiragongo volcano, East African Rift // Lithos. 2014. V. 206. P. 164-178.

Berger J., Ennih N., Mercier J.-C.C., Liégeois J.-P., Demaiffe D. The role of fractional crystallization and late-stage peralkaline melt segregation in the mineralogical evolution of Cenozoic nephelinites/phonolites from Saghro (SE Morocco) // Mineralogical Magazine. 2009. V. 73. P. 59-82.

Pekov I.V., Zubkova N.V., Chukanov N.V., Sharygin V.V., Pushcharovsky D.Y. Crystal chemistry of delhayelite and hydrodelhayelite // Doklady of Earth Sciences. 2009. V. 428. P. 1216-1211.

Pekov I.V., Zubkova N.V., Chukanov N.V., Zadov A.E., Pushcharovsky D.Y. Fivegite, $K_4Ca_2[AlSi_7O_{17}(O_{2-x}OH_x)]$ $[(H_2O)_{2-x}OH_x]Cl$: a new mineral from the Khibiny alkaline complex, Kola Peninsula, Russia // Geology of Ore Deposits. 2011. V. 53(7). P. 591-603.

Sahama T.G., Hytönen K. Delhayelite, a new silicate from the Belgian Congo // Mineralogical Magazine. 1959. V. 32. P. 6-9.

Sharygin V.V., Kamenetsky V.S., Zaitsev A.N., Kamenetsky M.B. Silicate-natrocarbonatite liquid immiscibility in 1917 eruption combeite-wollastonite nephelinite, Oldoinyo Lengai volcano, Tanzania: melt inclusion study // Lithos. 2012. V. 152. P. 23-39.

Sharygin V.V., Pekov I.V., Zubkova N.V., Khomyakov A.P., Stoppa F., Pushcharovsky D.Y. Umbrianite, $K_7Na_2Ca_2[Al_3Si_{10}O_{29}]F_2Cl_2$, a new mineral species from melilitolite of the Pian di Celle volcano, Umbria, Italy // European Journal of Mineralogy. 2013. V. 25. P. 655-669.

Zaitsev A.N., Marks M.A.W., Wenzel T., Spratt J., Sharygin V.V., Strekopytov S., Markl G. Mineralogy, geochemistry and petrology of the phonolitic to nephelinitic Sadiman volcano, Crater Highlands, Tanzania // Lithos. 2012. V. 152. P. 66-83.

Ore depositions in connection with the Phanerozoic alkaline magmatism of East Azov region (Ukrainian shield)

Sheremet E.M.

M.P. Semenenko Institute of geochemistry, mineralogy and ore formation of the National Academy of sciences of Ukraine, Kiev

EvgSheremet@yandex.ru

Alkaline-ultrabasic-alkaline basaltoids of Devonian formation developed at the junction of the folded Donbas with Priazovsky crystalline massif. It includes the following series of rocks presumably from the older to the younger: 1. Alkaline-ultrabasic: wehrlites, pyroxenites, ore pyroxenites, gabbro-pyroxenites and gabbro composing shtoko shaped intrusion. Vein analogues of these rocks are monchikites, avgitites, camptonites, odinites, plagioclasites. 2. Alkaline basalts presented of limburgites, avgititites, picrite-basalts, alkaline basalts, and pseudo- epileucitic basaltoids, trachytes (ortophyres). 3. Alkaline rocks: nepheline syenite, malignites and syngenetic them subvolcanic fonolitoid rocks. 4. Explosive rocks (kimberlite pipes).

With alkaline-ultrabasic series of rocks associated Pokrovo-Kireevsky vanadium containing ilmenite-titanium-magnetite deposit. Ore bearing are basic-ultrabasites of Pryazovsky complex composing three tectonically separate massifs – Kumachevsky, Central and Northern. Thickness of ore bodies within the massifs ranges from 100 to 600 m. Ore bodies are small and medium disseminated, finely schlieren. The basic mass of titanomagnetite and ilmenite is in the intergranular spaces ferruginous silicates. The ores are represented by squalid differences (TiO_2 - up to 5 %) and poor (TiO_2 up to 5-7 %), to medium (7-10 % TiO_2) and less rich (over 10 % TiO_2). There is an alternation of the rich, middle and poor ore deposits in within the ore-bearing ultrabasite-basite rocks.

East Azov Region to the wide dissemination of fluorine in igneous rocks is fluorine metallogenic region. In the Phanerozoic stands out: a) the group of late Caledonian-early Hercynian fluorite formations associated with Devonian alkaline-ultrabasic-alkaline-basaltic complex; b) the group of late Paleozoic-early Mesozoic associated with post Carbon activation of tectono-magmatic activity (it is the intercession Pokrovo-Kireevsky deposit of fluorite). The source of fluorine was mostly rocks of Devonian magmatic complex, especially his later differentiates from which fluorine was leached fluids. About 50 % of total content of fluorine in the Devonian rocks associated with calcium rinkite attributed by analogy with the known array of alkaline rocks (Kolsky peninsula) to the formations of late-magmatic stage. Occurences of fluorite known in the East Azov Region, fall into two main formations – carbonate-fluorite and quartz-fluorite, each of which are allocated separate rare subtypes. Pokrovo-Kireevsky deposit refers to the type of dissent metasomatic deposits encountered in carbonate rocks near low-amplitude thrust. The deposit is formed at shallow depths (probably no more than 1,5 km from the surface).

Gold occurrences are located in the lower Carboniferous thicker of Carbon. The main ore-controlling structure is a tectonic melange. There are two types of gold mineralization – endogenous, associated with hydrothermal-metasomatic processes and exogenous, associated with karst formation. Gold-bearing rocks are jasperoides, argilizites, sulfidized and dolomitized terrigenous-carbonate formation, silicified marls and limestones. Found native gold mercuriferous and cupriferous species. In addition to gold mineralization encountered silver-polymetallic and molybdenum manifestations.

Rare earth mineralization is widespread in the zone of articulation of the Donbas fold with Priazovsky crystalline massif and is localized within the melange lower Carboniferous strata of carbonate rocks. Highlighted promising areas – Zhogolevskaya, Stylskaya, Dalnaya, Vostochnaya, Dokuchaevskaya, Novotroitskaya. There is developed the body of pyroxenites and gabbro-pyroxenites lower Devonian, volcanogenic and volcanogenic-sedimentary formations Antonovskaya formation of the upper Devonian, sediments Razdolnenskaya formation of the upper Devonian, terrigenous-sedimentary deposits of the Lower Carboniferous. The most investigated Zhogolevskoe occurence. In it the ore-bearing rocks are argillisites – clay rocks, developed in the form of bodies of irregular shape with sharp geological boundaries. Ore manifestation is classified as ionic genetic group yttrium-rare earth formations in alumosilicate rocks. The average content of trioxide of rare earths in argillite is 0,144 % at maximum contents to 1,03 %. The content of rare earth elements of the cerium group is 66,77 % and yttrium group – 33,23 %.

Polymetallic ore mineralization within the square Kalmius of East Azov Region refers to veinlet-disseminated type. Ore-metasomatic zones are controlled by zones of feldspathization, silicification, argillization, muscovitization, pyritization and metasomatic magnetitization, probably, associated with subvolcanic bodies trachyte-trachyandesite and liparite formation of Paleozoic age. Identified molybdenum ore (Novoselovsky, Kalanovsky areas) lead (Kichiksu), tungsten (Verbov area), molybdenum and tungsten (Kirillovsky area).

Diamond and nondiamondiferous kimberlites (pipes "Nadia", "Yuzhnaja", "Novolaspinskaya", dike "Novolaspinskaya" and dike rocks comagmatic the kimberlite rocks) are located in the northern part of the East Azov subblock **Ukrainian Shield (USh)**, in the area of dynamic influence on the Dnieper-Donetsk aulacogen on the Azov megablock. Pipe "Petrovckaya" and kimberlitic occurence of "Gorniatskoe", are located in the junction zone of the Donbas with Azov crystalline massif in the field development of Devonian volcanogenic-sedimentary rocks.

Considered Phanerozoic magmatism and related occurences of minerals in the Azov megablock due to the onset of tensile stresses in a collision at the end of the Carboniferous Epipaleozoic West Siberian platform with Russian platform. At the junction of the Azov megablock with Dnieper-Donetsk depression formed faults stretching are the natural channels out of deep magma Devonian alkaline-ultrabasic-alkaline basaltic and kimberlite compositions on the surface of the Earth. They were followed by the arrival of magmatic deep fluids that formed during the processes of tectogenesis in the host rock occurrences and deposits of a range of different ore minerals.

On the origin of high potassium magmas in subduction zones
Simakin A.G.*, Salova T.P.*
* IEM RAS, Chernogolovka, Russia
simakin@iem.ac.ru

Typical magmas of subduction zones have normal alkalinity and sodium specification (Na/K>1). Their origin is connected with water fluid released at the dehydration of the descending oceanic slab. In some occasions the potassic subalkaline or alkaline magmas appear at the active continental margins. Decade and half ago no clear source of such magmas was proposed (Price et al., 1999). Recently role of CO_2 in the potassic magmas formation is becoming accepted (Gupta, 2015).

We perform experiments that directly demonstrate process of the potassic melt assembling on the olivine-Spl matrix from the components transported by the dry reduced CO_2 fluid from the basaltic source at the crustal pressures 2-5 Kbar and T=900-1000°C. Novel technique was applied. Carbonic fluid was generated during experiment by the decomposition of the $(Fe,Mg)CO_3$ according to the reactions: $FeCO_3=Fe_3O_4+CO+CO_2$ $MgCO_3=MgO+CO_2$

Natural siderite was placed into the small open capsule while source material (spilitized basalt) was placed into the main capsule hosting small one. Natural siderite aggregate contains quartz and feldspar grains. In the experiment these grains become the centers of the melting. Fluid transfer dissolved components from source basalt towards oxide matrix. As a result of this transfer olivines and spinels (predominantly $MgFe_2O_4$) form. Melt domains expand by consuming first of all K_2O and Al_2O_3 from the dry reduced carbonic fluid. Compositions of all

components of the studied system are characterized by ICP-MS (siderite), XRF (basalt) and SIMS (experimental products).
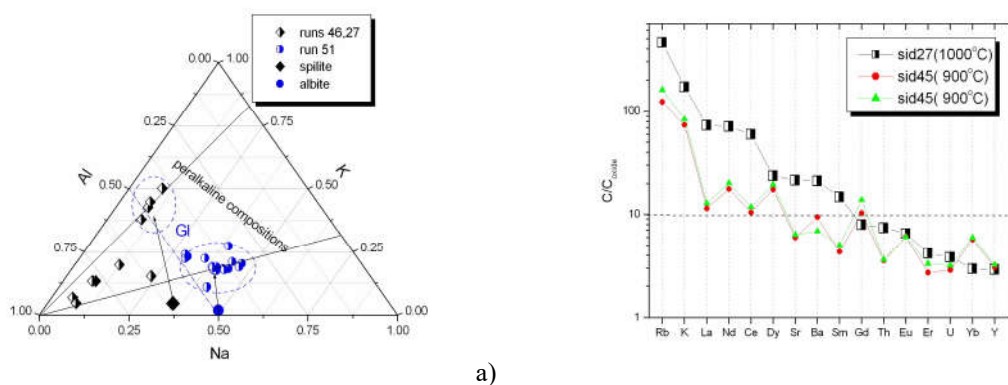
Fig. 1. Composition of the fluid modified oxide matrix a) potassium enrichment relative albite and basalt sources b) composition of the glass + crystals mixture with SIMS normalized on the initial oxides matrix composition.

Experiments with basalt and albite sources demonstrate that melt formed in the oxide matrix has K/Na ratio that is 25-28 time higher than in the source basalt. Fluid mediated melt has rather high Rb, LREE contents. Ba, Sr, Yb enrichments relative source are moderate. Ti shows the least mobility among studied elements. Since HFSE (Zr, Hf) contents in the spilite appears to be below high determination limit for of ICP-MS method source of these elements in the matrix melt is unclear. Level of Zr content (no more than 50-60 ppm) is substantially lower than usually registered in the high-K basalts (200-350 ppm). We explain this fact by the involvement of fluorine in the HFSE transport. As shown by the results of our thermodynamic modeling and petrologic data reduced carbonic fluid would accumulate fluorine from the melt.

Gupta (2015) declared universal connection of the high potassic low silica magmas with contamination of the mantle with crustal carbon. At the routine smooth subduction only small fraction of the sediments is transported with descending slab. Large fraction of carbon sinks into the lower mantle due to slab heating slower than pressurization that keeps carbonates stable. At the same time continent arc collision and accretion events creates dynamic irregularities that greatly enhance mantle contamination with the crustal material. In the numerical study (Simakin, 2014) it was shown that temporary reversal of the subduction direction can create and push large pieces of the continental of island crust under the mantle wedge.

Fig. 2. Break of the accreted terrain edge during subduction restarting (to the right island, to the left oceanic plate), numerical modeling from (Simakin, 2014). Results of the analogous modeling from (Boutelier and Chemenda, 2011) are in the inset.

We anticipate that Kronotsky paleo-arc accretion to Kamchatka 5-10 Mys ago put carbonates and organic material (coal) under mantle wedge. Several kilometers blocks of carbonaceous and siliceous rocks in the mantle are gravitationaly unstable and have extremely low relative viscosity that empowers their pluming and dyking propagation upwards. For the mechanical failure at the zone of collision it is essential that locking of subduction is local and slab continues to descend aside. Alkaline melts produced in the carbonatized mantle under Klyuchevskaya group of volcanoes can contribute to the basalts erupted in Tolbachik 2012-2013 voluminous fissure eruption. In the described by Pirce et al.(1999) case with high-K volcanism in North Island (New Zealand) direction of subduction is reversed along the New Zealand Plate Boundary. Pacific plate subduction propagates westwards and delamination of Australian crust is anticipated (Furlong, 2015) similar to N.Kamchatka case.

References:

Boutelier, D. and Chemenda, A. Physical Modeling of Arc - Continent Collision: A Review of 2D, 3D, Purely Mechanical and Thermo-Mechanical Experimental Models // In D.Brown and P.D. Ryan (Eds.), Arc-Continent Collision, Frontiers in Earth Sciences. 2011.

Gupta, A.K. Origin of Potassium-rich Silica-deficient Igneous Rocks. Springer, India. 2015. 536 P.

de Hoog, J.C.M. and van Bergen M.J.. Volatile induced transport of HFSE, REE, Th and U in arc magmas: evidence from zirconolite-bearing vesicles in potassic lavas of Lewotollo volcano (Indonesia) // Contrib.Mineral.Petrol. 2000. 139. 485-502.

Price, R.C., R.B. Stewart, J.D. Woodhead and Smith, I.E.M. Petrogenesis of High-K Arc Magmas:Evidence from Egmont Volcano, North Island, New Zealand// J.Petrology. 1999. 40. 1. Pages. 167–197.

Simakin, A.G. Numerical modelling of the late stage of subduction zone transference after an accretion event // Terra Nova. 2014. 26. 1. 26-28.

REE mineralogy of the Lofdal carbonatite, Namibia

Sitnikova M.A.*, DoCabo V.N.**, Wall F.***, Graupner T.*
*BGR, Hannover, Germany
**Namibian Geological Survey, Windhoek, Namibia
***Camborne Scholl of Mines, University of Exeter, UK
maria.sitnikova@bgr.de

The Lofdal Alkaline Carbonatite Complex, which is located 36 km northwest of Khorixas in Damaraland, Kunene Region, Namibia, occupies an area of about 24 km^2. The complex is composed of nepheline syenites, carbonatite plugs and dykes, phonolite dykes and breccias associated with the intrusions. Some mafic dykes also occur, including one possible lamprophyre. Although exposed within pre-Damara basement and lacking any contact with Damara rocks, the Lofdal intrusion belongs to an early magmatic event and is pre-orogenic related to an intra-continental rift environment (Miller, 1983).

The carbonatite forms at least three central plug-like bodies composed of coarse-grained calcite carbonatite (sövite) with scattered concentrations of apatite, magnetite and pyrite. The carbonatite often gives an anomalous radiometric response due to its elevated thorium contents. These carbonatite bodies occur in close vicinity to the syenite intrusions. The carbonatite dykes at Lofdal form part of a swarm of about one hundred carbonatite and phonolite dykes. Some of the dykes exceed five meters in width with an extension in length of usually several hundred meters; however, they may reach a linear extension of up to 15 km. The carbonatite dykes clearly cross-cut all the other dykes and, consequently, represent the youngest intrusion event.

Carbonatites at Lofdal are recently classified into eight main carbonatite groups based on field evidence, and their petrographical, geochemical and mineralogical characteristics (DoCabo, 2013).

The carbonatites vary significantly in their whole rock REE concentrations. The sövite in the plugs and large calcite carbonatite dykes are almost devoid of significant quantities of rare earth minerals and contain different rare earth phases than all other carbonatite dykes. Rarely, they contain accessory burbankite, cordylite-(Ce), carbocernaite, and monazite-(Ce). Some veinlets cross-cutting the early magmatic carbonatite contain hydrothermal rare earth minerals – synchysite-(Ce), pariste-(Ce) and ancylite-(Ce). Late carbonatite types are represented by highly sheared carbonatite dykes of calcite, dolomite or ankerite lithology, overprinted by a multi-stage hydrothermal assemblage having significantly elevated REE concentrations of up to 8 wt.% REE (average REE is 1.2 wt.%) or 2.8 wt.% of heavy REE. In these rocks the hydrothermal assemblage consists of both, LREE and HREE-bearing minerals, which are represented by synchysite-(Ce), parisite-(Ce), monazite-(Ce), xenotime-(Y) and fluorite.

Some of the dykes are of particular interest because of their contents of substantial amounts of xenotime-(Y) (Wall et al., 2008) and their elevated heavy to light rare earths ratios (HREE / LREE). Xenotime-(Y) forms a number of mineral paragenesis and assemblages ranging from magmatic to metasomatic stages in Lofdal carbonatites.

The majority of rare earth minerals formed during the hydrothermal / carbothermal stages of carbonatite formation. REE mineralisation in carbonatite dykes is highly variable following sub-parallel zones. Such mineralisation probably formed by multiple stages of hydrothermal / metasomatic overprinting of the primary carbonatite by fluids at variable intensities. Apatite and fluorite represent two important gangue minerals, which possibly played an important role in the transportation and deposition of the REE at Lofdal.

The location of the HREE-mineralisation is strongly controlled by intensive shearing within the carbonatites dykes. In addition, HREE precipitation partly took place in the fractured albitised country rocks and carbonatite-free shear zones. Thus, at least some of the the xenotime mineralisation in the Lofdal alkaline complex seems to trace back to intensive interaction of an HREE-rich hydrothermal fluid with the carbonatites. Fractionation of REE during hydrothermal activity can produce an enrichment of mid-atomic number REEs and Y in carbonatites (Mariano, 1989). This hydrothermal fractionation seems to have caused the unusually high HREE/LREE ratios in the Lofdal carbonatites. The carbonatites at Lofdal generally show higher HREE concentrations than most other carbonatites. The HREE concentration considerably increases from the early magmatic to the hydrothermal stages of mineralisation. It culminates in the formation of a xenotime cement in the brecciated dolomite carbonatites.

References

DoCabo V.N. Geological, mineralogical and geochemical characterization of the Heavy Rare Earth-rich carbonatites at Lofdal, Namibia. // Unpublished PhD Thesis, University of Exeter, UK. 2013.

Mariano, A.N. (1989) Nature of economic mineralization in carbonatites and related rocks. Pp. 149-176) In Carbonatites: Genesis and Evolution (K.Bell, editor). Unwin Hyman, London

Miller, R. McG. The Pan-African Damara orogen of South West Africa/Namibia // In Evolution of the Damara Orogen of South West Africa/Namibia (R. McG., Miller, Ed., 1983) Special Publication, Geological Society of South Africa,). 1983. 11. 431-515.

Wall F., Niku-Paavola V.N., Storey G., Müller A., Jeffries T. Xenotime-(Y) from carbonatite dykes at Lofdal, Namibia: unusually low LREE:HREE ratio in carbonatite, and the first dating of xenotime overgrowths on zircon // Canadian Mineralogist. 2008. 46. 861-877

Characterisation of zirconolite from alkaline pegmatites of the Larvik plutonic complex, south Norway

Škoda R., Haifler J., Hönig S.
Department of Geological Sciences, Masaryk University, Kotlářská 267/2, Brno, Czech Republic,
rskoda@sci.muni.cz

Zirconolite, ideally $CaZrTi_2O_7$, is an accessory mineral occurring in silica-poor rocks such as carbonatites, alkaline rocks and their pegmatites as well as in contaminated marbles. Minerals with composition close to $CaZrTi_2O_7$ were called zirconolite, polymignite or zirkelite in the past. Currently, polytypoids with fluorite-type structure should be called zirconolite-2*M*, -3*T* or -3*O* depending on their symmetry. Zirkelite should be a cubic mineral with formula $(Ti,Ca,Zr)O_{2-x}$. However, the exact relationships between zirconolite polytypoids and zirkelite is still not well understood.

Zirconolite from alkaline pegmatites of the Larvik plutonic complex in Norway, localities Stålaker, Håkestad, and Agnes, has been examined. Zirconolite forms euhedral black lathy crystals up to 3 cm long with striated prismatic and pinacoidal faces in those pegmatites. Associating minerals are mainly albite, K-feldspar, biotite, magnetite, britholite-(Ce), zircon, pyrochlore, nepheline, and aegirine. All samples are quite homogeneous in BSE image without any significant zonation or alteration, the only narrow altered zones line the old fractures of zirconolite. Electron probe microanalysis in WDS mode give analytical totals of 97.2 to 98.9 wt% for the fresh parts. Mineral formula and Fe^{2+}/Fe^{3+} ratio was calculated on the basis of 4 cations and 7 anions. Chemical composition of zirconolite is similar in the range of a single crystal as well as among all localities examined, whereas the highest variability shows zirconolite from Agnes, see Fig 1. Zirconolite from Larvik Plutonic complex is enriched in Y+REE, Nb, Ta and Fe giving the resulting formulae as follows:

Stålaker
$(Ca_{0.45-0.50}REE^{3+}_{0.44-0.46}Th_{0.04-0.06}U_{0.01-0.02})(Zr_{0.94-0.97}Hf_{0.01})(Ti_{0.91-0.96}Nb_{0.46-0.53}Ta_{0.01-0.02}Me^{2+}_{0.48-0.54}Fe^{3+}_{0.04-0.10})O_{7.00}$,
Håkestad
$(Ca_{0.55-0.58}REE^{3+}_{0.36-0.38}Th_{0.04-0.06}U_{0.01})(Zr_{0.94-0.96}Hf_{0.01})(Ti_{0.93-0.97}Nb_{0.50-0.55}Ta_{0.02}Me^{2+}_{0.47-0.50}Fe^{3+}_{0.05-0.09})O_{7.00}$,
and Agnes
$(Ca_{0.50-0.60}REE^{3+}_{0.34-0.39}Th_{0.05-0.09}U_{0.02-0.04})(Zr_{0.95-1.01}Hf_{0.01})(Ti_{0.97-1.12}Nb_{0.36-0.48}Ta_{0.02}Me^{2+}_{0.43-0.50}Fe^{3+}_{0.04-0.10})O_{7.00}$,

where REE^{3+} are represented by Ce>Nd>Y>La dominating over Pr, Sm, Gd, Dy, Er, Yb; Me^{2+} includes most of Fe dominating over Mn, and Mg. The calculated $Fe^{2+}/(Fe^{2+}+Fe^{3+})$ ratio vary from 0.79-0.92 with the average of 0.88 for Stålaker, 0.86 for Håkestad and Agnes is with a very good agreement with the results obtained from Mössbauer spectroscopy (0.83). The reliable determination of the substitution vectors is

complicated by a quite homogenous chemical composition and many variables, but the positive correlation of the Me^{2+} vs. Me^{5+}, Me^{2+} vs. REE^{3+} and Me^{5+} vs. REE could indicate substitution involving $REEZrMe^{5+}Me^{2+}O_7$ end-member. The only zirconolite from Agnes corresponds to the Ca-, Zr-, and Ti-dominated composition. Material from Håkestad shows prevalence of $Me^{5+}+Me^{2+}$ over Ti^{4+}. Similarly $Me^{5+}+Me^{2+}$-enriched, but REE-poorer zirconolite were described from the Kovdor carbonatite (Williams 1996). Some analyses from Stålaker show also the prevalence of $Me^{5+}+Me^{2+}$ over Ti^{4+} as well as the slight prevalence of REE over Ca corresponding to about (51 %) $REEZrMe^{5+}Me^{2+}O_7$ end-member. Similar composition with slightly dominant $REEZrMe^{5+}Me^{2+}O_7$ molecule also described Della Ventura *et al.* (2000) from Eifel (Germany), but their analysis have Mn>Fe.

The radiation dose the zirconolite have suffered, assuming the geological age of 295 Ma, is about 2.0-2.8 x 10^{16} α decays/mg, which is one order of magnitude higher than is the transition from crystalline zirconolite to metamict (Lumpkin *et al.,* 1997a,b). XRPD study also confirms its metamict nature. The annealing of the zirconolite powder from Håkestad under an inert atmosphere at 800°C caused recrystallization to a phase with the cubic space group *Fm*3*m* and with the cell parameter a = 5.104(3) Å that is close to the cubic ZrO_2, tazheranite, $(CaTiZr_2O_8)$ phase or zirkelite. This result is very similar to that which was gained by Bulakh *et al.* (1998), but their specimen was described as zirkelite because of its cubic morphology. Crystal morphology of the metamict zirconolite (polymignite) from Larvik plutonic complex is of the orthorhombic symmetry (Larsen 2010). During the heating to 900°C the cubic structure turned to the orthorhombic symmetry and the diffraction pattern corresponds to zirconolite-3O, which could indicate the heating at 900°C recovered its original structure.

Some narrow zones along the rim or the cracks within the crystal were altered by penetrating hydrothermal fluid that significantly affected the chemical composition of these zones. The most distinct changes are the enrichment of SiO_2 (from nearly Si-free fresh parts increased to about 5–6 wt.% SiO_2 in altered region), Al_2O_3 (increased from 0.14 to 0.27 wt.%), WO_3 (increased from nearly W-free to 0.3–0.4 wt.%), F (increased from 0.3 to 0.5 wt.%) and the content of actinides and lanthanides is also relatively slightly higher in altered parts. The hydration of the mineral is also probable. On the other hand there is a great loss of Fe (decreased from about 7.6 wt.% FeO to about 1 wt.%), quite distinct loss of Ca (decreased from 7 to 4 wt.% CaO), Ti (decreased from 20.5 to 18 wt.% TiO_2), Zr (decreased from 28 to 26.5 wt.% ZrO_2), and lower disparities in Pb, Mg and Mn content. This behaviour during alteration is in agreement with published data (Bulakh *et al.*, 1998). The content of U, Th and Y+REE does not seems significantly affected by the alteration.
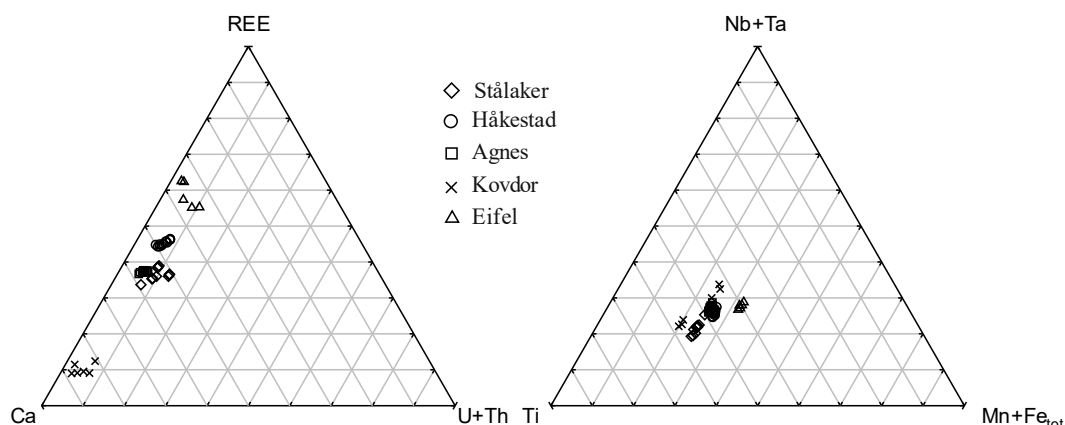
Figure 1: Chemical composition of the zirconolite from Larvik Plutonic complex (Stålaker, Håkestad, and Agnes) and another localities is plotted in two ternary plots.

References:

Bulakh A.G., Nesterov A.R., Williams C.T. & Anisimov I.S. Zirkelite from the Sebl'yavr carbonatite complex, Kola Peninsula, Russia: an X-ray and electron microprobe study of a partially metamict mineral. Mineralogical Magazine, (1998), 62: 837–846.

Della Ventura G., Bellatreccia F., & Williams C.T. Zirconolite with significant $REEZrNb(Mn,Fe)O_7$ from a xenoliths of the Laacher see eruptive center, Eifel volcanic region, Germany. Canadian Mineralogist, (2000), 38: 57–65.

Larsen A.O. The Langesundsfjord, Bode Verlag GmbH, Germany, (2010), 239

Lumpkin, G.R. – Smith, K.L. – Gieré, R. Application of analytical electron microscopy to the study of radiation damage in the complex oxide mineral zirconolite. – Micron. (1997a), 28 (1), *57-68.*

118

Lumpkin G.R., Smith K.L., Blackford M.G., Gieré R. and Williams C.T. The Crystalline-Amorphous Transformation in Natural Zirconolite: Evidence for Long-Term Annealing. In: McKinley, I. G – McCombie, C. (eds.): MRS Proceedings. (1997b), 506, *215-222*.

Williams T.S. The occurence of niobian zirconolite, pyrochlore and baddeleyite in the Kovdor carbonatite complex, Kola Peninsula, Russia. Mineralogical Magazine, (1996), 60, 639-646.

Specific features of eudialyte decomposition in oxalic acid

Smirnova T.N.*, Pekov I.V.*,**, Varlamov D.A.***, Kovalskaya T.N.***, Bychkov A.Y.*,
Bychkova Y.V.****

*Faculty of Geology, Moscow State University, Moscow, Russia
**Vernadsky Institute of Geochemistry and Analytical Chemistry RAS, Moscow, Russia
***Institute of Experimental Mineralogy RAS, Chernogolovka, Russia
****Institute of Geology of Ore Deposits, Petrography, Mineralogy and Geochemistry RAS, Moscow,
Russia

One of the main aspects of a possible practical use of eudialyte today is extracting of Zr, Hf, *REE* (especially *HREE*) and U. Numerous attempts to solve this problem using full decomposition of eudialyte by strong inorganic acids were not successful in technological aspect: silicon converts into solution forming a filterable gel which strongly hampers any processes of isolation and purification of valuable components.

We have studied the processes and products of eudialyte decomposition in dilute oxalic acid, $H_2C_2O_4$, and for comparison in HCl at t <100°C. For the experiments, two eudialyte varieties were used: (1) from rischorritic pegmatite, the Oleniy Ruchey apatite deposit (sample OLE-9), Khibiny, and (2) from naujaitic pegmatite, Mt. Alluaiv (sample UMB-2), Lovozero (both Kola peninsula, Russia). The Lovozero eudialyte is enriched with *REE* and Zr and has, according to our data, more defective crystal structure in comparison with the Khibiny sample.

Experiments with 1 and 3% $H_2C_2O_4$ gave similar results for the Khibiny eudialyte: it alters only from the surface to opal-like phase with overgrowing crystals (Fig. 1). Using the EMPA and IR spectroscopy data, we undoubtedly identified these crystals as Ca-Zr oxalates. In experiments with 7% $H_2C_2O_4$ the Khibiny eudialyte completely decomposes with the formation of a gel-like opal phase closely associated with crystalline oxalates of Ca and Zr with admixed *REE*.

The Lovozero eudialyte fully decomposes in 3, 5 and 7% $H_2C_2O_4$. On the surface of the formed opal phase, crystals (up to 40 μm) of both Ca-Zr and *REE* oxalates (Fig. 2) are abundant. Two types of *REE* oxalates occur: (1) with essentially yttrium cationic composition (enriched also with *HREE*) and (2) *LREE*–rich.

Thus, after the decomposition of eudialyte in $H_2C_2O_4$ *REE* separate from other cations fotming the *solid crystalline phases, oxalates*. They are almost insoluble in water and oxalic acid, and release of *REE* into the solution is minor, unlike a system with HCl. It seems very important for further extraction of *REE* because we see a relatively easy way to convert them into the molecular (rather than colloid!) solution using a complexing agent without any reaction with opal, a dried silica gel. It seems also important that a dilute solution of $H_2C_2O_4$ is used: oxalic acid is a chemical which, unlike corrosive and volatile mineral acids, may be easily transported and stored in an environmentally safe solid form.

Extraction of Zr (and Hf) into solution in experiments with $H_2C_2O_4$ is reduced as compared to HCl, but still significant. Also note the solubility of eudialyte significantly depends on the perfection of its structure (Ca-Fe-Zr-Si heteropolyhedral framework): the Khibiny sample is considerably more resistant to acid degradation than the Lovozero mineral.
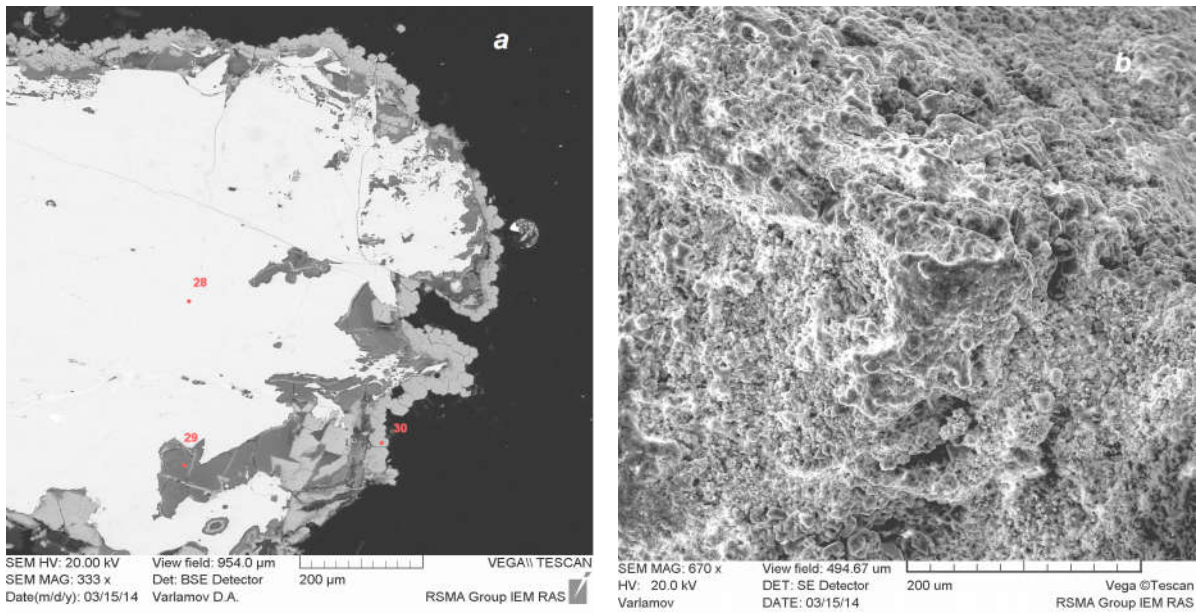
Fig. 1. The Khibiny eudialyte after the experiment with 1% $H_2C_2O_4$. On section (a), an opal-like phase (p.29) and Ca-Zr oxalate crusts (30) overgrowing unaltered eudialyte (28) are observed. On the rough surface (b), Ca-Zr oxalate crystals are abundant. SEM image: (a) BSE, (b) SE.
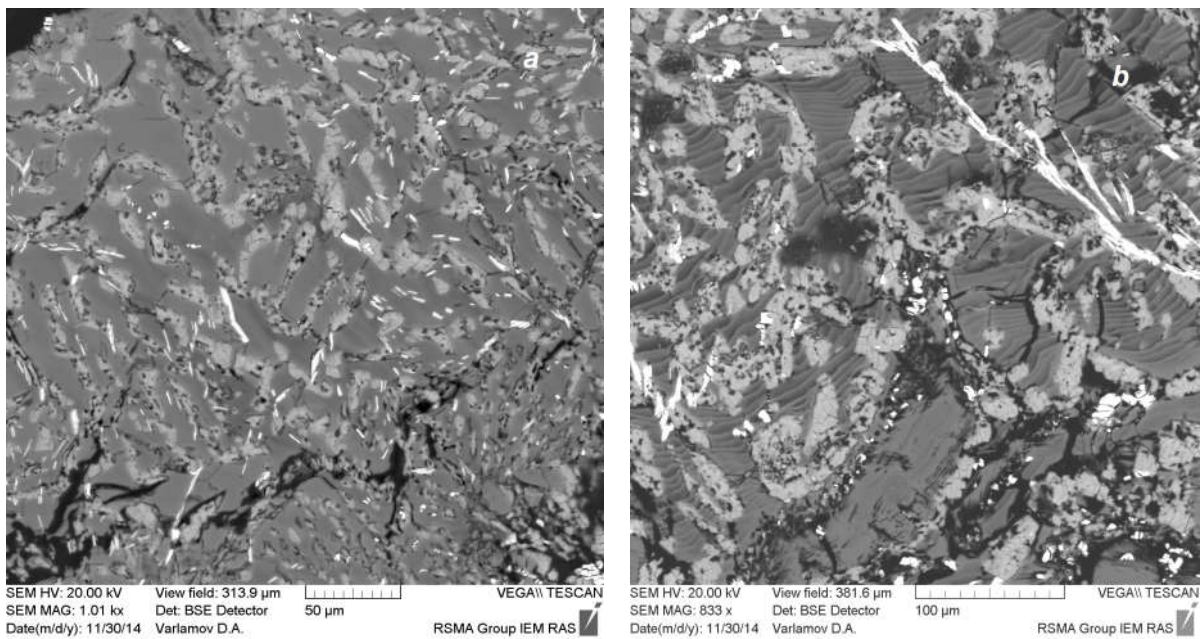
Fig. 2. Surface of the opal-like product formed as a result of full decomposition of eudialyte in 7% (a) and 5% (b) $H_2C_2O_4$ [SEM (BSE) image]. White zones correspond to *REE* oxalates and light gray zones to Ca-Zr-oxalates.

Table. Contents of rare elements and Ti (ppm) in thousandfold diluted solutions after the experiments with HCl and $H_2C_2O_4$ of different concentrations and eudialyte from Khibiny (OLE-9) and Lovozero (UMB-2). ICP MS data; bdl – below detection limit; dash – not analysed.

| | HCl | | | | | | $H_2C_2O_4$ | | | | | | |
| | OLE-9 | | | UMB-2 | | | OLE-9 | | | | UMB-2 | | |
	10%	7%	2%	10%	7%	2%	7%	5%	3%	1%	7%	5%	3%
Zr	2486	1671	135	1600	1528	390	306	260	477	122	1100	1739	1311
Hf	36	20	1.2	28	26	5	-	bdl	-	1.8	22	35	28
Ti	93	91	-	79	72	41	-	-	-	-	-	85	57
Ta	bdl	0.1	bdl	bdl	0.3	0.6	-	-	-	0.7	4	5	0.7
Th	0.8	0.8	0.3	0.8	1.1	0.4	bdl	bdl	bdl	bdl	0.2	0.6	0.3
U	1.5	1.6	0.5	0.5	0.7	0.3	0.4	0.3	0.5	0.3	0.2	0.6	0.5
Sr	176	182	56	210	157	94	5	4	4	3	5	5.5	5.5
Ba	44	45	13	2	1.8	2	10	7	6	4	0.8	0.6	0.1
Y	43	44	12	107	86	53	0.4	0.2	bdl	bdl	0.9	1.1	0.9
La	25	26	7	49	5	24	0.7	0.3	bdl	bdl	1	1.8	0.1
Ce	32	31	14	101	87	50	1	0.4	bdl	0.1	0.9	1.2	0.2
Pr	5.5	5.5	1.5	13	18	6	bdl	bdl	bdl	bdl	bdl	0.1	bdl
Nd	22	23	6	58	79	28	0.3	0.15	bdl	bdl	bdl	0.1	bdl
Sm	5	5	1.5	17	24	9	bdl	bdl	bdl	bdl	bdl	bdl	bdl
Eu	2	2	0.5	6	8	2.9	bdl	bdl	bdl	bdl	bdl	bdl	bdl
Gd	6.5	6.5	1.5	18	27	8.5	0.1	bdl	bdl	bdl	bdl	bdl	bdl
Tb	1.2	1.2	0.3	3.8	5	2	bdl	bdl	bdl	bdl	bdl	bdl	bdl
Dy	8	8	2	24	32	12	bdl	bdl	bdl	bdl	bdl	bdl	0.1
Ho	1.8	1.8	0.5	4.6	6.5	2	bdl	bdl	bdl	bdl	bdl	bdl	bdl
Er	5.5	6	1.5	14	20	7	bdl	bdl	bdl	bdl	bdl	0.1	0.1
Tm	0.8	0.9	0.2	2	2.8	1	bdl	bdl	bdl	bdl	bdl	bdl	bdl
Yb	5	5	1.5	12	17	6	bdl	bdl	bdl	bdl	0.2	0.4	0.3
Lu	12	8	0.2	1.7	17	0.8	bdl	bdl	bdl	bdl	bdl	8.5	7

Thermal analysis of carbonaceous shales as a way to forecasting of gold mineralization (at the example of Beloretsk metamorphic dome, Southern Urals)

Snachev A.V.
Institute of geology of the Ufa centre of science of the Russian Academy of Science,
Ufa, the Russian Federation
EMail: SAVant@rambler.ru

The Beloretsk zonal methamorphic complex is situated in the eastern part of the Bashkirian meganticlinorium in the limits of Mayardak anticlinorium. It bends in a horseshoe way around the northern periclinal end of the Zilair synclinorium and stretches in the northeastern direction at a distance of about 120 km, being 20 to 40 km wide. The complex is composed of the Lower- to Upper Riphean deposits, with a thickness of $4-5$ km (Alexeev et al, 1984).

The initial rocks of the complex are mainly sandy-argillaceous, carbonate and carbonaceous terrigenous deposits, and much less often - intrusive bodies and effusions of basic composition. In the Late Vendian (?) time the rocks have been exposed to a metamorphism exerted by a deep-seated large granite or granite-migmatite intrusive body, reliably fixed by geophysical methods. Therefore a zonal metamorphic complex was formed, with a core (diameter of 7-8 km) composed of rocks of eclogite facies; the intermediate zone (width of 2-10 km) belongs to amphibolitic and external (width of 15-20 km) – to greenschist facies (Alexeev & al., 2009). The carbonaceous deposits are developed in the Yusha, Mashak, Zigalga and Zigazino-Komarovo Formations. Their position in sections and lithological character are described in detail in a monograph (Snachev et al. 2012) and are not considered here. The most widely developed are the carbonaceous schists in the Zigazino-Komarovo Formation (RF_2zk). They are combined in various proportions with chlorite-sericite-quartz, micaceous-quartz, micaceous-fieldspar-quartz schists, quartz siltstones and sandstones, enriched with carbonaceous substance; by their petrochemical features they can be attributed to a terrigenous-carbonaceous

complex (Snachev, 2015). In schists a sulphidization is very frequently observed, varying from individual interspersed grains of pyrite to sulphidic veins up to 1 cm thick; the content of sulfides in the rocks may reach 25-30 %. More often in exposures and eluvial-deluvial debris, weathered rocks are developed in which in a place of initial sulfides remain either hollows of a cubic habitus, or zones of cavernous structures, intensely ferruginous. The further weathering of such rocks leads to a formation of limonite crusts.

The results of thermal (Rock-Eval) analysis of carbonaceous schists of the Zigazino-Komarovo Fotmation from the Beloretsk methamorphic complex have shown C_{org} contents from 0,76 up to 7,22 % that allows to relate them to low carbonaceous, and less often to carbonaceous types. Geneticaly, the carbonaceous substance of the considered rocks belongs to a sedimentary-diagenetic type and is represented by a finely dispersed form of allocation. Particles with a size of no more than 0,005 mm impregnate in a regular manner all mass of the rocks or concentrate as spots, irregular and lenticular accumulations. Such a form of a presence of carbonaceous substance testifies for a syngenetically initial C_{org} matter and a deposit (Sidorenko, Sidorenko, 1971). As a result of study of carbonaceous sediments of different age in the Far East by V.P. Ivanova & al (1974), a dependence between temperature of burning out of dispersed organic substance and a degree of metamorphism of rocks was established. In a process of increase of a regional metamorphism the temperature C_{org} of burning out is naturally increased.

The thermogravimetric analysis of carbonaceous shists of Zigazino-Komarovo Formation was carried out on a derivatograph Q-1500 (Hungary) (analyst T.I. Chernikova, IG USC, Russian Academy of Science). The heating was accomplished on air under a temperature from 20 to 1000 °C with a speed of 10 °C/min. The samples of the least changed rocks outside zones of intrusive exocontacts and intensive tectonic reworking were selected for the analysis, which allowed to exclude the influence of local factors and to reconstruct a degree of the regional metamorphism.

For the schists of the Zigazino-Komarovo Formation, the exothermal effect occurs in the range 630-730 °C, that corresponds to a biotite-muscovite greenschist facies and is close to a staurolite-andulusite-biotite level of metamorphism (epidote-amphibolite facies) (Bluman et al, 1974).

It is necessary to note, that the greater interest is represented not by absolute numbers, neither by a distribution of temperatures on the area. Bilding the map of isopleths of temperatures of exothermic effect (a method of interpolation Kriging) allows, using the results of termogravimetrical analysis, to establish zones with various degrees of metamorphic transformations. The boundary between a greenschist and epidote-amphibolite facies for the Zigazino-Komarovo Formation, received in a such way, coincide with an isopleth of 660 °C, and it is well coordinated with the results received A.A. Alekseev who constructed a map of a metamorphic zonation of the Beloretsk dome. The boundary between amphibolite and greenschist facies was tstablished at the isograde of granate, and external border of the greenschist facies – along the isograde of biotite (Alexeev & al, 1984).

Moreover, in the result of a processing and summarizing of the collected, published and archive material on gold-bearing carbonaceous sediments of the Beloretsk methamorphic complex and its frame, including ca. 200 our own analyses of piece and groove samples, very precise regularity in localization of elevated concentrations of gold has come to light: all points with industrial values of gold are situated in the area of development of rocks of greenschist facies of metamorphism (Snachev, Snachev, 2014).

The mechanism of redistribution of precious metals is considered in detail in an experimental work of L.P. Pljusnina et al (2011). The metamorphism of carbonaceous substance is accompanied by a generation of water-organic oleophilic fluid-mobilizate, gas phases and solid kerogen. In this process, a part of precious metals migrate beyond limits of host rocks together with the mobilizate, and the part concentrates in the resdual volume of kerogen. The process is finished by a crystallization of graphite at the expense of kerogen at temperature of 500 °C. At that, its sorption capacity reaches the maximum at 2700 g/t and 1000 g/t for Au and Pt correspondingly. In the graphite itself, under degazation, pores and hollows from 200 up to 500 microns in dimensions are formed, creating a fine-meshed porous framework. As a consequence, the layers of rocks with a similar graphite are loosened, that raises their permeability for ore-bearing solutions, and reducing conditions promote an ore mineralization and favour an introduction of metallo-fullerenes between the planes (002).

According to data of A.I. Hanchuk et al. (2009), the early form of segregation of platinum are finely dispersed agglomerates, with dimensions of one to tens microns, containing in its structure carbon and a plenty of other elements. The subsequent progress of metamorphism and, probably, redeposition lead to a partial purification of precious metals and to formation of lamellar and crystal forms.

Thus, the work that had been carried out shows an opportunity of use thermogravimetric analysis which is cheap enough, in the aim of a forecasting of gold mineralization in metamorphosed carbonaceous complexes. Gold-ore objects, having a precise confinement to the greenschist facies (Snachev & al, 2013), in most cases are concentrated close or almost on the boundary between the greenschist and amphibolite facies of metamorphism.

References

Alekseev A.A. Rifejsko-Vendskij magmatizm zapadnogo sklona Yuzhnogo Urala. M.: Nauka, 1984. 136 p.

Alekseev A.A., Kovalev S.G.,Timofeeva E.A. Beloretsky metamorficheskij kompleks / Ufa: DizajnPoligrafServis, 2009. - 210 p.

Blyuman B.A., Djyakonov Yu.S., Krasavina T.N., Pavlov M.G. Ispoljzovanie termo- i radiograficheskikh kharakteristik grafita dlya opredeleniya urovnya i tipa metamorfizma. Zapiski Vsesoyuznogo.Mineralogicheskogo Obschestva, 1974, p. 103, vyp. 1, s. 95-103.

Ivanova V.P., Kasatov B.K., Krasavina T.N, Rozinova E.L. Termicheskij analiz mineralov i gornykh porod L.:Nedra, 1974. - 399 p.

Plyusnina L.P., Likhojdov G.G., Kuzmina T.V. Grafitizatsiya i naftorudogenez/ Litosfera, 2011, № 5. p. 111-116.

Sidorenko A.V., Sidorenko Sv.A. Organicheskoe veschestvo v dokembrijskikh osadochno-metamorficheskikh porodakh i nekotorye geologicheskie problemy. - " Sovetskaya Geologiya ", 1971, № 5, p. 3-20.

Snachev A.V. Geologiya i petrokhimicheskie osobennosti uglerodistykh otlogenij Zigazino-Komarovskoj svity Beloretskogo metamorficheskogo kupola (Yuzhnyj Ural) / Problemy mineralogii, petrografii i metallogenii. Nauchnye chteniya pamyati P.N. Chirvinskogo. Perm SU, Perm, 2015. p. 328-333.

Snachev A.V., Snachev V.I., Rykus M.V., Savel'ev D.E., Bazhin E.A., Ardislamov F.R.Geologiya, petrogeokhimiya i rudonosnost uglerodistykh otlozhenijYuzhnogo Urala / Ufa. DizajnPress, 2012. 208 p.

Snachev V.I.,Snachev A.V. Zakonomernosti razmescheniya zolotorudnykh proyavleniyakh v uglerodistykh otlozheniyakh Beloretskogo metamorficheskogo kompleksa (Yuzhnyj Ural) // Bulletin VSU. 2014. № 2. p. 79-87.

Hanchuk A.I., Berdnikov N.V., Cherepanov A.A., Konovalova N.S., Avdeev D.V. Pervye nakhodki vidimykh platinoidov v cyornoslantsevykh tolschakh Burejnskogo massiva (Khabarovskij Kraj i Evrejskaya AO) / Doklady AN , 2009, vol. 424, № 5, p. 672-675

Composition and thermodynamic parameters of the metasomatic agent beneath east Antarctica from results of study inclusions

Solovova I.P.*, Kogarko L.N.**
*Institute of the Geology of Ore Deposits, Petrography, Mineralogy, and Geochemistry (IGEM), Russian Academy of Sciences, Staromonetnyi per. 35, Moscow, 109017 Russia. solovova@igem.ru
**Vernadsky Institute of Geochemistry and Analytical Chemistry, Russian Academy of Sciences, ul. Kosygina 19, Moscow, 119991 Russia. kogarko@geokhi.ru

We investigated deformed xenoliths of garnet-spinel peridotites from alkaline mafic and ultramafic bodies from oasis Jetty (East Antarctica). Isotope-geochemical investigation of these xenoliths (Михальский и др., 1998) demonstrated that during the range of 1023 – 1240 Ma mantle material was metasomatised which led to the enrichment of the generated alkaline magmas. Because of this, the investigation of the composition and evolution of fluids and products of their interaction with mantle peridotites is of certain interest. The findings of fluid inclusions in the rock-forming minerals proves the presence of free fluid at great depths, and presence of sulfides concentrating transitional and precious metals (Ni, Cu, Pt, Pd и Au) suggests high concentrations of sulfur.

The minerals of the investigated xenoliths contain coexisting sulfide and fluid inclusions of high density. The evidence of partial loss of material (haloes) around vacuoles appear during their partial dehermetization at the decompression. Therefore, the estimated from the study of inclusions P-T parameters correspond to one of the stages of the mantle material evolution.

Sulfide inclusions represent isolated one- and two-phase drop-like grains grouping into clusters. Their compositions on the Ni – M/S plot form two diverging trends with positive and negative correlations. According to the experimental data (Ballhaus et al., 2001) the inclusions represent coexisting sulfide melt and Ni-enriched monosulfide solid solution (*mss*) (рис. 1). Ni partition coefficient (D_{Ni}*mss*/melt) permitted to evaluate minimal temperature of the stabilization of two-phase sulfide assemblage in the range 1060-920ºC.
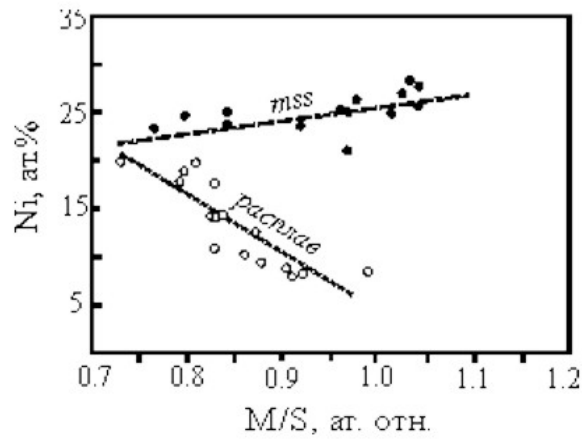
Fig. 1. Two evolution trends of the composition of sulfide inclusions.

The investigation of fluid inclusions by thermobarogeochemical method and Raman-spectroscopy demonstrated that fluid is characterized by polycomponent composition - CO_2, N_2, H_2S и H_2O; mole fractions were estimated as как ~ 0.7 CO_2, 0.15-0.2 N_2 и 0.1 H_2S. The presence of water has been established cryometrically. Our isotope studies confirmed mantle origin of fluid (Buikin et al., 2014). The measured density of fluid of partially decrepitated inclusions yielded calculated pressure of 1.1-1.5 GPa.

Using the results of our studies and experimentally established fields of coexistence of mss+sulfide melt and peridotite solidus at -0.9CO_2 + 0.1H_2O as well as the positions of isochores of 0.8CO_2+0.2N_2 fluid the reconstructed initial temperature and pressure of the action of metasomatizing substance on mantle material were estimated as 1270-1280ºC и ~2.2 GPa (рис. 2).

In spite of the relatively minor contribution of N_2, H_2S и H_2O into the overall budget of deep fluids these volatiles play an important role in the processes of mantle metasomatism, and it is reflected in the geochemical features of generated magmas. Not only H2O but other components as well transport significant amounts of ore metals and REE. For example, H_2S-bearing fluid in the preserce of H_2O is capable of the transporting of Zr, Ti and REE. The appearance in xenoliths of intergranular veinlets of glass with the immersed newly formed crystals of clinopyroxene, spinel, Ba-Ti phlogopite, olivine, S-bearing chlorapatite, henrymeyerite, calcite and dolomite is related to the metasomatism (Kogarko et al., 2007).
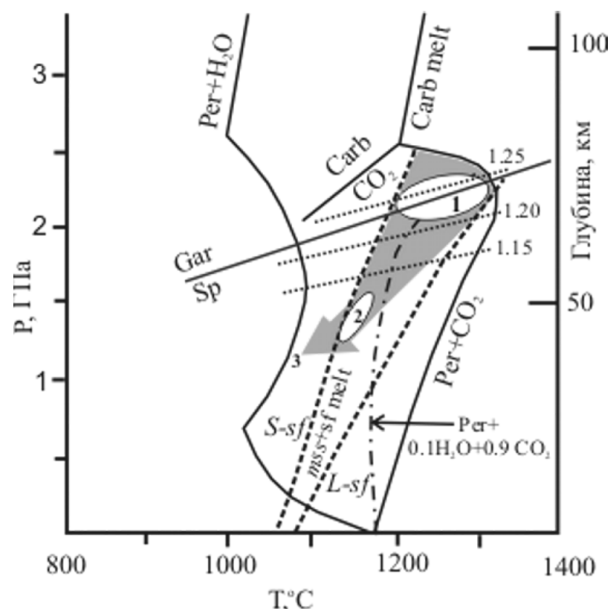
Fig. 2. Temperature and pressure of the evolution of sulfide fluid association. Dash-point line is solidus of peridotite -0.9CO_2 + 0.1H_2O. *L-sf* – liquidus and *S-sf* – solidus of sulfide system (dashed line), *mss*+sf melt – field of the coexistence of monosulfide solid solution and sulfide melt. Dotted lines – isochores of the fluid 0.8CO_2+0.2N_2. 1 - starting PT-parameters of sulfide fluid assemblage, 2 – PT-parameters of partially decrepitated inclusions, 3 – the field of the stability of intergranular sulfide aggregates.

124

The active carbonate metasomatism of mantle peridotite which resulted in the formation of calcite and dolomite in the metasomatized zones, took place according to the following reactions

$$2\ Mg_2SiO_4\ +\ CaMgSi_2O_6\ +\ 2\ CO_2\ =\ 2\ Mg_2Si_2O_6\ +\ CaMg(CO_3)_2 \qquad (1)$$
olivine   clinopyroxene   fluid   orthopyroxene   melt

$$3\ CaMg(CO_3)_2 + CaMgSi_2O_6 = 4\ CaCO_3 + 2\ Mg_2SiO_4\ +\ CO_2 \qquad (2)$$
melt   clinopyroxene   calcite   olivine   fluid
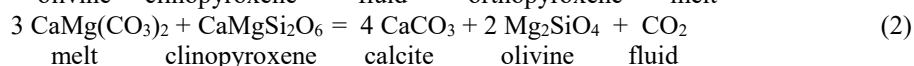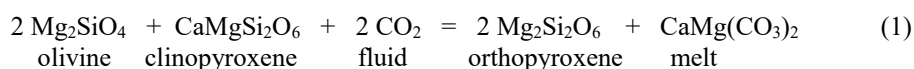
The metasomatic character of sulfide mineralization of the investigated mantle material is confirmed by the elevated concentrations of chalcophile and siderophile elements. It was set that concentration Cu in 1.5 times higher by comparison with the mantle (Palme, O'Neill, 2003), Ag in 83 times, As in 8 times, Au in 2.5 times and Ir in 1.7 times. The introduced character of sulfides is consistent with the high sulfur concentration in the investigated xenolith (1400 ppm, which is 7 times higher by comparison with the S content in the mantle.

References:
1. Mikhalsky E.V., Laiba A.A., Surina N.P. The Lambert province of alkaline-basic and alkaline-ultrabasic rocks in East Antarctica: Geochemical and genetic characteristics of igneous complexes // Petrology. 1998. V. 6. No 5. P. 512-527.
2. Buikin A.I., Solovova I.P., Verchovsky A. V., Kogarko L.N., Averin A.A. *PVT* Parameters of Fluid Inclusions and the C, O, N, and Ar Isotopic Composition in a Garnet Lherzolite Xenolith from the Jetty Oasis Area, East Antarctica // Geochemistry International, 2014, V. 52, No. 10, P. 805–821
3. Ballhaus C., Tredoux M., Späth A. Phase Relations in the Fe–Ni–Cu–PGE–S System at Magmatic Temperature and Application to Massive Sulphide Ores of the Sudbury Igneous Complex // J. Petrol. 2001. V. 42 (10). P. 1911–1926
4. Kogarko L.N., Kurat G., Ntaflos. Henrymeyerite in the metasomatized upper mantle of eastern Antarctica // Can. Miner. 2007. V. 45. P. 497-501
5. Palme H., O'Neill H. Cosmochemical Estimates of Mantle Composition // In Treatise on Geochemistry, Geochemistry of the Mantle and Core. Elsevier. 2003. V. 2. P. 1–35

Magnesite mineralization of the Safianovskoe massive sulfide deposit (Middle Ural, Russia)

Soroka E.I., Pritchin M.R.
Institute of geology and geochemistry Ural Branch of RAS, Ekaterinburg, Russia, soroka@igg.uran.ru

In our work the results of a physic-chemical study of carbonate mineralization occur in ore-bearing rocks of the Safianovskoe copper sulfide ore deposit are considered (the Middle Urals, Russia). Safianovskoe deposit is situated in the southern part of the Rezhevskaya tectonic structural zone. At the present time massive pyrite-chalcopyrite, pyrite-sphalerite and sulfide impregnated obtained by quarrying.

Ore-bearing series of the deposit consist of the hydrothermal altered volcanic and volcanic-sedimentary rocks of the Devonian age. Carbonates in ore-bearing rocks are presented by Mg-Fe ($MgCO_3$ - $FeCO_3$) varieties of magnesite (breunnerite, siderite) and dolomite. According Mg-Fe content and morphological characteristics the four types of magnesite (breunnerite) mineralization have been distinguished at the eastern-southern part of a deposit near the large ore bodies. Each type has a definite mineral association. It's shown a relationship between a carbonate mineralization and ores. The most ferruginous type of breunnerite mineralization (with siderite) occurs at a contact with pyrite-sphalerite ore bodies.

A sequence of Fe-magnesite mineralization has been defined: 1) an earlier mineralization – impregnation and fine veins of breunnerite in a whole ore-bearing rock and breunnerite-siderite in pyrite-sphalerite ore; 2) incrustation breunnerite mineralization of veins; 3) dolomitic mineralization in the cavities of carbonate (breunnerite) veins; 4) a late mineralization – magnesite veins with quartz and kaolinite.

In carbonate veins' monofractions (magnesite, dolomite), hand-selected by the binocular Loupe, were analysed stable isotopes $\delta^{13}C$, $\delta^{18}O$ (Group of isotopic studies, the Institute of geology of the Komi UB of RAS). The decomposition of carbonates in the phosphoric acid and the measurement of the isotopic composition of carbon and oxygen flow mass spectrometry method in the mode of continuous flow of helium (CF-IRMS) were produced on the analytical complex company Thermo Fisher Scientific (Bremen, Germany), which includes training and sample input Gas Bench II, connected to the mass spectrometer DELTAV Advantage. Values of

$\delta^{13}C$ are given in ppm relative to the PDB standard, $\delta^{18}O$ -standard SMOW. Sizing used international standards NBS NBS 19 and 18. $\delta^{13}C$ and $\delta^{18}O$ definition error is $\pm$ 0.1 ‰ (1σ). The results are shown in table 1.

Table 1. Data of O, C isotopic composition of the vein carbonates of the Safianovskoe copper sulphide deposit (‰).

№	Samples	Mineral	$\delta^{13}C$, PDB	$\delta^{13}C$, PDB, CO_2	$\delta^{18}O$, SMOW	$\delta^{18}O$, SMOW H_2O
1	2/14	magnesite	-3.9		16.8	6.7
2	3/14	magnesite	-4.3		16.7	6.6
3	7/14(m)	magnesite	-5.9		19.4	9.3
4	7/14(d)	dolomite	-5.1	- 5.9	22.9	12.9
6	6/14(m)	magnesite	-5.9		19.0	8.9
7	6/14(d)	dolomite	-5.7	- 6.3	19.3	9.3
8	8/14	magnesite, siderite	-0.6		27.8	

Analyses were carried out in the EEC "Geonauka" Institute of geology of the Komi UB RAS. Analyst I.V. Smoleva.

Isotopic studies of carbonates have shown (table 1), that their $\delta^{13}C$ are in the values area of the carbon granite magma chambers (-8.0 to -5 ‰) (Ohmoto, Goldhaber, 1997) and in the sample 8/14 (siderite-breunnerite)-close to carbon of marine limestones ($\delta^{13}C$ about 0 ‰). In magnezite veins and the dolomites (the third type of mineralization) is a noticeable relief of the isotopic composition of oxygen compared with $\delta^{18}O$ marine carbonates (for sedimentary carbonates $\delta^{18}O > +20$ ‰). Values of $\delta^{18}O = 27.8$ ‰ in a sample 8/14 are values marine carbonates. Ratios of isotopes in the water and carbonic acid contained in fluids, equilibrium with carbonates (table 1), calculated according to the equations of fractionation in dolomite, CO_2 (Ohmoto, Rye, 1979; Sheppard, Schwarcz, 1970) and magnesite-H_2O, dolomite -H_2O (Zheng, 1999) subject to mineralization temperature 200° C. Fluid contains light isotope^{13}C ($\delta^{13}C_{CO2}$ = -5.9-до -6.3‰). $\delta^{18}O_{H2O}$ is 6.6 - 12.9‰.

According to isotope studies of carbonates (magnesite, dolomite, breunnerite-siderite) of the Safianovskoe deposit fluid was enriched by light isotopes because of the probably ratio of isotopes in fluid was interconnected with the composition of the enclosing rocks that previously noted (Murzin et al., 2002) at the Mindyak gold deposit (the Southern Ural). At the Safianovskoe deposit ore-bearing rocks contain rhyodacites. In fluid equilibrium with a maximum value of $\delta^{13}C_{CO2}$ is similar to carbon dating of magmatic origin of ($\delta^{13}C$= -5 to -10 ‰). There is a possibility of participation of a deep fluid ore mineralization with Mg^{2+}.

References:

Murzin V.V., Bortnikov N.S., Sazonov V.N. Evolution of carbon and oxygen isotopic composition of carbonate and rudoobrazuûŝego fluid Mindâkskogo gold/ Ezhegonik-2001. Ekaterinburg: UB RAS, **2002**. P. 252-254.

Ohmoto H., Rye R. O. Isotope of sulfur and carbon, in Barnes, H. L. Ed. Geochemestry of Hydrothermal deposits. N.Y.: John Wiley & Sons, **1979**. P. 509-567

Ohmoto H., Goldhaber M.B. Sulfur and carbonisotopes. Geochemistry of hydrothermal ore deposites. N.Y.: John Wiley and Sons, **1997**. P. 517-611.

Sheppard S.M.F., Schwarcz H.P. Fractionation of carbon and oxygen isotopes and magnesium between coexisting metamorphic calcite and dolomite. Contrib. Mineral. Petrol. **1970**. 26. P. 161-198.

Zheng Y.-F. Oxygen isotope fractionation in carbonate and sulfate minerals. Geochemical Journal. **1999**. 33. P. 109-126.

Au and Ag in carbonatites of the Guli Massif (Polar Siberia)

Sorokhtina N.V., Kogarko L.N.
Vernadsky Institute of Geochemistry and Analytical Chemistry RAS, Moscow
nat_sor@rambler.ru

The average Au and Ag contents in samples from ore deposits were estimated from 1 to 5 ppm and from 10 to 100 ppm, respectively [Avdonin et al., 1998]. According to Gavrilenko et al. (2002) average concentration of these elements in carbonatites are significantly lower than in noble metals ores (Au up to 0.005 ppm and Ag up to 0.1 ppm, respectively). Sulphide-bearing carbonatites and flotation concentrates of the sulphide minerals from carbonatites are enriched in Au and Ag at the most. This is typical for the carbonatite ores of Loolekop deposit (Phalaborwa massif, South Africa) and sulphide-bearing carbonatites of Kovdor, Vuoriyarvi, Sallanlatvi and others alkaline massifs of the Kola Peninsula. [Gavrilenko et al., 2002, Rudashevsky et al., 2001; 1995]. For example, flotation concentrates of chalcopyrite from Kovdor shows 8.7 ppm gold и 323 ppm silver [Gavrilenko et al., 2002, Putintseva et al., 1997]. According to the geochemical mapping of the Karelian-Kola region for noble metals, different formational types have been identified [Sokolov et al., 2011]. Platinum-titanomagnetite type is located in the basic-ultrabasic rocks Kola-Karelian region (Elet'ozero, Gremyakha-Vyrmes, Lesnaya Varaka, Afrikanda, Salmagora, Vuoriyarvi). Au-Ag-Pt sulphide type is known in phoscorites and carbonatites (Kovdor, Seblyavr, Vuoriyarvi, Sallanlatvi), in alkaline rocks and metasomatic rocks, which contacted with foidolites (Salmagora). The fact that the sulfide phases exhibit enrichments in the gold and silver which suggests that carbonatite deposits of this type should be considered as possible noble metal deposits. The high Au and Ag contents are presented in metasomatic altered pyroxenites, sulphide-bearing foidolites and U-REE-rare metal carbonatites of Ingiliyski massif of the Aldan Alkaline Province [Goroshko & Gur'yanov, 2004], in sulphide-bearing calcite carbonatites of the Taimyr Province [Proskurnin et al., 2010]. Significant quantities of Au and Ag are detected in melilites (Au up to 7 ppm, Ag up to 2.7 ppm) and sulphide-bearing carbonatites (Au up to 0.09 ppm, Ag up to 1.8 ppm) of Krestovsky intrusion of the Maymecha-Kotuy Province [Sazonov et al., 2001].

Guli massif of alkaline-ultrabasic rocks is the largest among the same massifs in the Maymecha–Kotuy Province. This massif consists of the following rocks: clinopyroxenites, dunites, picrite melanephelinites, ijolites, phoscorites and carbonatites. PGE mineralization was genetically related to dunite and chromitite of the Guli massif. The PGE and gold minerals from alluvial deposits are located within valleys of rivers and creeks draining rocks of the Guli massif [Malitch, 1999]. Recently, the inclusion of zirconolite and some typomorphic minerals of carbonatites we found in Guli native gold. We believe that the carbonatites may be sources of gold-bearing placers [Malitch et al., 2013].

The Au and Ag contents detected in some samples of early calcite carbonatite of the Guli massif and in magnetite and sulphide concentrates of these carbonatites by neutron-activation methods (Table 1). Our study indicates that the bulk noble metal abundances in sulphide concentrates are higher than the concentration of these elements in carbonatites and magnetite concentrates.

Table 1 Au and Ag contents in rocks and sulfide concentrates of Guli massif (ppm).

sample	calcite carbonatite					magnetite concentrate			Pyrrhotite-pyrite-chalcopyrite concentrate				
	85-109	85-133	87-58	85-125	85-112	85-109	85-133	85-112	85-109	85-133	87-58	85-125	85-112
Au	0.001	0.014	0.002	0.0004	0.001	0.0002	0.001	0.0005	0.022	0.062	0.008	0.006	0.011
Ag	0.015	0.36	0.17	0.09	0.08	0.033	0.2	0.08	0.72	1.45	0.84	0.77	3.64

The silver and gold is mainly impurity component and occurs in pyrite, pyrrhotite, chalcopyrite, and other copper sulphides. Pyrrhotite, djerfisherite, pyrite and chalcopyrite are the most common among sulphides of carbonatites of the Guli massif and the major sources of noble metals. These sulphides may accommodate significant concentrations of Au and Ag (Table 2). Pyrite and pyrrhotite from carbonatites contained up to 0.3 wt.% Ag and 0.2 wt.% Au. Chalcopyrite, djerfisherite, lenaite ($Ag_{1.21}Fe_{1.20}Al_{0.03}S_2$), argentopyrite ($Ag_{0.71}Fe_{2.30}Al_{0.02}Co_{0.01}S_3$) and Fe-Ag phases incorporate significant quantities of silver (Table 2). The composition of different specimens of djerfisherite shows a strong range in silver content. According to a diagram (fig.1) Ag-rich djerfisherite (up to 3.73 wt.% Ag) is occupied a separate field of compositions. Perhaps this mineral is a potentially new mineral species. Silver sulphides were found in multiphase carbonate-sulfide-magnetite inclusions in pyrrhotite from the calcite-phlogopite carbonatite.

Table 2 Compositions (wt.%) of Ag-rich sulfides and Fe-Ag phase from calcite carbonatites of the Guli massif

Mineral	Sample / analyses (n)	K	Na	Fe	Cu	Ni	Co	Ag	Au	Pb	Cd	Cl	S	Total
djerfisherite	97-57 (7)	8.38	0.01	36.37	15.65	0.01	0.07	3.47	0.12	0.07	nd	1.25	31.54	96.82
	G15-55 (5)	8.59	nd	39.55	15.85	0.01	0.07	0.69	nd	0.17	nd	1.33	31.06	97.32
chalcopyrite	97-57 (1)	nd	nd	41.38	19.46	0.03	0.1	2.56	0.16	nd	nd	nd	34.89	98.58
lenaite	97-57 (7)	nd	nd	17.79	0.05	nd	0.09	54.95	0.07	nd	0.40	nd	19.33	92.50
argentopyrite	97-57 (3)	nd	nd	43.72	0.02	0.02	0.20	18.49	0.06	nd	0.02	nd	31.43	93.93
Fe-Ag phase*	97-57 (3)	nd	nd	1.03	0.03	nd	0.01	72.73	0.07	nd	0.74	0.04	0.64	75.36

*Included 0.02 Mg, 0.08 Zn, nd – not detected

On the basis of phase relations of sulphide minerals in carbonatite deposits, noble metal minerals are crystallized under hydrothermal conditions between 80°C and 480°C for Phalaborwa [Rudashevsky et al., 2001], between 470°C and 500°C for Kovdor [Rudashevsky et al., 1995], between 105°C and 300°C for Vuoriyarvi [Shpachenko & Savchenko, 2004]. According to the experimental data [Taylor 1970] the assemblages argentite + pyrrhotite and argentite + pyrite become stable, with decreasing temperature, at 622 ± 2 °C and 607± 2 °C, respectively.
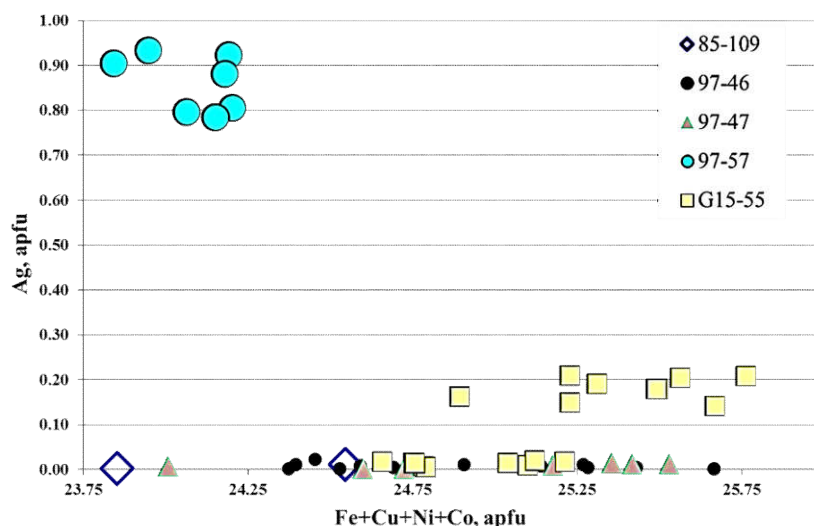
Fig. 1. Chemical variation of Ag in djerfisherite from carbonatites of the Guli massif.

In this case, less than 0.05 and 0.1 at.% Ag are soluble in pyrite and pyrrhotite. The phase relations in the Ag-Fe-S system remain essentially unchanged from 532 °C to 320 °C. Native silver and pyrite are formed below 248 °C. Argentopyrite is stable close to 152 °C [Taylor 1970]. We concluded that the range a temperature of Ag-rich sulphides in carbonatite of the Guli massif can be estimated by stability of the Ag phases between 150°C and 600°C. The sulphide-bearing carbonatites of Guli massif commonly contain elevated amounts of both gold and silver. The fact that the sulphide phases exhibit enrichments in the two precious metals suggests that deposits of this type should be considered as possible noble metal deposits.

References

Avdonin V.V., Bo'ytsov V.E., Grigor'ev V.M. et al. Deposits of metallic mineral resources / M.: ZAO"Geoinformmark", 1998. 269 p. (in Russ.).

Gavrilenko B.V., Shpachenko A.K., Skiba V.I. et al. Noble metals allocation in rocks, ores and flotation concentrates in apatite intrusive complexes of the Karelia-Kola region /Apatity. KSC RAS. 2002. Geology and mineral resources of Kola Peninsula. V. 2. Mineral resources, mineralogy, petrology, geophysics. P. 48-63. (in Russ.).

Rudashevsky N.S., Kretser Yu.L., Bulakh A.G. et al. Platinum-palladium and gold-silver mineralization in carbonatite ores of Loolekop deposit (Phalaborwa massif, South Africa) // ZVMO. 2001. 5. P. 21 – 35. (in Russ.).

Rudashevsky N.S., Knauf V.V., Krasnova N.I., Rudashevsky V.N. The first description of gold and platinum group minerals in ores and carbonatites of alkaline-ultramafic complex (Kovdor massif, Russia) // ZVMO. 1995. 5. P. 1-15. (in Russ.).

Putintseva E.V., Petrov S.V., Philippov N.B. Noble metals in the ore processing products of the Kovdor deposit // Obogashchenie Rud (Mineral processing). 1997. 5. P. 22-25. (in Russ.).

Sokolov S. V., Shevchenko S.S., Belyaev G.M. et al. Perspective estimate of the Karelia-Kola region on endogenous noble metals mineralization based on geochemical data // Regional geology and metallogeny. 2011. 48. P. 87-97. (in Russ.).

Goroshko M.V., Gur'yanov V.A. Conditions of location of complex uranium-rare metal mineralization in the massifs of

ultrabasic alkali rocks, south-eastern part of the Siberian platform //Tikhookeanskaya geology (Pacific Geology). 2004. V. 23. 2. P. 76-91. (in Russ.).

Proskurnin V. F., Petrov O. V., Gavrish A. V. et al. The Early Mesozoic carbonatite zone of Taimyr Peninsula // Lithosphere. 2010. 3. P. 95–102. (in Russ.).

Sazonov A.M., Zvyagina E.A., Leontiev S.I. et al. Platinum-bearing alkaline-ultrabasic intrusions of the Polar Siberia / Tomsk CSTI. 2001. 510 p. (in Russ.).

Malitch K.N. Platinum-group elements in clinopyroxenite-dunite massifs of the East Siberia (geochemistry,mineralogy, and genesis). / St.-Petersburg: Saint Petersburg Cartographic Factory VSEGEI Press. 1999. 296 p. (in Russ.).

Malitch K.N., Sorokhtina N.V., Badanina I.Yu., Kononkova N.N. Parent Sources of NobleMetal Placers of the Guli Massif (Polar Siberia): New Mineralogical Data // Doklady Earth Sciences, 2013. V. 451, P. 1, P. 743–745.

Shpachenko A.K., Savchenko E.E. Tellurium and bismuth minerals in carbonatites and alkaline rocks of the Kola Peninsula // Geology and mineral resources of European northeast part of the Russia. Mat. XIV of Geology congress of the Komi Republic. V. 2. Syktyvkar. Geoprint 2004. P. 244-246. (in Russ.).

Taylor L.A. The system Ag-Fe-S: Phase equilibria and mineral assemblages //Mineralium Deposita. 1970.5. P.41–58.

Ba-dominant fluoroaluminates from the Katugin rare-metal deposit (Transbaikalia, Russia): chemical and Raman data

Starikova A.E., Sharygin V.V.
V.S. Sobolev Institute of Geology and Mineralogy SB RAS, Novosibirsk, Russia, a_sklr@mail.ru

The Katugin rare-metal deposit is located at the Kalar district in northern Zabaikalskii region. It is one of the largest Precambrian Ta-Nb-Y deposits in Russia and belongs to the category of unique deposits containing industrial concentrations of Zr, Nb, Ta, U, REE and cryolite. The source of ore and host rocks genesis are still actively debatable. Some authors classify them as alkaline metamorphic metasomatites which are related to deep-seated faults without any connection with magmatism (Arkhangelskaya et al., 1993; 2012). However, in recent publications the host rocks are considered to be alkali granites and ore mineralization is related to magmatic or early post-magmatic stage (Levashova et al., 2014). According to the recent data, the U-Pb age of the Katugin alkali granites is 2066 ± 6 Ma (Larin et al., 2002).

Alkali granites of the Katugin deposit are mainly composed by quartz-albite-K-feldspar association. Mafic minerals (arfvedsonite, aegirine, fluorannite, astrophyllite) are in principal amounts and indicate a zonation in the host rocks of the deposit (Arkhangelskaya et al., 1993; 2012). From rim to center of the ore body annite and annite-arfvedsonite-bearing granites gradually pass into arfvedsonite-bearing and than aegirine-arfvedsonite and aegirite-bearing species. Pyrochlore, zircon, REE-rich fluorides and cryolite are main ore components. Cryolite Na_3AlF_6 commonly forms small isolations in granites and larger veins or lenticular bodies of cryolite-rich (>30-50 vol.%) rocks (Arkhangelskaya et al., 1993; 2012). This mineral is associated with other fluoroaluminates and fluorides (weberite Na_2MgAlF_7, chiolite $Na_5Al_3F_{14}$, neighborite $NaMgF_3$, fluorite, tveitite-(Y), fluocerite-(Ce), gagarinite-(Y), yttrofluorite, elpasolite K_2NaAlF_6, simmonsite Na_2LiAlF_6) and products of their alteration (gearksutite $CaAlF_4(OH) \cdot H_2O$, prosopite $CaAl_2(F,OH)_8$, thomsenolite $NaCaAlF_6 \cdot H_2O$, pachnolite $NaCaAlF_6 \cdot H_2O$, ralstonite $Na_xMg_xAl_{2-x}(F,OH)_6 \cdot H_2O$) (Bykov, Arkhangelskaya, 1995; Arkhangelskaya et al., 2012; Sharygin, Vladykin, 2014).

In aegirine-arfvedsonite granites we have found individual fluoroaluminate segregations, which are dominant in Ba-rich fluoroaluminates (Fig.1a). Their sizes are up to 1 cm and they are red-colored due to the presence of iron oxides and hydroxides. Three Ba-containing fluoroaluminates were identified in the segregations: usovite $Ba_2CaMgAl_2F_{14}$, $BaAlF_4(OH)$ (possible Ba-analogue of jakobssonite $CaAlF_4(OH)-CaAlF_5$) and $BaCa_2AlF_9$ (Table, Fig. 1). It should be noted that these Ba-minerals have never been described in the Katugin rocks, and the two last phases are firstly found in natural conditions, although their synthetic analogues are known (Weil et al., 2001; Groß et al., 2007). Ba-rich phases are associated with minor cryolite, weberite, prosopite, pachnolite, thomsenolite and fluorite and seem to be primary in the fluoroaluminate segregations. Silicates are absent in these segregations. Usovite is close to ideal composition. The $BaAlF_4(OH)$ phase forms prismatic or splintery grains and contains up to 5.5-6 wt.% oxygen (Table). Raman data confirm the presence of OH-group: all spectra show strong stretching vibration bands in the 3500-3600 cm⁻ region (Fig. 2). Four modifications are known for synthetic $BaAlF_5$ (Weil et al., 2001). Assuming geological conditions, phase transitions and phase stability for $BaAlF_5$, we suggest that the Katugin $BaAlF_4(OH)$ phase is seems to be *alpha* or *beta* polymorph. The $BaCa_2AlF_9$ phase was identified around weberite grains in one of segregations and it forms intergrowths with fluorite (Fig.1b). Microprobe analyses did not indicate the presence of oxygen. Unfortunately, we failed to determine the presence or absence of the OH-group or H_2O in the structure of this mineral due to high luminescence under Raman laser in the 2000-4000 cm⁻ region.

Table. Chemical composition (EDS, wt.%) of Ba-dominant fluoroaluminates from the Katugin deposit.

| Phase	Usovite $Ba_2CaMgAl_2F_{14}$				$BaAlF_4(OH)$				$BaCa_2AlF_9$		
	1	2	3	4	5	6	7	8	9	10	11
Si	0.14	0.22	0.24	0.32	0.19	0.16	0.24	0.18	0.16	0.27	0.22
Al	7.63	7.50	7.91	7.68	10.11	10.18	9.99	10.10	6.61	6.27	6.59
Mg	3.26	3.23	3.32	3.24	-	-	-	-	-	-	-
Ca	5.97	5.94	5.83	5.92	-	-	-	-	19.03	19.98	18.85
Ba	43.08	43.03	42.24	42.30	53.32	53.34	53.08	53.59	33.58	32.40	34.30
Sr	-	-	0.37	0.42	-	-	-	-	0.65	0.62	-
F	40.57	39.15	40.49	39.90	30.81	30.74	30.71	30.34	41.97	41.73	41.46
O	-	-	-	-	5.71	5.45	5.77	5.73	-	-	-
Total	100.65	99.07	100.40	99.78	100.14	99.87	99.79	99.94	102.00	101.27	101.42

Note: Na, Fe, Mn, K are below detection limits (<0.1 wt.%).
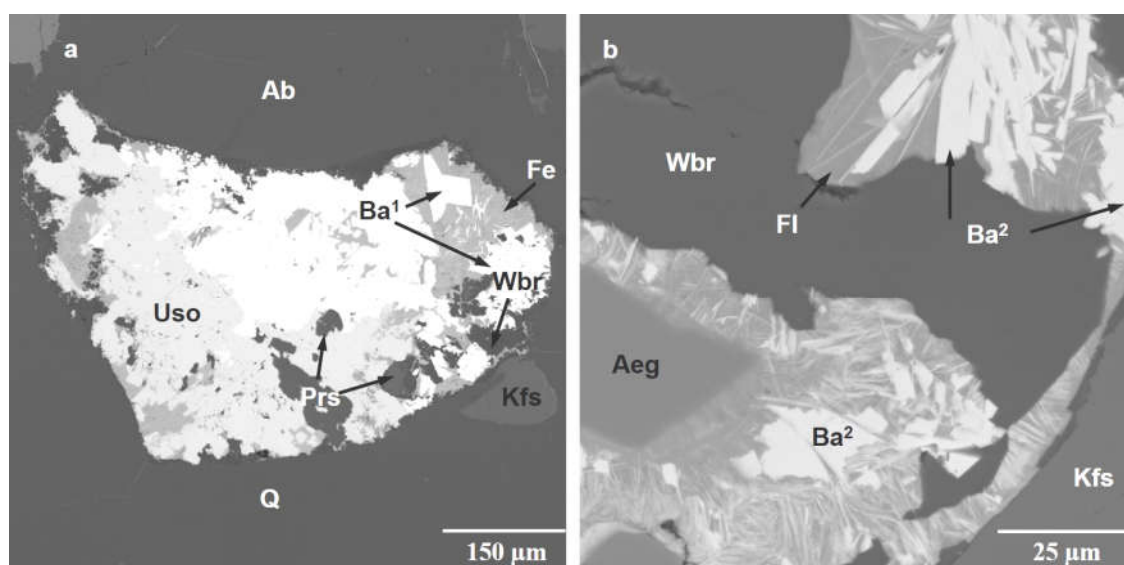
Figure 1. BSE images of fluoroaluminate segregations. Ba[1] - $BaAlF_4(OH)$, Ba[2] - $BaCa_2AlF_9$, Prs – prosopite, Wbr- weberite, Uso – usovite, Fl – fluorite, Ab – albite, Aeg – aegirine, Fe - iron oxides and hydroxides, Kfs – K-feldspar, Q – quartz.
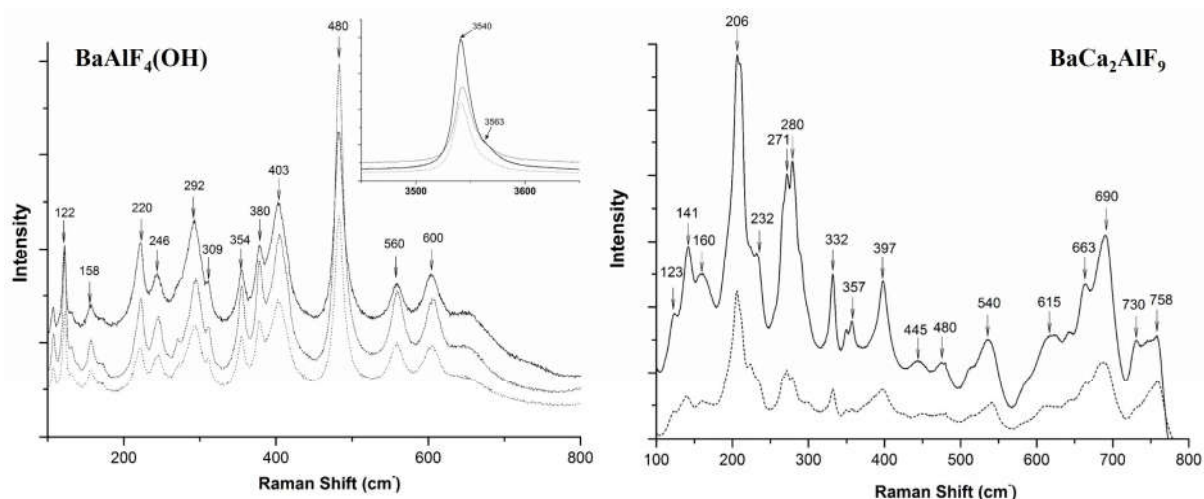
Figure 2. Raman spectra of BaAlF$_4$(OH) and BaCa$_2$AlF$_9$ phases.

References:

Arkhangelskaya V.V., Kazan V.I., Prokhorov K.V., Sobachenko V.N. Geological structure, zoning and conditions of formation of Katugin Ta-Nb-Zr-deposit (Charo-Udokan region, Eastern Siberia) // Geology of Ore Deposits. 1993. Vol. 35. P. 115-131.

Arkhangelskaya V.V., Ryabtsev V.V., Shuriga T.N. Geology and mineralogy of the Russian Ta deposits. Mineral raw materials. 2012. № 25. Moscow: VIMS. 318 p.

Bykov Y.V., Arkhangelskaya V.V. The Katugin rare-metal deposits // *In:* Deposits of Transbaikalia. 1995. Vol. 1, Chita-Moscow, Geoinformmark. P. 76-86.

Groß U., Rüdiger S., Kemnitz E. Alkaline earth fluorides and their complexes: A sol-gel fluorination study // Solid State Sciences. 2007. V. 9. P. 838-842.

Larin A.M., Kotov A.B., Sal'nikova E.B., Kovalenko V.I., Kovach V.P., Yakovleva S.Z., Berezhnaya N.G., Ivanov V.E. About the age of Katugin Ta-Nb deposit (Aldan-Stanovoi shield: the problem of selection of a new global epoch of rare metallogeny) // Doklady Akademii Nauk. 2002. V. 383. № 6. P. 807-811.

Levashova E.V., Skublov S.G., Marin Yu., Lupashko T.N., Ilchenko E.A. Trace elements in zircon from rocks of Katugin rare metal deposits // Zapiski Rossiiskogo Mineralogicheskogo Obshchestva. 2014. Vol. 143. № 5. P. 17-31.

Sharygin V.V., Vladykin N.V. Mineralogy of cryolite rocks from Katugin massif, Transbaikalia, Russia // Abstract book of 30th International Conference "Ore Potential of Alkaline, Kimberlite and Carbonatite Magmatism" (eds., Ilbeyli N., Yalcin M.G.), Antalya, Turkey.2014. P. 166-168.

Weil M., Zobetz E., Werner F., Kubel F. New alkaline earth aluminium fluorides with the formula (M, M′)AlF$_5$ (M, M′ = Ca, Sr, Ba) // Solid State Sciences. 2001. V. 3. P. 441-453.

Adakites: compositions of melts, residual glasses and rocks

Tolstykh M.L., Naumov V.B.

V.I. Vernadski Institute of Geochemistry and Analytical Chemistry of Russian Academy of Sciences, *Russia, Moscow, mashtol@mail.ru*

The assumption was based on geodynamic location of magmatic centers (Kay, 1978, Yogodzinsky, Kelemen, 1998), as well as on the results of experiments on the partial melting of basic rocks (Beard, Lofgren, 1991; Rapp, 1995).

This term have become popular, there are more than 500 analyses of adakites in the GEOROCK database (www.georoc.mpch-maigwdg.de). These rocks are located in different geodynamic conditions: subduction, collision, continents, orogens, etc. In fact, the adakites are most widely presented at the Kurile-Kamchatkan, Aleutian, Filipine island arcs, and at the Chinese greenstone belts.

Now we have several different assumptions about adakites origin (Castillo, 2012).

- melting of oceanic crust
- melting of mantle wedge, metasomatized by subduction melt or fluid
- melting of mafic lower crust
- differentiation of parental basaltic magma

All points of view are based on ideas about adakites as melts of different genesis. But it's not an easy problem to find an adakitic melt.
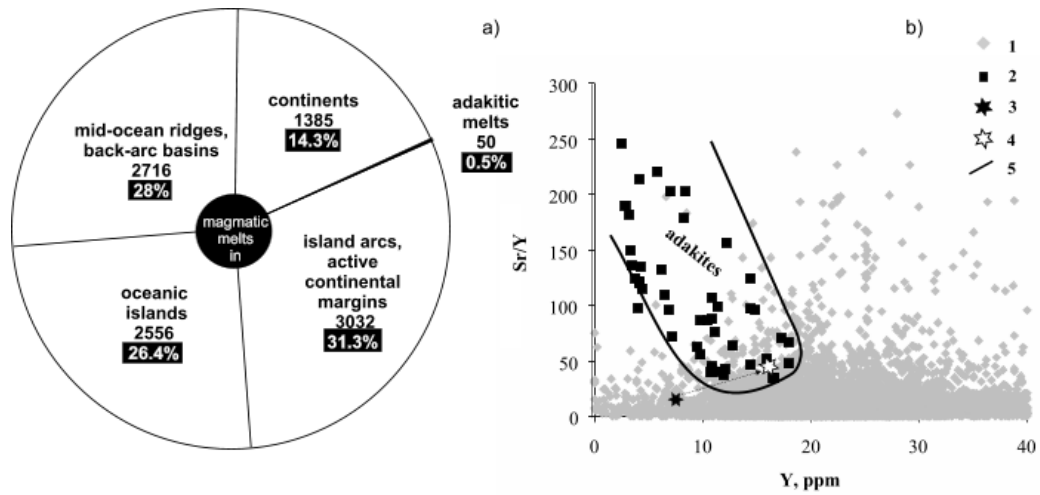
Fig.1. Adakitic melts among another types of glasses (Naumov et al., 2010)
a) The ratio of the total number of glasses in different rocks and adakitic glasses (only analyses with reported trace element composition were used for this plot).
b) Variation diagram for all types of glasses
1 - andesitic and dacitic glasses; 2 – glasses with the "adakitic mark"; 3 – melt inclusion (average value) from andesites of Sheveluch volcano (Kamchatka); 4 – rocks (average value) from Sheveluch; 5 – field of adakites (Castillo, 2012).

Andesitic and dacitic melts with the high Sr and low Y content were not detected in the GEOROCK database among 20000 assays of glasses. In a specialized database of glasses (Naumov et al., 2010) only 50 adakitic melts were found among 65000 analyses (fig.1). 22 analysis are glasses of the melt inclusions, the others are "vein glass" and "pocket melts" of mantle xenolithes and groundmass residual glasses. We can't regard the xenolithic glasses as rudiments of the initial melt, because they are most likely the result of the secondary non-equilibrium melting (Borisov, 2011). The residual glass of volcanic rocks groundmass is a result of differentiation of the rock-forming melt. Consequently, the true adakitic melts are currently represented by 22 melt inclusions from volcanic rocks of the Saint-Helens, Shasta, Paricutin, Colima (North and Central America). Thus, adakitic melts are extremely rare in the area of the finding adakitic rocks.

For example, on the Sheveluch volcanic massif despite of abundance of the adakitic rocks (Volynets et al., 2000) adakitic melts are not detected (Tolstykh et al., 2015) (Fig. 1b). Howewer these rocks could get the adakitic mark in a processes of accumulation of crystalline phases, if we consider andesites as cumulative rocks with a predominance of plagioclase (fig.2).
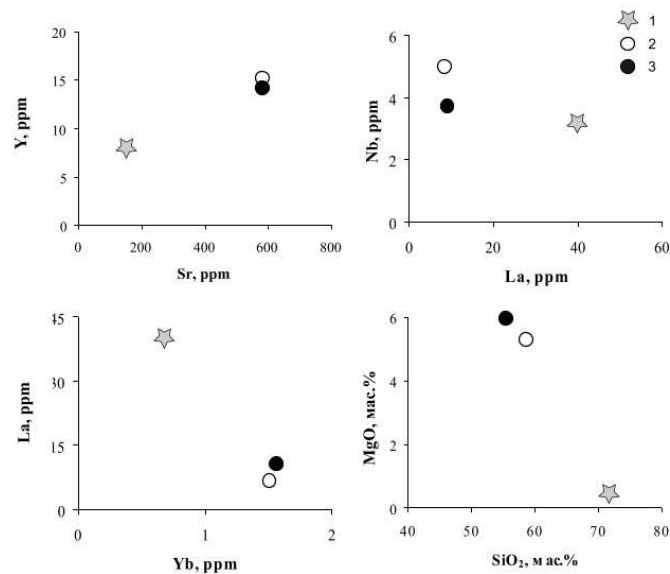

Fig.2. Sr-Y, La-Yb, La, SiO$_2$-MgO diagrams for melts and natural and modeled rock compositions.
1 – melt (measured), 2 – rock (measured), 3 – rock (calculated): glass 18vol.% +Amph vol. 30%+ Cpx 9vol. % + Pl 42vol.% + (Mt+Sp) 2 vol.% +Ol 1 vol%. R^2=0.99.

132

Based on the analysis of the available literature data and our own research, we propose the following conclusions:

1. Distribution of adakitic melts are extremely limited and rarely coincides with the distribution of adakitic rocks.

2. Ideas about the genesis of adakites associated with the crystallization of adakitic melts are rarely reflected in reality.

3. "Adakite mark" in rocks may be the result of fractionation/accumulation of mineral phases.

4. The using of the term "adakite" as a marker of a certain geodynamic conditions (f.e. collision or subduction) may be unjustified.

References:

Beard J.S., Lofgren G.E. Degydration Melting and Water-Saturated Melting of Basaltic and Andesitic Greenstones and Amfibolites at 1, 3, and 6-9 kb // J. Petrology. 1991. V.32. P. 365-401.

Borisov A. Diopside melting in sodium vapor: an experimental study // Abstracts of International conference "Ore potential of alkaline, kimberlite and carbonatite magmatism". 2011.

Castillo P. R. An overview of adakite petrogenesis // Chinese Science Bulletin. 2006. V. 51. P. 257-267.

Defant M.J., Drummond M.S. Derivation of some modern arc magmas by melting of young subducted lithosphere // Nature. 1990. V. 347. P 662-665.

Kay R.W. Aleutian magnesian andesites: melts from subducted Pacific Ocean Crust. // J. Volcan. Geotherm. Res. 1978. V. 4. P. 117-132.

Naumov V.B., Kovalenko V.I, Dorofeeva V.A., Girnis A.V., Yarmoluk V.V. Average compositions of igneous melts from main geodynamic settings according to the investigation of melt inclusions in minerals and quenched glasses of rocks // Geochemistry International. 2010. V. 12. P. 1185-1207.

Rapp R. Amphibole-out phase boundary in partially melted metabasalt, its control over liquid fraction and composition, and source permeability // J. Geophys. 1995. Res. 100. P. 15601-15610.

Tolstykh M.L., Pevzner M.M., Naumov V.B., Babanskiy A.D., Kononkova N.N. Types of melts from pyroclastic rocks of different structural-age complexes of the array Sheveluch (Kamchatka): melt inclusion evidence // Petrology. 2015. In press.

Volynets O., Woerner G., Babansky A., Dorendorf F., Churikova T., Yogodzinski G., Goldsman Yu., Agapova A. Variation in geochemistry and Sr-Nd isotopesin lavas from Northern Volcanic group, Kamchatka: Evidence for distinct sources at the subducting transform system // Amer. Geoph. Union. Fall meetimg. 1997. EOS supplements 78-46.

Yogodzinskiy G.M., Kelemen P.B. Slab melting in the Aleutians: Implication of an ion probe study of clinopyroxene in primitive adakite and basalt // Earth Planet Sci. Letter. 1998. V. 121. P. 227-244.

Formational typification of Early-Hercynian volcanic complexes in Archangelsk kimberlite-picrite province

Tretyachenko V.V.*, Garanin V.K.**,***, Bovkun A.V.***, Garanin K.V.***
*SRGE SC "ALROSA", Archangelsk, Russia;
**A.E. Fersman Mineralogical Museum of RAS, Moscow, Russia;
***Geological Faculty, M.V. Lomonosov Moscow State University, Moscow, Russia
VTretiyachenko@severalmaz.ru

The first in Europe discovery of primary/kimberlitic diamond deposits at the Winter Coast of White Sea: named after M.V. Lomonosov and V. Grib, predetermined the region as the global impact source of diamonds. Currently, more than one hundred kimberlites, its converged rocks and tholeiitic basalts have discovered within the White Sea-Kuloskoye plateau and Onega Peninsula (Bogatikov et al., 1999). The largest regional formational taxon specified accordingly (Tretyachenko, 2008): Zimneberezhny Mega-Complex of kimberlites and non-pyroxene alkaline picrites, Nenokso-Chidvinsky Mega-Complex of feldspar picrites-olivine melilitites, and Soyana-Pinezhsky dolerite-basalt Complex (Fig. 1).

1. Diamondiferous kimberlites of Zimneberezhny Mega-Complex presented by Zolotitsky Complex (Mg-Al) and Chernoozersky Complex (Fe-Ti). Zolotitsky Complex includes of 10 pipes (Fig. 1) where five pipes (Archangelskaya, Karpinskogo-1, Karpinskogo-2, Pionerskaya, Lomonosovskaya) are among M.V. Lomonosov diamond deposit. Chernoozersky Complex (Tretyachenko, 2008) is presented by a single V. Grip pipe/diamond deposit.

Diamondiferous kimberlites have following petrochemical characteristics: high magnesium content, low concentrations of alumina, almost a total absence of silicate calcareous earth and Ca-Na type of alkalinity. Zolotitsky Complex kimberlites belong to type-I (low-titaniferous) and V. Grib kimberlites belong to type-II (moderately-titaniferous) according to Ti-content (Bogatikov et al., 2007).

There is a significant domination of olivine-I phenocrysts within these kimberlites matrix. Cr-diopside-pyrope-chromite assemble is peculiar to Zolotitsky Complex and pyrope-picroilmenite assemble is peculiar to V. Grib pipe kimberlites among high-barophilic accessory minerals of kimberlites. An important feature of diamondiferous kimberlites is typomorphic specialization of groundmass microcrystalline oxides: chromites prevail within Zolotitsy Complex kimberlites, but picroilmenites-chromites are dominated in V. Grib pipe kimberlites groundmass.

Zolotitsky and Chernoozersky Complexes kimberlites are significantly different from other non-diamondiferous rocks of the region according to Nb- and Zr-contents, Sm-Nd and Rb-Sr parameters (Tretyachenko et al., 2010). Generally Zolotitsky Complex kimberlites are similar to diamondiferous kimberlites of Srednemarkhinsky district, Yakutian Diamondiferous Province and Chernoozersky Complex kimberlites are similar to kimberlites of Malo-Botuobinsky and Daldyno-Alakitsky districts, Yakutian Diamondiferous Province. Zolotitsy and Chernoozersky Complexes kimberlites hold transitional position between Groups I and II of South African kimberlites, and, thus, are defined in individual Zolotitsky type (Bogatikov et al., 2007).

2. Non-diamondiferous and poor-diamondiferous kimberlites and alkaline picrites of Zimneberezhny Mega-Complex (Mg-Al rocks of Verkhotinsky and Fe-Ti rocks of Kepinsky, Megorsky, and Melsky Complexes) and Mg-Al-feldspar picrites-olivine melilitites Nenoksko-Chidvinsky Mega-Complex (Nenoksky, Chidvinsko-Izhmozersky and Suksomsky Complexes) in contrast to the above-described diamondiferous kimberlites are characterized by clear predominance of olivine-II phenocrysts, as well as the presence of a significant variable number of melilite, nepheline and clinopyroxene microliths.

Monticellite and richterite are identified in some pipes of Chidvinsko-Izhmozersky Complex. Clinopyroxene phenocrysts are dominated among rocks matrix of Nenoksky Complex pipes. Wide-spread occurrence of phlogopite phenocrysts is one of the most important features of Verkhotinsky and Melsky Complexes picrites. Fe-Ti kimberlites and picrites of Kepinsky and Megorsky Complexes are characterized by elevated and high concentrations of total Fe and Ti, these rocks are attributed to type-III (high-titaniferous) according to Bogatikov et al. classification (Bogatikov et al., 2007). Mg-Al-picrites of Verkhotinsky Complex are characterized by low-magnesium content and elevated contents of aluminous and silicate calcareous earth. Generally, Nenoksko-Chidvinsky Mega-Complex volcanites have significant contents of alumina, silicate calcareous earth and total alkali with stable prevalence of sodium over potassium, and low magnesium content.

Picroilmenite concentrations are significantly higher than pyrope concentrations in high-barophilic accessory minerals of kimberlites of Kepinsky Complex, but chromite is dominated in picrites of Kepinsky Complex and Nenoksko-Chidvinsky Mega-Complex volcanites. Non-diamondiferous volcanites are characterized by titanomagnetite-rutile specialization of groundmass microcrystalline oxides within Fe-Ti-type rocks matrix, and chromite-titanomagnetite specialization is a feature of Mg-Al-type rocks matrix.

Generally, indicative characteristics of non-diamondiferous Fe-Ti-kimberlites and non-pyroxene picrites of Zimneberezhny Mega-Complex allow to assign these rocks with Group I of South African kimberlites, kimberlites and picrites of northern fields of Yakutian Diamondiferous Province. These rocks are related to type-III (high-titaniferous) kimberlites (Bogatikov et al., 2007). Feldspar picrites and olivine melilitites of Nenoksko-Chidvinsky Mega-Complex are similar to alnoite-picrites, and attracted to Group II kimberlites of South Africa according to Sm-Nd and Rb-Sr isotopic systems parameters.

3. Soyana-Pinezhsky dolerite-basaltic Complex join three groups of pipes in eastern part of Winter Coast of White Sea: Soyanskaya, Kovalgsko-Poltozerskaya, Chuplega-Pinezhskaya (Fig. 1). Petrological features of these rocks are similar to tholeiitic basalts of intra-platform continental environment, it allows to consider this Complex in the structure of Early-Hercynian dolerite-basaltic formation of Eastern-Europian platform (Tretyachenko, 2008; Tretyachenko et al., 2010).

It should be pointed that diamondiferous kimberlites of Zolotitsky and Chernoozersky Complexes have been formed during Late Devonian-Early Carboniferous Eras (Fammenian-Visean Age, 370-340 ma), similar to kimberlites of Malo-Botuobinsky, Daldyno-Alakitsky and Verkhnemunsky districts (Yakutian Diamondiferous Province). The other bodies of kimberlites, its converged rocks and tholeiitic basalts have been formed earlier: Pragian-Frasnian Age, 410-375 ma (Kepinsky, Megorsky, and Melsky Complexes), Zhivetian-Frasnian Age, 387-375 ma (pipes of Nenoksko-Chidvinsky Mega-Complex and Soyana-Pinezhsky Complex) (Tretyachenko, 2008; Tretyachenko et al., 2010).
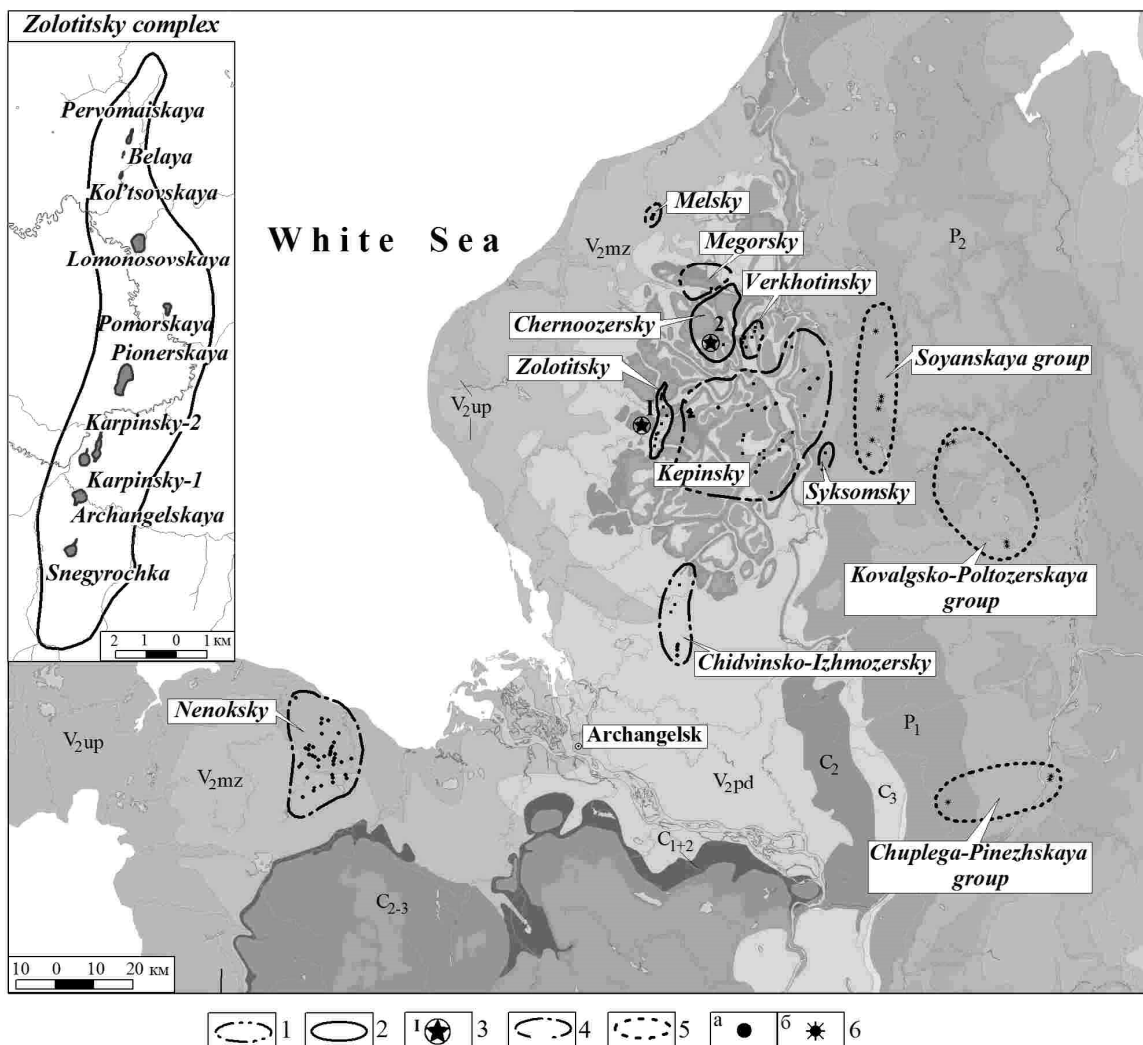
Fig. 1. The location of kimberlites, its converged rocks and basaltic diatremes of Early-Hercynian complexes within Southern-Eastern White Sea region. 1-3 - Zimneberezhny Mega-Complex: 1 – Fe-Ti type (Kepinsky, Megorsy, Melsky, Chernoozersky Complexes); 2 – Mg-Al type (Zolotitsky, Verkhotinsky Complexes); 3 – Diamond deposits (1 – M.V. Lomonosov, 2 – V. Grib); 4 – Nenoksko-Chidvinsky Megacoplex (Nenoksky, Chidvinsko-Izhmozersky, Suksomsky Complexes); 5 – Soyana-Pinezhsky basaltic Complex pipes groups (Soyanskaya, Kovalgsko-Poltozerskaya, Chuplega-Pinezhskaya); 6 – Diatremes: a – kimberlites, picrites, olivine melilitites, b – tholeiitic basalts.

References:

1. Bogatikov, O.A., Garanin, V.K., Kononova, V.A., Kuryavtseva, G.P. et al. Archangelsk Diamondiferous Province. Moscow. 1999. 524 p. *In Russian*

2. Bogatikov, O.A., Kononova, V.A., Nosova, A.A., et al. Kimberlites and lamproites of Eastern-Europian platform//Petrology. 2007. № 4, V. 15. 339-360 pp. *In Russian*

3. Tretyachenko, V.V. Mineragenetic zonation of kimberlitic region of Southern-Eastern Belomorie. PhD. Thesis. Moscow, MSU. 2008. 28 p. *In Russian*

4. Tretyachenko, V.V., Bovkun, A.V., Garanin, K.V. Formational features of Early-Hercynian alkaline-ultrabasic and basic volcanic complexes and criteria of kimberlitic diamond grade// Collected papers after 3-4 Scientific Readings named after G.P. Kudryavtseva. Moscow, Institute of Applied Mineralogy. 2010. 219-252 pp. *In Russian*

Composition of mineral-forming environment of Kulemshor rare metal occurrence (Subpolar Urals)

Udoratina O.V.*, Varlamov D.A.**, Shevchuk S.S.*
*IG Komi SC UB RAS, Syktyvkar, Russia
**IEM RAS, Chernogolovka, Russia
udoratina@geo.komisc.ru

Rare, REE, radioactive metal mineralization is localized in cataclased and albitized granites in the Kulemshor area in the southern part of Torgov-Keftalyk granite massif (upper courses of the Torgovaya River, Subpolar Urals) (Udoratina et al., 2014b).

Ore-bearing granitoids are located in Riphean metamorphites of Central Ural uplift (southern part of Lyapinsky anticlinorium). The granitoids show changing microstructures from graphitic granite to structures of initial cataclase and to emergence of signs of initial milonitization. Dynamometric transformations are defining for localization of complex mineralization.

The sampled rocks were studied in transparent thin sections made on epoxy base and polished sections, because the crushed samples do not reveal ore minerals. Large quantity of zircon is observed together with uranium-thorium, rare metal and REE minerals, which is dispersed inside veinlets and composed of micrograined (1-10 mcm) aggregates.

Minerals, forming the rare metal-rare earth mineralization, are as follows (Udoratina, 2014d): (a) main – fergusonite, yttrialite, aeshynite, baestnesite; (b) rarer: thorite, fergusonite (including Yb- or Dy- selectively enriched), xenotime, monacite, synchysite, calcioancylite, brannerite, policrase, columbite, Nb-rutile, baddeleyite; (c) single: herenite-(Y), thorianite, various thorium phosphatosilicates. Primary minerals of niobium are fergusonite, columbite, Nb-rutile as inclusions in ilmenite or small separate individuals, for thorium – thorite (inclusions in primary zircon). REE primary minerals are monacite, xenotime and zircon. Imposed minerals are observed as fringes and margins of grains of rock-forming minerals and also fill the fractures and intergranular space. Imposed mineralization formed as a result of primary accessories transformation – allanite, titanite, apatite, zircon under influence of potassium-carbon dioxide metasomatosis.

BSE images revealed relation between rare metal ore minerals with zircon generation without certain crystalline shape and with rather specific look (Udoratina et al., 2014a). Distribution of ore minerals and zircon underlines cataclastic microstructure of the rocks. In these local zones, enriched by ore accessories, total Th+U, Nb+Ta, Zr, HREE content sharply, in tens times, increases.

Two types of zircons were found: primary crystals Zrn_1 (fig. 1, a), and plumose-lens-like aggregates of small crystallites Zrn_2 located in intercataclase space and with a complex look (fig. 1, b). We consider this zircon as newly formed.
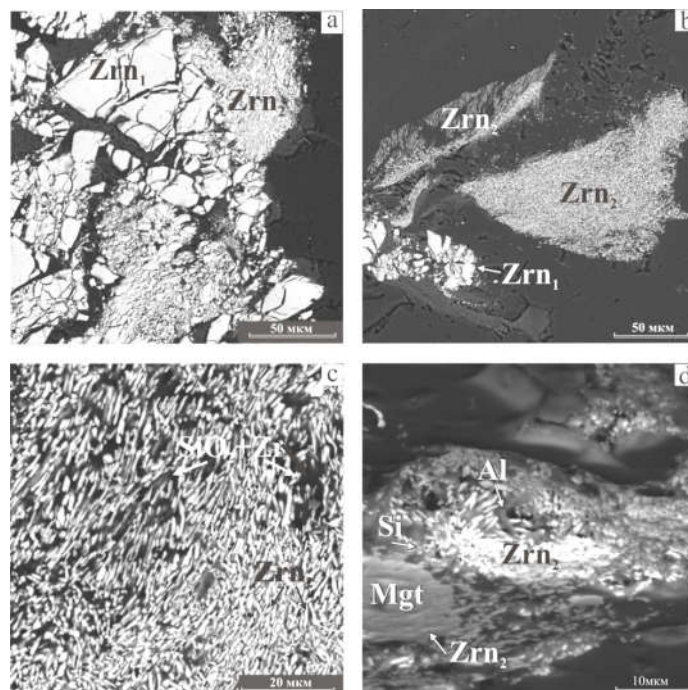

Fig.1 Examples of morphology of crystals and zircon aggregates: a – crystals of primary cataclased zircon Zrn_1; b – "flowing" structure generated by regenerated crystals of zircon Zrn_2, their intrusion in minerals; c – view of the regenerated crystals of zircons; d – regenerated crystals Zrn_2 in the alumosilicate matrix

The conducted isotope-geochemical studies revealed (Udoratina et al., 2014c) that apart from newly formed crystallites Zrn_2 the newly formed (non-cataclized) crystalline zircon Zrn_3 (grey in cathodoluminescent imaging) occurs here. The studies revealed that Zrn_1 substance was inherited and redistributed, but newly formed Zrn_3 shows sharply increased content of light rare earth elements. The age of magmatic (primary, cataclase) zircon Zrn_1 is 540.0±8.1 Ma, the age of newly formed crystallites Zrn_2 is impossible to determine due to small sizes less 20 mkm, the age of newly formed (non-cataclased) zircon Zrn_3 is 249.0±30 Ma.

Thus, we determine that the observed zircon structures formed in the process of metamorphic and hydrothermal-metasomatic transformation of primary zircon as result of cataclase (1), insignificant transfer (2) and regeneration of fragments to full crystals (3).

We studied environment where newly formed zircon crystals, associated with ore (radioactive - rare earth - rare metal) minerals, were located. According to microprobe studies it is a heterogeneous pseudoamorphous phase, in which alumosilicate matrix was observed during scanning. In some of analytic points albite and quartz was determined, but it was often impossible to determine the composition of alumosilicate, in which zirconium content is increased – protosubstance for its crystallization from heterogeneous solution (fig. 1 c-d). We think that the heterogeneous solution (suspension) transferred in intergranular space and fractures, formed at cataclase, and liquid and solid phases occurred within this solution. The crystallization of newly formed zircon crystallites occurred from hydrothermal solution enriched with ore elements and existing at temperatures and pressures that not exceeded level of epidote-amphibole and even greenshist faces.

References

Udoratina O. V., Varlamov D. A., Rakin V. I.(a) Gidrotermal'no-metasomaticheskii tsirkon (Kulemshorskoe proyavlenie, Pripolyarnyi Ural) (Hydrothermal-metasomatic zircon Kulemshor deposit, Subpolar Urals) // Problemy i perspektivy sovremennoi mineralogii (Yushkinskie chteniya – 2014): Materialy dokladov Mineralogicheskogo seminara. Syktyvkar: Geoprint, 2014. pp. 25-27.

Udoratina O. V., Kalinin E. P., Andreichev V. L., Kapitanova V. A., Ronkin Yu.L., Savatenkov V. M. (b) Granitoidy Torgovsko-Keftalykskogo massiva (Pripolyarnyi Ural): izotopno-geohimicheskie dannye (Granitoids of Torgov-Keftalyk massif (Subpolar Urals): isotope-geochemical data) // Izvestiya Komi SC 2014, No 3 (19), pp. 93-104.

Udoratina O. V., Coble M. A., Varlamov D. A. (c) Gidrotermal'no-metasomaticheskii tsirkon: geohronologiya rudnogo protsessa (Kulemshor, Pripolyarnyi Ural, Russia) (Hydrothermal-metasomatic zircon: geochronoly of ore process (Kulemshor, Subpolar Urals, Russia) // Granity i evolyutsiya Zemli: granity i kontinental'naya kora: Materialy II mezhdunarodnoi geologicheskoi konferentsii, 17-20 August 2014, Novosibirsk: SO RAN, 2014, pp. 205-207 ISBN 978-5-7692-1386-1

Udoratina O. V., Kapitanova V. A., Varlamov D. A. (d) Redkometall'nye granitoidy (Kulemshor, Pripolyarnyi Ural) (Rare metal granitoids (Kulemshor, Subpolar Urals) // Izvestiya Komi Nauchnogo Tsentra UrO RAN, No 1(17), Syktyvkar, 2014, pp. 57-70.

Titanium behavior in the Kryvbas rocks (Ukraine)

Velikanov Y.F., Velykanova O.Y.
M.P. Semenenko Institute of geochemistry, mineralogy and ore formation of NAS of Ukraine, Kiev, Ukraine
olgavelikanova1@rambler.ru

The Kryvy Rig iron basin is a complicated Precambrian structure composed by the Kryvy Rig series strata including volcanogenic, terrigenous, sedimentary-volcanogenic and terrigenous-chemogenic beds metamorphosed at different stages of regional metamorphism. The Kryvy Rig series consists of five suites.

The dominantly volcanogenic beds of the New Kryvy Rig suite covering the Archean granitoids represent the oldest beds of the series. The New Kryvy Rig suite, up to 1500 m in thickness, occurs as amphibolites and basic schists resulted from the amphibolite alterations during later metasomatism and metamorphism. The Skelevatsk suite represents arkose-fillite beds covering the New Kryvy Rig rocks. These formations occur as clastogenic (metasandstones, metagravelites, metaconglomerates) and fillitic (quartz-sericite and quartz-chlorite schists) beds, but also as talc-carbonate metamorphic schists derived from ultrabasic volcanic rocks. The Skelevatsk suite thickness varies from tens to 300-400 m. The Saksagan suite, up to 1500 m thick, covers the Skelevatsk rocks and represents the strata of sedimentary-volcanogenic and chemogenic-sedimentary rocks consisting of seven schistose horizons divided by seven ferrous horizons. The Gdantsi suite covers different horizons of the weathered Saksagan beds represented by metaconglomerates, metasandstones, and calcareous and mica schists. Marbles and quartz-calcareous rocks are of limited occurrence in the suite. The Gdantsi suite thickness reaches 2000m. The uppermost Gleyevatsk suite units terrigenous beds consisting of metasandstones, microgneisses and quartz-calcareous rocks in the bottom section and metasandstones, metagravelites and metaconglomerates in the top section.

The Kryvbas is surrounded by the Archaean and Proterozoic granitoid terrains. To the east, the Saksagan and Demurinsky granitoid complexes bound the Kryvy Rig sedimentary-volcanogenic formations. To the west, the structure abuts on the Ingulets plagiogranites and Kirovograd granites.

The ultrabasic rocks are developed in the Devladovo fault zone and Vysokopilska structure.

The Kryvy Rig structure and surrounding complexes do include neither Ti deposits nor big Ti ore showings, although geochemical behavior of Ti in the rocks is prospective.

Mineralogical-geochemical specialization and ore potential of Ti are different for different petrographic groups of the rocks, depending on their mineral composition, geotectonic history, and grade of metamorphic and metasomatic alterations. Geochemically, Ti always positively correlates with iron and is incorporated into many minerals. Many scientists have proved that Ti ores are concentrated in supergene zones of magmatic rocks but also in Ti placers. The magmatic deposits are spatially and genetically connected with ultrabasic, basic, alkali and carbonatite intrusions. Ultrabasites and volcanites of different complexes are different by Ti concentration. The highest Ti concentrations are related to the oceanic tholeiitic basalts.

In the metabasites of Kryvbass, V.V. Pokalyuk and Y.A. Kulish (2004) and other researchers established a range of volcanic associations including tholeiite, komatiite-tholeiite and basite-andesite associations.

The metamorphosed hyperbasites are less enriched in Ti than cumulative hyperbasites. Concentration and distribution of Ti in the rocks of the region significantly depends on its concentration in Ti-bearing minerals and their abundance. Ti forms ore minerals (ilmenite, titanomagnetite, rutile, titanite etc.) and is isomorphically incorporated into many accessories up to several percents.

Ti content in the ultrabasites of the Devladovo regional scale tectonic fault zone varies widely. Average and maximum concentrations of TiO_2 in ultrabasites of the Ternovka massif is 0.19 and 0.29 %, Veseloternovka massif – 0.8 and 0.88 %, Promijny massif – 0.12 and 0.14 %, Pryvorotnensky massif – 0.1 and 2.15 %, Kodaksky massif – 0.09 % and 0.34 %, Vodyansky massif – 0.43 and 0.49 %, Devladovo massif – 0.27 and 0.8 %, Krasnoyarsky massif – 0.03 and 0.05 %, Gulaypolsky massif – 0.31 and 0.42 %.

Olivines, ortho- and clinopyroxenes, chlorites, hornblende, kersutite and accessory chrome spinelides are Ti-bearing minerals in the ultrabasites of the above-noted massifs.

High-Ti monoclinic amphibole kersutite was at first time established during detailed mineralogical-petrographical investigations in the contact zone of the Devladovo massif with the host Demurino porphyry-like granites. Kersutite replaces pyroxene or fills interstitials of the rock-forming minerals.

In the host granitoids Ti content is usually less than 1 % at maximum of 0.75 % in granitoids of the Demurino complex. Ti is incorporated into titanomagnetite, feldspars, biotite, amphibole, epidote etc.

In the New Kryvy Rig metabasites, Ti content varies from 0.46 to 2.91 %. Ti is incorporated into ilmenite, titanomagnetite, titanite, biotite, but also into hornblende, tremolite, chlorite etc.

Average Ti concentrations in the rocks of the Skelevatsk suite is 0.3 % at maximum of 1 %. Obviously, major Ti minerals are mica, garnet, chlorite, magnetite, titanomagnetite and other accessory minerals of terrigenous origin.

The lowest Ti concentrations (0.07%) were found in iron horizons of the Saksagan beds whereas the schistose horizons contain up to 0.5 % of Ti. The schistose horizon K_2^{4c} of the Karl Liebknecht, Komintern and Frunze mines is especially enriched in Ti (up to 3 %). Magnetite, hematite, actinolite and chlorite are the major Ti concentrators in this horizon.

Carbonaceous and quartz-biotite schists of the Gdantsi suite near the Lenin mine contain up to 1 % Ti. Magnetite, titanomagnetite, biotite, sericite etc. are the major Ti concentrators in these rocks.

Ti content in mica schists, metasandstones and microgneisses of the Gleyevatsk suite reaches 2.65 %. Ti is incorporated into garnet, biotite, muscovite, sericite etc.

Summarizing, the highest and spatially most stable Ti concentrations are related to metabasites of the New Kryvy Rig suite. With the aim to investigate geochemical properties and Ti behavior in the volcanic rocks, a set of 165 chemical analyses of the rock samples with Ti contents varying from 0.46 to 2.91 % from different location along the Kryvy Rig structure were geochemically investigated.

Petrochemical coefficients calculated from the analyses data show their basaltic, tholeiitic, tholeiite-komatiitic and andesite-basaltic composition. These rocks form different beds of the strata, vary from several to several tens meters, with no visible regularities in their alternation. The andesite-basaltic association has higher alkalinity, contents of total Fe and Ti at decreased contents of MgO, CaO and Al_2O_3 comparatively to the komatiite-tholeiitic and tholeiitic associations.

Multiple alteration of the rocks in the sections, varied thickness of the petrochemical groups of the beds, interbedding of amigdaloid and massive metabasites may reflect recurrent volcanic activity in the region.

K_2O-Na_2O diagram demonstrates three major petrochemical groups of the rocks: high, normal and low alkalinity groups.

In summary, chemically different rocks of the Kryvbas contain numerous locations of anomalous Ti concentrations with their dominance in the metabasites of the New Kryvy Rig suite.

Nd and Sr isotopic composition of mineralized carbonatites

Verplanck P.L.*, Farmer G.L., Mariano A.N.***, Verplanck E.P**_**
*US Geological Survey, Denver, Colorado, USA
**University of Colorado, Boulder, Colorado, USA
***48 Page Brook Road, Carlisle, Massachusetts, USA
plv@usgs.gov

In this study we utilize Nd and Sr isotopic compositions from a suite of mineralized carbonatites to constrain the nature of the source of these magmas. Although radiogenic isotopic studies of carbonatites clearly point to a mantle origin, the wide range in isotopic compositions has led to contrasting views for which mantle reservoir or reservoirs are responsible for carbonatites. In recent years a renewed interest in carbonatite magmatism has occurred because carbonatite-related ore deposits are the principal source of the world's niobium and light rare earth elements (REEs) including La, Ce, Pr, and Nd. Carbonatites primarily occur in intracontinental settings associated with crustal thinning but have been identified in convergent margin and ocean island settings. Although there are more than 500 known carbonatites in the world, currently only four are being mined for REEs and three for Nb. To achieve ore-grade REE enrichment, the initial carbonatitic magma requires an adequate endowment of Nb and REEs and needs to evolve in such a way that these elements are concentrated in Nb- or REE-bearing mineral phases.

Carbonatite samples evaluated in this study are from four continents and span a wide range in age (~51 Ma to 1385 Ma), Nd concentrations (1,690 to 18,000 ppm), and Sr concentrations (2,290 to 159,500 ppm). Our new Nd and Sr isotopic data includes multiple samples for Mountain Pass (USA; $\varepsilon_{Nd\ i}$= -3.2 to -3.7, Sr_i = 0.70512 to 0.70594) and Elk Creek (USA; ~ε_{Ndi} = 1.7, Sr_i = 0.7035) and one sample each from Bear Lodge (USA; ε_{Ndi} = 0.1, Sr_i = 0.70441), Kangankunde (Malawi; ε_{Ndi} = 3.3, Sr_i = 0.70310), Adiounedj (Mali; ε_{Ndi} = -0.1, Sr_i = 0.70558), Mushgai Khudag (Mongolia; ε_{Ndi} = -1.3, Sr_i = 0.70636), and Araxá (Brazil; ε_{Ndi} = -4.4, Sr_i = 0.70495). Of this suite, only Mountain Pass and Araxá are mineralized carbonates currently in production for REEs and Nb respectively, with Araxá being the dominant source of the world's Nb. Other current primary carbonatite sources of light REEs are Bayan Obo (Inner Mongolia, China) and the Maoniuping and Dalucao (Daluxiang) deposits (Sichuan, China). Xu et al (2003) published Nd and Sr isotopic data for fluorite gangue minerals from Maoniuping (ε_{Ndi} = -3.7 to -4.3, Sr_i = 0.70603 to 0.70624). For this analysis we have not included isotopic data from Bayan Obo because it is an extremely complex deposit such that published isotopic data is difficult to evaluate. Interestingly, isotopic data from the 3 producing carbonatite REE/Nb deposits (Mountain Pass, Araxá, and Maoniuping) have broadly similar isotopic compositions (ε_{Ndi} =-3.2 to -4.4 and Sr_i=0.7051 to 0.7062). These isotopic compositions clearly point to a carbonated source within the lithospheric mantle for these REE and Nb carbonatite-related ore deposits. The other mineralized but unmined carbonatites have higher Nd initial isotopic compositions (ε_{Ndi} = -1.3 to 3.3) and a wider range in Sr isotopic compositions (Sr_i=0.70310 to 0.70637), but these data are consistent with the involvement of a lithospheric mantle reservoir as well.

References:
Xu, C., Huang, Z.-L., Liu, C.-Q., Qi, L., Li, W.-B., and Guan, T., 2003, Sources of ore-forming fluids in the Maoniuping REE deposit, Sichuan Province, China: Evidence from REE, radiogenic Sr, Nd, and stable-isotope studies: International Geology Review, 45:7, 635-645.

Petrology, geochemistry and composition rare-metal alkaline rocks in the South Gobi Desert, Mongolia

Vladykin N.V., Radomskaja T.A.

Institute of Geochemistry, Siberian Branch of the Russian Academy of Sciences, Russia

E-mail: vlad@igc.irk.ru

Earlier, a belt of alkali-granite plutons and a carbonatite province were discovered in the South Gobi Desert, Mongolia. The Lugingol pluton of pseudoleucitic syenites with carbonatites was assigned to the alkali-granite belt (Fig.1). However, new dating showed that it is 40 Myr younger than the Khan-Bogdo pluton and a large fault separates it from the alkali-granite belt. In the same part of the South Gobi Desert, a dike series of alkaline K-shonkinites with a rare-metal carbonatite vein was found by V.I. Kovalenko west of the Lugingol pluton, near Mt. Baruun Hasar Uula, and a dike series of alkali and nepheline syenites was found by us northeast of the Lugingol pluton.

These data give grounds to distinguish an intrusive complex of K-alkaline shonkinites and leucitic syenites with Late Paleozoic REE-bearing carbonatites. Thus, three alkaline-rock complexes of different ages are distinguished in the South Gobi Desert. We present refined geological maps of these complexes. The plutons of all three complexes are deposits of trace elements (REE, Nb, Zr, Y, P). The chemical composition of the silicate rocks of the complex, rare-metal agpaitic pegmatites, and carbonatite and apatite rare-metal ores was considered in detail. Shonkinites from Mt. Baruun Hasar Uula and the Mountain Pass mine (United States) and their carbonatites, along with the Lugingol carbonatites, belong to a single association of K-alkaline rocks and carbonatites, as evidenced by their identical chemical, mineral, and geochemical rare-metal compositions. Rare-earth element patterns and spidergrams show similarities and differences between the rare-metal rocks of three complexes as well as paragenetic differences between their rare-metal minerals. A rare process is described—the amorphization of rare-metal minerals, related to their high-temperature crystallization in a medium with abnormal silica contents of the Khan-Bogdo pegmatites. Three rare-metal complexes of different ages, associated with large trace-element deposits, are distinguished in the South Gobi Desert. They are characterized by different behavior of trace elements during ore formation and different assemblages of minerals concentrating trace elements.
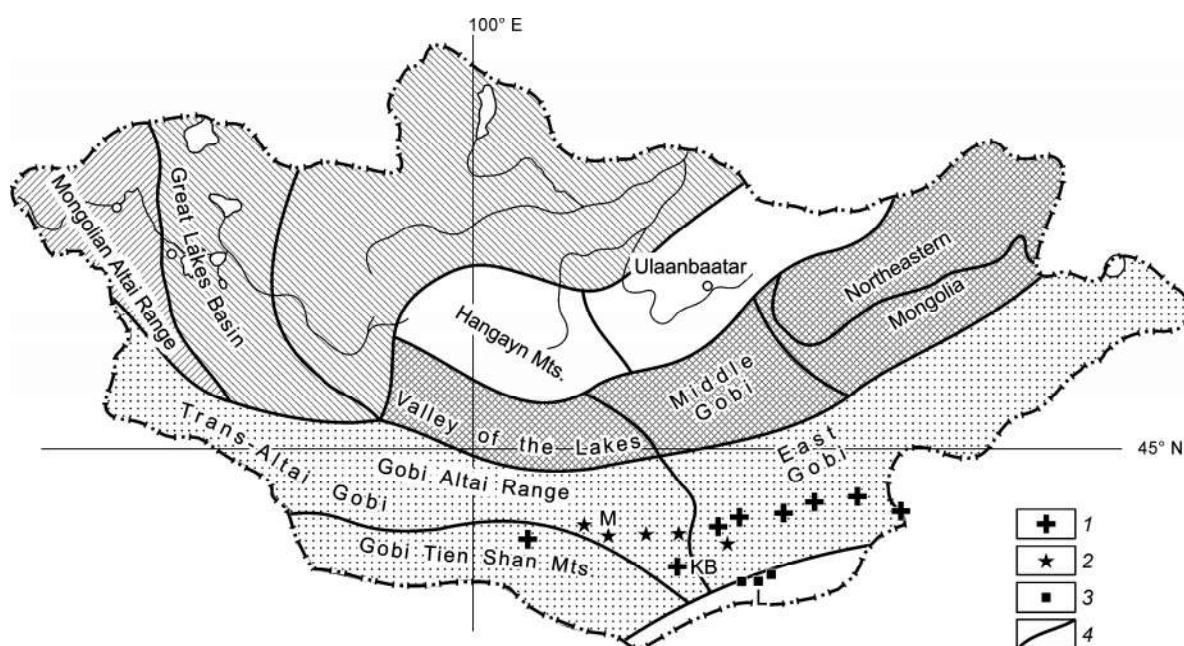
Fig. 1. Arrangement of alkaline plutons in the South Gobi area. *1*, alkali granites; *2*, plutons of a MZ-carbonatite complex; *3*, plutons of a PZ-carbonatite complex: M, Mushugai-Khuduk; KB, Khan-Bogdo; L, Lugingol; *4*, tectonic-block boundaries.

The Mushugai-Khuduk and Lugingol carbonatite complexes, like the large Mountain Pass and Baiyun Obo deposits, have many common geochemical features in the trace-element behavior and belong to the association of K-alkaline rocks. The volcanic-tuff process in the Mushugai-Khuduk complex produces peculiar enriched rocks with Pb, REE, F, and Ba mineralization. The parental magmas of the alkali-carbonatite complexes were generated from the EM-2 contaminated mantle that had undergone recycling, whereas the parental magmas of the Khan-Bogdo agpaitic alkali granites were produced from depleted mantle.

140

Rare earth elements in hot water

Williams-Jones A.E.
Department of Earth and Planetary Sciences, McGill University, Montreal, Canada
anthony.williams-jones@mcgill.ca

Although REE ore-formation is commonly dominated by magmatic processes, in many cases the REE have been remobilised by hydrothermal fluids and in some cases the deposits are almost exclusively hydrothermal in origin. Genetic models for the hydrothermal transport and deposition of the REE have generally assumed that the REE are transported mainly as fluoride complexes. Partly, this is because of a common association of the hydrothermal REE mineralisation with fluorite and partly because aqueous REE-fluoride complexes are orders of magnitude more stable than REE species involving most other plausible ligands. As a result, the potential role of these other ligands in transporting the REE to the sites of ore formation has largely been ignored. This contribution evaluates the nature of hydrothermal REE transport and the processes of REE mineral deposition in chlorine-, fluorine-, and sulphate-bearing hydrothermal fluids.

To provide a context for this study, features of four deposits that have been the subject of detailed investigation by the author and his students are reviewed. The Gallinas Mountains deposit, New Mexico, USA, is an exclusively hydrothermal light REE deposit of marginal economic interest in which a fluorite-bastnäsite-(Ce)-barite assemblage cemented quartz-syenite and sandstone breccias. Based on a detailed study of fluid inclusions, the deposit is interpreted to have formed between 300 and 400 ºC from brines containing 12 to 18 wt% NaCl equivalent (Williams-Jones et al., 2000). The Lofdal deposit, Namibia, is of considerably greater economic interest because it hosts a potentially economic resource containing 1.7 million tons of ore containing 0.6 wt% of heavy REE (HREE) oxide in the form of xenotime-(Y). An earlier study (Wall et al. 2008) had interpreted the ores to be hosted by carbonatites. However, our observations show that the mineralisation is concentrated in xenotime-(Y) veinlets that cut albitites developed along curvilinear structures and are in turn overprinted by calcite and/or dolomite. Significantly, the xenotime-(Y) grades outward and along strike into a monazite-(Ce)-rich halo. A carbonatite is inferred to be the source of the fluids. The Wicheeda deposit, British Columbia, Canada, is an example of potentially economic light REE mineralization (LREE), 11.3 million tons, grading 1.95 wt.% REE oxide hosted by carbonatite (Trofanenko et al., in press). However, the REE mineralisation, dominantly bastnäsite-(Ce), occurs with dolomite and fluorite in vugs and veins, and on the basis of C and O isotopic data, is clearly hydrothermal or carbo-hydrothermal. The fluids are inferred to have originated from the carbonatite magma and deposited the ores at a temperature between 300 and 400 °C. In addition to these dominantly hydrothermal deposits, there are a number of important deposits in which hydrothermal fluids remobilised magmatically concentrated REE. Among these are the Nechalacho and Strange Lake deposits in Canada. Both are characterised by appreciable proportions of HREE. The Nechalacho deposit contains a resource of 62 million tons grading 1.65 wt.% REE oxide (22% HREE) and 0.4 wt.% Nb oxide in a layered, silica-undersaturated alkaline complex in which the primary magmatic REE mineralisation formed as a result of gravity settling of eudialyte (a complex zirconosilicate containing $\sim$ 7 wt% REE_2O_3) and zircon (containing $\sim$ 3 wt.% REE_2O_3) (Sheard et al 2012). Hydrothermal fluids subsequently dissolved these minerals and re-precipitated the REE as fergusonite-(Y), secondary zircon, allanite-(Ce), bastnäsite-(Ce) and monazite-(Ce) together with fluorite. The HREE were deposited proximal to the precursor minerals, whereas the LREE were mobilised on a scale of metres and perhaps 10s of metres. At Strange Lake, the REE deposit (20 million tons grading 1.44 wt% REE, of which 50% are HREE, and 0.3 wt.% Nb) is hosted by rare metal pegmatites in a peralkaline granite pluton, and was the product of the product of late stage accumulation of an immiscible fluoride melt into which the REE were preferentially partitioned (Vasyukova and Williams-Jones, 2014). Hydrothermal fluids remobilised a complex assemblage of primary REE minerals and deposited the LREE as bastnäsite-(Ce) and fluocerite-(Ce) and the HREE as Gadolinite group minerals (Gysi and Williams-Jones, 2013). The remobilisation was effected by brines containing 26 wt% NaCl eq. at temperatures between 400 and <150ºC (Salvi and Williams-Jones, 1990, 1992).

Experimental studies have shown that the REE form very stable fluoride complexes in hydrothermal fluids, that REE-sulphate complexes have lower stability and that REE complexes with chloride ions are less stable than with the other two ligands (Migdisov and Williams-Jones, 2008; Migdisov et al., 2009). There are no experimental data on the stability of other potentially important REE complexes, e.g., those involving carbonate. Theoretical calculations suggest, however, that the stability of REE-carbonate complexes is comparable to that of REE-fluoride complexes. The Experimental studies have shown that the stability of the REE fluoride and chloride complexes decreases with increasing atomic number of the lanthanides, implying that the LREE are likely to be more mobile than the HREE. This effect, however, is not observed with sulphate complexes.

From our earlier description of a selection of REE deposits in which hydrothermal fluids played a role in REE concentration, it is evident that in some cases at least the fluids were chloride-bearing brines and from the association of the ores with fluorite and in some cases barite, that they may have contained significant fluorine and sulphate ions. Unfortunately, the only reliable measurements of the fluorine and sulphate concentrations of

fluids known to have precipitated REE minerals are those of Banks et al. (1994). These fluids contained ~500 ppm F and 2 wt.% SO_4^{2-}. We have modelled the transport of the REE for a fluid containing these concentrations of fluoride and sulphate and a concentration of chloride equivalent to 10 wt.% NaCl, and temperatures up to 400 °C. From this modelling, it is evident that significant concentrations of REE can only be transported as chloride complexes and at low pH, or as sulphate complexes at mildly acidic pH and high temperature. There are no conditions at which fluoride complexes can transport significant REE, and the reason for this is that at low pH, fluoride activity is low because HF is a weak acid and at higher pH, saturation of the fluid with fluocerite buffers fluoride activity to very low values. The modelling showed that REE ore deposition is promoted by a decrease in temperature and an increase in pH. Earlier, we noted that the REE form very stable complexes with carbonate ions. We do not believe, however, that carbonate complexes are significant in REE transport. On the contrary, because of the very low solubility of bastnäsite (Williams-Jones, et al., 2012; Migdisov and Williams-Jones, 2014), the main role of carbonate ions is to promote REE ore deposition. To conclude, a strong case can be made that in many REE ore-forming environments, the REE are transported predominantly as REE-chloride complexes, that deposition is promoted by processes that increase pH and decrease temperature and that because of the greater stability of LREE chloride complexes, hydrothermal processes will tend to preferentially mobilise the LREE, thereby explaining why in some deposits LREE are concentrated distally to HREE.

References:

Banks, D.A., Yardley, B.W.D., Campbell, A.R., and Jarvis, K.E. (1994) REE composition of an aqueous magmatic fluid: A fluid inclusion study from the Capitan Pluton, New Mexico, U.S.A. Chemical Geology 113, 259-272.

Gysi, A.P., and Williams-Jones, A.E. (2013) Hydrothermal mobilization of pegmatite-hosted REE and Zr at Strange Lake, Canada: A reaction path model. Geochimica et Cosmochimica Acta, 122, 324-352.

Migdisov, A.A., Williams-Jones, A.E. (2008). A spectrophotometric study of Nd(III), Sm(III) and Er(III) complexation in sulphate-bearing solutions at elevated temperatures. Geochimica et Cosmochimica Acta, 72, 5291-5303

Migdisov, A.A., Williams-Jones, A.E., Wagner, T. (2009). An experimental study of the solubility and speciation of the rare earth elements (III) in fluoride- and chloride-bearing aqueous solutions at temperatures up to 300ºC. Geochimica et Cosmochimica Acta 73, 7087-7109.

Migdisov, A.A., and Williams-Jones, A.E. (2014). Hydrothermal transport and deposition of the rare earth elements by fluiorine-bearing aqueous liquids. Mineralium Deposita 49, 987-997.

Salvi, S., and Williams-Jones, A.E. (1990). The role of hydrothermal processes in the granite-hosted Zr, Y, REE deposit at Strange Lake, Quebec/Labrador: Evidence from fluid inclusions. Geochimica et Cosmochimica Acta, 54, 2403-2418.

Salvi, S., and Williams-Jones, A.E. (1992). Reduced othomagmatic C-O-H-N-NaCl fluids in the Strange Lake rare-metal granitic complex, Quebec/Labrador. European Journal of Mineralogy, 4, 1155-1174.

Sheard, E.R., Williams-Jones, A.E., Heiligmann, M., Pederson, C., Trueman, D.L. (2012). Controls on the concentration of zirconium, niobium and the rare earth elements in the Thor Lake rare metal deposit, Northwest Territories, Canada. Economic Geology, 107, 81-104.

Trofanenko, J., Williams-Jones, A.E., Simandl, G., and Migdisove, A.A. (2015). The nature and origin of the REE mineralization in the Wicheeda carbonatite, British Columbia, Canada. Economic Geology (in press).

Vasyukova, O and Williams-Jones, A.E. (2014). Fluoride-silicate immiscibility and its role in REE ore formation: Evidence from the Strange Lake rare metal deposit, Québec-Labrador. Geochimica et Cosmochimica Acta, 139, 110-130.

Williams-Jones, A.E., Samson I.M, and Olivo, G.R (2000) The genesis of hydrothermal fluorite-REE deposits in the Gallinas Mountains, New Mexico. Economic Geology, 95, 327-342.

Williams-Jones, A.E., Migdisov, A.A., and Samson, I.M., 2012. Hydrothermal mobilisation of the rare earth elements – a tale of "Ceria" and "Yttria". Elements, 8, 355-360.

REE and trace elements in rocks of the Catanda carbonatite massif (W. Angola)

Wolkowicz S.**, **Bojakowska I., Wolkowicz K., Jackowicz E.
Polish Geological Institute – National Research Institute,
4 Rakowiecka Str. 00-975 Warsaw, Poland;
stanislaw.wolkowicz@pgi.gov.pl;

The Catanda carbonatites from the Cuanza Sul province of W Angola and other carbonatite massifs hitherto identified in that country belong to the Parana-Angola-Namibia large igneous province characterized by intrusions ranging in age from the Early to Late Cretaceous and even Paleocene in the case of Namibia (Gomes et al., 2006). Carbonatites of that igneous province represent intrusive bodies located in central parts of alkaline complexes or sometimes products of extrusive or effusive volcanic activity. The igneous and volcanic phenomena were related to tectonic activity in deep crustal propagating faults cutting the South American and African platforms far landward. In Angolan, both extrusive and intrusive carbonatites are exceptionally well exposed due to fault tectonics combined with advanced weathering and deep erosion. In some carbonatite complexes, weathering processes led to origin of mineral deposits of high economic value.

In the vicinities of Catanda, there are exposed relics of deeply eroded volcanic structures built of pyroclastic and lava carbonatite rocks. These and other carbonatite complexes found in that country form a lithological unit related to the crossing of four fault systems of a NE-SW oriented Lucapa transcontinental rift structure (Lapido-Loureiro, 1973). On the basis of datings of co-occurring alcaline rocks, both this structure and the whole lithological unit are assumed to be of the Cretaceous age, from 138 to 109 My old (Issa Filho, 1991) or even only c. 92 My old (Silva, 1973).

The studies covered 40 samples of rocks of the massif: 18 samples of pyroclatic rocks (tuffs) and 22 of lavas. Concentrations of elements in these rocks were established using the ICP-OES, ICP-MS and XRF methods.

Contents of REE in the studied rocks range from 659 to 9,564 mg/kg. Mean content of REE in lavas equals 2184 mg/kg, being markedly lower than in tuffs – 3331.5 mg/kg. The levels of REE in lavas show strong positive correlation with those of MnO, CaO and F and negative correlation with SiO_2 and Al_2O_3 contents. In turn, the levels of REE in tuffs show strong correlation with contents of MnO but it should be noted that levels of HREE exhibit strong positive correlation with contents of Fe_2O_3, MgO, P_2O_5 and F.

Nb concentrations range from 14 to 652 ppm, with mean levels equal 383 ppm for tuffs and 285 ppm for carbonatite lavas. Li concentrations range from 9 to 55 ppm, attaining 21 ppm at the average. Cr concentrations range from 25 to 161 ppm, being markedly higher in tuffs (49 ppm) than in carbonatite lavas (33 ppm). Cu concentrations range from 11 to 356 ppm, being much lower in tuffs than in carbonatite lavas (29 and 48 ppm at the average, respectively). V concentrations range from 33 to 222 ppm (98 ppm at the average). Zn concentrations change from 57 to 551 (124 ppm at the average). Ba concentrations change from 250 to 1700 ppm (950 ppm at the average). Sr concentrations change from 0,08 to 0,54%, with mean levels clearly higher in carbonatite lavas (0.21%) than in tuffs (0.16%). Concentrations of Ga, Hf, Ni, Pb, As and Co are low and poorly differentiated as they appear generally unrelated to petrology. The studied rocks are relatively poor in radioactive elements. Contents of uranium range from 1 to 20 mg/kg (6.8 mg/kg at the average), being higher in tuffs than lavas (8.4 and 5.9 mg/kg at the average). Contents of thorium range from 5 to 52 mg/kg, being very similar in lavas and tuffs (30.4 and 30.6 mg/kg at the average, respectively).

Conclusions

Carbonatite lavas of the Catanda Massif are characterized by higher mean levels of Cu, Zr, Th and HREE and the tuffs – by higher mean levels of Cr, U, V, Rb, Mo, Zn, Nb, Li and LREE. In turn, concentrations of As, Ba, Ga, Hf, Ni, Pb, Y and Sc appeared not related to the types of rocks of that massif.

Acknowledgements.

References

1. Gomes C. B., Comin Chiaramonti P., Ruberti., Azzone R. G., 2006 - A review of the carbonatitic magmatism in the Parana-Angola-Namibia Province. http://www.vssagi.com/igcp478/AbstractsVSSAGI/416.pdf
2. Issa Filho A., Dos Santos A. B. R. M. D., Riffel B. F., Lapido-Loureiro F. E. V., Mc Reath I., 1991. Aspect of the geology, petrology and chemistry of some Angolan carbonatites. In: Rose A. w., Taufen P. M. (Editors), Geochemical Exploration 1989. J. Geochem. Explor., 40: 205-226
3. Lapido-Loureiro F. E. 1973. Carbonatitos de Angola, t. 11: Memórias e Trabalhos, Instituto de Investigação Científica de Angola, Instituto de Investigação Científica de Angola, 242 p Lloyd F. E.,
4. Silva, M. V. 1973. Estrutura vulcânica-carbonatitica de Catanda (Angola). ServoGeol. Min. Angola, 24, pp. 5-14.

Magnetite-hosted multiphase inclusions in phoscorites and carbonatites of the Kovdor complex, Kola alkaline province

Zaitsev A.N.*, Kamenetsky V.S.**, Chakhmouradian A.R.***
*Department of Mineralogy, St. Petersburg State University, St. Petersburg, Russia
**School of Physical Sciences, University of Tasmania, Hobart, Australia
***Department of Geological Sciences, University of Manitoba, Winnipeg, Canada

Kovdor is a Devonian plutonic complex in the Kola Peninsula, Russia, consisting of various ultrabasic and alkaline rocks that include olivinites, clinopyroxenites, melilitolites, ijolite-urtites, phoscorites and carbonatites (Kukharenko et al., 1965). Phoscorites and carbonatites occur in the south-western part of the complex, at the contact between clinopyroxenites and ijolite-urtites, and form a multistage pipe-like stockwork approximately 2 km from north to south, 0.5-1 km from east to west and up to 1.5 km deep (Krasnova et al., 2004).

Phoscorites are mineralogically diverse rocks that contain variable proportions of forsterite, hydroxylapatite, magnetite, phlogopite, tetraferriphlogopite with subordinate calcite and/or dolomite. Several varieties of phoscorites are distinguished on the basis of their mineralogy and emplacement ages. Carbonatites are represented by calcite, calcite-dolomite and dolomite varieties containing subordinate magnetite, forsterite, phlogopite, tetraferriphlogopite and hydroxylapatite (Krasnova et al., 2004). The Kovdor phoscorites and carbonatites were formed between 380 and 376 Ma, and are obviously genetically related, but the exact nature of that relationship (e.g., fractional crystallisation versus liquid immiscibility) is still under discussion.

In this work, we studied one variety of phoscorite (calcite-forsterite-magnetite phoscorite) and one variety of carbonatite (calcite carbonatite with magnetite, phlogopite, forsterite and apatite). Both rocks were formed at an early stage of phoscorite-carbonatite formation and show no sign of hydrothermal alteration. Magnetite is a major to minor mineral in the studied samples. Both rocks types commonly contain euhedral ($\{111\} \pm \{110\}$) magnetite crystals up to 1 cm in size. Published bulk wet chemistry data show that the mineral is a Ti-Mg-Al-enriched variety (1.3-4.2, 1.4-6.1, 0.6-2.6 wt.% respective oxides), whereas other components, such as MnO, are present at lower levels (Krasnova et al., 2004). Magnetite in the early stage calcite phoscorites and carbonatites contains numerous inclusions of spinel due to exsolution during cooling. Exsolved spinel typically occurs as equant inclusions up to 10 μm, with rare large grains reaching 20 μm across. Also, spindle-like inclusions and their cross-like intergrowths are observed.

An SEM study of this magnetite revealed the presence of abundant mono-, bi- and polymineralic solid inclusions (Fig. 1). The inclusions are randomly distributed within the host magnetite crystal and vary from 20×20 to 150×200 μm. The majority of inclusions are characterised by well-faceted shape and sharp boundaries with the host magnetite and can be classified as negative crystals. Our interpretation is that small portions of a conjugate melt were trapped by magnetite during its growth, and subsequently solidified to form various minerals. Few inclusions can be identified as entrapped crystals of early-crystallising phases (forsterite, phlogopite, apatite, calcite and dolomite).
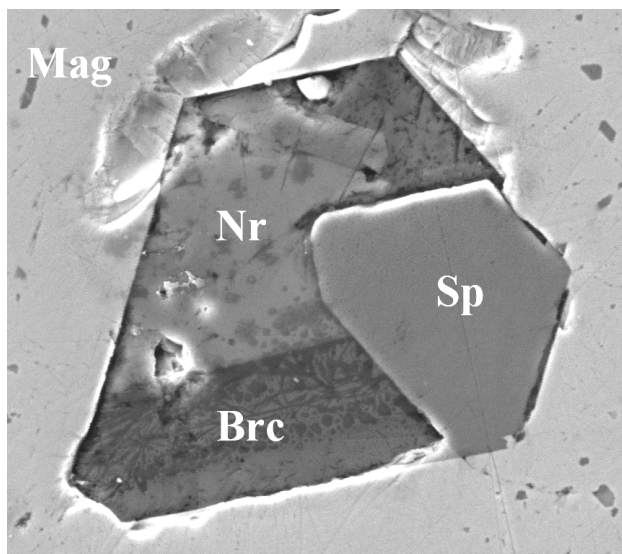

Figure 1. A negative crystal composed of euhedral spinel (Sp), brucite (Brc) and nyerereite (Nr) in magnetite (Mag) from calcite carbonatite.

Data from SEM/EDS analyses and Raman spectroscopy indicate that the inclusions host a great diversity of carbonate minerals (see below, under 1), accompanied by non-carbonate minerals commonly found in carbonatites and present in the host rock (e.g., forsterite), and several oxysalt-, halide- and hydroxide-bearing species that have not been previously reported from this environment. These constituent phases can be grouped chemically into:

(1) carbonates – nyerereite $Na_2Ca(CO_3)_2$, calcite $Ca(CO_3)$, dolomite $CaMg(CO_3)_2$, shortite $Na_2Ca_2(CO_3)_3$, eitelite $Na_2Mg(CO_3)_2$, norsethite $BaMg(CO_3)_2$;

(2) carbonates with additional anions – bradleyite $Na_3Mg(PO_4)(CO_3)$, tychite $Na_6Mg_2(SO_4)(CO_3)_4$, northupite $Na_3Mg(CO_3)_2Cl$;

(3) oxides – spinel $MgAl_2O_4$, baddeleyite ZrO_2, pyrochlore $CaNaNb_2O_6F$;

(4) hydroxides – brucite $Mg(OH)_2$;

(5) silicates – forsterite $Mg_2(SiO_4)$, phlogopite $KMg_3(AlSi_3O_{10})(OH)_2$;

(6) phosphates – hydroxylapatite $Ca_5(PO_4)_3(OH)$;

(7) sulphates – tenardite $Na_2(SO_4)$;

(8) halides – sylvite KCl; and

(9) a number of rare phases whose identification is only tentative at this point – burbankite $(Na,Ca)_3(Sr,Ca,REE,Ba)_2(CO_3)_5$, fairchildite $K_2Ca(CO_3)_2$, wüstite FeO, valleriite $4(Fe,Cu)S•3(Mg,Al)(OH)_2$ and quintinite $Mg_4Al_2(CO_3)(OH)_{12}•3H_2O$.

Mineral parageneses vary among the inclusions. Mono- and bimineralic inclusions contain calcite, dolomite, apatite, calcite+apatite, nyerereite+spinel, brucite+spinel. Those observed in polymineralic inclusions consist of calcite+dolomite+spinel, spinel+nyerereite+brucite, etc. Statistically, only three minerals occur in the majority of the examined inclusions: spinel (about 80 % of all inclusions), nyerereite (65 %) and brucite (60 %). No reaction between the constituent minerals was observed (Fig. 1), which implies no addition or removal of components after these inclusions crystallised.

The mineral assemblages documented in the inclusions from the Kovdor carbonatites and phoscorites and in particular, the association of primary brucite, nyerereite and spinel, indicate the existence of a hydrous, Mg- and alkali-rich, phosphate-sulphate-bearing carbonate melt, which gave rise to the early carbonatitic rocks at Kovdor. This melt can be considered a hydrous analogue of the Kerimasi/Tinderet-type Ca-alkali-Mg-rich carbonatitic magma. The Oldoinyo Lengai natrocarbonatites, although showing some similarities to the melt inclusions described here, appear have derived from melts distinct from those that produced the Kovdor rocks.

References:

Krasnova, N.I., Balaganskaya, E.G., Garcia, D. Kovdor — classic phoscorites and carbonatites // In: Wall, F., Zaitsev, A.N. (Eds.), Phoscorites and Carbonatites from Mantle to Mine: The Key Example of the Kola Alkaline Province.Mineralogical Society Series, 10. Mineralogical Society, London, pp. 99–132.

Kukharenko, A.A., Orlova, M.P., Bulakh, A.G., Bagdasarov, E.A., Rimskaya-Korsakova, O.M., Nefedov, E.I., Ilinskiy, G.A., Sergeev, A.S., Abakumova, N.B. The Caledonian complex of ultramafic, alkaline rocks and carbonatites of the Kola Peninsula and Northern Karelia // 1965. Nedra, Leningrad, 772 pp. (in Russian).

Some notes about LIP (large ignieos provinces) temporal distribution in Earth history.

Zaitsev V.A.
Vernadsky Institute of Geochemistry and Analytical Chemistry RAS, Moscow
va_zaitsev@inbox.ru

The concept of mantle plumes is one of the central ideas in geological sciences during resents decades. It is widely believed that plumes result in intraplate magmatic events like large igneous provinces (LIPs), alkaline-ultramafic formations with carbonatites, kibmerlirtes and limproites (even if someone do not believe to plumes, he relate these magmatic events to the special conditions in the earth mantle). From these point of view, analysis of they temporal distribution looks an attractive way to study the Earth mantle history. In spite of plenty of papers, dedicated to the geological interpretation of intraplate magmas ages distribution, published by the several authors (Ernst, Condy, etc), temporal distribution was not examine as stochastic process. To fill this gape we use database, published by Large Igneous Provinces Commission of International Association of Volcanology and Chemistry of the Earth's Interior (http://www.largeigneousprovinces.org/downloads).

The most popular form of LIP record is histogram of ages (diagram, where quantity of events in each time interval – N(t) plotted vs. the age of thus interval-t). It is clear, that quantities of LIP in time intervals depend on the splitting, and for each splitting we can count intervals, containing 1, 2, 3… LIPs (intervals with N(t)=1, 2, 3…). From the other hand, it is possible to estimate these quantities of intervals from the Poisson's law, on the assumption of random distribution of LIP events in geological time.

χ^2 –test was used to determine whether there is a significant difference between the observed and expected quantitys of time intervals containing 1, 2, 3…n LIPs. It was found that for the different splitting (time step from 10 to 100 Ma) the distributions are quite close to the Poisson's law, especially if only the best known part of geological history is taken into account (1-1,5-2 Ga). There are only few exclusions: 75-150 Ma, 1000, 1100, 1250 1800 and 1900 Ma. First of they may be explaned by presence of contain oceanic LIPs, which mainly do not preserve for older parts. The excesses of 1000, 1100 and 1250 Ma looks to be attributed to the effect of rounding of poorly dated events (like 1Ga, 1.1Ga, 1-1.5 Ga) the nature of 1800 and 1900 Ma excesses need to be understood. On the fig. 1B showed example of LIP number distribution for 25 Ma time-step, we have also tested all time-steps from 9 to 40 Ma, some of biger time-steps, and some splitting moved from 0-age. In all cases we received the similar results.
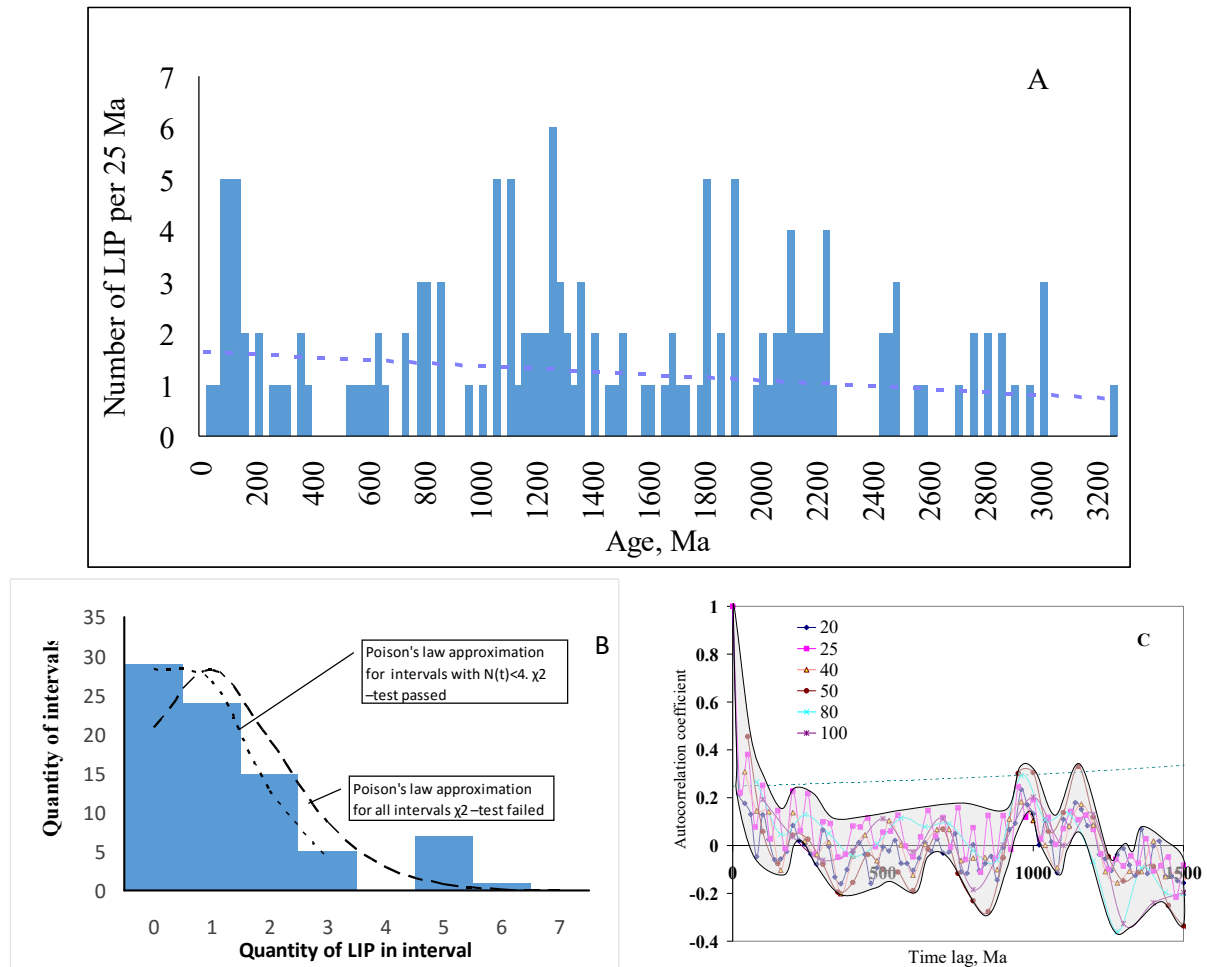

Fig. 1 A- Histogram of LIP ages (time interval 25 Ma), and its statistical characteristics: B- distribution of time intervals by number of LIPs (splitting 25Ma), and corellogram

One of the very popular ideas is cycling of geological processes cycles with periods 30, 100, 170,330, 550-700. For strict validation whether Earth activity in LIP generation in time have regular recurrence, we calculate autocorrelation coefficients (correlation coefficients N(t) vs N(t+Δt)) with Δt (time lag) 0-1500 Ma for LIP histograms with 20, 25, 40, 50, 80, 100 Ma splitting. Autocorrelation coefficients, plotted against time lag (correlogram) showed on the fig. 1. Autocorrelation coefficients quickly decrease, significant values found only for lags<100 Ma. It shows that there is no regular repetition of plume activity of the Earth. High autocorrelation coefficients for small lags connected with obvious trend of LIP quantity grown during geological time.

So, our statistical tests evident that LIP formation (plume events as soon as we consider LIP a reflection of mantle plumes) in geological time can be considered as a continuous-time stochastic process of rare events. This fact is not to deny the importance of plumes for continental break-up, ore-deposit formation etc. From other hand, this fact give additional limitation for plume origin models: birth of plumes must be insignificant for energy and material balance in plume-generating system, but this process must need trigger, which may be result of some rare combination of conditions.

Typomorphic features of allanite in rocks of the Tsakhirin site of the Khaldzan-Buregteg alkali-granite complex (Western Mongolia)

Zenina K.S., Konovalenko S.I.

National Research Tomsk State University, Tomsk, Russia

kseniazenina@ngs.ru

The Khaldzan-Buregteg alkali-granite massive with the same-name rare-metal deposit and the Tsakhirin occurrence is located in Western Mongolia in the zone of a regional fault separating Caledonian structures of the Mongolian Altai and the Early Caledonian structures of the Ozernaya zone. Tsakhirin Y-Zr-Nb occurrence located is in exocontact metasomatic zone of Northern outcrop of Khaldzan Buragtag alkaline massif. The deposit is represented by two linear ore zones Western and Eastern, located some Northern of Mt. Ulyn Khuren. The occurrence is represented by two genetic types of mineralized pegmatite and pneumatolytic-hydrothermal. Pegmatites mainly developed in endocontact array on the Northern slope of the mountain Ulan-Huren among first phase and alkaline granites second. Metasomatites associated with pneumatolytic-hydrothermal process, on the contrary concentrated in the exocontact of the array are more effusive rocks of the ophiolite complex of the frame. The ore minerals are allanite, zircon, fergusonite, chevkinite, ilmenite, etc.

Allanite is most widely developed in pegmatites and metasomatites of the Tsakhirin site. The mineral is metamict, optically isotropic, with variable chemical composition. Al and Fe grades vary most significantly, which testifies to the fact that the main isomorphic substitutions occur in the octahedral position of the structure of the mineral. Meanwhile, it is common knowledge that the main isomorphic substitution in minerals of the allanite group occurs by the aliovalent pattern and is associated with substitution of Ca^{2+} and Al^{3+} by Fe^{2+} with TR^{3+}. In this relation the Fe^{2+} to TR^{3+} ratio in allanites shall not exceed 1 theoretically. However it is much higher in recalculated microprobe analyses and makes 1.48-2.2 in pegmatites and metasomatites respectively. The current knowledge of allanite crystal chemistry does not allow for using the direct calculation of formulas on the basis of oxygen with the supposition that whole iron in the mineral is presented by a bivalent form only. It is explained by the fact that a specific part of Fe^{3+} cations occupying the Al^{3+} position in the crystal lattice of the mineral thus compensates the excess of cation charges occurring when Ca^{2+} is substituted by TR^{3+}. The scale of such substitution is evidently sometimes extremely significant, and the value of the Fe_2O_3/FeO ratio in the mineral will fall abruptly. The quantitative prevalence of Fe^{3+} over Fe^{2+} in the studied allanite is likely preconditioned by not only structural features of the mineral but also increased background of alkalinity, when a trivalent form of iron is the one that is active. Therefore, a part of total iron in samples calculated for a bivalent form is undoubtedly related to a trivalent form. One should also remember that the significant quantity of allanite inclusions, as the observations show, is formed by means of substitution of epidote preceding it, in which whole iron is presented by a trivalent form.

Crystallochemical formula allanite array data from the chemical analysis, has the following form: $(Ca_{1,15}Ce_{0,33}La_{0,20}Nd_{0,1})_{1,78}(Al_{1,65}Fe_{1,36}Ti_{0,01})_{3,02}[Si_2O_7][SiO_4](O_{0,44}OH_{0,56})(OH)$.

The content of lanthanides varies in samples as well, (Σ TR_2O_3 10.6-24.0 % wt), falling within the interval typical for the mineral. The rare earth spectrum remains unchanged. Ce always prevails in it; La is second and Nd is third. The Ce/Nd, La/Nd and Ce/La ratio variations make respectively 8.3; 2.8; 2.9 in pegmatite allanite and 2.44; 1.11; 2.18 in metasomatite allanite.

For allanite metasomatites radiographs were obtained, taken before calcination after calcination at 900° C and 1000° C. Crystal structure of a mineral is recovered during annealing up to 900° C. In this case, when shooting, he gives the diffraction pattern close to the reference. Calculated according to the parameters of the unit cell is equal to: a_0 = 8,97Å; b_0 = 5,70Å; c_0 = 10,13Å; β = 115°00′. Upon further heating of allanite (above 1000° C) according diffraction pattern, becomes a mixture of the oxides present in the composition of chemical elements (CE, Fe, etc.). On the differential curve of heating allanite found three well-defined exothermic peaks: 273, 772 and 803°C. First effect at a temperature of 273°C is likely to be associated with the oxidation of Fe^{2+}. Two high-temperature peaks (803 and 772°C) obviously, related to the processes of recrystallization and the transition of the mineral in a crystalline state.

Spectral analysis established the impurity elements listed in Table.

Table. The content of trace elements in allanite.

Element	Content	Element	Content
Pb	11	U	100
Cu	15	Th	100
Ti	3000	Be*	50
Mn	250	P*	2000
Sr	1000	Y*	5000
Ba	260	Yb*	100
Nb*	5000	Zr	4450

Note: * - semiquantitative determination; 1 g/t = 0.0001%

Analyst Agapova E.D., Center for collective use "Analytical Center geochemistry of natural systems" Tomsk State University.

Studies allanite manifestations Tsahirin show that the main of typomorphic its feature composition is abnormal iron content with increased role of trivalent element. This, apparently, reflects the specificity of the process of mineralization in the area, characterized by high levels of alkalinity, when the active form of trivalent iron. allanite characterized by a relatively high content of impurity components: Zr, Sr, Nb, Y, Yb, P, U and Th. This list reflects all metallogenic the specific manifestation specialized in relation to Zr, TR, Nb, partly, Be and Th.

References

Armbruster T., Bonazzi P., Akasaka M. Recommended nomenclature of epidotegroup minerals // Eur. J. Mineral. 2006. vol. 18. P. 551–567.

Kovalenko V.I., Tsaryeva G.M., Goreglyad A.V., Yarmolyuk V.V., Troitsky V.A. The peralkaline granite-related Khaldzan-Buregtey rare metal (Zr, Nb, REE) deposit, Western Mongolia // Econ. Geol. 1995. Vol. 90. P. 530–547

Zenina K.S. Typochemistry of allanite in rocks of the Tsakhirin site of the Khaldzan-buregteg alkali-granite complex (Western Mongolia) // Geology in the developing world. Collection of scientific works (on materials of the V scientific-practical conference of students, postgraduates and young scientists with international participation. 2015. (in press)

Geodynamic Reconstruction of the Palaeozoic Kola Alkaline Large Igneous Province

Zhirov D.V.

Geological Institute of Kola Science Centre RAS, Apatity, Russia, zhirov@geoksc.apatity.ru

The Palaeozoic Kola Alkaline Large Igneous Province (LIP) is one of the best studied and representative in terms of number and manifestation forms of alkaline-ultramafic magmatism with carbonatites (AUC). The origination of this province was dominated by plume and relevant mantle-lithospheric geodynamics [1-10]. Such conclusions were mainly drawn based on substance evidences (mantle genesis indicators). And the descriptions of the Palaeozoic plume tectonics and geodynamics are generally illustrated by simplified figures of a conventional Newton (mushroom-like) plume with such controlling factors as thermal gradient, number and depth of magma generating hearths [1,4,9]. Alongside, studies of modern (young) plumes and accompanying processes have provided abundant material for laws of plume origination and evolution, and allowed modelling their shape and surface topography in detail. All these data demonstrate quite a complicated nature of plume geodynamics and interaction with the lithosphere [11]. This means that the description of the Kola alkaline LIP also requires a more detailed and complicated model, and any comprehensive attempts to reconstruct the specifics of its geodynamics are still relevant and of scientific interest.

This research represents results of morphometric and tectonophysical analysis of the Palaeozoic AUC intrusions in order to reconstruct geodynamics and evolution of the whole LIP. The analysis was based on the following geological background and logics of reasoning:

The origination of geological bodies (AUC intrusions) took place at a depth of 0-8 km from the surface (3-5 on the average). With due regard to heterogeneous and sign-variable differentiated vertical motions, further erosion yields a modern range of represented intrusion origination depths from 0 to 10 km (4-7 km on the average). The shape of intrusion and individual igneous phases reflects tectonophysical conditions of the Palaeozoic upper crust with variability and homogeneity / heterogeneity along the whole LIP. It is defaulted that the tectonophysical conditions and crust tectonics were caused by plume tectonics (or mantle – lithospheric processes). These processes were recorded in the shape and sizes of intrusions, and in relationships of igneous phases. The heterogeneity and contrast nature of the conditions are namely most informative. Thus, recovery of structural laws for alkaline-ultramafic intrusions and their shape varying with time dynamics of igneous phase origination shall describe features of the Kola LIP geodynamics. This, in turn, provides prerequisites for the reconstruction. Very tentatively, the sequence of main igneous phases in the AUC intrusion origination is conditionally represented as follows (from ancient to young): ultramafic → alkaline → carbonatite stages. The majority of the Kola LIP AUC intrusions show minimum two of three above stages with the relative sequence being always persistent. Upon the completion of the Palaeozoic tectonomagmatic activity, the regional evolution was due to differentiated vertical (modular and button-like) motions with no significant lateral (or horizontal) movements and deformations. The boundaries of the largest geological bodies and structures preserved initial contours, shape, and relative position up to present.

The analysis of each individual AUC intrusion divided into certain igneous phases has identified the geometric center and axes of the maximum and minimum body length in the horizontal section, orientation, and ratio. During further events, the center offset directions and axis swivel were detected. The maximum elongation axis was taken as a direction of the quasi-principal compression (minimum extension) in the horizontal plane. The orthogonal direction, or the minimum length axis, was considered as a direction of maximum extension. The resultant information was applied to the geological basis [12], grouped and analyzed both individually for each

igneous stage, and in general. In the course of AUC intrusion grouping, a few single-point, areal, and linear controlling factors that regularly unite groups of intrusions in terms of tectonophysical features and dynamics of variation in igneous phases were substantiated (Fig. 1). The analysis has allowed identifying and shaping structures that control magmatism in the Kola LIP and significantly complicate, extend, and sometimes fundamentally differ from those earlier accepted (see Figure 1). In the Kukharenko zone (Kuh), there are several clear sub-zones varying in study features (see I-III) with one representing a near east-west branch (or arm). The Kandalaksha rift zone is less relevant than it was earlier supposed. The identification of near east-west (stretching east-south-east) linear zone L1 along the Sallanlatva-Vuoriyarvi-Kovdozero-Tury Mys-Zimny Bereg line regularly and sequentially manifested in all stages of the Kola LIP evolution.

The revealed magmatism-controlling elements and structures are interpreted as follows: elongated zones are correlated with comb-shaped protrusions/rays on the plume surface, linear zones with deep-seated faults that constrain the rift zone of a plume, and maximum extension directions correspond to vectors of heat and mass transfer of convective motion. Thus, the geodynamics of the Palaeozoic Kola LIP was caused by a plume with complicated morphology and surface topography. Linear (linear areal) and single-point plume elements were of main importance. The results obtained may be interpreted by a few options of geodynamics, of which the three-ray plume origination model with rare apophyses in the form of hot spots is simplest and consistent at the current level of knowledge. The plume center located near zone I, from which heat and mass transfer flows spread radially along the Kukharenko zone (II and III) with a turn along the Linear zone L2. A deep-seated fault and linear zone L1 are of key importance. This is most probably a normal deep-seated fault that constrains the rift in accordance with a regular quasi-parallel arrangement of AUC intrusions (maximum extension direction is perpendicular). Extending, it is traced eastwards through the Tersky shore explosion pipes to the Zolotitsa kimberlite fields. This gives reasons to further extend boundaries of the kola alkaline LIP.
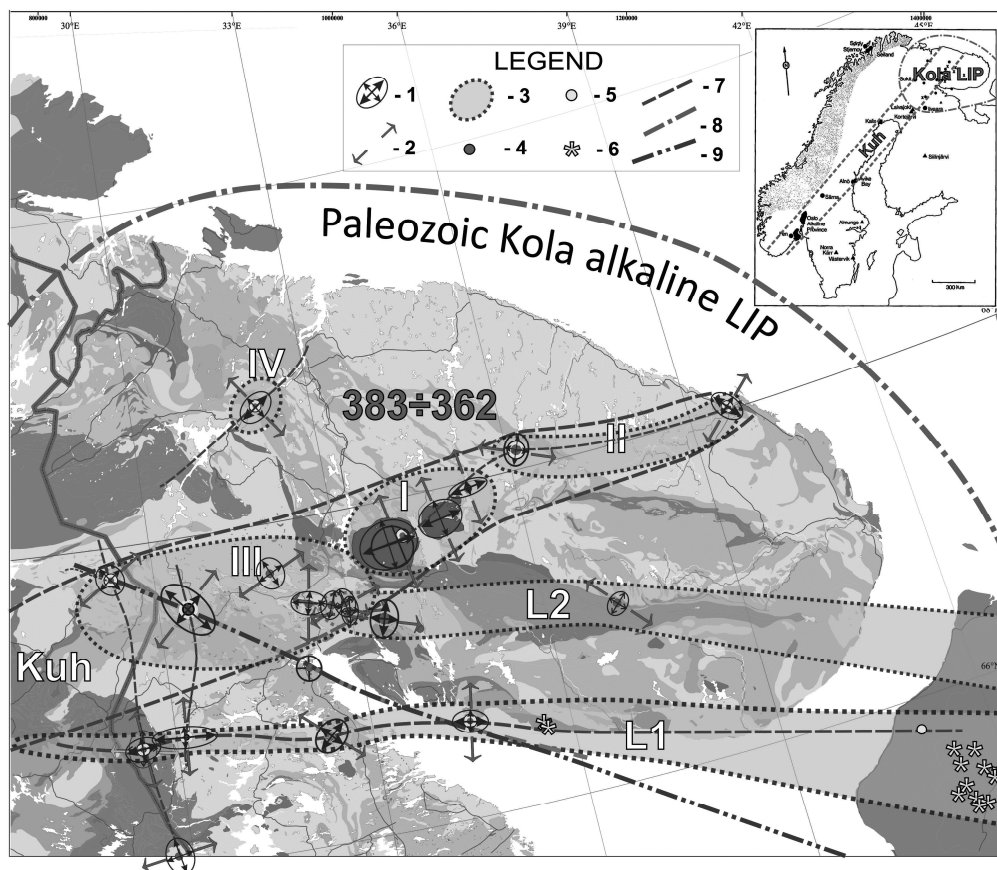
Figure 1. Zoning and controlling factors for the AUC intrusions location in the Kola LIP, summary chart for alkaline and carbonatite stages. Legend: 1 – long to short intrusion side ratio along the outlined ellipse; 2 – maximum stretching direction; 3 – zones for grouping areal type intrusions: I – Khibiny-Lovozero, II - Kontozero-Ivanovka, III - Sokli-Kovdor-Niva-Salmagora, IV - Seblyavr; 4 – AUC intrusion; 5 – carbonatites; 6 – explosion pipes (kimberlites); 7 – linear zones of deep faults: Kuh – Kukharenko zone, L1 – Sallanlatva-Vuoriyarvi-Tury-Mela/Zolotitsa fault, L2 – assumed Afrikanda-Ozernaya Varaka-Ingozero-Pesochny-Zimny Bereg fault; 8 – rough boundaries of the Kola LIP; 9 – main lineament of the Kandalaksha Graben.

References:

1. Arzamastsev A.A., Bea F., Glaznev V.N., Arzamastseva L.V., Montero P. Kola alkaline province in the Paleozoic: evalution of primary mantle magma composition and magma generation conditions. // Russian Journal of Earth Sciences. 2001. Vol.3. No.1. pp.1-32.

2. Kogarko L.N., Kononova V.A., Orlova M.P., Woolley A.R. Alkaline rocks and carbonatites of the World. Pt.2: Former USSR. London: Chapman & Hall, 1995. 226 p.

3. Arzamastsev A.A., Glaznev V.N. Plume-lithosphere interaction in the presence of an ancient sublithospheric mantle keel: an example from the Kola alkaline province. // Doklady Earth Sciences. 2008. Vol. 419. 2. pp. 384-387.

4. Arzamastsev A.A., Mitrofanov F.P. Paleozoic plume-lithospheric processes in Northeastern Fennoscandia: evaluation of the composition of the parental mantle melts and magma generation conditions. // Petrology. 2009. Vol. 17. No.3. pp. 300-313.

5. Arzamastsev A.A., Fedotov Zh.A., Arzamastseva L.V. and Travin A.V. Paleozoic Tholeiite Magmatism in the Kola Igneous Province: Spatial Distribution, Age, Relations with Alkaline Magmatism. // Doklady Earth Sciences, 2010, Vol. 430, Part 2, pp. 205–209.

6. Kramm U., L.N. Kogarko L.N., Kononova VA, Vartiainen H. The Kola Alkaline Province of the CIS and Finland—precise Rb-Sr ages define 380–360 Ma age range for all magmatism. // Lithos. 1993. 30(1):33–44.

7. Downes, H., Balaganskaya, E., Beard, A.D., Liferovich, R., Demaiffe, D. Petrogenetic processes in the ultramafic, alkaline and carbonatitic magmatism in the Kola Alkaline Province: a review. // Lithos. 2005. 85 (1-4), pp. 48-75.

8. Rukhlov A. S. & Bell K. Geochronology of carbonatites from the Canadian and Baltic Shields, and the Canadian Cordillera: clues to mantle evolution. // Miner Petrol. 2010. 98:11–54.

9. Zaitsev, A.N., Williams T., Jeffries, C., Teresa E., Strekopytov, S., Jacques, M., Ivashchenkova, O.V., John, S., Petrov, S.V., Frances, W., Reimar, S., Borozdin, A.P., Rare earth elements in phoscorites and carbonatites of the Devonian Kola Alkaline Province, Russia: examples from Kovdor, Khibina, Vuoriyarvi and Turiy Mys complexes. // Ore Geology Reviews. 09. 2014 pp. 204–225.

10. Kravchinsky V.A. Paleozoic large igneous provinces of Northern Eurasia: Correlation with mass extinction events. // Global and Planetary Change. 86-87. 2012. pp. 31–36.

11. Foulger G.R. and Jurdy D.M. (eds). Plates, Plumes, and Planetary Processes. // The Geological Society of America. Special Paper 430. 2009. 999 p.

12. Eilu, P., Bergman, T., Bjerkgård, T., Feoktistov, V., Hallberg, A., Ihlen, P.M., Korneliussen, A., Korsakova, M., Krasotkin, S., Muradymov, G., Nurmi, P.A., Often, M., Perdahl, J-A., Philippov, N., Sandstad, J.S., Stromov, V. & Tontti, M. Metallogenic Map of the Fennoscandian Shield, 1:2,000,000. Geological Surveys of Finland, Norway, Sweden and the Russian Federation. 2009.

Magnetoelastic effects in the magnetite-calcity rocks of the Kovdor massif

Zhirova A.M.
Geological Institute of the KSC of the RAS, Apatity, Russia
anzhelaz@geoksc.apatity.ru

INTRODUCTION

The work is devoted to studying of the magnetoelastic effects in the magnetite-containing rocks of the Kovdor massif. The features of influence of an ultrasonic wave radiation on magnetization of rocks in the conditions of change of parameters of radiation are considered. It is known that magnetoelastic effects are characteristic for ferrites (for example, the yttrium ferrite-garnet). However natural ferriferous oxides with other chemical composition can have properties of ferrites also. Within the Kovdor massif the calcite-forsterit-magnetite, magnetite and other ores are marked (Katseblin et al., 1980). The main minerals composing these varieties are magnetite and other ferriferous minerals: ilmenite, hematite, maggemit, pseudo-brookite. Magnetoacoustic researches consist in studying of influence of ultrasonic fluctuations on residual magnetization of the magnetite-containing rocks. Thus the influence on residual magnetization of such parameters as time of radiation and the direction of mechanical oscillations is studied. The researches are conducted in development of the works begun by V.A. Tyuremnov (Glaznev et al., 2008). V.A.Tyuremnov has revealed that the residual magnetization and its direction change depending on the frequency of fluctuations and from a magnetic state of rocks.

The received results and further researches in this area present undoubted interest in development of problems of nonlinear geophysics, and in the solution of some questions in science of materials also. In this research the magnetoacoustic experiment is carried out in two directions. These are the "Influence of the

direction of ultrasonic radiation concerning the vector of residual magnetization for strongly magnetic samples of Kovdor in the conditions of cyclic radiation and demagnetization" and "Influence of time of ultrasonic radiation on residual magnetization of strongly magnetic samples of Kovdor".

EXPERIMENT AND RESULTS

1. "Influence of the direction of ultrasonic radiation concerning the vector of residual magnetization for strongly magnetic samples of Kovdor in the conditions of cyclic radiation and demagnetization"

The purpose of experiment is research of the possible relation between the direction of ultrasonic radiation and magnetization of the samples. The experiment consists in cyclic ultrasonic radiation of the samples previously demagnetized under following conditions: radiation time - 60 s, the frequency of ultrasonic fluctuations - 100kHz. The feature of experiment is change of parameters of radiation: ultrasonic radiation is carried out in the direction of the maximum axis of magnetization and against it. Magnetic cleaning of the sample consists in influence of the sinusoidal magnetic field (variable on amplitude).

On the basis of the first studies of influence of the direction of ultrasonic radiation concerning the vector of residual magnetization for the strongly magnetic samples of Kovdor massif at the cyclic radiation and demagnetization the following conclusions are received:

1.   Ultrasonic radiation influences the vector of residual magnetization of the magnetite-calcity rocks. The change of residual magnetization (the module and component), and its spatial situation (the magnetic variation and inclination).

2.   Changes of parameters of the vector of residual magnetization are significant, i.e. exceeding inaccuracy of the measurements on the magnetometer.

3.   In general it is possible to note growth of values of the module of the vector of residual magnetization during the ultrasonic radiation in the direction of the maximum axis of magnetization. That correlates with results of other researchers (Glaznev et al., 2008). During ultrasonic radiation against the direction of magnetization the results are ambiguous.
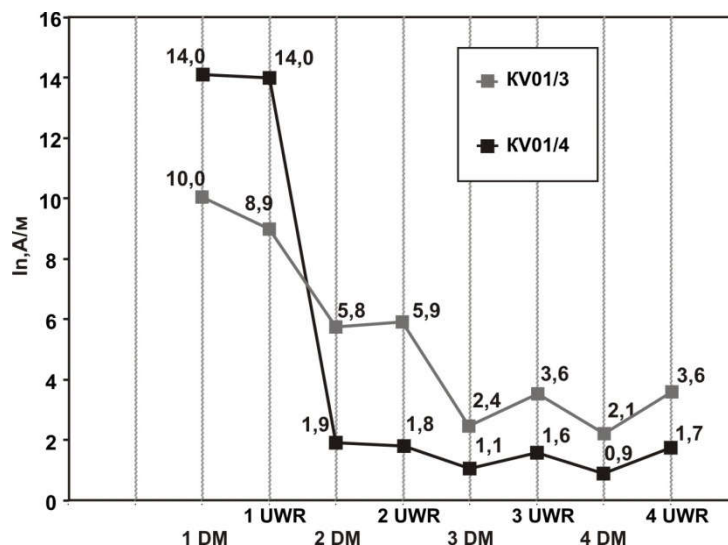

Fig. 1. Change of value of the module of residual magnetization vector during carrying out series of ultrasonic wave radiations (UWR) in the direction of the vector and demagnetization (DM) of the KV01/3 and KV01/4 samples

4.   The spatial behavior of the vector of residual magnetization at the ultrasonic radiation has ambiguous character. Return of the vector of magnetization of the samples (after demagnetization) to an initial state is not observed.

2."Influence of time of ultrasonic radiation on residual magnetization of magnetic samples of Kovdor".
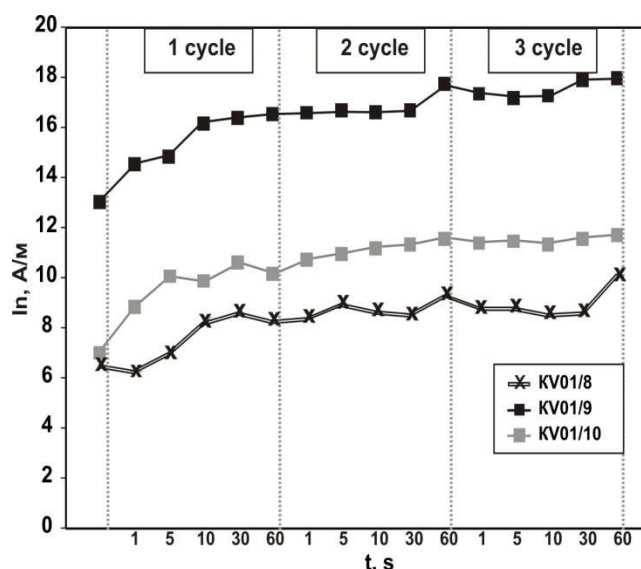
Fig. 2. Change of value of the module of residual magnetization vector in terms of increasing time of the ultrasonic wave radiation of the KV01/8, KV01/9, KV01/10 samples

One of the issues of the magnetoacoustic research, as mentioned above, is to studying the possible relationship between the time of the ultrasonic wave radiation and magnetization of the samples. Each cycle is ultrasonic radiation in the direction of vector of the remanent magnetization with increasing time of influence: 1s-5s-10s-60s-30s. On the basis of the first studies of influence of time of ultrasonic radiation on residual magnetization of magnetic samples of the Kovdor massif at the cyclic radiation and demagnetization the following conclusions are received:

1. In the process of ultrasonic radiation of samples an increase of modulus of vector of the remanent rock magnetization is revealed.

2. It was found that the first cycle of acoustic wave radiation the increase of modulus of vector of the remanent rock magnetization is more significant (in comparison with other cycles). And in subsequent cycles: an abrupt increase of the modulus with increasing time of ultrasonic sounding from 30 s to 60 s is observed (fig.2).

3. The clear relationship between the spatial behavior of the magnetization vector and the time of the ultrasonic radiation is not found.

This study was supported by the Russian Science Fund (project nos. 14-17-00751).

References:

1. Katseblin P.L., Tyuremnov V.A., Shaposhnikov V.A. Magnetic parameters of the Kovdor magnetites in connection with the composition // Collection of the proceedings "The method and results of geophysical researches of northeast part of Baltic Shield". Apatity: Kola branch of Academy of Sciences of the USSR. 1980. P. 111-119.

2. Glaznev V.N., Tyuremnov V.A., Neradovsky Yu.N., Osipenko L.G. Research of influence of acoustic fluctuations on the magnetic state and residual magnetization of the magnetite ores (Kola Peninsula) // Proceedings of the International Conference "Deposits of the natural and technogenic mineral raw: geology, geochemistry, geochemical and geophysical methods of search, ecological geology". Voronezh. 2008. P. 63-65.

The geochemical features of melilite-bearing rocks and initial magmas of Cupaello and Colle Fabbri (Central Italy)

Isakova A.T.

V.S. Sobolev Institute of geology and mineralogy SB RAS, Novosibirsk, Russia,
atnikolaeva@igm.nsc.ru

Kamafugites being Ca-rich potassic alkaline ultramafic rocks are common in Central Italy within Apennine range. There are small volcanic centers such as Cupaello lava, Colle Fabbri stock, San Venanzo volcano, Polino diatreme and others (Stoppa, Lavecchia, 1992; Lavecchia et al., 2006), which are found in the Pleistocene / Quaternary continental tectonic depressions which cross cut the Pliocene Apennine thrust-fold system.

Currently researchers obtained a lot of data (Cundari, Ferguson, 1991; Stoppa, Lavecchia, 1992; Stoppa, Cundari, 1995; Stoppa et al., 2003 and others) on geological setting and petrographic composition of the italian kamafugites. The melt inclusion study in minerals of melilite-bearing rocks from Cupaello volcano (Nikolaeva, 2012 et al.), Pian di Celle volcano (Panina et al., 2003), and Colle Fabbri stock (Stoppa, Sharygin, 2009; Panina et al., 2013) indicates that the high temperature (1140-1320 °C) melilitite magma is initial for the considered kamafugites. It was found that the silicate-carbonate-salt immiscibility occurred in this magma at lower temperature. Moreover sources of magma, which formed italian kamafugite-carbonatite complexes consisting of rocks of unusual composition and isotopic characteristics, are under discussion. In order to obtain additional information for explanation of this question, geochemical studies were conducted: trace-element compositions of kalsilite (Ks) melilitite and carbonatite tuff from Cupaello volcano, leucite-wollastonite (Lc-Wo) melilitolite and contact rock from Colle Fabbri stock as well as melt inclusions conserved in rock-forming minerals were studied.

This study evidences that the content of trace element in Ks melilitite and carbonatite tuff from Cupaello is significantly higher than the mantle norm: the content of LILE (Rb, Ba) is 2.5-3.5 orders higher, and that of HFSE (Zr, Hf, Ta, Nb) is 1-2 orders higher than the primitive mantle values (McDonough, Sun, 1995). The content of REE in the rocks is higher than in the primitive mantle: they are more than 2-2.5 orders richer in LREE, 1.5-2 orders richer in MREE, and less than an order in HREE. Besides Ks melilitite is enriched in trace elements more than carbonatite tuff. Primitive mantle-normalized spidergrams of Ks melilitite and carbonatite tuff of Cupaello have a negative slop (fig. 1). The La/Yb_n ratio is 64-71 for Ks melilitite and 57 for carbonatite tuff. Both spidergrams have a deep negative Ta, Nb, Ti, and K and the small Eu anomalies (Eu/Eu^*_n = 0.62-0.65). It should be noted that the presence of a small Eu/Eu^*_n negative anomaly is believed (Balashov, 1976) to be the result of fractional crystallization, in which plagioclase or melilite is involved.

The content of trace elements in Lc-Wo melilitolite from Colle Fabbri is also predominantly higher than the mantle norm: the content of LILE (Rb, Ba) is two orders higher, and that of HFSE (Zr, Hf, Ta, Nb) is an order higher than the primitive mantle values (McDonough, Sun, 1995), the content of REE in the rock is more than an order richer in LREE and MREE and less than an order richer in HREE (Panina et al., 2013). Primitive mantle-normalized (McDonough, Sun, 1995) spidergram of the Colle Fabbri Lc-Wo melilitolite (fig. 1) has a similar pattern if compared to the Ks melilitite from Cupaello and a negative slope. The La/Yb_n ratio is 8-10 for Lc-Wo melilitolite. The spidergram of Cupaello Ks melilitite is localized an order higher than that of Colle Fabbri Lc-Wo melilitolite. The spidergram of Colle Fabbri rock as well as Cupaello rocks has a deep negative Ta, Nb, Hf, Zr, and Ti and positive Ba anomalies. The Eu/Eu^*_n ratio is 0.6-0.7 for Lc-Wo melilitolite (Stoppa, Sharygin, 2009).
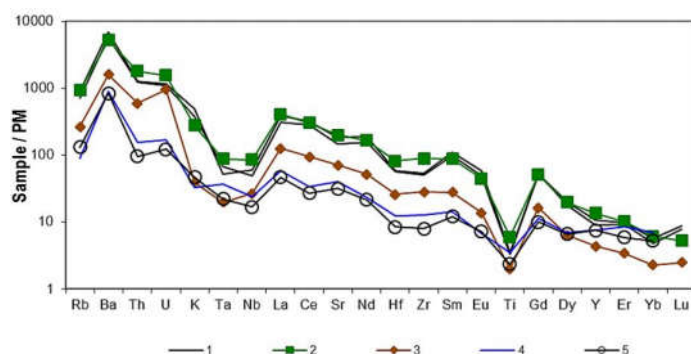

Figure 1. Primitive mantle-normalized trace element spidergram (McDonough, Sun, 1995): 1 – glass of melt inclusion hosted in diopside from Cupaello Ks melilitite; 2 – Cupaello Ks melilitite; 3 – Cupaello carbonatite tuff; 4 - glass of melt inclusion hosted in melilite from Colle Fabbri Lc-Wo melilitolite; 5 – Colle Fabbri Lc-Wo melilitolite.

The observed contents of rare and rare-earth elements in the glass (fig. 1) of the homogenized melt inclusions in clinopyroxene from Cupaello Ks-melilitite and in melilite from Colle Fabbri Lc-Wo melilitolite reflect an increased trace element contents of initial melts for the considered rocks. Primitive mantle-normalized trace element spidergrams of initial melts show the noncoherent element enrichment and is similar to that of Ks melilitite and Lc-Wo melilitolite, respectively. This fact shows that the trace element composition of considered rocks reflects that of initial melts. The La/Yb_n and Eu/Eu^*_n ratios are 67-70 and 0.65-0.72 for the glass of clinopyroxene-hosted melt inclusion in Ks melilitite, respectively. The La/Yb_n and Eu/Eu^*_n ratios are 9 and 0.53 for glasses of melilite-hosted melt inclusion in Lc-Wo melilitolite, respectively.

Thus, the key feature of the studied rocks from Cupaello and Colle Fabbri and melts conserved in minerals is a strong enrichment in LILE and LREE and less significant in HREE, which indicates the presence of enriched mantle source. The relative HREE depletion and high La/Yb_n value of considered rocks and glass of melt inclusions conserved in minerals are usually associated with the possible presence of a garnet in a mantle source. The content of LREE usually increases in primitive magma and the content of HREE remains in garnets at low degree of partial melting of the mantle source. Garnet-bearing mantle source is located at a depth of 30-60 km. The distinctive feature of studied rocks and melts is the presence of HFSE and Ti negative anomalies in primitive mantle-normalized pattern. The similar anomalies are typical for most continental flood basalts. It should be noted that the trace element enrichment and such anomalies are observed not only in Cupaello Ks melilitite and Colle Fabbri Lc-Wo melilitolite but in almost all kamafugites and associated with them carbonatites in Central Italy. The considered rocks are characterized by high $^{87}Sr/^{86}Sr$ and low $^{143}Nd/^{144}Nd$ isotopic ratios: for example, $^{87}Sr/^{86}Sr$ – 0.7112, $^{143}Nd/^{144}Nd$ – 0.5121 for Cupaello Ks melilitite; $^{87}Sr/^{86}Sr$ – 0.7097, $^{143}Nd/^{144}Nd$ – 0.51207 for Colle Fabbri Lc-Wo melilitolite (Stoppa et al., 2003; Bell et al., 2006).

These unique features of rocks from Central Italy are explained by either crustal contamination of kamafugite magma (Turi, Taylor, 1976; Peccerillo, 2004) or presence of ITEM source (Italian Enriched Mantle; Bell et al., 2006, 2013; Lavecchia, Bell, 2012). The version of crustal contamination for italian kamafugites is not consistent with the thermobarogeochemical studies and, in addition, cannot explain systematically observed Nb negative anomaly and very high $^{87}Sr/^{86}Sr$ ratio (Bailey, 2005; Boari et al., 2012). It is more likely that these anomalies are related to ITEM source, which has the highest $^{87}Sr/^{86}Sr$ (> 0.7200), low $^{143}Nd/^{144}Nd$ (0.5118) and intermediate $^{206}Pb/^{204}Pb$ (18.70) isotopic ratios (Bell et al., 2006, 2013). The researchers (Bell et al., 2006, 2013; Lavecchia, Bell, 2012) believe that ITEM could be produced by either partial melting of ancient pre-Alpine continental crust, which was involved in the mantle, or metasomatic activity caused by the presence of deep plume.

References:

Balashov Yu.A. Geochemistry of rare-earth elements. M.: Nauka. 1976. 267 p.

Stoppa F., Lavecchia. G. Late Pleistocene ultra-alkaline magmatic activity in the Umbria – Latium region (Italy): An overview // J. Volcanol. Geotherm. Res. 1992. 52. P. 277-293.

Lavecchia G., Stoppa F., Creati N. Carbonatites and kamafugites in Italy: mantle-derived rocks that challenge subduction // Ann. Geophys. 2006. 49(1). P. 389-402.

Cundari A., Ferguson A.K. Petrogenetic relationships between melilitite and lamproite in Roman Comagmatic Region: the lavas of S. Venanzo and Cupaello // Contrib. Mineral. Petrol. 1991. 107. P. 343-357.

Nikolaeva A.T. The composition of melt forming Cupaello kalsilite melilitite, Central Italy // Abstracts of TBG-XV. 2012. P. 119-120.

Panina L.I., Stoppa F., Usol'tseva L.M. Genesis of melilite rocks of Pian di Celle volcano, Umrian kamafugite province, Italy: evidence from melt inclusions in minerals // Petrol. 2003. 11(4). P. 365-382.

Stoppa F., Sharygin V. V. Melilitolite intrusion and pelite digestion by high temperature kamafugitic magma at Colle Fabbri, Spoleto, Italy // Lithos. 2009. 112. P. 306-320.

Panina L. I., Nikolaeva A. T., Stoppa F. Genesis of melilitolites from Colle Fabbri: inferences from melt inclusions // Miner. Petrol. 2013. 107. P. 897-914.

McDonough W. F., Sun S. S. The composition of the Earth // Chemical Geology. 1995. 120. P. 223-253.

Stoppa F., Cundari A., Rosatelli A., Woolley A. R. Leucite melilitolites in Italy: genetic aspects and relationships with associated alkaline rocks and carbonatites // Per. Mineral. 2003. 72. P. 223-251.

Bell K., Castorina F., Rosatelli G., Stoppa F. Plume activity, magmatism, and the geodynamic evolution of the Central Mediterranean // Ann. Geophys. 2006. 49(1). P. 357-371.

Bell K., Lavecchia G., Rosatelli G. Cenozoic Italian magmatism – Isotope constraints for possible plume-related activity // J. South Am. Earth Sci. 2013. 41. P. 22-40.

Lavecchia G., Bell, K. Magmatectonic Zonation of Italy: A Tool to Understanding Mediterranean Geodynamics // Stoppa, F. (Eds.) Updates in Volcanology – A Comprehensive Approach to Volcanological Problems. 2012. P.153-178.

Turi B., Taylor H.P., Ferrara G. A criticism of the Holm-Munksgaard oxygen and strontium isotope study of the Vulsinian district, Central ltaly // Earth Planet. Sci. Lett. 1986. 78. P. 447-453.

Peccerillo A. Carbonate-rich pyroclastic rocks from central Apennines: carbonatites or carbonated rocks? A commentary // Per. Mineral. 2004. 73. P. 165-175.

Bailey D. K. Carbonate volcanics in Italy: numerical tests for the hypothesis of lava-sedimentary limestone mixing // Per. Mineral. 2005. 74(3). P. 205-208.

Boari E., Tommasini S., Laurenzi M. A., Conticelli S. Transition from ultrapotassic kamafugitic to sub-alkaline magmas: Sr, Nd, and Pb isotope, trace element and ^{40}Ar-^{39}Ar age data from the Middle Latin Valley volcanic field, Roman Magmatic Province, Central Italy // J. Petrol. 2009. 50(7). P. 1327-1357.

The chemical composition of lamprophyllite group minerals and crystal structure of a new fluorine-rich barytolamprophyllite from the agpaitic dyke, area " Mokhnatye Roga" (Kola Peninsula)

Filina M.I.[1], Aksenov S.M.[2], Sorokhtina N. V. [1], Kogarko L.N. [1], Kononkova N.N. [1]
[1]*Vernadsky Institute of Geochemistry and Analytical Chemistry RAS,*
[2]*Shubnikov Institute of Crystallography RAS*
makimm@mail.ru

Explore a unique mineral association agpaitic dyke area "Mokhnatye Roga" (Kola Peninsula), located 55 km to the southeast of the Kovdor massif (67°15′ N, 31°30′ E) [1], in which one of the rock-forming minerals are the lamprophyllite group minerals (LGM). LGM crystallize during of formation of the dikes and form 3 generations, differ in their chemical composition (Table 1) and morphology.

Lamprophyllite-I formed large zonal composition prismatic crystals. SrO content ranges - 8.5 to 12.57 wt.%. Crystals enriched Sr in the central zone, the Ba/Sr relations achieve value 2/1. The content of BaO increases in the boundary zones - from 6.71 to 12.33 wt.%. Lamprophyllite-I is characterized by a maximum content of F - 3.22 and MgO - 1.63 wt. %. SiO_2 content of 30.50 wt. % With a minimum content of Al2O3 - 0.14 wt. %. Established the following limits concentration of impurity elements: Nb_2O_5 - 0.78, Ta_2O_5 - 0.25, ZrO_2 - 0.41, ThO_2 - 0.24, UO_2 - 0.32 (wt.%).

Lamprophyllite-II form interstitial crystals characterized by isolation and content is reduced relative to Sr Ba. The limits of variations content (wt.%): SrO from 4.21 to 8.49, and BaO - from 10.57 to 16.08 (in marginal parts), F to 2.52 wt. %. The proportion of impurity components as a whole is growing: MgO - 0.95, Nb_2O_5 - 1.05, Ta_2O_5 - 0.17, ZrO_2 - 0.42, UO_2 - 0.95, ThO_2 - 0.32, Al_2O_3 - 0.48 (wt.%).

Lamprophyllite-III forms a small needle crystals and their intergrowths formed together with the late Association - quartz-organic globules, Nb-rutile astrophyllite, shcherbakovite, carbonates Mn, sulphides, barite. SrO content varies from 5.17 to 5.54, BaO up to 16.39, F concentration drops to 1.2 wt. %. The concentration of impurity components in general decrease changing their relationship - the MgO content is reduced to 0.35 wt. %, With a decrease in the content of Na_2O K_2O increases to 3.11 wt. %, Zr, Ta, Th are close to the detection limit, U is not detected. FeO grow to 7.01, Nb2O5 to 1.63 wt.%

According to variations in the chemical composition, the fluorine content and the ratio Ba / Sr can distinguish four types of LGM. When variations relationship Ba / Sr from 0.4 to 0.97 and the fluorine content below 2.33 wt. % - to lamprophyllite, when Ba / Sr from 0.4 to 0.88 and F> 2.38 wt. % of such phases can be classified as fluorlamprophyllite. If the ratio Ba / Sr varies from 1.03 to 2.6, with a fluorine content below 2.31 - mineral relates to barytolamprophyllite, when Ba / Sr - 1.08 and F> 2.43 wt. % -fluorbarytolamprophyllite.

The crystal structure of fluorine-rich barytolamprophyllite from generation **I** was studied using single crystal X-ray analysis. The structure is similar to that of other monoclinic members of lamprophyllite group which are corresponding to type **I** (2*M*-polytype) [2]. The main structural features are reflected in its crystal chemical formula (Z = 2): ^{A}(Ba$_{0.36}$Sr$_{0.33}$K$_{0.18}$Ca$_{0.06}$Na$_{0.01}$)$_2$ [^{M1}Na$_{1.0}$^{M2}(Na$_{0.75}$Fe$_{0.21}$Mn$_{0.04}$)$_2$ ^{M3}(Ti$_{0.82}$Mg$_{0.16}$Fe$_{0.02}$) ^{X}(F$_{1.05}$O$_{0.52}$OH$_{0.43}$)] [^{L}Ti$_2$(Si$_2$O$_7$)$_2$O$_2$], where square brackets are denote the main structural units: *O*-layer of edge-shared *M*(1-3)-octahedra and heteropolyhedral net which is formed by *L*-semi-octahedra and (Si$_2$O$_7$)-diorthogroups. Fluorine-rich barytolamprophyllite differs from barytolamprophyllite be the predominance of fluorine over oxygen as well aas OH-groups in anionic *X*-site. It makes studied mineral a potential new member of the lamprophyllite group named "fluorbarytolamprophyllite" in analogues with fluorlamprophyllite [3]. Idealized formula of "fluorbarytolamprophyllite" should be written as (Z = 2): (Ba,Sr)$_2$[(Na,Fe)$_3$(Ti,Mg)F$_2$][Ti$_2$(Si$_2$O$_7$)$_2$O$_2$].

Sequential formation of all generations of LGM study agpaitic syenite held in conditions of rapid crystallization without interruption in time, the melt composition changed from high-sodium and magnesium to high-potassium and high-niobium, and barium fluoride content throughout remained extremely high. Comparison of the obtained and published data on the composition and properties of LGM [4-8] of the deposits in the world has shown that agpaitic associations at a relatively rapid crystallization of rocks can form high-F and high-Ba member of this group of minerals that are potentially new mineral species.

Table 1. Representative compositions of LGM from agpaitic dyke (wt %).

Component	I generation			II generation			III generation
	C	I	R	C	I	R	
SiO_2	29.85	29.7	29.69	29.98	29.4	29.79	27.63
TiO_2	27.9	27.53	27.94	27.28	27.57	28.01	25.48
Al_2O_3	0.18	0.18	0.17	0.25	0.2	0.35	0.39
FeO	4.59	4.33	4.82	5.2	4.71	5.14	6.23
MnO	0.77	0.71	0.87	0.87	0.91	0.65	0.4
MgO	1.24	1.17	0.95	0.76	0.71	0.58	0.35
CaO	0.96	0.91	1.02	0.86	0.96	0.79	0.54
Na_2O	9.91	9.98	9.72	9.36	9.51	8.32	8.61
K_2O	1.67	1.63	2.04	2.36	2.34	3.13	3.02
BaO	9.47	9.41	10.77	13.48	12.72	14.57	15.16
SrO	10.11	10.39	9.05	7.18	7.44	5.05	5.36
ZrO_2	0.11	0.2	0.06	0.11	0.22	0.08	0.04
Nb_2O_5	0.22	0.4	0.19	0.26	0.67	0.61	1.61
Ta_2O_5	0.08	0.08	0.07	0.08	0.05	0.05	0.09
ThO_2	0.06	0.01	0.01	0.01	0.09	0.02	0.07
UO_2	0.01	B.d.l.	B.d.l.	0.24	B.d.l.	0.6	B.d.l.
F	2.29	2.24	2.14	2.02	2.03	2.01	1.68
Total	99.42	98.87	99.47	100.30	99.48	99.75	96.53
O=F	0.96	0.94	0.90	0.85	0.85	0.85	0.71
Total (recalculated for the concentration of fluorine)	98.46	97.93	98.57	99.45	98.63	98.90	95.82
The average of X analyses	$\sum 12$	$\sum 16$	$\sum 6$	$\sum 5$	$\sum 3$	$\sum 4$	$\sum 2$

Microprobe analyses were performed at the laboratory of Vernadsky Institute of Geochemistry and Analytical Chemistry RAS (Cameca SX-100). Grain zones: (C) center; (R) rim; (I) intermediate zone. B.d.l., below the detection limits.

Reference

1. Akimenko M. I., Kogarko L. N., Sorokhtina N. V., Kononkova N. N., Mamontov V. P.. A New Occurrence of Alkaline Magmatism on the Kola Peninsula: An Agpaitic Dyke in the Kandalaksha Region // Doklady Earth Sciences. 2014, Vol. 458, Part 1, pp. 1125–1128.
2. Rastsvetaeva R.K., Chukanov N.V., Aksenov S.M. The crystal chemistry of lamprophyllite-related minerals // Eur. J. Mineral. 2015. (in print)
3. Andrade. M.B., Yang, H., Downs, R.T., Färber, G., Contreira Filho, R.R., Evans, S.H., Loehn, C.W. & Schumer, B.N. Fluorlamprophyllite, IMA 2013-102. CNMNC Newsletter No. 19, February 2014, page 166 // Mineral. Magazine. 2014, V. 78, pp. 165-170.
4. Arzamastsev A.A., Belyatsky B.V., Arzamastseva L.V. Agpaitic magmatism in northeastern Baltic Shield: A study of the Niva intrusion, Kola Peninsula, Russia // Lithos. 2000. V. 51. № 1-2. pp. 27.
5. Azarova Y. V., Genesis and minerals typochemism series lamprophyllite-baritolamprohyllite of complex lujaurite-malignites Khibiny massif // New Data on Minerals. 2004. V. 39. pp. 66.
6. Zaitsev V.A., Kogarko L.N., The compositions of lamprophyllite group minerals of alkaline massifs of the world // Geochemistry. 2002. № 4. pp. 355.
7. Ivanyuk G. Y., Yakovenchuk V.N., Pakhomovsky Y. A., Kovdor. Apatity // 2002. 320 p.
8. Chukanov N.V., Moiseev M.M., Pekov I.V., Labeznik K.A., Rastsvetaeva R.K., Zayakina N.V., Ferraris J.,. Ivaldi G., Nabaritolamprophyllite Ba(Na,Ba) {Na$_3$Ti[Ti$_2$0$_2$Si$_4$0$_{14}$](OH,F)$_2$ new layered titanosilicate lamprophyllite group of alkaline-ultrabasic massifs Inagli and Kovdor, Russia // ZVMO. 2004. № 1. pp. 59-72.